THE DYNAMICS AND CONTROL OF THE SHUTTLE SUPPORTED TETHERED SUBSATELLITE SYSTEMS

by

DA MING XU

Department of Mechanical Engineering
McGill University

Submitted to the Faculty of Graduate Studies and Research of McGill University, in partial fulfillment of the requirements for the degree of Doctor of Philosophy

ABSTRACT

In this thesis, the dynamics and control of the shuttle supported tethered subsatellite system are investigated. At first, a dynamical model is developed that takes into account the three dimensional rotational motion of the system as well as the nonlinear vibrations of the tether, both in longitudinal and transverse directions. Using the extended Hamilton's principle, a set of nonlinear partial differential equations to govern the vibrations and nonlinear ordinary differential equations to describe the rotations are derived. These equations are applicable whether the length is constant or changing with time. Galerkin's method (with slight modification) is then used to get the discretized equations for the vibrations.

Attention is then focused on the control of the motions during the retrieval stage since both rotations and vibrations are inherently unstable during this phase and effective control schemes are not available. In the thesis, control laws are derived using simplified analyses and validated through numerical integration of the original unsimplified equations.

To start with, rotations both in and out of the orbital plane are considered in the absence of the vibrations of the tether. A length rate control law using linear feedback of pitch rate and quadratic feedback of roll rate is proposed and proved to be quite effective during the retrieval phase. As an extension of this control law, a non-linear tension control law is also suggested and verified to be of the same effectiveness.

The vibrations of the tether are then taken into account. Longitudinal vibrations along with the rotational motions are examined first and a length change control law is proposed to control them during retrieval using that scheme. The rotations can be limited to very small ranges and the longitudinal vibrations can be damped out without slackening the tether. In the following step, transverse vibrations are considered as well. It is noted that both longitudinal and transverse vibrations must be considered together, especially for very short tether lengths. A length acceleration scheme is suggested to control all the vibrations of the tether. In addition, fast retrieval concepts are examined to maintain certain minimum tension during the terminal phase of retrieval thus avoiding the problem of slackening the tether.

Finally, thruster augmented active control is investigated as it might have great advantage in the practical design. Thrusters in three perpendicular directions (one of them along the direction of the tetherline) are used. Required thrust time histories are determined. It is noted that using the proposed schemes, successful control of all the rotational and vibrational motions can be achieved during the retrieval of the subsatellite while the retrieval time can be limited to about two to four orbital periods.

SOMMAIRE

Cette thèse a pour objet l'étude de la dynamique et de la commande d'un système à satellite déployé à partir d'une navette au moyen d'un fil. Un modèle dynamique a d'abord été établi; ce modèle tient compte du mouvement de rotation du système dans les trois sens, de même que des vibrations non-linéaires du fil, dans le sens longitudinal et transversal. En étendant l'application du principe de Hamilton, l'auteur a produit un ensemble d'équations différentielles partielles non-linéaires décrivant les vibrations, et un ensemble d'équations différentielles ordinaires non-linéaires décrivant les rotations. Ces équations s'appliquent que la longueur du fil soit constante ou variable dans le temps. L'auteur a ensuite utilisé la méthode de Galerkin (en la modifiant légèrement) pour formuler les équations discrètes qui s'appliquent aux vibrations.

L'auteur examine ensuite le contrôle des mouvements à l'étape de la récupération; en effet, les rotations et les vibrations sont fondamentalement instables à cette étape, et nous ne disposons actuellement d'aucun schéma efficace de contrôle. L'auteur dégage donc des lois de contrôle à l'aide d'analyses simplifées et validées par l'intégration numérique des équations non-simplifiées initiales.

Il examine d'abord les rotations du système de part et d'autre du plan de l'orbite, en l'absence de toute vibration du fil. Il propose ensuite une loi de contrôle du taux de raccourcissement du fil, à partir de la rétroaction linéaire du taux de tangage et de la

rétroaction quadratique du taux de roulis; cette loi s'est révélée très efficace à l'étape de la récupération. Comme complément à cette loi, il propose une loi de contrôle de la tension non-linéaire. Cette dernière loi s'est révélée aussi efficace que la première.

Il est alors tenu compte des vibrations du fil. Les vibrations dans le sens longitudinal accompagnant le mouvement de rotation sont d'abord examinées; l'auteur propose une loi de contrôle de la variation de la longueur du fil afin de maîtriser ces vibrations pendant la récupération. Les rotations peuvent être gardées sous de très faibles amplitudes, et les vibrations longitudinales peuvent être absorbées sans relâchement du fil. A l'étape suivante, l'auteur examine également les vibrations dans le sens transversal. Il fait remarquer qu'il faut tenir compte à la fois des vibrations dans le sens longitudinal et des vibrations dans le sens latéral, particulièrement lorsque le fil est très court. Il propose un schéma d'accélération pour contrôler toutes les vibrations du fil. De plus, il examine certaines notions de récupération rapide qui visent à maintenir une certaine tension minimum sur le fil, à la dernière étape de la récupération, afin d'en éviter le relâchement.

Enfin, l'auteur examine le problème du contrôle actif assisté par propulseurs, car cette technique pourrait présenter des avantages considérables sur le plan pratique. Les propulseurs disposés perpendiculairement dans les trois plans (l'un d'eux se trouvant dans le plan du fil) sont utilisés à cette fin. Les durées de mise à feu nécessaires sont déterminées. L'auteur fait remarquer, qu'à l'aide des schémas qu'il propose, on peut arriver à bien contrôler tous les mouvements de rotation et de vibration pendant la récupération de sous-satellites, et que cette opération peut s'exécuter sur une période de deux à quatre orbites.

ACKNOWLEDGEMENTS

The author wishes to express his deep gratitude to his research director, Dr. A.K. Misra for his guidance and encouragement consistently throughout the preparation of this thesis. His personality and kindness and sincerity also impress the author deeply.

The author is grateful to Dr. V.J. Modi for his help and valuable research advice.

Sincere thanks are also due to the Department of Mechanical Engineering for awarding the author a Departmental Fellowship in 1982-83 and to the University for awarding the Major Bindra Fellowship in 1983-1984. Many professors in the Department including Professor G.G. Bach, Professor M.P. Paidoussis, Professor J.W. Provan and Professor A.M. Ahmed helped make the author's stay at University a pleasant one and helped him to feel at home.

Finally, sincere thanks also to Ms. Evelyn Schliecker for the excellent job of typing a difficult manuscript.

TABLE OF CONTENTS

PAGE

PAGE

LIST OF FIGURES

REJECTED/REJETE

AUTHOR'S NAME/
NOM DE L'AUTEUR: XU, DA Ming.

THESIS NO./
NO. DE THESE 133

REASONS/RAISONS:

Les feuillets XIII et XIV

manquent à la thèse.

LIST OF TABLES

NOMENCLATURE

a	semi-major axis of the orbit
a_0	semi-major axis of the earth
A	cross section of the tether
$[A]$	a square matrix defined in Appendix G
A_b	projected area of the subsatellite normal to the relative velocity of air
A_i	nondimensional $\tilde{A}_i$; $A_i = \tilde{A}_i/\ell_0$
$\tilde{A}_i$	i^{th} generalized modal coordinate used in the discretization of the inplane transverse displacement u of the tether
A_p	projected area, in general, normal to the relative velocity of air
A_u, A_α	differential operators
b	semi-minor axis of the orbit
b_0	semi-minor axis of the earth
$[B]$	inverse of the square matrix [A]
B_i	nondimensional $\tilde{B}_i$, $B_i = \tilde{B}_i/\ell_0$
$\tilde{B}_i$	i^{th} generalized modal coordinate used in the discretization of the out-of-plane transverse displacement w of the tether
c	retrieval constant [sec^{-1}]
$\tilde{c}$	nondimensional retrieval constant, $\tilde{c} = c/\omega$
C_{1d}	dynamic part of C_1
C_{1s}	quasi-static part of C_1
C_d	drag coefficient in general
C_{db}	drag coefficient for the subsatellite
C_{dc}	drag coefficient for the tether

C_i	nondimensional $\tilde{C}_i$
$\tilde{C}_i$	i^{th} generalized coordinate used in the discretization of the longitudinal displacement v of the tether
dA_c	projected area of an element dy_c of the tether normal to the relative velocity of air
d_c	diameter of the tether
e	eccentricity of the orbit
E	Young's modulus of the tether material
E*	complex Young's modulus of the tether material
E_1	real part of E*
E_2	imaginary part of E*
F	$2e\ s\theta/(1+e\ c\theta)$
$\vec{F}$	aerodynamic force in general
$\vec{F}_b$	aerodynamic force acting on the subsatellite
$\vec{f}_c$	aerodynamic force acting on an element dy_c of the tether
G	universal gravitational constant
h	height above the earth's surface; also, angular momentum per unit mass of the system
H	altitude parameter, equation (2.8.7)
h_0	a constant in metres
i	angle of inclination of the orbit to the equatorial plane; also square root of -1.
$\vec{I}, \vec{J}, \vec{K}$	unit vectors along inertial coordinate axes X, Y, Z
$\vec{i}_0, \vec{j}_0, \vec{k}_0$	unit vectors along orbital coordinate axes x_0, y_0, z_0
$\vec{i}_c, \vec{j}_c, \vec{k}_c$	unit vectors along tether based coordinate axes x_c, y_c, z_c
K	$K = \sqrt{2}/\pi$
K_1, K_2	constants in equation (1.2.1)

K_{AB}	gain associated with transverse vibrations
K_c	gain associated with longitudinal vibration
K_α	gain associated with inplane rotation
K_γ	gain associated with out-of-plane rotation
K_θ	a function of θ, constant for a circular orbit
L	Lagrangian $L = T - V$
L_c	commanded length of the tether
ℓ_{fin}	final unstretched length of the tether
ℓ_{fr}	a specified length beyond which fast retrieval is carried on
ℓ_i	initial unstretched length of the tether
$\vec{\ell}_j$	length vector of the tether after elongation along y_c direction, equation (2.3.5)
ℓ_0	unstretched length of the tether at any instant; $\ell_0 = \ell_0(t)$ during deployment and retrieval
ℓ_s	stretched length of the curved tether
ℓ_t	a specified length beyond which tetherline thruster fires additionaly to maintain a certain amount of tension in the tether
M	total mass of the SSTS system
M_a	mass of the shuttle
M_b	mass of the subsatellite
M_c	mass of the deployed part of the tether at any instant
M_{earth}	mass of the earth
P_{Ai}, P_{Bi}, P_{Ci}	nondimensional values of Q_{Ai}, Q_{Bi}, Q_{Ci}, respectively
P_E	strain energy in the tether
Q_{Ai}, Q_{Bi}, Q_{Ci}	generalized forces due to aerodynamic forces corresponding to the generalized coordinates A_i, B_i and C_i, respectively; $i = 1,2$.

Q_{ua}, Q_{va}, Q_{wa} generalized forces due to aerodynamic forces corresponding to displacements u, v, w of an element of the tether, respectively

Q_{vab} generalized force due to aerodynamic forces corresponding to displacement v at the subsatellite

Q_α, Q_γ generalized forces due to the nonpotential forces corresponding to generalized coordinates α and γ, respectively

$Q_{\alpha a}$, $Q_{\gamma a}$ generalized forces due to the aerodynamic forces corresponding to generalized coordinates α and γ, respectively

$\vec{R}_a$ position vector from the centre of mass of the SSTS system to the centre of mass of the shuttle

$\vec{R}_b$ position vector from the centre of mass of the SSTS system to the centre of mass of the subsatellite

$\vec{R}_c$ position vector from the centre of mass of the SSTS system to any arbitrary point on the tether

$\vec{r}_c$ position vector from the centre of mass of the shuttle to any arbitrary point on the tether

r_{earth} radial distance of the surface of the earth from its centre for a given θ

R_{earth} average radius of the earth, equal to $\frac{1}{2}(a_0 + b_0)$

$\vec{R}_{Ea}$ position vector of the centre of mass of the shuttle from the centre of the earth

$\vec{R}_{Eb}$ position vector of the centre of mass of the subsatellite from the centre of the earth

$\vec{R}_{Ec}$ position vector of any arbitrary point on the tether from the centre of the earth

$\vec{R}_0$	position vector from the centre of the earth E to the instantaneous centre of mass S of the SSTS system
S_{C_1}	nondimensionalized generalized force due to the thrust T_c corresponding to generalized coordinate C_1
S_α	nondimensionalized generalized force due to the thrust T_α corresponding to generalized coordinate α
S_γ	nondimensionalized generalized force due to the thrust T_γ corresponding to generalized coordinate γ
t	time
T	kinetic energy of the SSTS system
T_a	kinetic energy of the shuttle
T_b	kinetic energy of the subsatellite
T_c	kinetic energy of the tether
T_{nonorb}	kinetic energy associated with the rotational motion and vibrations of the tether
T_{orb}	orbital kinetic energy of the SSTS system
T_{uvw}	kinetic energy $T_{uvw} = T_{nonorb} - T_{\alpha\gamma}$
$T_{\alpha\gamma}$	kinetic energy associated with rotations only
$\vec{u}$	displacement vector $\vec{u} = u\vec{i}_c + v\vec{j}_c + w\vec{k}_c$
u	inplace displacement of the tether
$\bar{u}$	average inplace displacement of the tether
v	longitudinal displacement of the tether
$\bar{v}$	average longitudinal displacement of the tether
V	potential energy of the system
$\vec{V}$	velocity in general
$\vec{V}_a$	velocity of the SSTS system relative to atmosphere

V_G	gravitational potential energy of the SSTS system
V_{Ga}	gravitational potential energy of the shuttle
V_{Gb}	gravitational potential energy of the subsatellite
V_{Gc}	gravitational potential energy of the tether
V_{nonorb}	potential energy associated with the rotational motion of the subsatellite and vibrations of the tether
V_{orb}	orbital potential energy
v_s	longitudinal displacement of the tether at the subsatellite end
$\vec{V}_s$	velocity of the atmosphere at the subsatellite altitude due to the rotation of the earth
$\vec{V}_{sa}$	velocity of the subsatellite relative to the atmosphere
V_{xa}, V_{ya}, V_{za}	components of $\vec{V}_a$ along x_0, y_0 and z_0 directions, respectively
V_{xc}, V_{yc}, V_{zc}	components of $\vec{V}_a$ along x_c, y_c and z_c directions, respectively
$V_{xsa}, V_{ysa}, V_{zsa}$	components of $\vec{V}_s$ along x_0, y_0 and z_0 directions, respectively
V_{uvw}	potential energy, $V_{uvw} = V_{nonorb} - V_{\alpha\gamma}$
$V_{\alpha\gamma}$	gravitational energy associated with rotations only
w	out-of-plane displacement of the tether
$\bar{w}$	average out-of-plane displacement of the tether
W	work done by the external forces (both potential and nonpotential forces)
W_a	work done on the SSTS system by the aerodynamic forces
W_{ab}	work done by the aerodynamic forces acting on the subsatellite

W_{ac}	work done by the aerodynamic forces acting on the tether
W_{np}	work done by the external nonpotential forces
$\{Y\}$	vector of state variables
y_i	i^{th} state variable, $i = 1, 2, \ldots$
x_c, y_c, z_c	tether-based local coordinate system
X, Y, Z	earth centre based inertial coordinate system
x_0, y_0, z_0	orbital coordinate system
α	inplane rotational angle (pitch)
γ	out-of-plane rotational angle (roll)
δ	a nondimensional parameter, equation (4.2.32)
ε	strain in the tether at any arbitrary point
ε_1	strain in the tether at the shuttle end
ε_2	strain in the tether at the subsatellite end
η	nondimensional length, $\eta = \ell n(\ell_0/\ell_{ref})$; also, a parameter $\eta = (E_2/E_1)$
θ	true anomaly
$\dot{\theta}$	instantaneous orbital rate
θ_0	argument of the perigee
μ	a constant, $\mu = G \cdot M_{earth}$
ν	mass ratio between the subsatellite and the tether at any instant, equation (4.2.13)
ξ_1, ξ_2	nondimensional parameters, equations (4.2.33) and (4.2.34) respectively
ρ_a	density of air, equation (3.3.2)
ρ_c	mass per unit length of the tether
ρ_0, ρ_{00}	constants, equations (3.1.3) and (3.3.3), respectively

σ	tension in an arbitrary element of the tether
σ_1	tension in the tether at the shuttle end
σ_2	tension in the tether at the subsatellite end
σ_0	rotational rate of the earth
ϕ_i	i^{th} admissible function used in discretization of transverse vibrations
ψ_i	i^{th} admissible function used in discretization of longitudinal vibrations
ω	mean orbital rotational velocity
ω_1, ω_2	two lowest frequencies of transverse vibrations
$\vec{\omega}_c$	angular velocity of x_c, y_c, z_c cordinate system with respect to the inertial coordinate system X, Y, Z
ω_{xc},ω_{yc},ω_{zc}	components of $\vec{\omega}_c$ along x_c, y_c and z_c axes, respectively
ω_ε	lowest frequency of longitudinal vibration of the tether
Ω	$(EA/\rho_c \ell_0^2 \dot{\theta}^2)^{(1/2)}$

CHAPTER 1

INTRODUCTION

1.1 PRELIMINARY REMARKS

Tether connected two-body systems have a great potential for future space applications. Interest in the tethered systems was initially associated with the retrieval of stranded astronauts [1,2]. However, the problems associated with such retrieval was clearly demonstrated in a study by Starly and Adlhoch [2], in which it was shown that the rotational motions grew continuously as the tether was reeled in. The retrieval scheme was not developed further because more suitable rescue techniques were developed subsequently.

Proposals have been made to use a tether for stationkeeping between two orbiting space vehicles [3]; however, the method has been abandoned due to the difficulties involved in determining and controlling the required tether tension. On the other hand, Gemini XI and XII flight tests have successfully demonstrated the feasibility of a short tethered system. The former used a rotating configuration while the latter had a gravity-gradient stabilized configuration [4].

With the advent of the space shuttle, a variety of fascinating uses of these systems have been proposed during the last ten years. Some examples are given below.

(i) Upper atmospheric experiments: A subsatellite may be deployed into the upper atmosphere from the shuttle using a 100-120 Km long tether called 'Skyhook' [5]. This would provide an economic and reliable way to carry out measurement of the physical properties of the atmosphere, ionosphere and magnetosphere as well as observation of various phenomena in the thermosphere.

ii) Artificial gravity uses: A system of two bodies linked by a long tether aligned with the local vertical can produce an artificial gravity for both the end bodies due to the tension in the tether caused by the gravity gradient. The tension pulls both bodies towards the center of mass of the system and neither body moves in a freely orbiting state. Although the artificial gravity level produced may be very weak (0.01 g - 0.1 g depending on the length), it may be of great help to the crew-support systems in a space station. In addition, such a tether connected system can be used for low-gravity experiments. It must be pointed out that this concept is somewhat different from the rotating space station-cable-counterweight systems [6].

iii) Electrodynamic uses: A long insulated conducting tether moving around the earth will generate electric current by intersecting the earth's magnetic field. In some cases of emergency, electric power can still be supplied in this way although a price is paid in terms of lowering the altitude of the spacecraft.

iv) Radio astronomy and low frequency communication uses: A tether can be used as an antenna for radio astronomy and very low frequency communications. In this case, the tether itself is used as part of the scientific instrument.

v) Transportation and space constellation uses: A tether can be used for orbital transfer. If the subsatellite supported by the tether is released at an appropriate time with correct initial velocity, it will reach the desired orbit [7].

There are many other possible applications of tethered satellite systems which will not be described here for the sake of brevity; the interested reader is referred to the works of Bekey [7] and Rupp, et al. [8].

Of particular interest among the above-mentioned systems is the shuttle supported tethered subsatellite system and in recent years many investigators have paid attention to its dynamics and control. The system is approaching a practical design stage and the first space flight test will take place in the mid-eighties. This mission will be a joint project of the NASA and the Government of Italy. The effects of various environmental forces on the equilibrium configuration of the tether during the station-keeping stage and the effectiveness of different deployment and retrieval schemes will be tested in this mission.

The operation of a tethered satellite system consists of three stages: (i) deployment; (ii) station-keeping and (iii) retrieval. During the deployment, a reel mechanism equipped at the shuttle releases the tether to send the subsatellite to a planned altitude. At the beginning, an initial push may be needed to overcome the weightlessness situation until the tether is taut. In the following process of deployment, the reel mechanism functions somewhat like a brake. A certain experiment could be carried out during the station-keeping stage after the instrumented subsatellite has been placed at the desired altitude. Once the experiment is completed, the reel mechanism reels the subsatellite back to the shuttle; this is termed the retrieval stage.

This proposed shuttle supported tethered subsatellite (SSTS)* system is really a revolutionary means to send a subsatellite into a desired orbit

---

* This abbreviation will be used from now on.

compared with traditional ones. It not only avoids an extra launch operation but also provides a totally recoverable and reusable system thus having the possibility of a very low recurrent cost [9]. However, the task involved is rather comprehensive and not at all routine. The core of the difficulty lies in the system dynamics and control, especially during the retrieval stage.

Dynamics of the SSTS system involves orbital dynamics as well as attitude dynamics. The center of mass of the system moving around the earth is called orbital dynamics while the motion of the system relative to the center of mass is termed attitude dynamics. Orbital dynamics is negligibly affected by the attitude dynamics [10] as the energy associated with the former is much larger than that of the latter. On the other hand, the orbital motion does affect the attitude dynamics significantly.

It is not difficult to see that the dynamics of the SSTS system is rather complicated. The shuttle flies around the earth; the subsatellite swings around the shuttle; the tether vibrates longitudinally as well as in the transverse directions; the tether moves away from or towards the shuttle during deployment or retrieval, respectively, making the system non-autonomous; tension in the tether ranges from less than 0.1 N (very weak) to around 100 N, when the length of the tether changes from say, 20 m (quite short) to 100 Km (very long). The fact that the density of air varies by several orders of magnitude along the tether complicates the motion further. A good modelling of the system is necessary to provide a basis for the analysis and control of its dynamics.

It has been shown that the rotational motions are inherently unstable during retrieval [11]. The faster the retrieval is, the larger is the rate of growth of motion. Even during the deployment stage, if the initial conditions are large and the deployment is required to be reasonably fast, control of motion is still needed although it is much easier compared with the control during retrieval.

The problems related to retrieval control of SSTS systems have not completely been solved yet. Some of these problems will be tackled in this thesis.

1.2 LITERATURE REVIEW

This literature review is not meant to be exhaustive. Rather a few key references are mentioned to indicate the general development of the subject of cable connected orbiting bodies. As for a more detailed review, the interested reader is referred to the paper by Misra and Modi [12]. However, all the papers on the SSTS system are discussed here.

The literature review is carried out based on the nature of scientific development rather than time sequence. This approach is believed to be more suitable for describing where the spots of difficulty lie, thus, what this thesis must really attack. The topics of dynamical modelling and control strategies are considered below separately.

1.2.1 Dynamical Modelling

The general dynamics of SSTS systems shown in Figure 1.1 is rather complex. Many parameters play major roles in governing the system behaviour. An important consideration is whether the unstretched length of the tether is constant (station-keeping phase) or varies with time (if increasing, deployment; if decreasing, retrieval). During the station-keeping stage, the dynamics is simpler compared to the other two stages and is quite similar to the dynamics of another cable connected system, the space station-cable-counterweight system, which has been investigated extensively. The latter system had been proposed for the creation of artificial gravity in a space station by rotating the entire system around its center of mass.

The investigations of the dynamics of the space station-cable-counterweight systems (see [12]) are relevant to this study and can be regarded as preliminary research. It is important to note that the gravity gradient can excite longitudinal as well as transverse vibrations of the tether [13,14]. However, a small amount of damping (1% critical damping) is quite effective in stabilizing the system although the spin rate decreases slightly [15].

The effort to study the dynamics of the SSTS system was first made by Rupp [11]. He made a key development in this area; however, his dynamical model is a drastic simplification of the actual system. The tether was assumed to be massless and inextensible and the rotational motion was confined to the orbital plane. His conclusion that the deployment is basically stable and the retrieval is inherently unstable is valid even when the dynamical models are made more sophisticated. A tension control law was proposed by him to control the motion of the system. This law will be discussed later in Section 1.2.2.

During either deployment or retrieval, the out-of-plane rotational motion cannot be neglected if the orbit is in a non-equatorial plane. This is because the out-of-plane rotation is excited by the out-of-plane component of the aerodynamic drag caused by a rotating atmosphere. Even when the orbit is equatorial, there might be some initial out-of-plane disturbances. During retrieval, this initial disturbance grows without bounds. Thus, the investigations [16-26] subsequent to Rupp's work have included the out-of-plane rotation in the dynamical model.

The mass of the tether is expected to be of the same order of magnitude as that of the subsatellite when the tether is long enough and hence cannot be ignored. Another important parameter is the elasticity of the tether. Proposed tethers are very thin (less than 1 mm in diameter) and very long (up to 100 Km). Payload mass limitation forces us to make the tether so thin. This makes it very flexible and extensible. Thus, the longitudinal stretch of a 100 Km long tether can be several hundred meters. The tether vibrates axially if there is any initial disturbance during deployment, station-keeping or retrieval stage . This vibration has been represented by a single longitudinal displacement similar to that of a spring-mass system in the works [16,20,22]. However, as the mass is distributed along the tether, a more accurate representation is in terms of combination of axial modes similar to that of an elastic bar; this has been done by Banerjee and Kane [25].

Furthermore, the tether can have transverse displacements making the tether curved. This happens mainly due to two reasons. Aerodynamic drag not only pushes the subsatellite to lag behind the shuttle but also forces the tether to assume a curved equilibrium configuration. In addition, if the tether is moving axially during deployment or retrieval stage, then the Coriolis force again curves the tether. Since the tether has distributed mass and elasticity (i.e., an elastic string), transverse vibrations occur. This is especially serious in the orbital plane and in a fast retrieval or deployment situation. The transverse vibrations of the tether have been taken into account recently by several investigators such as Kohler, et al.

[21], Modi and Misra [20,22,23] and Glaese and Pastrick [26]. Kalaghan, et al. [19] did consider the transverse motion of the tether; but since the co-ordinate system in which displacements are calculated does not follow the attitude rotations, the transverse vibrations are masked by the rotational motion.

A comparison of dynamical modes of SSTS systems used in various investigations is given in Table 1. Because there are so many factors affecting the dynamics, no model is exactly the same as another even though the main considerations may be the same.

1.2.2 Control of the SSTS System

Control of the dynamics of the SSTS system during deployment and retrieval is a challenging problem. Since all the motions are inherently unstable during the retrieval stage, corresponding control is much more difficult than that during deployment.

During the past ten years or so, the control problem has been of great concern since it is directly related to the feasibility of the SSTS system. Various types of control laws have been proposed. These control laws can basically be categorized into three types:

(i) Tension control laws;

(ii) Laws based on rotational rate of the tether reel, for example, length rate control law and torque control law;

(iii) Thruster augmented active control laws.

They are reviewed below briefly.

1.2.2.1 Tension Control Laws

Among the three types of control laws, the tension control law was developed first. Rupp [11] formulated a tension control law to control the inplane rotation during deployment and station-keeping. The retrieval problem was touched upon only briefly. In his control law, the tension level in the tether is modulated in the form

$$T = K_1 L + C_1 \dot{L} + K_2 L_c \tag{1.2.1}$$

where L and $\dot{L}$ are instantaneous length and length rate, respectively, L_c is a commanded length while K_1 , K_2 and C_1 are a set of constants. No feedback from the swing angle was used. The most significant feature was to design properly the tetherline spring and the viscous damping associated with the reel mechanism, so that the frequency of the swing motion and that of the oscillation of the length are the same. Since the two motions are strongly coupled, the inplane rotations can be damped by adding damping to the length equation. It may be pointed out here that this longitudinal motion is different from the very high frequency longitudinal vibrations of the tether associated with its elasticity.

Several subsequent investigations modified Rupp's tension control law to improve the performance. Baker, et al. [16] modified the tension law to

$$\frac{T}{m_s + \frac{1}{2} m_t} = (R^2 + 3)\Omega^2 L + 2\xi_c R\Omega L - R^2\Omega L_c \tag{1.2.2}$$

where R is the ratio between control law stretch frequency and orbital frequency, ξ_c is the control law damping while m_s and m_t are the mass of the subsatellite and tether, respectively. The most significant modification is to make the commanded length a function of the actual length rather than an arbitrary set of commands, i.e.,

$$L_c = K_1 L + K_3 \tag{1.2.3}$$

Kulla [27] and Kalaghan, et al. [19] used laws similar to Baker's law in their investigations.

Bainum and Kumar [24] developed an optimal tension control law based on an application of the linear regulator problem. The inplane swing angle and its rate were used as feedback in this tension control law, i.e.,

$$T = K_\ell \ell + K_{\ell'} \ell' + K_\alpha \alpha + K_{\alpha'} \alpha' + T_0 \tag{1.2.4}$$

where T_0 is the equilibrium tension, K_ℓ etc. are a set of constants and ℓ is defined as

$$\ell = L_c/L - 1 \tag{1.2.5}$$

The control strategy was very effective during deployment but was not very successful during retrieval.

Now, the following question arises. Are these control laws effective if the out-of-plane rotation is considered and the system is being retrieved instead of being deployed? Modi, et al. [28] have indicated that the answer is negative. Out-of-plane rotation could grow up to 45°, which is unacceptable. The above-mentioned authors thus proposed a nonlinear strategy in which the tension uses feedback of the rate of the out-of-plane rotation in a quadratic form*. The pitch motion is damped and the roll bounded to a limit cycle of about 10° amplitude through this control. It

* This tension control law is based on a similar length rate control law proposed in this thesis and published earlier.

appears to be one of the most promising tension control laws for retrieval. If the vibrations of the tether, both longitudinally and in transverse directions are taken into account in the dynamical model, the tension control law might have to use the feedback of these vibrational variables as well. However, no such development has been made to the best of the author's knowledge.

1.2.2.2 Length Change Control

As opposed to the tension control laws, the length change laws, the nominal unstretched length or its time derivatives are modulated using feedback of the state variables. This is quite direct to the reel mechanism. The law corresponds to modulating the rotation of the drum of the reel mechanism.

This type of control was originally proposed by Kohler, et al. [21], but its effectiveness has been investigated only recently (since 1980).

Misra and Modi [29] proposed such a control law to investigate a planar situation in the presence of longitudinal and transverse vibrations. The numerical results were obtained using a length rate involving linear pitch rate feedback only. Although the rotations during retrieval were bounded, both transverse and longitudinal vibrations grew. This suggests that feedback of vibrations is necessary for successful retrieval. Most of the analysis in this thesis uses this type of control law.

1.2.2.3 Thruster Augmented Active Control

During retrieval, as the length of the tether reduces to a small value, the equilibrium tension in the tether due to the gravity gradient approaches zero and during a dynamical situation the tether may become slack. Thus a tension control law (for example, the one suggested by Baker, et al. [16]) or any modification of that such as a length rate law [29] becomes ineffective. To alleviate this difficulty, Banerjee and Kane [30] proposed to use a set of thrusters (in addition to a torque control law) to control the retrieval dynamics. In this active control scheme, the thrusters are placed at the subsatellite to help reduce the motion and speed up the retrieval process. The thrusters are capable of exerting forces in both transverse and longitudinal directions. In their dynamical model, the transverse vibrations are not considered in the dynamical model. About five to six orbital periods (approximately nine hours) are needed to complete the retrieval.

The comparison of various control laws for the SSTS system is shown in Table 2.

1.3 PURPOSE AND SCOPE OF THE INVESTIGATION

From the literature review, it is clear that for the SSTS system the most difficult problem is controlling the motion during retrieval compared with deployment or station-keeping. Hence, the goal of this thesis is aimed at studying retrieval dynamics and control.

There are two key problems associated with retrieval:

(i) control of unstable out-of-plane rotation;

(ii) preventing the tether from becoming slack due to unstable vibrations during the terminal stage of retrieval.

The latter is much more challenging than the former, and very little effort has been directed towards studying this aspect. Most investigators are concerned with the rotational motions only. The vibrations of the tether, both longitudinal and transverse, have often been ignored as if the continuous tether always remains straight and is inextensible. This thesis emphasizes studying the out-of-plane rotations as well as the vibrational aspects of the tether.

The thesis may be divided into two parts. The first part (Chapters 2 to 5) presents a general dynamical model of the SSTS system while the second part (Chapters 6 to 9) deals with control of the dynamics during retrieval of the subsatellite.

In Chapter 2, the dynamical model is developed taking into account:

(i) three dimensional rotations;

(ii) mass of the tether;

(iii) longitudinal vibrations including variation of the longitudinal strain along the tether;

(iv) three dimensional transverse vibrations;

(v) aerodynamic drag in a rotating atmosphere considering the oblateness of the earth;

(vi) material damping of the tether;

(vii) geometric nonlinearity, i.e., nonlinear relation between strain and displacements, which becomes important for short tethers.

Equations governing the dynamics of the system are derived using the extended Hamilton's principle.

In Chapter 3, the generalized forces arising due to the aerodynamic forces are formulated.

In order to get approximate solutions to the equations of motion, the latter are discretized in Chapter 4. The ordinary differential equations thus obtained are nondimensionalized and numerical procedures to analyse them are discussed.

In Chapter 5, the quasi-equilibrium configuration in the case of circular orbits for a specified tether length is calculated. The effects of various parameters on the quasi-equilibrium configuration are examined.

The four chapters described above form the first part of the thesis. In the following chapters (the second part of the thesis), attention is focused on the control of the motions during retrieval of the subsatellite. In Chapter 6, a nonlinear length rate control law is developed to control the rotations (both pitch and roll) during retrieval.

In Chapter 7, the tether is regarded as an elastic string and the longitudinal vibrations of the tether are thus introduced. An appropriate length rate change law is proposed to control rotations and longitudinal vibrations simultaneously.

In Chapter 8, the transverse vibrations of the tether is brought into consideration. Vibrations of the tether, both longitudinal and transverse, are investigated. At first, only the terminal phase of retrieval is considered. Subsequently, both rotations and vibrations of the tether are analysed from the very beginning of the retrieval process. Several length change laws are examined for this case.

In Chapter 9, thruster augmented control is investigated with a goal of controlling the motions during a very short retrieval time. A mixed control strategy, using first a length change control followed by thruster control, is also presented. Some closing comments and suggestions for further work are given in Chapter 10.

CHAPTER 2

DERIVATION OF EQUATIONS OF MOTION

2.1 SYSTEM DESCRIPTION

The system under consideration is shown in Figure 2.1. It consists of three bodies: the shuttle, a subsatellite and a long thin tether. The shuttle enters its orbit carrying the subsatellite and the tether. When a scientific experiment is to be carried out, the subsatellite equipped with the instruments and the tether are deployed to the required altitude using a reel mechanism placed on the shuttle. The experiment is conducted during the station-keeping stage. Then follows the retrieval to bring the subsatellite back into the shuttle.

In Figure 2.1, body A represents the shuttle while body B is the subsatellite, having masses M_a and M_b, respectively. The tether has a mass ρ_c per unit length and an instantaneous mass of the deployed tether $M_c(=\rho_c \ell_0)$. The instantaneous center of mass S can be located with respect to the center of the earth E by the radial distance R_0, the inclination angle i of the orbital plane to the equatorial plane, argument of the perigee θ_0 and true anomaly θ. Body B is attached to the tether at pont P_b and body A at point P_a through which the tether is deployed or retrieved. A and B are the mass centers of bodies A and B, respectively.

Coordinate systems, X, Y, Z; x_0, y_0, z_0 and x_c, y_c, z_c are introduced to describe the motion. The last two coordinate systems are rotating coordinate systems, while the first is an inertial system having its origin at the center of the earth. The set of coordinate axes x_0, y_0, z_0 located at origin S is so oriented that x_0-axis is along the orbit normal, y_0-axis concides with the local vertical while z_0-axis completes the triad. The unit vectors $\vec{i}_0$, $\vec{j}_0$ and $\vec{k}_0$ are along the x_0, y_0 and z_0 axes, respectively. The orientation of the axes x_c, y_c, z_c (y_c coinciding with the nominal tetherline) are defined by only two rotations α and γ, implying an assumption that the rotation about the axis of the tether is ignored. At first, rotation α is given about x_0-axis resulting in x_c', y_c', z_c' and then rotation γ is applied about z_c'-axis yielding axes x_c, y_c, z_c. α is called the pitch angle while γ is the roll angle. The unit vectors $\vec{i}_c$, $\vec{j}_c$ and $\vec{k}_c$ are along x_c, y_c, z_c axes, respectively.

The flexibility of the tether must be taken into account since the tether is very long and thin. It has longitudinal as well as transverse displacements due to the gravity gradient, atmospheric drag and Coriolis forces during deployment or retrieval. The transverse vibrational displacements along x_c and z_c (nominally perpendicular and in the orbital plane, respectively) are denoted by u and w, while the longitudinal vibrational displacement is represented by v. The displacements u, v, w are functions of both time as well as space coordinate y_c and form the elastic displacement vector $\vec{u}$.

One must distinguish between the undeformed and deformed tether length. Here ℓ_0 (associated with "material coordinate") denotes the length of the undeformed tether while ℓ_s is the length of the deformed tether from point P_a to P_b measured along the curved tetherline. Obviously, if there is no transverse vibration in the tether, ℓ_s will be measured along a straight line, but it is still not equal to ℓ_0, since there is a longitudinal strain in the tether.

For given α and γ, the line connecting the shuttle and the subsatellite can be defined uniquely with respect to S; with u, v and w, the position of any arbitrary point of the tether can be determined uniquely with respect to this line. Since u, v, w are measured from the already rotated tetherline, the small displacement assumption would be reasonable.

With this understanding of the geometry, it can be seen that there are three kinds of motion:

(i) The entire system rotates around the earth (orbital dynamics);

(ii) The subsatellite rotates around the center of mass of the system or that of the space shuttle because the system center of mass is alomst coincident with that of the space shuttle (attitude dynamics);

(iii) The tether vibrates longitudinally and transversely (structural dynamics).

These three kinds of motion are coupled to each other. The last two motions affect the first (orbital motion) only slightly [10]. Hence the orbit could be calculated separately without any significant loss of accuracy. It is assumed here to be Keplerian. As for the rotational and vibrational motions, they are certainly affected by the orbital motion and are more complicated. The equations governing these motions are derived in this Chapter.

2.2 BASIC ASSUMPTIONS

Some assumptions based on the physical insight to the problem are necessary to get a reasonable dynamical model. Without such assumptions, the mathematical model becomes very complicated; but on the other hand, if the assumptions are not quite correct or are overly simplifying, the mathematical model will not represent the real situations. For example, in the early stage of research on this subject, some investigators neglected the out-of-plane rotation of the system and the vibrations of the tether. Corresponding mathematical models of the SSTS system are oversimplified and do not describe the dynamics of real systems very well. The most important thing is to grasp the significant factors and eliminate the trivial ones.

The following basic assumptions are made in this thesis to obtain a reasonable model of the system:

(i) Orbital motion is assumed to be unaffected by the attitude motions and vibrations of the tether and is maintained Keplerian. This assumption allows separate calculation of orbital motion.

(ii) The masses of the subsatellite and the tether are much smaller than that of the shuttle.

The shuttle has a mass of $M_a = 0(10^4 - 10^5\ \mathrm{Kg})$. The mass of the subsatellite M_b is $0(10^2\ \mathrm{Kg})$. As for the tether, its mass is variable depending on the length; for a 100 Km tether, the mass M_c is $0(10^2\ \mathrm{Kg})$ and less for smaller tethers. Thus the assumption cited above is reasonable. The consequence of this assumption is that terms like M_bM_c, M_b^2, M_c^2, can be ignored compared to M_a^2 making the algebra significantly simpler, as will be seen later.

(iii) Since the sizes of the shuttle and the subsatellite are much smaller than the length of the tether, both the shuttle and the subsatellite are regarded as point masses.

When the length of the tether is small during the terminal phase of retrieval or initial phase of deployment, the assumption is not valid; however, it holds good for the major part of the mission.

(iv) Vibrations of the tether are small in amplitude compared to the instantaneous length. In spite of this assumption, the nonlinearity in the strain-displacement relation is taken into account. The reason for retaining this nonlinearity is described later.

(v) The effects of solar radiation pressure and the earth's electromagnetic field are neglected since they are small compared with the earth's gravity gradient. The only environmental force taken into account is the atmospheric drag (apart from gravity). The density of air is assumed to vary exponentially with altitude.

(vi) Perturbing forces due to attractions of the sun and the moon are ignored. The effect of a nonspherical earth on the earth's gravity gradient is ignored as well.

The present dynamical model includes the following features:

(i) <u>3-D rotations</u> which are <u>allowed to be large</u>;

(ii) the tether is <u>not massless</u> and <u>not inextensible</u>; the material damping of the tether is included;

(iii) <u>both longitudinal and transverse vibrations</u> of the tether are considered;

(iv) <u>variation of longitudinal strain along the tether</u> is taken into account; nonlinearity in the relation between longitudinal strain and vibrational displacements (i.e., geometric nonlinearity) is retained;

(v) aerodynamic drag is calculated considering the oblateness of the earth, rotation of the atmosphere and eccentricity of the orbit.

2.3 KINEMATICS OF THE SYSTEM

Let the position vectors of the centers of mass of the shuttle and the subsatellite from the center of mass S of the entire system be denoted by $\vec{R}_a$ and $\vec{R}_b$, respectively (refer to Figure 2.1). Furthermore, let $\vec{R}_c$ denote the position vector of any arbitrary point on the tether relative to S. These position vectors can be expressed in terms of the rotations α and γ of the tether and vibrational displacements u, v and w.

Since S is the center of mass of the system, we have

$$M_a\vec{R}_a + M_b\vec{R}_b + \int_{M_c} \vec{R}_c \, dm = 0 \tag{2.3.1}$$

From geometric considerations, the following relation holds:

$$\vec{R}_a + \vec{AB} - \vec{R}_b = 0 \tag{2.3.2}$$

where $\vec{AB}$ is the vector from the center of mass of the shuttle to that of the subsatellite. Since the tether has some elongation, the magnitude of $\vec{AB}$ is larger than the undeformed length ℓ_0 of the tether.

The term $\int_{M_c} \vec{R}_c \, dm$ in (2.3.1) and $\vec{AB}$ in (2.3.2) need to be expressed in terms of the deformations of the tether. An arbitrary point P on the unstretched tether moves to point Q after deformation (Fig. 2.2). This can be expressed as

$$P(0,\ y_c,\ 0) \rightarrow Q(u(y_c,\ t)\ ,\ [y_c + v(y_c,\ t)]\ ,\\ w(y_c,\ t)) \tag{2.3.3}$$

In (2.3.3), it is clear that y_c is used to denote position along the unstretched tether, i.e., y_c is a material coordinate. We have,

$$y_c \in (0,\ \ell_0(t)) \tag{2.3.4}$$

where ℓ_0 is the instantaneous unstretched length of the tether. During deployment or retrieval, ℓ_0 changes, thus it is a function of time. With the above geometric understanding, $\vec{AB}$ may be written as

$$\vec{AB} = \vec{\ell}_j = [\ell_0(t) + v(\ell_0,\ t)]\vec{j}_c \tag{2.3.5}$$

Let $\vec{r}_c$ denote the position vector of any arbitrary point of the tether from the point A. Thus, $\vec{r}_c$ is related to u, v, w as

$$\vec{r}_c = u(y_c,\ t)\vec{i}_c + [y_c + v(y_c,t)]\vec{j}_c + w(y_c,\ t)\vec{k}_c\ , \tag{2.3.6}$$

and

$$\vec{R}_c = \vec{r}_c + \vec{R}_a \tag{2.3.7}$$

The integral $\int_{M_c} \vec{R}_c dm$ is then given by

$$\int_{M_c} \vec{R}_c dm = \int_0^{\ell_0} (\vec{R}_a + \vec{r}_c)\rho_c dy_c = M_c\vec{R}_a + \rho_c \int_0^{\ell_0} \vec{r}_c dy_c \tag{2.3.8}$$

Substituting (2.3.5) and (2.3.8) into (2.3.2) and (2.3.1), respectively, we have,

$$(M_c + M_a)\vec{R}_a + M_b\vec{R}_b = -\rho_c \int_0^{\ell_0} \vec{r}_c dy_c \tag{2.3.9}$$

and

$$\vec{R}_a - \vec{R}_b = -\vec{\ell}_j \tag{2.3.10}$$

It may be noted that the terms on the right hand side of equations (2.3.9) and (2.3.10) involve tether deformations. $\vec{R}_a$, $\vec{R}_b$ can be solved from these two equations as

$$\vec{R}_a = [-1/(M_a + M_b + M_c)][\rho_c \int_0^{\ell_0} \vec{r}_c dy_c + M_b\vec{\ell}_j] \tag{2.3.11}$$

$$\vec{R}_b = [-1/(M_a + M_a + M_c)]\ [-(M_c + M_a)\vec{\ell}_j + \rho_c \int_0^{\ell_0} \vec{r}_c dy_c] \tag{2.3.12}$$

Notice that

$$M_a + M_b + M_c = M = \text{constant} \quad , \tag{2.3.13}$$

where M is the mass of the whole system. During deployment or retireval, M_c and M_a are variable; however, the total mass is conserved. Putting (2.3.13) into (2.3.11) and (2.3.12), we have

$$\vec{R}_a = (-1/M)[\rho_c \int_0^{\ell_0} \vec{r}_c dy_c + M_b\vec{\ell}_j] \tag{2.3.14}$$

$$\vec{R}_b = (-1/M)[-(M - M_b)\vec{\ell}_j + \rho_c \int_0^{\ell_0} \vec{r}_c dy_c] \tag{2.3.15}$$

where $\vec{r}_c$ and $\vec{\ell}_j$ are given by (2.3.6) and (2.3.5), respectively. Note that $\vec{R}_c$ can be obtained from (2.3.7) and (2.3.14).

$\vec{R}_a$, $\vec{R}_b$ and $\vec{R}_c$ are related to u, v, w as well as rotations α and γ. The latter is not directly evident; however, $\vec{\ell}_j$ is along $\vec{j}_c$ direction, and the orientation of $\vec{j}_c$ is determined by rotations α and γ.

2.4 KINETIC ENERGY OF THE SYSTEM

The total kinetic energy of the system T consists of three parts, i.e.,

$$T = T_a + T_b + T_c \tag{2.4.1}$$

where T_a, T_b and T_c are the kinetic energy of the shuttle, the subsatellite and the tether, respectively. They are calculated separately as follows.

(i) Since the shuttle is regarded as a point mass (see the basic assumptions), T_a may be expressed as

$$\begin{aligned} T_a &= (1/2)M_a(\dot{\vec{R}}_0 + \dot{\vec{R}}_a)\cdot(\dot{\vec{R}}_0 + \dot{\vec{R}}_a) \\ &= (1/2)M_a(\dot{\vec{R}}_0\cdot\dot{\vec{R}}_0 + 2\dot{\vec{R}}_0\cdot\dot{\vec{R}}_a + \dot{\vec{R}}_a\cdot\dot{\vec{R}}_a) \quad , \end{aligned} \tag{2.4.2}$$

where $\vec{R}_0$ is the radius vector of the center of mass S of the system from the center of the earth and the dot represents differentiation with respect to time.

(ii) Similar to T_a, T_b is given by

$$\begin{aligned} T_b &= (1/2)M_b(\dot{\vec{R}}_0 + \dot{\vec{R}}_b)\cdot(\dot{\vec{R}}_0 + \dot{\vec{R}}_b) \\ &= (1/2)M_b(\dot{\vec{R}}_0\cdot\dot{\vec{R}}_0 + 2\dot{\vec{R}}_0\cdot\dot{\vec{R}}_b + \dot{\vec{R}}_b\cdot\dot{\vec{R}}_b) \end{aligned} \tag{2.4.3}$$

(iii) The tether is a continuous body and its kinetic energy involves integration over the distributed mass of the tether. It is given by

$$T_c = (1/2)\int_{M_c} (\dot{\vec{R}}_0 + \dot{\vec{R}}_c)\cdot(\dot{\vec{R}}_0 + \dot{\vec{R}}_c)dm$$

$$= (1/2)M_c\dot{\vec{R}}_0\cdot\dot{\vec{R}}_0 + \dot{\vec{R}}_0\cdot\int_{M_c}\dot{\vec{R}}_c dm + (1/2)\int_{M_c}\dot{\vec{R}}_c\cdot\dot{\vec{R}}_c dm \qquad (2.4.4)$$

Substituting (2.4.2 - 2.4.4) into (2.4.1), we get

$$T = (1/2)M\dot{\vec{R}}_0\cdot\dot{\vec{R}}_0 + \dot{\vec{R}}_0\cdot(M_a\dot{\vec{R}}_a + M_b\dot{\vec{R}}_b + \int_{M_c}\dot{\vec{R}}_c dm)$$

$$+ (1/2)M_a\dot{\vec{R}}_a\cdot\dot{\vec{R}}_a + (1/2)M_b\dot{\vec{R}}_b\cdot\dot{\vec{R}}_b + (1/2)\int_{M_c}\dot{\vec{R}}_c\cdot\dot{\vec{R}}_c dm\ . \qquad (2.4.5)$$

Using (2.3.7), T can be written as

$$T = (1/2)M\dot{\vec{R}}_0\cdot\dot{\vec{R}}_0 + \dot{\vec{R}}_0\cdot[(M_a + M_c)\dot{\vec{R}}_a + M_b\dot{\vec{R}}_b + \int_{M_c}\dot{\vec{r}}_c dm]$$

$$+ (1/2)(M_a + M_c)\dot{\vec{R}}_a\cdot\dot{\vec{R}}_a + (1/2)M_b\dot{\vec{R}}_b\cdot\dot{\vec{R}}_b + (1/2)\int_{M_c}\dot{\vec{r}}_c\cdot\dot{\vec{r}}_c dm$$

$$+ \dot{\vec{R}}_a\cdot\int_{M_c}\dot{\vec{r}}_c dm \qquad (2.4.6)$$

It is shown in Appendix A that the second term is equal to zero.* Hence, the kinetic energy can be rewritten as

* Derivation of this result from (2.3.1) is not trivial since M_a and M_b vary with time.

$$T = T_{orb} + T_{nonorb} \tag{2.4.7}$$

where

$$T_{orb} = (1/2)M\dot{\vec{R}}_0 \cdot \dot{\vec{R}}_0 \tag{2.4.8}$$

and

$$T_{nonorb} = (1/2)(M_a + M_c)\dot{\vec{R}}_a \cdot \dot{\vec{R}}_a + (1/2)M_b\dot{\vec{R}}_b \cdot \dot{\vec{R}}_b + (1/2)\int \dot{\vec{r}}_c \cdot \dot{\vec{r}}_c dm$$

$$+ \dot{\vec{R}}_a \cdot \int_{M_c} \dot{\vec{r}}_c dm \tag{2.4.9}$$

Here, T_{orb} is the orbital kinetic energy while T_{nonorb} is the remaining part of the kinetic energy associated with rotational motion of the system and vibrations of the tether. T_{nonorb} is much smaller than T_{orb} and does not affect the orbital motion. Hence, the orbital motion may be calculated separately.

T_{nonorb} can be developed further. Differentiating (2.3.14) and (2.3.15) and using equation (A.5)

$$\dot{\vec{R}}_a = (-1/M)[\rho_c \frac{d}{dt}\int_0^{\ell_0} \vec{r}_c dy_c + M_b\dot{\vec{\ell}}_j]$$

$$= (-1/M)[\rho_c \int_0^{\ell_0} \dot{\vec{r}}_c dy_c + M_b\dot{\vec{\ell}}_j] \tag{2.4.10}$$

and

$$\dot{\vec{R}}_b = (-1/M)[\rho_c \int_0^{\ell_0} \dot{\vec{r}}_c dy_c - (M - M_b)\dot{\vec{\ell}}_j] \tag{2.4.11}$$

Here

$$(\dot{\vec{r}}_c) = (\frac{\partial}{\partial t} + \dot{\ell}_0 \frac{\partial}{\partial y_c})(\vec{r}_c) \tag{2.4.12}$$

which takes into account the fact that the tether may be moving axially. It is similar to the convective derivative that is encountered in fluid mechanics. Substituting (2.4.10) and (2.4.11) into (2.4.9) and using (2.3.13), we get

$$T_{nonorb} = (1/2)(M_b/M)(M_a + M_c)\dot{\vec{\ell}}_j\cdot\dot{\vec{\ell}}_j - (M_b/M)\cdot\rho_c\dot{\vec{\ell}}_j\cdot\int_0^{\ell_0}\dot{\vec{r}}_c dy_c$$

$$+ (1/2)\rho_c\int_0^{\ell_0}\dot{\vec{r}}_c\cdot\dot{\vec{r}}_c dy_c \qquad (2.4.13)$$

Equation (2.4.13) is valid for any combination of values of M_a, M_b and M_c. The magnitudes of M_a, M_b and M_c are of the same order in the case of two space stations linked by a tether, for example. However, in the present SSTS system, M_a is much larger than M_b and M_c (see Section 2.2). Thus from (2.4.13), we have

$$T_{nonorb} = (1/2)M_b\dot{\vec{\ell}}_j\cdot\dot{\vec{\ell}}_j - (1/2)(M_b^2/M)\dot{\vec{\ell}}_j\cdot\dot{\vec{\ell}}_j$$

$$- (M_bM_c/M)\dot{\vec{\ell}}_j\cdot(1/\ell_0)\int_0^{\ell_0}\dot{\vec{r}}_c dy_c + (1/2)M_c(1/\ell_0)\int_0^{\ell_0}\dot{\vec{r}}_c\cdot\dot{\vec{r}}_c dy_c$$

$$\approx (1/2)M_b\dot{\vec{\ell}}_j\cdot\dot{\vec{\ell}}_j + (1/2)M_c(1/\ell_0)\int_0^{\ell_0}\dot{\vec{r}}_c\cdot\dot{\vec{r}}_c dy_c \qquad (2.4.14)$$

ignoring second order terms involving M_b and M_c. Equation (2.4.14) is quite neat in vector form and has a very clear physical meaning. The first term represents the kinetic energy of the subsatellite, while the second is the kinetic energy of the tether.

Since $\vec{\ell}_j$ and $\vec{r}_c$ are related to ℓ_0, u, v and w while $\dot{\vec{\ell}}_j$, $\dot{\vec{r}}_c$ are absolute velocities with respect to the inertial coordinate system X, Y, Z thus dependent on rotations α and γ as well, T_{nonorb} is a function of

α, γ, ℓ_0, u, v, w and their derivatives. The explicit form will be developed later in Section 2.7.

2.5 STRAIN ENERGY IN THE TETHER

The tether is very long and thin thus flexible. When it deforms, some strain energy is stored in the tether. In the linear elastic theory of strings, it is assumed that the initial tension in the string is large enough and the transverse displacements cause negligible change in this tension. But, in the present case, the tension in the tether is not large enough all the time. When the tether is long, gravity gradient and centrifugal force are large enough to cause reasonably large tension in the tether; however, when the tether becomes shorter and shorter during retrieval of the subsatellite, these forces weaken since they are proportional to the length ℓ_0 in general. In an extreme case when ℓ_0 approaches zero, the tension tends to zero. Therefore we cannot neglect transverse displacement induced changes in the tension. This implies that the longitudinal vibration is strongly coupled with the transverse vibrations [31] during the terminal stage of retrieval.

Consider an infinitesimal element PQ having an undeformed length dy_c (see Fig. 2.2). The strain in the element is given by

$$\varepsilon = \frac{ds-dy_c}{dy_c} = \{\{[dy_c+v(y_c+dy_c,t)-v(y_c,t)]^2+[u(y_c+dy_c,t)-u(y_c,t)]^2$$

$$+[w(y_c+dy_c,t)-w(y_c,t)]^2\}^{1/2}-dy_c\}/dy_c \approx \frac{\partial v}{\partial y_c} + (1/2)[(\frac{\partial u}{\partial y_c})^2$$

$$+(\frac{\partial w}{\partial y_c})^2] = \varepsilon_1 + \varepsilon_2 \qquad (2.5.1)$$

Here

$$\varepsilon_1 = \frac{\partial v}{\partial y_c} = \text{strain caused by longitudinal displacement } v$$

$$\varepsilon_2 = (1/2)[(\frac{\partial u}{\partial y_c})^2+(\frac{\partial w}{\partial y_c})^2] = \text{extensional strain caused by transverse displacements } u \text{ and } w.$$

The tension at point P is $EA\varepsilon$. If ε_1 is very large compared to ε_2, the tension can be regarded as $EA\varepsilon_1$, if not, it is $EA(\varepsilon_1 + \varepsilon_2)$. When the tether is long, $\varepsilon_1 = 0(10^{-2}\text{-}10^{-3})$ and $\varepsilon_2 = 0(10^{-4})$, i.e., ε_1 is reasonably large and dominant; when the tether is shorter than 1 Km, $\varepsilon_1 = 0(10^{-5}\text{-}10^{-6})$ while ε_2 could be large if the transverse vibrations are not damped out.

The strain energy in the tether is given by

$$P_e = (1/2)EA \int_0^{\ell_0} \varepsilon^2 dy_c$$

$$= (1/2)EA \int_0^{\ell_0} \{ \frac{\partial v}{\partial y_c} + (1/2)[(\frac{\partial u}{\partial y_c})^2 + (\frac{\partial w}{\partial y_c})^2]\}^2 dy_c \qquad (2.5.2)$$

2.6 MATERIAL DAMPING

As the tether is deformed, usually some energy is dissipated in the deforming process, which can be accounted for through material damping. The mechanism is quite complex and may be explained adequately only by using micromechanics. Irreversible sliding of the dislocations inside the material dissipates energy [34]. Hence, the relation between strain and stress is not exactly elastic. There is some hysteresis phenomenon when the material is subject to vibration. The area enclosed by the hysteresis curve indicates the energy dissipation which turns to heat. In engineering applications, it is usually accounted for by introducing a material damping or structural damping coefficient which is determined by experiments [33]. One can introduce an equivalent complex Young's modulus

$$E^* = E_1 + iE_2 \tag{2.6.1}$$

where i is the square root of -1. Then,

$$\sigma = E^*\varepsilon = (E_1 + iE_2)\varepsilon = E_1(1 + i\eta)\varepsilon \tag{2.6.2}$$

where usually

$$\eta = E_2/E_1 << 1 \quad . \tag{2.6.3}$$

If ε is harmonic with frequency ω_0,

$$i\varepsilon = \dot{\varepsilon}/\omega_0$$

and (2.6.2) becomes

$$\sigma = E_1[\varepsilon + (\eta/\omega_0)\dot{\varepsilon}] \tag{2.6.4}$$

The coefficient η is often assumed to be a constant, although it somewhat varies with frequency as well as other factors such as the stress level, etc. For metals, in the environment of 1g, η is between 0.01 ~ 0.001. In the space environment, experiments have shown that the damping increases. In the calculations in this thesis η was chosen as 0.005. This is a conservative estimation.

2.7 GRAVITATIONAL POTENTIAL ENERGY

The total gravitational potential energy of the system consists of three parts; that due to the shuttle, subsatellite and the tether, respectively, i.e.,

$$V_G = V_{Ga} + V_{Gb} + V_{Gc} \tag{2.7.1}$$

From the definition of gravitational potential energy,

$$V_{Ga} = \frac{-\mu M_a}{|\vec{R}_0 + \vec{R}_a|} \tag{2.7.2}$$

$$V_{Gb} = \frac{-\mu M_a}{|\vec{R}_0 + \vec{R}_b|} \tag{2.7.3}$$

$$V_{Gc} = - \int_0^{\ell_0} \frac{\mu \rho_c dy_c}{|\vec{R}_0 + \vec{R}_c|} \tag{2.7.4}$$

where $\mu = G \cdot M_{earth}$, while G is the universal gravitational constant and M_{earth} is the mass of the earth. Here the end-bodies are assumed to be points and the earth is assumed to be spherical.

Equation (2.7.2) may be expanded as

$$V_{Ga} = \frac{-\mu M_a}{\sqrt{(\vec{R}_0 + \vec{R}_a)\cdot(\vec{R}_0 + \vec{R}_a)}} = -\mu M_a \, (\vec{R}_0\cdot\vec{R}_0 + 2\vec{R}_0\cdot\vec{R}_a + \vec{R}_a\cdot\vec{R}_b)^{-1/2}$$

$$= -\mu \frac{M_a}{R_0} [1 - \frac{1}{R_0^2} \vec{R}_0\cdot\vec{R}_a - \frac{\vec{R}_a\cdot\vec{R}_a}{2R_0^2} + \frac{3}{8} (\frac{2\vec{R}_0\cdot\vec{R}_a}{R_0^2}) + 0(\frac{|\vec{R}_a|^3}{R_0^3})]$$

Ignoring higher than third order terms, we have

$$V_{Ga} \cong -\mu \frac{M_a}{R_0} [1 - \frac{1}{R_0^2} \vec{R}_0 \cdot \vec{R}_a - \frac{\vec{R}_a \cdot \vec{R}_a}{2R_0^2} + \frac{3}{8} (\frac{2\vec{R}_0 \cdot \vec{R}_a}{R_0^2})^2] \tag{2.7.5}$$

Similarly,

$$V_{Gb} \cong -\mu \frac{M_b}{R_0} [1 - \frac{1}{R_0^2} \vec{R}_0 \cdot \vec{R}_b - \frac{\vec{R}_b \cdot \vec{R}_b}{2R_0^2} + \frac{3}{8} (\frac{2\vec{R}_0 \cdot \vec{R}_b}{R_0^2})^2] \tag{2.7.6}$$

and

$$V_{Gc} \cong - \frac{\mu\rho_c}{R_0} [\ell_0 - \frac{1}{R_0^2} \vec{R}_0 \cdot \int_0^{\ell_0} \vec{R}_c dy_c - \frac{1}{2R_0^2} \int_0^{\ell_0} \vec{R}_c \cdot \vec{R}_c dy_c + \frac{3}{2} \int_0^{\ell_0} R_0^{-4} (\vec{R}_0 \cdot \vec{R}_c)^2 dy_c \quad \ldots \tag{2.7.7}$$

Now, using (2.7.1) and (2.3.1), we get

$$V_G = -\mu \frac{M}{R_0} + \frac{\mu}{2R_0^3} \{M_a[\vec{R}_a \cdot \vec{R}_a - 3(\vec{J}_0 \cdot \vec{R}_a)^2] + M_b[\vec{R}_b \cdot \vec{R}_b - 3(\vec{J}_0 \cdot \vec{R}_b)^2]$$

$$+ \rho_c \int_0^{\ell_0} [\vec{R}_c \cdot \vec{R}_c - 3(\vec{J}_0 \cdot \vec{R}_c)^2] dy_c\} \tag{2.7.8}$$

The potential energy V, which includes V_G and P_E, can be written as

$$V = V_{orb} + V_{nonorb}$$

Here

$$V_{orb} = -\mu \frac{M}{R_0} \tag{2.7.9}$$

and is relevant to orbital motion. On the other hand,

$$V_{nonorb} = \frac{\mu}{2R_0^3}\{M_a[(R_a^2 - 3(\vec{J}_0 \cdot \vec{R}_a)] + M_b[R_b^2 - 3(\vec{J}_0 \cdot \vec{R}_b)]$$

$$+ \rho_c \int_0^{\ell_0} [R_c^2 - 3(\vec{J}_0 \cdot \vec{R}_c)]dy_c\}$$

$$+ \frac{1}{2} EA \int_0^{\ell_0} \{\frac{\partial v}{\partial y_c} + [(\frac{\partial u}{\partial y_c})^2 + (\frac{\partial w}{\partial y_c})^2]\}^2 dy_c \qquad (2.7.10)$$

and is associated with rotational and vibrational motions. Obviously, V_{orb} is much greater than V_{nonorb} since $V_{orb}/V_{nonorb} = O(R_0^2/\ell_0^2)$.

2.8 ORBITAL MOTION

The system has the kinetic energy T_{orb} and the gravitational potential energy V_{orb}, if other much smaller terms associated with the attitude motion of the system and vibrations of the tether are ignored. With this, the orbital motion can be calculated separately and can be shown to be Keplerian. A Keplerian orbit is a planar orbit and is characterized by [38]

$$\dot{\theta} = h/R_0^2 \qquad (2.8.1)$$

and

$$R_0 = h^2/\{\mu[1 + e \cos \theta]\} \qquad (2.8.2)$$

where h is a constant, representing angular momentum per unit mass of the system and e is the eccentricity of the orbit. R_0, θ and θ_0 are as defined earlier. Equation (2.8.2) represents an ellipse. When e is zero, the orbit is circular.

It can be shown that the mean orbital rate is given by

$$\omega = [\mu/a^3]^{1/2} \tag{2.8.3}$$

where a is the semi-major axis of the orbit and is given by

$$a = h^2/[\mu(1 - e^2)] \tag{2.8.4}$$

Equation (2.8.3) represents what is known as Kepler's third law. Using (2.8.1) - (2.8.4), it can be shown that

$$\dot{\theta} = \omega(1 - e^2)^{-3/2} \cdot [1 + e \cos \theta]^2 \tag{2.8.5}$$

$$R_0 = [\mu/\omega^2]^{1/3}(1 - e^2)/[1 + e \cos \theta] \tag{2.8.6}$$

Relations (2.8.5) and (2.8.6) would prove useful later. If e is nonzero, the instantaneous orbital rotational velocity $\dot{\theta}$ varies with θ, oscillating around ω.

In this thesis, for convenience, a parameter H is used to specify the orbit rather than the semi-major axis a or mean orbital rate ω of the orbit. The parameter H is related to the semi-major axis a by

$$H = a - (1/2)(a_0 + b_0) \tag{2.8.7}$$

where a_0 and b_0 are the semi-major and semi-minor axes of the oblate earth. Since a_0 and b_0 are constants, specification of H is equivalent to specifying a. Clearly, H is equal to the altitude of the orbit if it is circular and the earth is assumed spherical. However, if the orbit is not circular, the altitude above the earth's surface varies and is not equal to H.

2.9 EXPLICIT EXPRESSIONS FOR V_{nonorb} and T_{nonorb}

Kinetic energy T_{nonorb} and potential energy V_{nonorb} have been obtained in vector form in (2.7.10) and (2.4.14), respectively. In this section they will be expressed explicitly in terms of rotations and vibrational displacements as

$$V_{nonorb} = V_{nonorb}\ (\alpha, \gamma, u, v, w, \ell_0) \tag{2.9.1}$$

and

$$T_{nonorb} = T_{nonorb}\ (\alpha, \gamma, u, v, w, \ell_0, \dot{\alpha}, \dot{\gamma}, \dot{u}, \dot{v}, \dot{w}, \dot{\ell}_0) \tag{2.9.2}$$

so that a set of equations of motion can be obtained through the extended Hamilton's principle.

Let us introduce notations $\bar{u}$, $\bar{v}$, $\bar{w}$ as follows:

$$\bar{u}(t) = \frac{1}{\ell_0(t)} \int_0^{\ell_0(t)} u(y_c, t) dy_c \tag{2.9.3}$$

$$\bar{v}(t) = \frac{1}{\ell_0(t)} \int_0^{\ell_0} v(y_c, t) dy_c \tag{2.9.4}$$

$$\bar{w}(t) = \frac{1}{\ell_0(t)} \int_0^{\ell_0} w(y_c, t) dy_c \tag{2.9.5}$$

Furthermore, the transformation relating the unit vectors of x_0, y_0, z_0 and x_c, y_c, z_c systems can be expressed as

$$\begin{Bmatrix} \vec{i}_0 \\ \vec{j}_0 \\ \vec{k}_0 \end{Bmatrix} = \begin{bmatrix} 1, & 0, & 0 \\ 0, & c\alpha, & -s\alpha \\ 0, & s\alpha, & c\alpha \end{bmatrix} \begin{bmatrix} c\gamma, & -s\gamma, & 0 \\ s\gamma, & c\gamma, & 0 \\ 0 & 0, & 1 \end{bmatrix} \begin{Bmatrix} \vec{i}_c \\ \vec{j}_c \\ \vec{k}_c \end{Bmatrix} \tag{2.9.6}$$

where $c\alpha = \cos\alpha$, $s\alpha = \sin\alpha$, etc., are used for abbreviation. With this, V_{nonorb} can be expressed as

$$V_{nonorb} = \frac{1}{2} EA \int_0^{\ell_0} \{\frac{\partial v}{\partial y_c} + \frac{1}{2} [(\frac{\partial u}{\partial y_c})^2 + (\frac{\partial w}{\partial y_c})^2]\}^2 dy_c$$

$$+ \frac{1}{2} [V_1 + V_2 + V_3] \tag{2.9.7}$$

where

$$V_1 = (\mu/R_0{}^3)(M_a/M^2)\{M_c{}^2\overline{u}^2 + [M_c(\frac{\ell_0}{2} + \overline{v}) + M_b(\ell_0 + v(\ell_0, t))]^2$$

$$+ M_c{}^2\overline{w}^2\} - 3M_a\{-(M_c/M)[c\alpha s\alpha\overline{u} + c\alpha c\alpha(\frac{1}{2}\ell_0 + \overline{v}) - s\alpha\overline{w}]$$

$$- \frac{M_b}{M} c\alpha c\gamma[\ell_0 + v(\ell_0, t)]\}^2 \quad . \tag{2.9.8}$$

V_2 and V_3 are similar to V_1 and are not listed here for brevity. They are given in Appendix B along with their derivations.

To simplify the lengthy expressions for V_1, V_2 and V_3, the basic assumptions defined earlier are used, i.e.,

(i) $M_a >> M_b, M_c$

(ii) $u, v, w << \ell_0$

With these assumptions

$$V_{nonorb} = \frac{EA}{2} \int_0^{\ell_0} \{\frac{\partial v}{\partial y_c} + \frac{1}{2} [(\frac{\partial u}{\partial y_c})^2 + (\frac{\partial w}{\partial y_c})^2]\}^2 dy_c$$

$$+ V_{\alpha\gamma} + V_{uvw} \tag{2.9.9}$$

where

$$V\alpha\gamma = \frac{1}{2}[\mu/R_0{}^3][M_b + \frac{1}{3}M_c](1 - 3\, c^2\alpha c^2\gamma)\ell_0{}^2 \qquad (2.9.10)$$

$$V_{uvw} = \frac{1}{2}[\mu/R_0{}^3]\{(1-3c^2\alpha c^2\gamma)[M_b\ell_0 v(\ell_0,\, t)$$

$$+ M_c \frac{1}{\ell_0}\int_0^{\ell_0} y_c v dy_c] - 3M_c[\frac{1}{\ell_0}\int_0^{\ell_0} c\alpha c\gamma(uc\alpha - ws\alpha)y_c dy_c]\} \qquad (2.9.11)$$

From the above, $V_{uvw}/V_{\alpha\gamma} = O([u,\, v,\, w]/\ell_0)$, thus $V_{\alpha\gamma} >> V_{uvw}$, i.e., u, v, w have a small contribution to the gravitational potential energy. This is expected since vibrations are small in amplitude. $V_{\alpha\gamma}$ depends on α, γ and ℓ_0 only while V_{uvw} is dependent on α, γ, ℓ_0 as well as the vibrational displacements u, v, w. If there are no vibrations and stretching of the tether, V_{uvw} is zero. Otherwise, we have both V_{uvw} and the strain energy term. In the simplifying procedure, care must be taken to retain the term V_{uvw} by using appropriate order of magnitude analysis, since we want α, γ equations as well as the vibrational equations both to a reasonable degree of accuracy.

In order to express T_{nonorb} given by (2.4.14) as a function of rotations and vibrational displacements, $\dot{\vec{\ell}}_j$ and $\dot{\vec{r}}_c$ must be expanded explicitly. Using (2.3.5) one obtains

$$\dot{\vec{\ell}}_j = [\ell_0 + v(\ell_0,\, t)]^{\bullet}\vec{j}_c + \vec{\omega}_c \times \vec{\ell}_j \qquad (2.9.12)$$

where $\vec{\omega}_c$ is the angular velocity of x_c, y_c, z_c coordinate system. The components of $\vec{\omega}_c$ along x_c, y_c, z_c directions can be written in matrix form

$$\begin{Bmatrix} \omega_{xc} \\ \omega_{yc} \\ \omega_{zc} \end{Bmatrix} = \begin{bmatrix} c\gamma, & s\gamma, & 0 \\ -s\gamma, & c\gamma, & 0 \\ 0, & 0, & 1 \end{bmatrix} \begin{bmatrix} 1, & 0, & 0 \\ 0, & c\alpha, & s\alpha \\ 0, & -s\alpha, & c\alpha \end{bmatrix} \begin{Bmatrix} (\dot{\theta}+\dot{\alpha}) \\ 0 \\ 0 \end{Bmatrix} + \begin{bmatrix} c\gamma, & s\gamma, & 0 \\ -s\gamma, & c\gamma, & 0 \\ 0, & 0, & 1 \end{bmatrix} \begin{Bmatrix} 0 \\ 0 \\ \dot{\gamma} \end{Bmatrix}$$

$$= \begin{Bmatrix} (\dot{\theta}+\dot{\alpha})c\gamma \\ -(\dot{\theta}+\dot{\alpha})s\gamma \\ \dot{\gamma} \end{Bmatrix} \tag{2.9.13}$$

Substituting (2.9.13) into (2.9.12), we get

$$\dot{\vec{\ell}}_j = [-[\ell_0 + v(\ell_0, t)]\dot{\gamma}, \; \dot{\ell}_0(1 + \frac{\partial v}{\partial y_c}(\ell_0, t)) + \frac{\partial v(\ell_0, t)}{\partial t} \; ,$$

$$[\ell_0 + v(\ell_0, t)](\dot{\theta} + \dot{\alpha})c\gamma] \begin{Bmatrix} \vec{i}_c \\ \vec{j}_c \\ \vec{k}_c \end{Bmatrix} \tag{2.9.14}$$

Similarly, using (2.3.6),

$$\dot{\vec{r}}_c = \{\frac{\partial u}{\partial t} + \ell_0 \frac{\partial u}{\partial y_c} - w(\dot{\theta} + \dot{\alpha})s\gamma - (y_c + v)\dot{\gamma}\}\vec{i}_c$$

$$+ \{\dot{\ell}_0(1 + \frac{\partial v}{\partial y_c}) + \frac{\partial v}{\partial t} + u\dot{\gamma} - (\dot{\theta} + \dot{\alpha})c\gamma w\}\vec{j}_c$$

$$+ \{\frac{\partial w}{\partial t} + \dot{\ell}_0 \frac{\partial w}{\partial y_c} + (\dot{\theta} + \dot{\alpha})s\gamma u + (\dot{\theta} + \dot{\alpha})c\gamma(y_c + v)\}\vec{k}_c \tag{2.9.15}$$

Substituting (2.9.14) and (2.9.15) in (2.4.14),

$$T_{nonorb} = \frac{M_b}{2}\{[(\dot{\alpha} + \dot{\theta})^2 c^2\gamma + \dot{\gamma}^2][\ell_0 + v(\ell_0, t)]^2$$

$$+ [(1 + \frac{\partial v}{\partial y_c}(\ell_0, t))\dot{\ell}_0 + \frac{\partial v}{\partial t}(\ell_0, t)]^2$$

$$+ \frac{1}{2} M_c \cdot \frac{1}{\ell_0} \int_0^{\ell_0} \{[\frac{\partial u}{\partial t} + \dot{\ell}_0 \frac{\partial u}{\partial y_c} - w(\dot{\theta} + \dot{\alpha})s\gamma - (y_c + v)\dot{\gamma}]^2$$

$$+ [\dot{\ell}_0 (1 + \frac{\partial v}{\partial y_c}) + \frac{\partial v}{\partial t} + u\dot{\gamma} - (\dot{\theta} + \dot{\alpha})c\gamma w]^2$$

$$+ [\frac{\partial w}{\partial t} + \dot{\ell}_0 \frac{\partial w}{\partial y_c} + (\dot{\theta} + \dot{\alpha})s\gamma u + (\dot{\theta} + \dot{\alpha})c\gamma(y_c + v)]^2\} dy_c \tag{2.9.16}$$

T_{nonorb} can be decomposed into two parts as (Appendix C):

$$T_{nonorb} = T_{\alpha\gamma} + T_{uvw} \tag{2.9.17}$$

where

$$T_{\alpha\gamma} = \frac{1}{2}(M_b + \frac{1}{3} M_c)[(\dot{\alpha} + \dot{\theta})^2 c^2\gamma + \dot{\gamma}^2]\ell_0^2 + \frac{1}{2}(M_b + M_c)\dot{\ell}_0^2 \tag{2.9.18}$$

and

$$T_{uvw} = M_b\{[(\dot{\alpha} + \dot{\theta})^2 c^2\gamma + \dot{\gamma}^2] v(\ell_0, t)\ell_0 + \dot{\ell}_0{}^2 \frac{\partial v}{\partial y_c}(\ell_0, t)$$

$$+ \dot{\ell}_0 \frac{\partial v}{\partial t}(\ell_0, t)(1 + \frac{\partial v}{\partial y_c}(\ell_0, t)) + (\frac{\partial v}{\partial t}(\ell_0, t))^2\}$$

$$+ \frac{1}{2} M_c \cdot \frac{1}{\ell_0} \int_0^{\ell_0} \{[(\frac{\partial u}{\partial t})^2 + (\frac{\partial v}{\partial t})^2 + (\frac{\partial w}{\partial t})^2]$$

$$+ \dot{\ell}_0{}^2[(\frac{\partial u}{\partial y_c})^2 + 2(\frac{\partial v}{\partial y_c}) + (\frac{\partial w}{\partial y_c})^2] + 2\dot{\ell}_0[\frac{\partial u}{\partial t}\frac{\partial u}{\partial y_c} + \frac{\partial v}{\partial t}\frac{\partial v}{\partial y_c}$$

$$+ \frac{\partial w}{\partial t} \cdot \frac{\partial w}{\partial y_c} - 2(\dot{\theta} + \dot{\alpha})s\gamma(u\frac{\partial w}{\partial t} - w\frac{\partial u}{\partial t}) + 2(y_c + v)$$

$$[(\dot{\theta} + \dot{\alpha})c\gamma\frac{\partial w}{\partial t} - \dot{\gamma}\frac{\partial u}{\partial t}] + 2(\dot{\theta} + \dot{\alpha})s\gamma y_c \cdot [\dot{\gamma}w + (\dot{\theta} + \dot{\alpha})c\gamma u]$$

$$+ 2\frac{\partial v}{\partial t}[u\dot{\gamma} - (\dot{\theta} + \dot{\alpha})c\gamma w]\}dy_c \qquad (2.9.19)$$

In obtaining (2.9.19) the basic assumptions cited in Section 2.2 have been used. In addition, some vibrational terms have been dropped based on order of magnitude analysis.

Again, as in the case of gravitational potential energy, $T_{\alpha\gamma}$ is much larger than T_{uvw}. One can expect that the rotational motion is affected to a smaller extent by the vibrations compared to the vice versa.

2.10 GOVERNING EQUATIONS OF MOTION

Once the energy expressions have been obtained, there are two ways to derive the equations of motion. One way is to expand at the outset, u, v, w in terms of a set of admissible functions. Then, the integrals with respect to the coordinate y_c in the energy functionals can be evaluated. Thus one obtains energy expressions explicitly in terms of α, γ, etc. and Galerkin coefficients which are functions of time only. Subsequently, Lagrange's equation is used to obtain the equations of motion. This approach has been followed by Misra and Modi [22,23]. Although this method may sometimes involve less work, it does not yield equations in terms of u, v, w in general form. Admissible functions are not unique anyway. If these functions are changed, the entire derivation must be repeated starting from the energy functionals.

The other way is to use directly the extended Hamilton's principle to get the general equations of motion (partial differential equations for vibrations and ordinary differential equations for rotations). These may be more useful, although more algebra is involved in the derivation. This second approach is followed here.

The extended Hamilton's principle is

$$\int_{t_1}^{t_2} (\delta T + \delta W)dt = 0 \tag{2.10.1}$$

where δT is the variation of the kinetic energy and δW is the virtual work done by all the forces acting on the system. Putting

$$\delta W = -\delta V + \delta W_{np} \tag{2.10.2}$$

where δV is the variation of the potential energy and δW_{np} is the work done by all the nonpotential forces, one has

$$\int_{t_1}^{t_2} \delta L dt = -\int_{t_1}^{t_2} \delta W_{np} dt \tag{2.10.3}$$

Here L is the Lagrangian given by

$$L = T-V \tag{2.10.4}$$

The expressions for T and V are given in (2.9.17 - 2.9.19) and (2.9.9 - 2.9.11), respectively.

For the sake of brevity, only equations for α and u degrees of freedom are developed in the main text. The other equations are derived in Appendix D.

2.10.1 Development of the α Equation

Let us define

$$\delta_\alpha L = L(\alpha + \delta\alpha, \gamma, u, v, w, \ell_0) - L(\alpha, \gamma, u, v, w, \ell_0) \tag{2.10.5}$$

Only the α degree of freedom has a generalized virtual displacement since we are interested in obtaining the corresponding equation. Using (2.10.3), (2.9.17-19) and (2.9.9-11)

$$\begin{aligned}\delta_\alpha L = & -3 \frac{\dot\theta^2}{1+e\cos\theta} c\gamma\ell_0^2\{s\alpha c\alpha c\gamma[M_b(1+2\frac{v(\ell_0,t)}{\ell_0})+\frac{M_c}{3}] \\ & + \rho_c \frac{1}{\ell_0^2}\int_0^{\ell_0} y_c[2\cdot s\alpha c\alpha c\gamma v+2s\alpha c\alpha s\gamma u + \cos(2\alpha)w]dy_c\}\delta\alpha \\ & + \{[(1+2\frac{v(\ell_0,t)}{\ell_0})M_b + \frac{1}{3}M_c](\dot\alpha+\dot\theta)c^2\gamma\ell_0^2 + \rho_c[2\dot\ell_0 c\gamma\int_0^{\ell_0} w dy_c \\ & + 2(\dot\theta+\dot\alpha)c\gamma\int_0^{\ell_0}(c\gamma v+s\gamma u)y_c dy_c+\int_0^{\ell_0}(s\gamma(u\frac{\partial w}{\partial t}-w\frac{\partial u}{\partial t})+c\gamma(v\frac{\partial w}{\partial t}-w\frac{\partial v}{\partial t})]dy_c\}\delta\dot\alpha\end{aligned}$$

$$\dots \quad (2.10.6)$$

Here, the following relation has been used

$$\mu/R_0^3 = \frac{\dot{\theta}^2}{1 + e\ c\theta} \qquad (2.10.7)$$

Integrating $\delta_\alpha L$ with respect to time from t_1 to t_2 and noticing that

$$\delta\alpha(t_1) = \delta\alpha(t_2) = 0 \qquad (2.10.8a)$$

$$\delta\dot{\alpha} = \frac{d}{dt}(\delta\alpha) \qquad (2.10.8b)$$

one can obtain

$$\int_{t_1}^{t_2} [A_\alpha]\delta\alpha dt = \int_{t_1}^{t_2} Q_\alpha \delta\alpha dt \qquad (2.10.9)$$

where A_α is the integral kernel and Q_α is the generalized force corresponding to α, which is derived in Chapter 3.

Since α is an independent generalized coordinate, $\delta\alpha$ is arbitrary and the only way the above equation can be satisfied is if

$$A_\alpha = Q_\alpha$$

or

$$\frac{d}{dt}\{\{M_b[\ell_0 + 2v(\ell_0,t)]\ell_0 + \frac{1}{3}\rho_c\ell_0^3\}(\dot{\alpha} + \dot{\theta})c^2\gamma\}$$

$$+ 3\frac{\dot{\theta}^2}{(1 + e\ c\theta)} s\alpha c\alpha c^2\gamma\{M_b\ell_0[\ell_0 + 2v(\ell_0,t)] + \frac{1}{3}\rho_c[\ell_0^3 + 2\int_0^{\ell_0} y_c\, v\, dy_c]\}$$

$$- 6\frac{\dot{\theta}^2}{1 + e\ c\theta}\rho_c s\alpha c\alpha s\gamma c\gamma \int_0^{\ell_0} uy_c dy_c - 3\frac{\dot{\theta}^2}{1 + e\ c\theta}\rho_c c\gamma c(2\alpha)\int_0^{\ell_0} wy_c dy_c$$

$$-2\rho_c\frac{d}{dt}\{\dot{\ell}_0\ c\gamma\int_0^{\ell_0} wdy_c\} + 2\rho_c\frac{d}{dt}\{(\dot{\theta} + \dot{\alpha})c^2\gamma\int_0^{\ell_0} y_c v dy_c\}$$

$$+ \rho_c\frac{d}{dt}\{s\gamma\int_0^{\ell_0}(u\frac{\partial w}{\partial t} - w\frac{\partial u}{\partial t})dy_c\} + \rho_c\frac{d}{dt}\{c\gamma\int_0^{\ell_0}(y_c + v)\frac{\partial w}{\partial t}dy_c\}$$

$$+\rho_c\frac{d}{dt}\{s\gamma\dot{\gamma}\int_0^{\ell_0} y_c\, w\, dy_c\} + 2\rho_c\frac{d}{dt}\{(\dot{\theta} + \dot{\alpha})s\gamma c\gamma\int_0^{\ell_0} y_c\ u\ dy_c\}$$

$$- \rho_c\frac{d}{dt}\{c\gamma\int_0^{\ell_0}\frac{\partial v}{\partial t} w\, dy_c\}$$

$$= Q_\alpha \qquad (2.10.10)$$

Equation (2.10.10) is very messy and contains many insignificant terms. It can be simplified further by ignoring these small terms. We do not know how large the local velocities $\frac{\partial u}{\partial t}$, $\frac{\partial v}{\partial t}$, $\frac{\partial w}{\partial t}$ are (vibrations have high frequencies), but at least the values of u, v, w are much smaller than ℓ_0. This fact can be used in the simplification process.

Finally, one obtains

$$\{M_b \ell_0^2 + \frac{1}{3}\rho_c \ell_0^3\} \frac{d}{dt}[c^2\gamma(\dot\theta + \dot\alpha)] + [c^2\gamma(\dot\theta + \dot\alpha)]\{[2M_b \ell_0 \dot\ell_0$$

$$+ 2M_b \ell_0 \frac{\partial v(\ell_0, t)}{\partial t}] + \rho_c \dot\ell_0 \ell_0^2\} + 3 \frac{\dot\theta^2}{1 + e\, c\theta} s\alpha c\alpha c^2\gamma\{M_b \ell_0^2$$

$$+ \frac{1}{3}\rho_c\, \ell_0^3\} + 2\rho_c \frac{d}{dt}\{-\dot\ell_0 c\gamma \int_0^{\ell_0} w dy_c + (\dot\theta + \dot\alpha)c\gamma[c\gamma \int_0^{\ell_0} y_c v dy_c$$

$$+ s\gamma \int_0^{\ell_0} y_c u dy_c] + s\gamma\dot\gamma \int_0^{\ell_0} y_c w dy_c + c\gamma \int_0^{\ell_0} y_c \frac{\partial w}{\partial t} dy_c\} = Q_\alpha \qquad (2.10.11)$$

2.10.2 Development of u Equation

Using a procedure similar to the one used in Section 2.10.2, let

$$\delta_u L = L(\alpha, \gamma, u + \delta u, v, w, \ell_0) - L(\alpha, \gamma, u, v, w, \ell_0) \qquad (2.10.12)$$

Here only a generalized virtual displacement δu is given. Again from (2.10.3), (2.9.17-2.9.19) and (2.9.9-2.9.11)

$$\int_{t_1}^{t_2} \delta_u L dt = \frac{1}{2}\rho_c \{\int_{t_1}^{t_2} \int_0^{\ell_0} \frac{\partial u}{\partial t} \frac{\partial}{\partial t} \delta u dy_c dt$$

$$+ \int_{t_1}^{t_2} \dot\ell_0^2 \int_0^{\ell_0} 2(\frac{\partial u}{\partial y_c}) \frac{\partial}{\partial y_c} \delta u dy_c dt$$

$$+ \int_{t_1}^{t_2} 2\dot\ell_0 \int_0^{\ell_0} (\frac{\partial u}{\partial t} \frac{\partial}{\partial y_c} \delta u + \frac{\partial u}{\partial y_c} \frac{\partial}{\partial t} \delta u_c) dy_c\, dt \qquad \ldots$$

...

$$+ \int_{t_1}^{t_2} 2\dot{\ell}_0 \int_0^{\ell_0} 2\dot{\gamma}\delta u dy_c dt$$

$$+ \int_{t_1}^{t^2} 2(\dot{\theta} + \dot{\alpha}) s\gamma \int_0^{\ell_0} [\frac{\partial w}{\partial t} \delta u - w \frac{\partial}{\partial t} \delta u] dy_c dt$$

$$+ \int_{t_1}^{t_2} (-\dot{\gamma}) \int_0^{\ell_0} 2(y_c + v) \frac{\partial}{\partial t} \delta u dy_c dt$$

$$+ \int_{t_1}^{t_2} 2(\dot{\theta} + \dot{\alpha})^2 \cdot s\gamma c\gamma \int_0^{\ell_0} y_c \delta u dy_c dt$$

$$+ \int_{t_1}^{t_2} 2\dot{\gamma} \int_0^{\ell_0} \frac{\partial v}{\partial t} \delta u dy_c dt$$

$$- EA \int_{t_1}^{t_2} \int_0^{\ell_0} \{\frac{\partial v}{\partial y_c} + \frac{1}{2} [(\frac{\partial u}{\partial y_c})^2 + (\frac{\partial w}{\partial y_c})^2]\} \frac{\partial u}{\partial y_c} \frac{\partial}{\partial y_c} \delta u dy_c dt$$

$$- \frac{\dot{\theta}^2}{(1 + e\ c\theta)} \int_{t_1}^{t_2} (-3\rho_c) c^2\alpha s\gamma c\gamma \int_0^{\ell_0} y_c \delta u dy_c dt$$

$$= \int_{t_1}^{t_2} \delta u\ W_{np} dt = -\int_{t_1}^{t_2} \int_0^{\ell_0} Q_u \delta u dy_c dt \qquad (2.10.13)$$

where Q_u is the generalized force acting on an element dy_c of the tether corresponding to displacement u. By definition,

$$\delta u(y_c, t_1) = \delta u(y_c, t_2) = 0 \quad \text{for} \quad y_c \in (0, \ell_0) \qquad (2.10.14)$$

Boundary condition for u can be obtained through the variational equation above, but from geometrical considerations, it is quite obvious that

$$u(0,t) = u(\ell_0,t) = 0 \tag{2.10.15}$$

Hence

$$\delta u(0,t) = \delta u(\ell_0,t) = 0 \tag{2.10.15'}$$

In the variational equation (2.10.13) the order of integration with respect to y_c and t cannot be exchanged in general since $\ell_0 = \ell_0(t)$ during retrieval and deployment. (If ℓ_0 is constant, the exchange is valid). Considering the first term, integrating by parts and using Leibnitz's rule, we have

$$\int_0^{\ell_0} \frac{\partial u}{\partial t} \cdot \frac{\partial}{\partial t} \delta u dy_c = \frac{\partial}{\partial t} \int_0^{\ell_0(t)} \frac{\partial u}{\partial t} \delta u dy_c - \int_0^{\ell_0} \frac{\partial^2 u}{\partial t^2} \delta u dy_c$$

$$- \dot{\ell}_0 \frac{\partial u}{\partial t} \delta u(\ell_0,t) = \frac{\partial}{\partial t} \int_0^{\ell_0} \frac{\partial u}{\partial t} \delta u dy_c - \int_0^{\ell_0} \frac{\partial^2 u}{\partial t^2} \delta u dy_c$$

Carrying out similar algebra (integration by parts and use of Leibnitz's rule) one can express (2.10.13) in the form

$$\int_{t_1}^{t_2} \int_0^{\ell_0} (A_u - Q_u) \delta u dy_c dt = 0 \tag{2.10.16}$$

Since δu is independent at every point of the tether and is arbitrary, equation (2.10.16) can be satisfied if and only if

$$A_u - Q_u = 0 \tag{2.10.17}$$

This leads to u equation as follows

$$(\frac{\partial}{\partial t} + \dot{\ell}_0 \frac{\partial}{\partial y_c})^2 u - 2(\dot{\ell}_0 + \frac{\partial v}{\partial t})\dot{\gamma} - 2(\dot{\theta} + \dot{\alpha})s\gamma \frac{\partial w}{\partial t}$$

$$- [\ddot{\gamma} + (\dot{\theta} + \dot{\alpha})^2 \frac{s(2\gamma)}{2}]y_c - \frac{EA}{\rho_c} \frac{\partial}{\partial y_c}\{\frac{\partial u}{\partial y_c} [\frac{\partial v}{\partial y_c} + \frac{1}{2} \overline{(\frac{\partial u}{\partial y_c})^2 + (\frac{\partial w}{\partial y_c})^2}]\}$$

$$- 3 \frac{\dot{\theta}^2}{1 + e\ c\theta} c^2\alpha s\gamma c\gamma y_c = Q_u \tag{2.10.18}$$

Corresponding boundary conditions at the two ends are already given in (2.10.15).

2.11 SYSTEM EQUATIONS

From Section 2.10 and Appendix D, one can summarize the equations for α, γ, u, v and w degrees of freedom with corresponding boundary conditions (when required) as follows:

α equation:

$$[c^2\gamma(\dot{\alpha} + \dot{\theta})]^{\cdot} (M_b\ell_0^2 + \frac{1}{3} \rho_c\ell_0^3) + [c^2\gamma(\dot{\theta} + \dot{\alpha})]\{2M_b\ell_0(\dot{\ell}_0 + \frac{\partial v(\ell_0,t)}{\partial t}) + \rho_c\dot{\ell}_0\ell_0^2\}$$

$$+ 3 \frac{\dot{\theta}^2}{1 + e\ c\theta} s\alpha c\gamma c^2\gamma\{M_b\ell_0^2 + \frac{1}{3} \rho_c\ell_0^3\} - 2\rho_c \frac{d}{dt}\{\dot{\ell}_0\ c\gamma \int_0^{\ell_0} w dy_c\}$$

$$+ \rho_c\frac{d}{dt} \{c\gamma \int_0^{\ell_0} y_c \frac{\partial w}{\partial t} dy_c\} + \rho_c \frac{d}{dt} \{s\gamma\dot{\gamma} \int_0^{\ell_0} y_c w dy_c\} + 2 \rho_c\frac{d}{dt}\{(\dot{\theta} + \dot{\alpha})c^2\gamma\int_0^{\ell_0} y_c v dy_c\}$$

$$+ 2 \frac{d}{dt} \{(\dot{\theta} + \dot{\alpha})s\gamma c\gamma \int_0^{\ell_0} y_c u dy_c\}$$

$$= Q_\alpha \tag{2.11.1}$$

γ equation:

$$\ddot{\gamma}\{M_b\ell_0{}^2+\frac{\rho_c}{3}\ell_0{}^3\}+\dot{\gamma}\{2M_b\ell_0(\dot{\ell}_0+\frac{\partial v(\ell_0,t)}{\partial t})+\rho_c\ell_0{}^2\dot{\ell}_0\}+\{(\dot{\alpha}+\dot{\theta})^2$$

$$+\frac{3\dot{\theta}^2}{1+e\ c\theta}c^2\alpha\}s\gamma c\gamma\{M_b\ell_0{}^2+\frac{1}{3}\rho_c\ell_0{}^3\}+2\rho_c\frac{d}{dt}\{\dot{\ell}_0\int_0^{\ell_0}udy_c\}$$

$$+\rho_c(\dot{\theta}+\dot{\alpha})s\gamma\int_0^{\ell_0}y_c\frac{\partial w}{\partial t}dy_c-\rho_c\frac{d}{dt}(\int_0^{\ell_0}y_c\frac{\partial u}{\partial t}dy_c)$$

$$+\rho_c\frac{d}{dt}\{(\dot{\theta}+\dot{\alpha})s\gamma\int_0^{\ell_0}y_cwdt_c\}+2\rho_c\frac{d}{dt}\{\dot{\gamma}\int_0^{\ell_0}y_cvdy_c\}=Q_\gamma \qquad (2.11.2)$$

u equation:

$$\frac{D^2}{Dt^2}u-2[\dot{\ell}_0+\frac{\partial v}{\partial t}]\dot{\gamma}-2(\dot{\theta}+\dot{\alpha})s\gamma\frac{\partial w}{\partial t}+[\ddot{\gamma}-(\theta+\alpha)^2\frac{s2\gamma}{2}]y_c$$

$$-\frac{\partial}{\partial t}[s\gamma(\dot{\theta}+\dot{\alpha})]w-\frac{EA}{\rho_c}\frac{\partial}{\partial y_c}\{\frac{\partial u}{\partial y_c}\cdot[\frac{\partial v}{\partial y_c}+\frac{1}{2}((\frac{\partial u}{\partial y_c})+(\frac{\partial w}{\partial y_c})^2)]\}$$

$$-3\frac{\dot{\theta}^2}{1+e\ c\theta}c^2\alpha s\gamma c\gamma y_c=Q_u \qquad (2.11.3)$$

Boundary conditions are

$$u(0,t)=0 \quad\text{and}\quad u(\ell_0,t)=0 \qquad (2.11.4)$$

w equation:

$$\frac{D^2w}{Dt^2}+2(\dot{\theta}+\dot{\alpha})c\gamma(\dot{\ell}_0+\frac{\partial v}{\partial t})+\frac{\partial}{\partial t}[(\dot{\theta}+\dot{\alpha})s\gamma]u+2(\dot{\theta}+\dot{\alpha})s\gamma\frac{\partial u}{\partial t}$$

$$+y_c\{\frac{\partial}{\partial t}[(\dot{\theta}+\dot{\alpha})c\gamma]-(\dot{\theta}+\dot{\alpha})s\gamma\dot{\gamma}\}-\frac{EA}{\rho_c}\frac{\partial}{\partial y_c}\{\frac{\partial w}{\partial y_c}[\frac{\partial v}{\partial y_c}$$

....

...

$$+ \frac{1}{2}((\frac{\partial u}{\partial y_c})^2 + (\frac{\partial w}{\partial y_c})^2)]\} + 3\frac{\dot{\theta}^2}{1 + e\,c\theta} s\alpha c\alpha c\gamma y_c = Q_w \tag{2.11.5}$$

Boundary conditions are

$$w(0,t) = 0 \quad \text{and} \quad w(\ell_0,t) = 0 \tag{2.11.6}$$

<u>v equation:</u>

$$\frac{D^2}{Dt^2}[\ell_0+v]-[(\dot{\alpha}+\dot{\theta})^2c^2\gamma+\dot{\gamma}^2 + \frac{(3c^2\alpha c^2\gamma-1)\dot{\theta}^2}{1 + e\,c\theta}]y_c + 2[\dot{\gamma}\frac{\partial u}{\partial t} - (\dot{\theta}+\dot{\alpha})c\gamma\frac{\partial w}{\partial t}]$$

$$-\frac{EA}{\rho_c}\frac{\partial}{\partial y_c}\{\frac{\partial v}{\partial y_c} + \frac{1}{2}[(\frac{\partial u}{\partial y_c})^2 + (\frac{\partial w}{\partial y_c})^2]\} = Q_v \tag{2.11.7}$$

Boundary conditions are

$$v(0,t) = 0 \tag{2.11.8}$$

and

$$M_b\frac{d^2}{dt^2}[\ell_0+v(\ell_0,t)]-M_b[(\dot{\alpha}+\dot{\theta})^2c^2\gamma+\dot{\gamma}^2+\frac{(3c^2\alpha c^2\gamma-1)\dot{\theta}^2}{1 + e\,c\theta}]\ell_0$$

$$+ EA\{\frac{\partial v}{\partial y_c} + \frac{1}{2}[(\frac{\partial u}{\partial y_c})^2 + (\frac{\partial w}{\partial y_c})^2]\}\Big|_{y_c=\ell_0} = Q_{vb} \tag{2.11.9}$$

where

$$\frac{D}{Dt} \equiv (\frac{\partial}{\partial t} + \dot{\ell}_0\frac{\partial}{\partial y_c}) \tag{2.11.10}$$

and Q_{vb} is the external force acting on the subsatellite along the axial direction of the tether.

CHAPTER 3

DERIVATION OF GENERALIZED AERODYNAMIC FORCES

3.1 BASIC DEFINITIONS AND ASSUMPTIONS

The Shuttle Supported Tethered Subsatellite (SSTS) system is subject to various environmental forces such as astmospheric resistance, solar radiation pressure, earth's magnetic field, luni-solar perturbations, etc. The most important external force is the atmospheric drag the magnitude of which is usually much larger than the other forces. Thus it is the only environmental force considered here.

Consider an orbit inclined at an angle i to the equatorial plane (Fig. 3.1). Let $\vec{I}$, $\vec{J}$, $\vec{K}$ be the unit vectors along the earth-centered axes X, Y, Z, respectively. X-axis is from south to north direction, Y-axis is in the equatorial plane along the line of nodes (assumed fixed) and Z-axis completes the triad. As defined earlier, $\vec{i}_0$, $\vec{j}_0$, $\vec{k}_0$ are unit vectors along rotating x_0, y_0, z_0 axes, which are along the orbit normal, local vertical and local horizontal, respectively.

The earth as well as the atmosphere assumed attached to it have an angular velocity $\sigma_0\vec{I}$. Since the rotational period is one day,

$$\sigma_0 = (2\pi/24 \times 60 \times 60)\cdot \text{Sec}^{-1} = 7.272 \times 10^{-5}\ \text{Sec}^{-1} \qquad (3.1.1)$$

From Fig. 3.1, it is clear that the inclination angle i, shape of the orbit and the oblateness of the earth determine how the aerodynamic forces affect the motion. If i = 0, the orbital and equatorial planes are coincident. Thus it could be expected that the aerodynamic forces have a great effect on the inplane α motion and no effect on out-of-plane motion γ since they produce no torque relevant to γ rotation. If i $\neq$ 0, then γ

motion will be affected through the rotation of the earth and this effect will be maximum for $i = 90°$.

The shape of the orbit is determined by eccentricity e. If $e = 0$, it is a circular orbit and the aerodynamic forces are the same at different θ when the earth is assumed to be spherical. If $e \neq 0$, then the effect of the drag varies with θ since the SSTS system dives into denser atmosphere at certain times. The deeper it dives, the thicker the atmosphere is, hence more drag is experienced by the system.

If the oblateness of the earth is taken into account, the situation becomes more complex. The earth is not exactly spherical. Along north-south direction, the radius of the earth is shorter than that along west to east. Thus, when SSTS system is in a polar orbit, the drag again varies with θ even if the orbit is circular. It is smallest above the north and south poles.

Due to the presence of the atmospheric drag the subsatellite cannot be deployed to an altitude as low as one wants without limit. This is because α and/or γ are increased very much due to increasing drag.

In this thesis, the following assumptions are made in order to calculate the aerodynamic forces.

(i) It is assumed that the aerodynamic force (based on free molecular flow) can be expressed as

$$\vec{F} = -\frac{1}{2} C_d \rho_a A_p |\vec{V}| \vec{V} \tag{3.1.2}$$

where A_p is the projected area of either the subsatellite or an element of the tether perpendicular to the relative velocity of air. Here ρ_a is the density of air at the altitude under consideration while C_d is the drag coefficient. C_d depends on the shape of the object experiencing the aerodynamic force [39]. If the shape is cylindircal (tether) C_d can be taken as 2. For a spherical subsatellite $C_d = 1$.

(ii) The variation of the density of air is assumed to be exponential, i.e.,

$$\rho_a = \rho_0 \exp[-(h-H_0)/h_0] \tag{3.1.3}$$

where h is the altitude in meters above the earth's surface, ρ_0 is the density of air at a reference altitude H_0 and h_0 is a scale factor. It is assumed here that ρ_0, h_0 and H are constants in the altitude range covered by the tether.

(iii) The relative velocity $\vec{V}$ depends on the orbital velocity of the center of mass of the system, the velocity of the atmosphere due to its rotation about the earth's axis and the velocity of the element relative to the center of mass of the system resulting due to the rotations and vibrations of the tether. The last one (vibrational velocity) is comparatively small and hence is ignored here.

3.2 RELATIVE VELOCITY OF AIR AND THE AERODYNAMIC FORCES

The unit vectors in the orbital and inertial coordinate systems are related by

$$\begin{Bmatrix} \vec{I} \\ \vec{J} \\ \vec{K} \end{Bmatrix} = \begin{bmatrix} ci & 0 & si \\ 0 & 1 & 0 \\ -si & 0 & ci \end{bmatrix} \begin{bmatrix} 1 & 0 & 0 \\ 0 & c\tilde{\theta} & -s\tilde{\theta} \\ 0 & s\tilde{\theta} & c\tilde{\theta} \end{bmatrix} \begin{Bmatrix} \vec{i}_0 \\ \vec{j}_0 \\ \vec{k}_0 \end{Bmatrix} \tag{3.2.1}$$

where

$$\tilde{\theta} = \theta + \theta_0 \tag{3.2.2}$$

and $c\tilde{\theta}$, etc. represent cos $\tilde{\theta}$, etc., respectively. Using the first row,

$$\sigma\vec{I} = \sigma(ci\ \vec{i}_0 + si\ s\tilde{\theta}\ \vec{j}_0 + si\ c\tilde{\theta}\ \vec{k}_0) \tag{3.2.3}$$

Let the location of a point on the tethered system be given by P (x_c, y_c, z_c). P could be either an arbitrary point on the tether or on the subsatellite. If P is on the subsatellite, the radius vector from the center of the earth E to P is

$$\vec{R}_{Eb} \simeq \vec{R}_0 + \ell_0\vec{j}_c \tag{3.2.4}$$

The velocity of atmosphere at the subsatellite altitude is given by

$$\vec{V}_s = \sigma\vec{I} \times (\vec{R}_{Eb}) = \sigma(ci\ \vec{i}_0 + si\ s\tilde{\theta}\ \vec{j}_0 + si\ c\tilde{\theta}\ \vec{k}_0) \times (\vec{R}_0 + \ell_0\vec{j}_c) \tag{3.2.5}$$

The velocity of the subsatellite is

$$(\vec{R}_0 + \ell_0\vec{j}_c)^{\bullet} = \dot{R}_0\ \vec{j}_0 + R_0\ \dot{\theta}\ \ \vec{k}_0 + (\ell_0\vec{j}_c)^{\bullet} \tag{3.2.6}$$

The first two terms represent the orbital velocity and the last term is the velocity of the subsatellite relative to the shuttle. Hence, the velocity of the subsatellite relative to the atmosphere is given by

$$\begin{aligned} \vec{V}_{sa} &= \dot{R}_0\vec{j}_0 + R_0\dot{\theta}\vec{k}_0 + (\ell_0\vec{j}_c)^{\bullet} - \vec{V}_s \\ &= \dot{R}_0\vec{j}_0 + R_0\dot{\theta}\vec{k}_0 + \dot{\ell}_0\vec{j}_c + \ell_0\dot{\vec{j}}_c - \sigma(ci\ \vec{i}_0 \\ &\quad + si\ s\tilde{\theta}\ \vec{j}_0 + si\ c\tilde{\theta}\ \vec{k}_0) \times (\vec{R}_0 + \ell_0\vec{j}_c) \end{aligned} \tag{3.2.7}$$

From (2.9.6)

$$\vec{j}_c = -s\gamma\ \vec{i}_0 + c\alpha\ c\gamma\vec{j}_0 + s\alpha\ c\gamma\ \vec{k}_0 \tag{3.2.8}$$

Furthermore,

$$\dot{\vec{j}}_c = \vec{\omega}_c \times \vec{j}_c$$

and using (2.9.13) and (2.9.6),

$$\dot{\vec{j}}_c = -\dot{\gamma}(c\gamma\ \vec{i}_0 + s\gamma\ c\alpha\ \vec{j}_0 + s\gamma\ s\alpha\ \vec{k}_0)$$

$$+ (\dot{\theta} + \dot{\alpha})c\gamma(-s\alpha\ \vec{j}_0 + c\alpha\ \vec{k}_0) \tag{3.2.9}$$

Substituting (3.2.8) and (3.2.9) into (3.2.7),

$$\vec{V}_{sa} = V_{xsa}\ \vec{i}_0 + V_{ysa}\ \vec{j}_0 + V_{zsa}\ \vec{k}_0$$

where

$$V_{xsa} = -\dot{\ell}_0\ s\gamma - \ell_0\ c\gamma\dot{\gamma} + R_0\ \sigma\ c\tilde{\theta}\ si - \sigma\ \ell_0\ si\ c\gamma$$

$$\cdot (s\tilde{\theta}\ s\alpha - c\tilde{\theta}\ c\alpha)$$

$$V_{ysa} = \dot{R}_0 + \dot{\ell}_0\ c\gamma\ c\alpha - \ell_0\ \dot{\gamma}\ s\gamma\ c\alpha - s\alpha\ c\gamma\ (\dot{\theta}+\dot{\alpha})\ell_0$$

$$+ \sigma\ \ell_0(ci\ c\gamma\ s\alpha + si\ c\tilde{\theta}\ s\gamma)$$

and

$$V_{zsa} = R_0\dot{\theta} + \dot{\ell}_0\, s\alpha\, c\gamma - \ell_0\, \dot{\gamma}\, s\gamma\, s\alpha + c\alpha\, c\gamma(\dot{\theta}+\dot{\alpha})\ell_0$$

$$- R_0\, \sigma\, ci - \sigma\ell_0(ci\, c\alpha\, c\gamma + si\, s\tilde{\theta}\, s\gamma) \tag{3.2.10}$$

Equation (3.2.10) includes the contribution of $\dot{\ell}_0$, $\dot{\alpha}$ and $\dot{\gamma}$ to the velocity of the subsatellite relative to the atmosphere. It is rather lengthy and in fact, many terms are quite small. The deployment or retrieval velocity $\dot{\ell}_0$ of the tether as well as $\dot{\alpha}\,\ell_0$ and $\dot{\gamma}\,\ell_0$ terms turn out to be negligible compared with the orbital velocity, even though ℓ_0 is quite large. In actual computations, they were ignored and the following expression was used

$$\vec{V}_{sa} = [R_0\, \sigma\, c\tilde{\theta}\, si,\ \dot{R}_0,\ R_0(\dot{\theta} - \sigma\, ci)] \begin{Bmatrix} \vec{i}_0 \\ \vec{j}_0 \\ \vec{k}_0 \end{Bmatrix}$$

$$\equiv [V_{xa}, V_{ya}, V_{za}] \begin{Bmatrix} \vec{i}_0 \\ \vec{j}_0 \\ \vec{k}_0 \end{Bmatrix} = \vec{V}_a \tag{3.2.11}$$

With the above approximation, one can assume that the velocity of any point on the system relative to the atmosphere is the same $\vec{V}_a$ and is given by (3.2.11).

It is more convenient to express $\vec{V}_a$ in terms of components along the tether coordinate system, x_c, y_c, z_c. Using (2.9.6) and (3.2.11)

$$\vec{V}_a = V_{xc}\, \vec{i}_c + V_{yc}\, \vec{j}_c + V_{zc}\, \vec{k}_c \tag{3.2.12}$$

where

$$V_{xc} = c\gamma(R_0\, \sigma\, c\tilde{\theta}\; si) + \dot{R}_0\, s\gamma$$

$$V_{yc} = -s\gamma\; c\alpha(R_0\, \sigma\, c\tilde{\theta}\; si) + \dot{R}_0\, c\gamma\; c\alpha + R_0(\dot{\theta} - \sigma\, ci)s\alpha$$

$$V_{zc} = s\alpha\; s\gamma(R_0\, \sigma\, c\tilde{\theta}\; si) - \dot{R}_0\, c\gamma\; s\alpha + R_0(\dot{\theta} - \sigma\, ci)c\alpha \qquad (3.2.13)$$

The aerodynamic forces acting on the subsatellite and an element dy_c of the tether are given by

$$\vec{F}_b = -\frac{1}{2}\, C_{db}\, \rho_{ab}\, A_b|\vec{V}_a|\vec{V}_a \qquad (3.2.14)$$

and

$$\vec{f}_c = -\frac{1}{2}\, C_{dc}\, \rho_{ac}\, dA_c|\vec{V}_a|\vec{V}_a \quad , \qquad (3.2.15)$$

respectively. Here C_{db} and C_{dc} are drag coefficients associated with the subsatellite and tether, respectively, A_b and dA_c are the projected areas of the subsatellite and an element of the tether normal to the relative velocity of the air while ρ_{ab} and ρ_{ac} are the density of air at the altitudes of the subsatellite and the element of the tether under consideration, respectively. A_b is governed by the shape of the subsatellite. Here the subsatellite is assumed to be spherical. Hence, whatever is the direction of the air flow, the projected area A_b remains the same.

The tether is assumed to be cylindrical with a diameter d_c. Now, dA_c depends on the angle between the tetherline and the relative velocity of air. Using the diagram shown below,

$$dA_c = (dy_c)(d_c)|\cos\ \beta|$$

$$= (d_c)(dy_c)\cdot\sqrt{V_{xc}^2 + V_{zc}^2}/\sqrt{V_{xc}^2 + V_{yc}^2 + V_{zc}^2} \qquad (3.2.16)$$

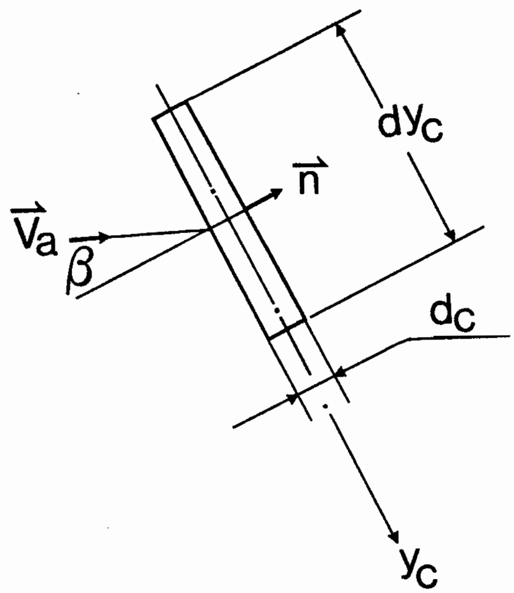

3.3 DENSITY OF ATMOSPHERE

As mentioned earlier in this thesis, the density of air ρ_a is represented approximately by an expression varying exponentially with the altitude, i.e.,

$$\rho_a = \rho_0 \exp[-(h-H_0)/h_0] \qquad (3.1.3)$$

Although ρ_0, H and h_0 vary somewhat with altitude, they are assumed to be constant here and chosen so as to yield the density of air identical to that used by Baker et al. [16]. Accordingly,

$$\frac{1}{h_0} = 0.1513 \times 10^{-3}\ m^{-1} \qquad (3.3.1)$$

while ρ_0 and H_0 are eliminated by using a value of ρ_a equal to 1.2321×10^{-13} kg/m³ at an altitude of 200 km, i.e.,

$$\rho_a = \rho_{00} \exp(-0.1513 \times 10^{-3} h) \mathrm{kg/m^3} \tag{3.3.2}$$

where

$$\rho_{00} = 1.2321 \times 10^{-13} \exp(0.1513 \times 10^{-3} \times 2 \times 10^5) \mathrm{kg/m^3} \tag{3.3.3}$$

The oblateness of the earth affects the calculation of altitude h. The earth and the SSTS system are shown in Fig. 3.1 schematically. Along the N-S direction, the axis is a bit shorter than that along the W-E direction since the earth is not exactly spherical. It is more like an ellipsoid. Measurements have shown that the semi-major axis a_0 of the earth is 6378.160 km while the semi-minor axis b_0 is 6356.778 km [38] and the equatorial plane is essentially a circle. Supposing that the density of air is the same everywhere on the earth's surface, this nearly 20 km difference between the semi-major and the semi-minor axes would affect the air density significantly even for a circular orbit. That is because the altitude would vary up to 20 km and variation of air density with altitude is exponential. The SSTS system will have a lower altitude and therefore experience larger aerodynamic force in the equatorial plane than over the north and south poles. Twenty km may be small compared with the radius of the earth, but it is of great significance while calculating the density of air because it changes by an order of magnitude within a 20 km layer.

The eccentricity e of the orbit obviously affects the density as well. R_0 is no longer constant when $e \neq 0$. Thus the SSTS system is sometimes far above the earth while dives into the atmosphere at some other time changing the aerodynamic force. The difference depends on how large e is.

Referring to Fig. 3.2, from geometric considerations, the instantaneous radius of the earth and the altitude above the earth's surface can be shown as [Appendix E]

$$r_{earth} = a_0\ b_0/[b_0^2(1 - s^2i\ s^2\theta) + a_0^2 s^2 i\ s^2\theta]^{\frac{1}{2}} \tag{3.3.4}$$

and

$$h = (R_0 - r_{earth} + y_c\ c\alpha\ c\gamma)\{1 + (a_0^2-b_0^2)^2(s^4i\ s^2\theta\ c^2\theta)/[b_0^2+(a_0^2-b_0^2)s^2i\ s^2\theta]^2\}^{-\frac{1}{2}} \quad \ldots(3.3.5)$$

3.4 GENERALIZED FORCES

The virtual work δW_a done by the aerodynamic forces is given by

$$\delta W_a = \int_{system} \vec{F} \cdot \delta\vec{R} \tag{3.4.1}$$

where $\vec{F}$ is the aerodynamic force acting at an element of the system and $\delta\vec{R}$ is the virtual displacement vector. $\vec{R}$ is the corresponding radius vector from the origin E of the inertial coordinate system, X, Y, Z. Considering the displacements u, v and w, the radius vectors for the subsatellite and an arbitrary point on the tether are given, respectively, by

$$\vec{R}_{Eb} = \vec{R}_0 + [\ell_0(t) + v(\ell_0,t)]\vec{j}_c \tag{3.4.2}$$

and

$$\vec{R}_{Ec} = \vec{R}_0 + u(y_c,t)\vec{i}_c + [y_c + v(y_c,t)]\vec{j}_c + w(y_c,t)\vec{k}_c \tag{3.4.3}$$

where

$$\vec{R}_0 = \vec{R}_0\ (\theta) \quad .$$

Corresponding to a virtual generalized displacement $\delta\alpha$, the variation in the radius vector $\vec{R}_{Eb}$ is given by

$$\delta_\alpha\ \vec{R}_{Eb} = \delta\alpha\{\vec{R}_0 + [\ell_0 + v(\ell_0,t)]\vec{j}_c\}$$

$$= (\ell_0+v)\delta_\alpha\ \vec{j}_c(\alpha,\gamma) \simeq \ell_0\ \delta_\alpha\ \vec{j}_c(\alpha,\gamma) \tag{3.4.4}$$

Clearly,

$$\delta_\alpha\ \vec{j}_c = \frac{\partial\vec{j}_c}{\partial\alpha}\ \delta\alpha \tag{3.4.5}$$

Using (2.9.6),

$$\frac{\partial\vec{j}_c}{\partial\alpha} = c\gamma\ \vec{k}_c \tag{3.4.6}$$

Substituting (3.4.5) and (3.4.6) into (3.4.4),

$$\delta_\alpha \vec{R}_{Eb} = \ell_0 \ c\gamma \ \delta\alpha \ \vec{k}_c \tag{3.4.7}$$

The virtual work done by the aerodynamic force F_b on the subsatellite due to the virtual generalized displacement $\delta\alpha$ is then

$$\delta_\alpha W_{ab} = \vec{F}_b \cdot \delta_\alpha \vec{R}_{Eb} = \ell_0 \ c\gamma(\vec{F}_b \cdot \vec{k}_c)\delta\alpha \tag{3.4.8}$$

Using (3.2.12) and (3.2.14)

$$\delta_\alpha W_{ab} = -\frac{1}{2} C_{db} \ \rho_{ab} \ A_b|\vec{V}_a|\ell_0 \ c\gamma \ V_{zc} \ \delta\alpha \tag{3.4.9}$$

In a similar way, we have

$$\delta_\alpha \vec{R}_{Ec} = y_c \ c\gamma \ \delta\alpha \ \vec{k}_c \tag{3.4.10}$$

and

$$\delta_\alpha W_{ac} = \int_0^{\ell_0} (\vec{f}_c \cdot \delta_\alpha \vec{R}_c)$$

$$= \int_0^{\ell_0} y_c \ c\gamma(\vec{f}_c \cdot \vec{k}_c)\delta\alpha \ dy_c \tag{3.4.11}$$

Using (3.2.12), (3.2.15) and (3.2.16)

$$\delta_\alpha W_{ac} = -\frac{1}{2} C_{dc} \int_0^{\ell_0} \rho_{ac}(V_{xc}^2 + V_{zc}^2)^{\frac{1}{2}} y_c \ c\gamma \ V_{zc} \ d_c \ dy_c \cdot \delta\alpha \tag{3.4.12}$$

Since

$$\delta_\alpha W_a = \delta_\alpha W_{ab} + \delta_\alpha W_{ac} = Q_{\alpha a} \cdot \delta\alpha \ , \tag{3.4.13}$$

using (3.4.9) and (3.4.12), we have

$$Q_{\alpha a} = -\frac{1}{2} c\gamma \, V_{zc} \{C_{dc} \, d_c (V_{xc}^2 + V_{zc}^2)^{\frac{1}{2}} \int_0^{\ell_0} y_c \, \rho_{ac} \, dy_c$$

$$+ C_{db} \, \rho_{ab} \, A_b |\vec{V}_a| \ell_0\} \tag{3.4.14}$$

Here $Q_{\alpha a}$ is the generalized force corresponding to α due to aerodynamic forces.

Following a similar procedure, one obtains the generalized aerodynamic force $Q_{\gamma a}$ corresponding to γ as

$$Q_{\gamma a} = \frac{1}{2} V_{xc} \{C_{dc} \, d_c (V_{xc}^2 + V_{zc}^2)^{\frac{1}{2}} \int_0^{\ell_0} \rho_{ac} \, y_c \, dy_c$$

$$+ C_{db} \, \rho_{ab} \, A_b |\vec{V}_a| \ell_0\} \tag{3.4.15}$$

Now, if a virtual displacement $\delta u(y_c,t)$ is imposed, the variations in the radius vector $\vec{R}_{Eb}$ and $\vec{R}_{Ec}$ are given by

$$\delta_u \, \vec{R}_{Eb} = 0 \tag{3.4.16}$$

and

$$\delta_u \, \vec{R}_{Ec} = \delta u(y_c,t) \vec{i}_c \tag{3.4.17}$$

Equation (3.4.16) is as expected because displacement u is not relevant to $\vec{R}_{Eb}$. It implies that the aerodynamic force acting on the subsatellite does no work due to the virtual displacement δu, thus contributing nothing to the generalized force Q_{ua}.

The virtual work $\delta_u(d\,W_{ac})$ done by the aerodynamic force acting on an element dy_c of the tether is given by

$$\delta_u(dW_{ac}) = (\vec{f}_c \cdot \vec{i}_c)\delta u(y_c,t) \tag{3.4.18}$$

Using (3.2.15) and (3.2.16)

$$\delta_u(d\,W_{ac}) = -\frac{1}{2} C_{dc} \cdot d_c\, \rho_{ac}(V_{xc}^2 + V_{zc}^2)^{\frac{1}{2}} V_{xc}\, dy_c \cdot \delta u(y_c,t)$$

$$= Q_{ua}\, dy_c\, \delta u(y,t) \tag{3.4.19}$$

where Q_{ua} is the generalized force corresponding to u per unit length of the tether acting on y_c. Clearly,

$$Q_{ua} = -\frac{1}{2} C_{dc}\, d_c\, \rho_{ac}\, (V_{xc}^2 + V_{zc}^2)^{\frac{1}{2}} V_{xc} \tag{3.4.20}$$

Similarly, the generalized force Q_{wa} corresponding to W can be obtained as

$$Q_{wa} = -\frac{1}{2} C_{dc}\, d_c\, \rho_{ac}\, (V_{xc}^2 + V_{zc}^2)^{\frac{1}{2}} V_{zc} \tag{3.4.21}$$

As opposed to the case of virtual displacements δu and δw, the work done due to the virtual displacement δv is dependent on the aerodynamic force applied on the subsatellite. This is because $v(\ell_0,t) \neq 0$ at the subsatellite end while $u(\ell_0,t)$ and $w(\ell_0,t)$ are. From (3.4.2) and (3.4.3),

$$\delta_v \vec{R}_{Eb} = \delta v(\ell_0,t)\vec{j}_c \tag{3.4.22}$$

and

$$\delta_v \vec{R}_{Ec} = \delta v(y_c,t)\vec{j}_c \tag{3.4.23}$$

The virtual work $\delta_v(dW_{ac})$ due to the aerodynamic force acting on the element dy_c of the tether corresponding to virtual displacement $\delta v(y_c,t)$ is given by

$$\begin{aligned}\delta_v(dW_{ac}) &= \vec{f}_c \cdot \delta_v \vec{R}_c \\ &= \delta v(y_c,t)\vec{f}_c \cdot \vec{j}_c \end{aligned} \tag{3.4.24}$$

Since by definition

$$\delta_v(dW_{ac}) = Q_{va}\, dy_c \cdot \delta v(y_c,t) \ , \tag{3.4.25}$$

using (3.2.15), (3.2.16) and (3.4.25)

$$Q_{va} = -\frac{1}{2} C_{dc}\, d_c\, \rho_{ac}\, (V_{xc}^2 + V_{zc}^2)^{\frac{1}{2}}\, V_{yc} \tag{3.4.26}$$

Where Q_{va} is the generalized force applied on the tether corresponding to v.

The virtual work done by the aerodynamic forces acting on the subsatellite due to the virtual displacement $\delta v(\ell_0,t)$ is given by

$$\begin{aligned}\delta_v W_{ab} &= \delta v(\ell_0,t)\ \vec{F}_b \cdot \vec{j}_c \\ &= Q_{vab} \cdot \delta v(\ell_0,t) \quad \text{(say)}\end{aligned} \tag{3.4.27}$$

Using (3.2.12) and (3.2.14)

$$Q_{vab} = - \frac{1}{2} C_{db} \rho_{ab} A_b |\vec{V}_a| V_{yc} \qquad (3.4.28)$$

As will be seen later, this Q_{vab} gives rise to a dynamic boundary condition for the longitudinal vibrations.

CHAPTER 4

DISCRETIZATION OF THE EQUATIONS GOVERNING VIBRATIONS USING GALERKIN'S METHOD

4.1 INTRODUCTORY REMARKS

We have already obtained a hybrid set of differential equations to describe the dynamics of the system. For α and γ, they are ordinary differential equations, because α and γ are functions of time only. For u, v, w, they are partial differential equations because u, v and w are not only functions of time but also of the space coordinate, i.e., at different y_c, u, v, w are different.

It is difficult if not impossible to get analytical solutions for these equations for given initial conditions, since the equations are non-linear, non-autonomous and coupled to each other. Therefore, we have to use an approximate method and get numerical solutions using a computer.

Generally for linear partial differential equations with constant coefficients the exact solution can be expressed in the form of separated variables as follows:

$$u = \sum_{i=1}^{\infty} T_i^u(t)\, Y_i^u(y_c) \tag{4.1.1}$$

$$v = \sum_{i=1}^{\infty} T_i^v(t)\, Y_i^v(y_c) \tag{4.1.2}$$

$$w = \sum_{i=1}^{\infty} T_i^w(t)\, Y_i^w(y_c) \tag{4.1.3}$$

where $Y_i^u(y_c)$, etc. are so called characteristic functions or modes. However, in the present case the equations are nonlinear and the length is time-dependent; thus one does not know if expansions of the form (4.1.1-4.1.3) are strictly correct or not. In any case, there are no modes Y_i^u, etc. in the classical sense if the length varies with time. However, one can express u, v and w <u>approximately</u> as

$$u = \ell_0 \sum_{i=1}^{n} A_i(t)\ \phi_i(y_c;\ell_0) \equiv \sum_{i=1}^{n} \tilde{A}_i\ \phi_i \tag{4.1.4}$$

$$w = \ell_0 \sum_{i=1}^{n} B_i(t)\ \phi_i(y_c;\ell_0) \equiv \sum_{i=1}^{n} \tilde{B}_i\ \phi_i \tag{4.1.5}$$

$$v = \ell_0 \sum_{i=1}^{p} C_i(t)\ \psi_i(y_c;\ell_0) \equiv \sum_{i=1}^{p} \tilde{C}_i\ \psi_i \tag{4.1.6}$$

Here ϕ_i and ψ_i are not modes, but a set of admissible functions satisfying at least the geometric boundary conditions. The problem that remains is to determine $A_i(t)$, $B_i(t)$ and $C_i(t)$ appropriately so that the errors involved in satisfying the equations of motion are reduced to as small as possible. In this thesis, Galerkin's method is used to minimize the errors.

While choosing the admissible functions, there are a variety of functions that could be candidates. Often, harmonic functions are selected due to their nice properties such as orthogonality and smoothness. At both ends ($y_c = 0$ and $y_c = \ell_0(t)$), u and w must be zero. Thus we can use the same set of admissible functions for both u and w, i.e.,

$$\phi_i(y_c;\ell_0) = \sqrt{2}\ \sin\ (i\pi y_c/\ell_0) \tag{4.1.7}$$

For displacement v, we have only one geometric boundary condition at $y_c = 0$ end given by $v(0,t) = 0$. At the $y_c = \ell_0(t)$ end, where the subsatellite is attached to the tether, the dynamic boundary condition (2.11.9) holds good which expresses a force equilibrium condition. Some mechanical understanding might be useful in choosing the admissible functions ψ_i in the expansion of v.

The tension τ in a <u>straight</u> tether is related to v through

$$\tau = EA \frac{\partial v}{\partial y_c} \tag{4.1.8}$$

It is caused mainly by the gravity gradient and the centrifugal force. This tension, in the static case, can be shown to vary quadratically with y_c (as $a + by_c^2$). From (4.1.8) then v_s, the corresponding static longitudinal displacement, has a form

$$v_s = \tilde{C}_1 \, y_c + \tilde{C}_2 \, y_c^{\,3} \tag{4.1.9}$$

If the tether is vibrating longitudinally due to the elasticity of the tether, it will have time-dependent tension. Thus $\tilde{C}_1$ and $\tilde{C}_2$ in (4.1.9) become time-dependent. In addition, some other longitudinal displacement terms may be included. One can simply analyse an elastic tether fixed at one end and a concentrated mass at the other and find the first mode of vibration as

$$v_d = \tilde{C}_3(t) \sin \left[(\rho_c \, \ell_0/M_b)^{\frac{1}{2}}(y_c/\ell_0)\right] \tag{4.1.10}$$

This suggests that an appropriate form of displacement v is

$$v = \tilde{C}_1(t)y_c + \tilde{C}_2(t)y_c^3 + \tilde{C}_3(t)\sin[(\rho_c \ell_0/M_b)^{\frac{1}{2}}(y_c/\ell_0)] \quad (4.1.11)$$

However, the third term nearly represents the same variation with y_c as the first two terms if $\rho_c \ell_0$ is small compared to M_b. Towards the terminal phase of retrieval of the subsatellite, this is valid more and more precisely. Therefore, the third term can be combined into the first two terms. This suggests a representation of the form

$$v = \tilde{C}_1(t)y_c + \tilde{C}_2(t)y_c^3, \quad (4.1.12)$$

or in nondimensional form

$$v/\ell_0 = C_1(y_c/\ell_0) + C_2(y_c/\ell_0)^3 \quad (4.1.13)$$

Thus in this thesis ψ_i in (4.1.6) are chosen as

$$\psi_i = (y_c/\ell_0)^{2i-1} \quad , \quad i = 1,2,\ldots,p. \quad (4.1.14)$$

In actual calculations, p is equal to 2. Generally, if more terms are chosen, less error is involved because a higher dimensional space is used to minimize the errors in the equations. However, the computing cost is also greatly increased. Since one cannot choose too many terms due to limitation on computer expenses, a mechanical understanding helps to choose the most important terms. Although only two terms are used in numerical computations, the trend is likely to remain the same if more terms are used.

4.2 DERIVATION OF ORDINARY DIFFERENTIAL EQUATIONS FOR GENERALIZED COORDINATES α, γ, A_i, B_i, C_i

Substituting expressions (4.1.4 - 4.1.7) and (4.1.14) into α, γ, u, v and w equations and using Galerkin's method, a set of ordinary differential equations can be obtained for the generalized coordinates α, γ, A_i, B_i, C_i. Only two terms are retained in the expansions of u, v and w henceforth implying i = 1,2. Thus one obtains eight second order ordinary differential equations corresponding to α, γ, A_1, A_2, B_1, B_2, C_1 and C_2.

For the α and γ equations, the integral terms in equations (2.11.1 - 2.11.2) are evaluated. After integration with respect to y_c and substitution of limits, y_c coordinate vanishes and one gets

$$f_\alpha(\ddot{\alpha},\dot{\alpha},\alpha,\ddot{\gamma},\dot{\gamma},\dot{\gamma},\ddot{A}_1,\ldots,\ddot{\ell}_0,\dot{\ell}_0,\ell_0) = 0 \tag{4.2.1}$$

and

$$f_\gamma(\ddot{\gamma},\dot{\gamma},\gamma,\ddot{\alpha},\dot{\alpha},\alpha,\ddot{A}_1,\ldots,\ddot{\ell}_0,\dot{\ell}_0,\ell_0) = 0 \tag{4.2.2}$$

Denoting u and w equations (2.11.3) and (2.11.5) as $A_u = 0$ and $A_w = 0$, respectively, Galerkin's method yields

$$\int_0^{\ell_0} A_u\, \phi_m dy_c = 0, \qquad m = 1,2 \tag{4.2.3}$$

and

$$\int_0^{\ell_0} A_w\, \phi_m dy_c = 0, \qquad m = 1,2 \tag{4.2.4}$$

Similarly, denoting v equation (2.11.7) as $A_v = 0$ and the boundary condition (2.11.9) as $\bar{A}_v = 0$, one obtains

$$\rho_c \int_0^{\ell_0} A_v \psi_m dy_c + \bar{A}_v = 0, \qquad m = 1,2 \tag{4.2.5}$$

from a variational formulation. It may be noted that ψ_m are not comparison functions but admissible functions and do not satisfy the dynamic boundary condition $\bar{A}_v = 0$. Thus a variational formulation starting from the energy integrals yields an additional term in (4.2.5). Omission of this term would result in drastically incorrect results.

Although the principles are straight-forward, the algebra involved is very lengthy and time-consuming. Some of the steps in the transformation of α equation and discretization of u equation are given in Appendix F. Those for γ, v and w are omitted from the Appendix for the sake of brevity. The resulting ordinary differential equations are nondimensionalized by using the true anomaly θ as the independent variable as opposed to time t. This is carried out by using

$$\frac{d}{dt}(\ ) \equiv (\ )^{\bullet} = \dot{\theta}\frac{d}{d\theta}(\ ) \equiv \dot{\theta}(\ )' \tag{4.2.6}$$

where prime refers to differentiation with respect to θ. Furthermore,

$$\frac{d^2}{dt^2}(\ ) = \frac{d}{dt}[\dot{\theta}\frac{d}{d\theta}(\ )] = \dot{\theta}\frac{d}{d\theta}[\dot{\theta}\frac{d}{d\theta}(\ )]$$

$$= \dot{\theta}^2 \frac{d^2(\ )}{d\theta^2} + \dot{\theta}\frac{d\dot{\theta}}{d\theta}\frac{d(\ )}{d\theta}$$

$$= \dot{\theta}^2 [\{\frac{d^2}{d\theta^2} - F(\theta)\frac{d}{d\theta}\}(\ )] \tag{4.2.7}$$

Here,

$$\frac{d\dot{\theta}}{d\theta} = -\dot{\theta}\ F(\theta) \tag{4.2.8}$$

and using (2.8.1) and (2.8.2) it can be shown that

$$F(\theta) = 2\ e\ s\theta/[1 + e\ c\theta] \tag{4.2.9}$$

In addition, a dimensionless length may be introduced as

$$\eta = \ell n[\ell_0/\ell_{ref}] \tag{4.2.10}$$

where ℓ_{ref} is a reference length, a constant. Clearly,

$$\eta' = \ell_0'/\ell_0 \tag{4.2.11}$$

With the definitions above, equations (4.2.1 - 4.2.5) yield the following:

<u>α equation</u>

$$\begin{aligned}
&(1 + \tfrac{1}{3}\nu)\{(\alpha''-F-F\alpha')\ c^2\gamma-2s\gamma c\gamma\gamma'(1+\alpha')+3s\alpha c\alpha c^2\gamma/(1 + e\ c\theta)\} \\
&+ 2(1+\alpha')c^2\gamma[(1+ \tfrac{1}{2}\nu)\eta' + \sum_{i=1}^{n} (C_i'+\eta' C_i)]-(2K\nu) \sum_{i=1}^{n} \{[1-(-1)^i]/i\} \\
&\cdot\{(\eta''-F\eta'+3\eta'^2)c\gamma-\eta'\gamma' s\gamma]B_i+\eta' c\gamma B_i'\}-(K\nu) \sum_{i=1}^{n} [(-1)^i/i] \\
&\cdot\{[B_i''+(6\eta'-F)B_i'+3(\eta''-F\eta'+3\eta'^2)B_i]c\gamma+[c\gamma\gamma'^2+(\gamma''-F\gamma') \\
&s\gamma]B_i\}+2\nu\{[(\alpha''-F-F\alpha')c^2\gamma-2s\gamma c\gamma\gamma'(1+\alpha')+3\eta'(1+\alpha')c^2\gamma] \sum_{i=1}^{n} \frac{C_i}{(2i+1)} \\
&+(1+\alpha')c^2\gamma \sum_{i=1}^{n} \frac{C_i'}{(2i+1)}\}-(2K\nu) \sum_{i=1}^{n} [\frac{(-1)^i}{i}]\{[(\alpha''-F-F\alpha')s\gamma c\gamma+(1+\alpha')c(2\gamma)\gamma' \\
&+3(1+\alpha')s\gamma c\gamma\eta']A_i+(1+\alpha')s\gamma c\gamma A_i'\} = P_\alpha + S_\alpha
\end{aligned} \tag{4.2.12}$$

where P_α and S_α are the nondimensionalized generalized forces corresponding to α due to the aerodynamic forces and control forces if any, respectively. The parameter ν is the ratio between the mass of the tether and that of the subsatellite, i.e.,

$$\nu = \rho_c \ell_0 / M_b \tag{4.2.13}$$

and

$$K = (\sqrt{2}/\pi) \tag{4.2.13'}$$

In the case of n=p=2, i.e., if only A_1, A_2, B_1, B_2, C_1 and C_2 are retained, then equation (4.2.12) becomes

$$\begin{aligned}
& c^2\gamma[\alpha''-F-F\alpha'](1+\frac{1}{3}\nu)-2s\gamma c\gamma\gamma'(1+\alpha')(1+\frac{1}{3}\nu) \\
& + c^2\gamma(1+\alpha')\{2(\eta'+C_1'+C_2'+\eta'C_1+\eta'C_2)+\nu\eta'\} \\
& + 3\frac{1}{1+e\ c\theta} s\alpha c\alpha c^2\gamma(1+\frac{1}{3}\nu)-4K\nu\{[(\eta''-F\eta'+3\eta'^2)c\gamma \\
& - \eta'\gamma's\gamma]B_1+\eta'c\gamma B_1'\}+(K\nu/2)\{[2B_1''-B_2'']c\gamma+(6\eta'-F)c\gamma(2B_1'-B_2') \\
& + [(3\eta''-3F\eta'+9\eta'^2)c\gamma+c\gamma\gamma'^2+s\gamma(\gamma''-F\gamma')](2B_1-B_2)\} \\
& + 2\nu\{[(\alpha''-F-F\alpha')c^2\gamma-2s\gamma c\gamma\gamma'(1+\alpha')+3\eta'(1+\alpha')c^2\gamma](\frac{1}{3}C_1+\frac{1}{5}C_2) \\
& + (1+\alpha')c^2\gamma(\frac{1}{3}C_1'+\frac{1}{5}C_2')\}+K\nu\{[(\alpha''-F-F\alpha')s\gamma c\gamma+(1+\alpha')c(2\gamma)\gamma' \\
& + 3(1+\alpha')s\gamma c\gamma\eta'](2A_1-A_2)+(1+\alpha')s\gamma c\gamma(2A_1'-A_2')\} = P_\alpha + S_\alpha
\end{aligned} \tag{4.2.14}$$

γ equation

$$[\gamma''-F\gamma'](1+\frac{1}{3}\nu)+\gamma'\{2(\eta'+C_1'+C_2'+\eta'C_1+\eta'C_2)+\nu\eta'\}+\{(1+\alpha')^2$$

$$+\frac{3}{1+e\,c\theta}c^2\alpha\}s\gamma c\gamma(1+\frac{1}{3}\nu)+4K\nu\{[\eta''-F\eta'+3\eta'^2]A_1+\eta'A_1'\}$$

$$-(K\nu/2)\{(2A_1''-A_2'')+(6\eta'-F)(2A_1'-A_2')+(3\eta''-3F\eta'+9\eta'^2)(2A_1-A_2)\}$$

$$+(K\nu/2)\ \{2(1+\alpha')s\gamma(2B_1'-B_2')+(2B_1-B_2)[(\alpha''-F-F\alpha')s\gamma+(1+\alpha')c\gamma\gamma'$$

$$+6(1+\alpha')s\gamma\eta']\}+2\nu\{(\gamma''-F\gamma'+3\eta'\gamma')(\frac{1}{3}C_1+\frac{1}{5}C_2)+\gamma'(\frac{1}{3}C_1'+\frac{1}{5}C_2')\}$$

$$=P_\gamma+S_\gamma \tag{4.2.15}$$

where P_γ and S_γ are dimensionless generalized forces corresponding to γ due to the aerodynamic forces and control forces if any, respectively.

A_1 equation

$$A_1''+(3\eta'-F)A_1'-\frac{8}{3}A_2'+[\frac{3}{2}(\eta''-F\eta')+(2-\frac{\pi^2}{3})\eta'^2]A_1$$

$$+[-\frac{4}{3}(\eta''-F\eta')-\frac{76}{9}\eta'^2]A_2-4K\eta'\gamma'-K(\gamma''-F\gamma')$$

$$-K(1+\alpha')^2s\gamma c\gamma-2K\gamma'\{C_1'+(1-\frac{6}{\pi^2})(C_2'-2\eta'C_2)\}$$

$$-3Kc^2\alpha s\gamma c\gamma/(1+ec\theta)+\pi^2\Omega^2\{[C_1+(1+\frac{3}{2\pi^2})C_2]A_1-\frac{20}{9\pi^2}A_2C_2$$

$$+\pi^2[\frac{3}{4}A_1^3+\frac{3}{4}A_1B_1^2+6A_1A_2^2+4A_2B_1B_2+2A_1B_2^2]\}$$

$$-2(1+\alpha')s\gamma(B_1'+\frac{3}{2}\eta'B_1)-\frac{8}{3}(1+\alpha')s\gamma\eta'B_2$$

$$-\{[(\alpha''-F(\alpha'+1)]s\gamma+\gamma'c\gamma(1+\alpha')\}B_1=P_{A1} \tag{4.2.16}$$

where P_{A1} is the nondimensionalized generalized force corresponding to the generalized coordinate A_1 due to the aerodynamic forces while Ω is defined by

$$\Omega = (EA/\rho_c \, \ell_0^2 \, \dot{\theta}^2)^{\frac{1}{2}} \tag{4.2.17}$$

Ω is related to the frequencies ω_n of transverse vibrations of the tether in the linearized case as follows:

$$\omega_n/\dot{\theta} = n\pi(EAC_1/\rho_c \, \ell_0^2)^{\frac{1}{2}}/\dot{\theta} = n\pi\Omega(C_1)^{\frac{1}{2}} \tag{4.2.18}$$

A_2 equation

$$\begin{aligned}
&A_2''+(3\eta'-F)A_2'+\frac{8}{3}A_1'+[\frac{4}{3}(\eta''-F\eta')-\frac{4}{9}\eta'^2]A_1 \\
&+[\frac{3}{2}(\eta''-F\eta')+(2-\frac{4}{3}\pi^2)\eta'^2]A_2+(K/2)(\gamma''-F\gamma')+(K/2)(1+\alpha')^2 s\gamma c\gamma \\
&+K\gamma'\{C_1'+(1-\frac{3}{2\pi^2})(C_2'-2\eta' C_2)\}+\frac{3}{2}Kc^2\alpha s\gamma c\gamma/(1+e\, c\theta) \\
&+4\pi^2\Omega^2\{[C_1+(1+\frac{3}{8\pi^2})C_2]A_2-\frac{5}{9\pi^2}A_1C_2+\pi^2[1.5A_1^2A_2+3A_2^3+A_1B_1B_2 \\
&+3A_2B_2^2+0.5A_2B_1^2]\}-2(1+\alpha')s\gamma(B_2'+2\eta' B_2)+\frac{8}{3}(1+\alpha')\eta' s\gamma B_1 \\
&-\{[\alpha''-F(1+\alpha')]s\gamma+(1+\alpha')c\gamma\gamma'\}B_2 = P_{A_2}
\end{aligned} \tag{4.2.19}$$

where P_{A_2} is the nondimensionalized generalized force corresponding to A_2 due to aerodynamic forces.

B_1 equation

$$B_1''+(3\eta'-F)B_1'-\frac{8}{3}B_2'+[\frac{3}{2}(\eta''-F\eta')+(2-\frac{\pi^2}{3})\eta'^2]B_1$$

$$+[-\frac{4}{3}(\eta''-F\eta')-\frac{76}{9}\eta'^2]B_2+4K\eta'(1+\alpha')c\gamma+K\{[\alpha''-F(1+\alpha')]c\gamma$$

$$-2(1+\alpha')\gamma's\gamma\}+2K(1+\alpha')c\gamma\{C_1'+(1-\frac{6}{\pi^2})(C_2'-2\eta'C_2)\}$$

$$+3Ks\alpha c\alpha c\gamma/(1+e\ c\theta)+\pi^2\Omega^2\{[C_1+(1+\frac{3}{2\pi^2})C_2]B_1-\frac{20}{9\pi^2}B_2C_2$$

$$+\pi^2[\frac{3}{4}B_1{}^3+\frac{3}{4}B_1A_1{}^2+6B_1B_2{}^2+4B_2A_1A_2+2B_1A_2{}^2]\}$$

$$+2(1+\alpha')s\gamma(A_1'+\frac{3}{2}\eta'A_1)+\frac{8}{3}(1+\alpha')s\gamma\eta'A_2+\{[\alpha''-F(1+\alpha')]s\gamma$$

$$+\gamma'c\gamma(1+\alpha')\}A_1 = P_{B1} \tag{4.2.20}$$

where P_{B1} is the nondimensionalized generalized force corresponding to B_1 due to aerodynamic forces.

B_2 equation

$$B_2''+(3\eta'-F)B_2'+\frac{8}{3}B_1'+[\frac{4}{3}(\eta''-F\eta')-\frac{4}{9}\eta'^2]B_1$$

$$+[\frac{3}{2}(\eta''-F\eta')+(2-\frac{4}{3}\pi^2)\eta'^2]B_2-(K/2)\{[\alpha''-F(1+\alpha')]c\gamma$$

$$-2(1+\alpha')\gamma's\gamma\}-(3K/2)s\alpha c\alpha c\gamma/(1+e\ c\theta)-K\ (1+\alpha')c\gamma[C'_1$$

$$+(1-\frac{3}{2\pi^2})(C_2'-2\eta'C_2)]+4\pi^2\Omega^2\{[C_1+(1+\frac{3}{8\pi^2})C_2]B_2-\frac{5}{9\pi^2}B_1C_2$$

$$+\pi^2[1.5B_1{}^2B_2+3B_2^3+B_1A_1A_2+3B_2A_2{}^2+0.5B_2A_1{}^2]\}+2(1+\alpha')s\gamma(A_2'+2\eta'A_2)$$

$$-\frac{8}{3}(1+\alpha')s\gamma\eta'A_1+\{[\alpha''-F(1+\alpha')]s\gamma+\gamma'(1+\alpha')c\gamma\}A_2 = P_{B_2} \tag{4.2.21}$$

where P_{B2} is the nondimensionalized generalized force corresponding to B_2 due to the aerodynamic forces.

C₁ equation

$$(1+\frac{1}{2}\nu+C_1+C_2)(\eta''-F\eta'+\eta'^2)+(1+\frac{1}{3}\nu)(C_1''-FC_1')$$

$$+(1+\frac{1}{5}\nu)(C_2''-F\ C_2')+(2+\nu)\eta'C_1'+(2+\frac{7}{10}\nu)\eta'C_2'$$

$$-(1+\frac{1}{3}\nu)\{(1+\alpha')^2c^2\gamma+\gamma'^2+\frac{1}{1+e\ c\theta}(3c^2\alpha c^2\gamma-1)\}$$

$$+\omega_\varepsilon^{\ 2}\{C_1+C_2+\frac{\pi^2}{2}(A_1^{\ 2}+4A_2^{\ 2}+B_1^{\ 2}+4B_2^{\ 2})\}-K\nu\{[(\alpha''-F\alpha'-F)c\gamma$$

$$-(1+\alpha')s\gamma\gamma'](2B_1-B_2)+(1+\alpha')c\gamma[(2B_1'-B_2')+3\eta'(2B_1-B_2)]$$

$$-(\gamma''-F\gamma')(2A_1-A_2)-\gamma'[(2A_1'-A_2')+3\eta'(2A_1-A_2)]\}=P_{C1}+S_{C1} \qquad (4.2.22)$$

where P_{C1} and S_{C1} are the nondimensionalized generalized forces corresponding to C_1 due to the aerodynamic and control forces, respectively, and

$$\omega_\varepsilon^{\ 2}=EA/M_b\,\ell_0\,\dot{\theta}^2 \qquad (4.2.22')$$

Modified C₂ equation

$$\frac{1}{2}(\eta''-F\eta'+\eta'^2)+\frac{2}{15}(C_1''-FC_1')+\frac{2}{35}(C_2''-FC_2')+\frac{1}{2}\eta'C_1'$$

$$+\frac{19}{70}\eta'C_2'-\frac{2}{15}[(1+\alpha')^2c^2\gamma+\gamma'^2+\frac{1}{1+e\ c\theta}(3c^2\alpha c^2\gamma-1)]+\Omega^2\{-\frac{4}{5}C_2$$

$$-\frac{3}{4}(A_1^{\ 2}+A_2^{\ 2}+B_1^{\ 2}+B_2^{\ 2})+\frac{40}{3}(A_1A_2+B_1B_2)\}-(12K/\pi^2)\{(\alpha''-F\alpha'$$

$$-F)c\gamma(B_1-\frac{1}{8}B_2)-(1+\alpha')s\gamma\gamma'(B_1-\frac{1}{8}B_2)+(1+\alpha')c\gamma[(B_1'-\frac{1}{8}B_2')$$

...

...

$$+\ 3\eta'(B_1 - \frac{1}{8}B_2)] - (\gamma'' - F\gamma')(A_1 - \frac{1}{8}A_2) - \gamma'[(A_1' - \frac{1}{8}A_2')$$

$$+\ 3\eta'(A_1 - \frac{1}{8}A_2)]\} + 4K(1 - \frac{6}{\pi^2})[(1+\alpha')c\gamma\eta' B_1 - \gamma'\eta' A_1]$$

$$-\ 2K(1 - \frac{3}{2\pi^2})[(1+\alpha')c\gamma\eta' B_2 - \gamma'\eta' A_2] = P_{C2} + S_{C2} \qquad (4.2.23)$$

where P_{C2} and S_{C2} are the nondimensionalized generalized forces corresponding to C_2 due to the aerodynamic control forces, respectively.

Using (3.4.14), (3.4.15), (3.4.20), (3.4.21) and (3.4.26) the generalized forces P_α, P_{A1}, etc. can be shown to be

$$P_\alpha = -\frac{1}{2}c\gamma V_{zc}/(M_b\,\ell_0^2\,\dot{\theta}^2)\{C_{dc}\,d_c(V_{xc}^2+V_{zc}^2)^{\frac{1}{2}}\int_0^{\ell_0} y_c\,\rho_a\,dy_c$$

$$+\ C_{db}\,\rho_{ab}\,A_b|\vec{V}_a|\ell_0\} \qquad (4.2.24)$$

$$P_\gamma = \frac{1}{2}V_{xc}/(M_b\,\ell_0^2\,\dot{\theta}^2)\{C_{dc}\,d_c(V_{xc}^2+V_{zc}^2)^{\frac{1}{2}}\int_0^{\ell_0} y_c\,\rho_a\,dy_c$$

$$+\ C_{db}\,\rho_{ab}\,A_b|\vec{V}_a|\ell_0\} \qquad (4.2.25)$$

$$P_{A1} = [\int_0^{\ell_0} Q_{ua}\sqrt{2}\,\sin\,(\pi y_c/\ell_0)dy_c]/\rho_c\,\ell_0^2\,\dot{\theta}^2 \qquad (4.2.26)$$

$$P_{A2} = [\int_0^{\ell_0} Q_{ua}\sqrt{2}\,\sin\,(2\pi y_c/\ell_0)dy_c]/\rho_c\,\ell_0^2\,\dot{\theta}^2 \qquad (4.2.27)$$

$$P_{B1} = \int_0^{\ell_0} Q_{wa}\sqrt{2}\,\sin\,(\pi y_c/\ell_0)dy_c/\rho_c\,\ell_0^2\,\dot{\theta}^2 \qquad (4.2.28)$$

$$P_{B2} = \int_0^{\ell_0} Q_{wa}\sqrt{2}\,\sin\,(2\pi y_c/\ell_0)dy_c/\rho_c\,\ell_0^2\,\dot{\theta}^2 \qquad (4.2.29)$$

$$P_{C1} = \{Q_{vab} + \int_0^{\ell_0} Q_{va}(y_c/\ell_0)dy_c\}/M_b\, \ell_0\, \dot{\theta}^2 \tag{4.2.30}$$

$$P_{C2} = \int_0^{\ell_0} Q_{va}[(y_c/\ell_0)-(y_c/\ell_0)^3]dy_c/\rho_c\, \ell_0^2\, \dot{\theta}^2 \tag{4.2.31}$$

Since ρ_a is assumed to vary exponentially with y_c as shown in equation (3.3.2), the integrals in the above generalized forces can be carried out exactly. Let us define the following nondimensional parameters

$$\delta = \{1 + (a_0^2-b_0^2)s^4i\; s^2\theta\; c^2\theta/[b_0^2 + (a_0^2-b_0^2)s^2i\; s^2\theta]\}^{-\frac{1}{2}} \tag{4.2.32}$$

$$\xi_1 = (R_0-R_{earth})\;\delta/h_0 \tag{4.2.33}$$

and

$$\xi_2 = \ell_0\; c\alpha\; c\gamma\; \delta/h_0 \tag{4.2.34}$$

Using equations (3.3.2), (3.3.4), (3.3.5), (3.4.20), (3.4.21) (3.4.26) and (3.4.28), after considerable algebra one obtains

$$P_\alpha = -\frac{1}{2} c\gamma\; V_{zc}\; \{C_{db}\; A_b\; \exp(-\xi_1-\xi_2)|\vec{V}_a|$$

$$+ C_{dc}\; d_c\; \ell_0\; (V_{xc}^{\;2}+V_{zc}^{\;2})^{\frac{1}{2}} \exp(-\xi_1)[-\frac{\exp(-\xi_2)}{\xi_2}(1+\frac{1}{\xi_2})$$

$$+ \frac{1}{\xi_2^{\;2}}]\;/M_b\; \ell_0\; \dot{\theta}^2 \tag{4.2.35}$$

$$P_\gamma = -V_{xc}\; P_\alpha/(V_{zc}\; c\gamma) \qquad (4.2.3.6)$$

$$P_{Ai} = -\frac{1}{2} C_{dc}\, d_c (V_{xc}{}^2 + V_{zc}{}^2)^{\frac{1}{2}}\, V_{xc} (\rho_{00}/\rho_c)/(\dot{\theta}^2\, \ell_0)$$

$$\cdot \frac{\sqrt{2}\, i\pi \exp(-\xi_1)}{(\xi_2{}^2 + i^2\pi^2)} \{1 - (-1)^i \exp(-\xi_2)\} \quad , \; i = 1,2. \tag{4.2.37}$$

$$P_{Bi} = V_{zc}\, P_{Ai}/V_{xc} \qquad i = 1,2 \tag{4.2.38}$$

$$P_{C1} = -\frac{1}{2} V_{yc} (\rho_{00}/\rho_c)/\ell_0\, \dot{\theta}^2 \{C_{db}\, A_b |\vec{V}_a| \exp(-\xi_1 - \xi_2)$$

$$+ C_{dc}\, d_c\, \ell_0 (V_{xc}^2 + V_{zc}{}^2)^{\frac{1}{2}} \exp(-\xi_1)[-\frac{\exp(-\xi_2)}{\xi_2}(1 + \frac{1}{\xi_2})$$

$$+ \frac{1}{\xi_2{}^2}]\} \tag{4.3.39}$$

$$P_{C2} = -\frac{1}{2} V_{yc} (\rho_{00}/\rho_c)/\ell_0\, \dot{\theta}^2 (C_{dc}\, d_c\, \ell_0)(V_{xc}{}^2 + V_{zc}{}^2)^{\frac{1}{2}} \frac{1}{\xi_2{}^2} \{1 - \frac{6}{\xi_2{}^2}$$

$$+ e^{-\xi_2}(2 + \frac{6}{\xi_2} + \frac{6}{\xi_2{}^2})\} \tag{4.2.40}$$

The nondimensionalized control forces S_α, S_γ, S_{C1} and S_{C2} are dependent on what kind of actuators are used. If there is no active control device apart from the tension control mechanism, then all of them are zero. On the other hand, if thrusters are placed on the subsatellite to help control the motion (as is done in Chapter 9), S_α, S_γ, etc. are nonzero.

4.3 NUMERICAL METHOD

For given initial conditions and specified length variation, the equations developed in Section 4.2 for the nondimensionalized generalized coordinates α, γ, A_1, A_2, B_1, B_2, C_1 and C_2 are solved numerically using a computer. The equations (4.2.14-4.2.16), (4.2.19-

4.2.21), (4.2.22-4.2.23) after some transformation and the length equation determined from the control law (nine in all) can be arranged in a matrix form as

$$[A]\{q''\} = \{T\} \tag{4.3.1}$$

where the vector {q} is given by

$$\{q\}^T = [\eta, \alpha, \gamma, C_1, C_2, A_1, A_2, B_1, B_2] \tag{4.3.2}$$

and [A] is given in Appendix G.

Here, η, the nondimensionalized length, is an input, while α, γ, A_1, A_2, B_1, B_2, C_1 and C_2 are outputs. The goal of the dynamical control considered in the second half of this thesis is to find a length rate η' or acceleration η'' using the feedback of the generalized coordinates α, γ, A_1, A_2, B_1, B_2, C_1, C_2, and their derivatives so that all outputs α, γ, A_1, A_2, B_1, B_2, C_1 and C_2 are stable during the retrieval process. Hence, we have added an η'' equation from the consideration of control law to the equations of motion.

In equation (4.3.1), [A] is a square matrix dependent on time and {q} while {T} is a column vector, again depending on time and {q}, and in addition {q'}.

For the convenience of numerical integration, let us define a set of state variables Y_j (j = 1, 18) as

$$\{Y\} = \begin{Bmatrix} \{q\} \\ \{q'\} \end{Bmatrix} \tag{4.3.3}$$

where the vector {q} is given by (4.3.2).

Then the second order matrix differential equation (4.3.1) can be transformed to an equivalent first order matrix differential equation

$$\{Y'\} \equiv \begin{Bmatrix} \{Y_i'\} \\ \{Y_{9+i}'\} \end{Bmatrix} = \begin{Bmatrix} \{Y_{9+i}\} \\ [A]^{-1}\{T_i\} \end{Bmatrix}, \quad i = 1, 2, \ldots 9, \tag{4.3.4}$$

Equation (4.3.4) is in the right form for numerical integration.

4.3.1 Comments on Numerical Integration

The execution of the computer programme to solve (4.3.4) is very time consuming because of the following main reasons:

(i) The dynamical model involves many state variables. The computing time is dramatically increased with the increased number of variables.

(ii) The set of equations is stiff in the numerical analysis sense. A system is said to be stiff if the time constants vary by several orders of magnitude. In the present case, the frequencies of vibrations are much higher than the frequencies associated with rotational motions α and γ and the difference becomes larger and larger during retrieval. The step size must be chosen to be very small to get the correct vibrational motion.

(iii) The inversion of matrix [A] takes a lot of computer time because the matrix is dependent on time and the generalized co-ordinates and must be inverted at every time step.

We can do very little about (i) and (ii). The dynamical model must be of certain minimum order to represent the actual dynamics of the system reasonably. The tether is vibrating longitudinally and transversely. These vibrations cannot be neglected. Consideration of only rotations may be inexpensive but not representative of the system dynamics.

As for (iii), a semi-analytical inverse programme was developed by using block inverse concept which saves 30% of the computer cost compared with the inversion of the entire matrix using an inversion subroutine.

The IMSL subroutine DGEAR suitable for integrating stiff differential equations is used to solve the equations numerically.

4.3.2 Method of Inverting Matrix [A]

If {q} is ordered in a sequence given in equation (4.3.2), it can be noted that the matrix [A] given in Appendix G involves a unit submatrix, i.e.,

$$[A] = \begin{bmatrix} [A_{11}]_{3\times3} & [A_{12}]_{3\times6} \\ [A_{21}]_{6\times3} & [I]_{6\times6} \end{bmatrix} \tag{4.3.5}$$

Since there is a unit submatrix in [A], the inverse of [A] could be done in an economical way. Let

$$[B] = [A]^{-1} = \begin{bmatrix} [B_{11}]_{3\times3} & [B_{12}]_{3\times6} \\ [B_{21}]_{6\times3} & [B_{22}]_{6\times6} \end{bmatrix} \tag{4.3.6}$$

We have

$$[A][B] = [I]_{9\times9} \tag{4.3.7}$$

Substituting (4.3.5), (4.3.6) into (4.3.7), we get

$$\begin{bmatrix} [A_{11}]_{3\times3} & [A_{12}]_{3\times6} \\ [A_{21}]_{6\times3} & [I]_{6\times6} \end{bmatrix} \begin{bmatrix} [B_{11}]_{3\times3} & [B_{12}]_{3\times6} \\ [B_{21}]_{6\times3} & [B_{22}]_{6\times6} \end{bmatrix} = \begin{bmatrix} [I]_{3\times3} & [0]_{3\times6} \\ [0]_{6\times3} & [I]_{6\times6} \end{bmatrix} \quad (4.3.8)$$

Writing the four submatrix equations and solving for the components of [B], one obtains

$$[B_{11}]_{3\times3} = [[A_{11}]_{3\times3} - [A_{12}]_{3\times6}\,[A_{21}]_{6\times3}]^{-1} \quad (4.3.9)$$

$$[B_{21}]_{6\times3} = -[A_{21}]_{6\times3}\,[B_{11}]_{3\times3} \quad (4.3.10)$$

$$[B_{12}]_{3\times6} = -[B_{11}]_{3\times3}\,[A_{12}]_{3\times6} \quad (4.3.11)$$

and

$$[B_{22}]_{6\times6} = [I]_{6\times6} + [A_{21}]_{6\times3}\,[B_{11}]_{3\times3}\,[A_{12}]_{3\times6} \quad (4.3.12)$$

In this way, the job of an inversion of a 9×9 matrix [A] is reduced to a job of an inversion of a 3×3 matrix, thus saving computing time greatly. Note that inversion is carried out thousands of times for a nonautonomous system.

CHAPTER 5

EQUILIBRIUM STATE

During stationkeeping, the reel mechanism does not reel the tether in or out.* Hence, the nominal unstretched length of the tether remains unchanged. Due to the gravity gradient and centrifugal force acting on the system, the tether remains taut while the atmospheric drag on the subsatellite and the tether forces the subsatellite to lag behind the local vertical. In addition, the tether does not remain straight but becomes slightly curved due to this drag. If the orbit is circular and in the equatorial plane, all the above forces are steady for a constant length tether. An equilibrium configuration can then be found by solving the equations of motion after putting $q_i' = q_i'' = 0$. For different lengths, the equilibrium configurations are clearly different.

If the orbit is elliptic or inclined to the equatorial plane, the above mentioned forces are not steady but change with true anomaly θ. Strictly speaking, in this case no equilibrium configuration exists. However, we can still consider a constant length tether and let $q_i' = q_i'' = 0$. This will yield quasi-static equilibrium positions and will give a broad picture of how the eccentricity of the orbit and the oblateness of the earth affect the quasi-static behaviour of the system.

5.1 STATIC EQUILIBRIUM EQUATIONS

Letting the length of the tether remain constant, putting $q_i' = q_i'' = 0$ and ignoring S_i in (4.2.14-16), (4.2.19-23), the resulting

---

* A small amount of reeling in or out may be required for control purposes.

equations are

$$-c^2\gamma F(1+\frac{1}{3}\nu)+\frac{3}{(1+e\ c\theta)}s\alpha c\alpha c^2\gamma(1+\frac{1}{3}\nu)-2\nu Fc^2\gamma(\frac{1}{3}C_1+\frac{1}{5}C_2)$$

$$-K\nu Fs\gamma c\gamma(2A_1-A_2) = P_\alpha \tag{5.1.1}$$

$$[1+\frac{3}{(1+e\ c\theta)}c^2\alpha]s\gamma c\gamma(1+\frac{1}{3}\nu)-(K\nu/2)Fs\gamma(2B_1-B_2) = P_\gamma \tag{5.1.2}$$

$$(1+\frac{1}{3}\nu)\{c^2\gamma+\frac{1}{(1+e\ c\theta)}(3c^2\alpha c^2\gamma-1)\}+\omega_\varepsilon{}^2\{C_1+C_2+\frac{\pi^2}{2}(A_1{}^2+4A_2{}^2+B_1{}^2+4B_2{}^2)\}$$

$$= P_{C1} \tag{5.1.3}$$

$$-\frac{2}{15}[c^2\gamma+\frac{1}{(1+e\ c\theta)}(3c^2\alpha c^2\gamma-1)]+\Omega^2\{-\frac{4}{5}C_2-\frac{3}{4}(A_1{}^2+A_2{}^2+B_1{}^2+B_2{}^2)$$

$$+\frac{40}{3}(A_1A_2+B_1B_2)\}+(12K/\pi^2)Fc\gamma(B_1-\frac{1}{8}B_2) = P_{C2} \tag{5.1.4}$$

$$-Ks\gamma c\gamma-3K\frac{1}{(1+e\ c\theta)}c^2\alpha s\gamma c\gamma+\pi^2\Omega^2\{A_1[C_1+(1+\frac{3}{2\pi^2})C_2]$$

$$-(20/9\pi^2)A_2C_2+\pi^2[\frac{3}{4}A_1{}^3+\frac{3}{4}A_1B_1{}^2+6A_1A_2{}^2+4A_2B_1B_1+2A_1B_2{}^2]\}$$

$$+Fs\gamma B_1 = P_{A1} \tag{5.1.5}$$

$$\frac{K}{2}s\gamma c\gamma+(3K/2)\frac{1}{(1+e\ c\theta)}c^2\alpha s\gamma c\gamma+\pi^2\Omega^2\{4A_2[C_1+(1+\frac{3}{8\pi^2})C_2]$$

$$-\frac{20}{9\pi^2}A_1C_2+\pi^2[6A_1{}^2A_2+12A_2{}^3+4A_1B_1B_2+12A_2B_2{}^2+2A_2B_1{}^2]\}$$

$$+Fs\gamma B_2 = P_{A2} \tag{5.1.6}$$

$$-KFc\gamma+3K\frac{1}{(1+e\ c\theta)}s\alpha c\alpha c\gamma+\pi^2\Omega^2\{B_1[C_1+(1+\frac{3}{2\pi^2})C_2]$$

$$-(20/9\pi^2)B_2C_2+\pi^2[\frac{3}{4}B_1^3+\frac{3}{4}B_1A_1^2+6B_1B_2^2+4B_2A_1A_2+2B_1A_2^2]\}$$

$$-Fs\gamma A_1 = P_{B1} \tag{5.1.7}$$

$$(KF/2)c\gamma-(3K/2)\frac{1}{(1+e\ c\theta)}s\alpha c\alpha c\gamma+\pi^2\Omega^2\{4B_2[C_1+(1+\frac{3}{8\pi^2})C_2]$$

$$-(20/9\pi^2)B_1C_2+\Omega^2[6B_1^2B_2+12B_2^3+4B_1A_1A_2+12B_2A_2^2+2B_2A_1^2]\}$$

$$-Fs\gamma A_2 = P_{B2} \tag{5.1.8}$$

The equations (5.1.1 - 5.1.8) are static equilibrium equations if the orbit is circular and equatorial, while they are quasi-static equilibrium equations if the orbit is elliptic or inclined to the equatorial plane.

5.2 NUMERICAL RESULTS

The nonlinear algebraic coupled equations (5.1.1 - 5.1.8) were solved numerically using an IMSL subroutine ZSYSTEM, based on a quadratically convergent Newton-like method.

5.2.1 Variation of Static Equilibrium Configuration with Length

A circular orbit in the equatorial plane at an altitude of H = 220 Km was considered. The following system parameters were used:

M_b = 170 (Kg)

d_c = 0.325 (mm)

ρ_c = 0.658 (Kg/Km)

$$E = 2.1 \times 10^{11} \text{ (Newton/m}^2\text{)}$$

$$A_b = 1 \text{ (m}^2\text{)}$$

$$C_{db} = C_{dc} = 2$$

Table 5.1 shows how the equilibrium values of $(\alpha-\pi)$, γ, $\tilde{A}_1$, $\tilde{A}_2$, $\tilde{B}_1$, $\tilde{B}_2$, C_1 and C_2 change with the length of the tether.* The results are plotted in Figure 5.1.

From the table, the following salient features may be noted:

(a) The atmoshperic drag has significant effects when the tethered subsatellite is at a low attitude. At ℓ_0 = 120 Km, the subsatellite lags behind the local vertical by about 27° and the maximum transverse displacement in the orbital plane is about 2.3 Km ($w_{eq}(\ell_0/2) = \sqrt{2}\,\ell_0\, B_1$). Because there is no atmospheric drag in the out-of-plane direction, out-of-plane rotation γ and transverse displacement u are zero.

The effect of atmospheric drag weakens rapidly with the raising of the subsatellite. The reason is that the aerodynamic force is proportional to the atmospheric density which reduces exponentially with the altitude. When the length of the tether is about 90 Km, the in-plane rotation is only 3°; thus the tether is very close to the vertical direction.

(b) Longitudinal displacements characterized by C_1 and C_2 are reduced gradually with the decrease of the length ℓ_0 (as

---

* α is measured from the upward local vertical. Thus $(\alpha-\pi)$ is the deviation from the downward local vertical.

opposed to the rapid change above). The longitudinal displacement is mainly caused by the gravity gradient and centrifugal forces acting on the concentrated-mass subsatellite and distributed-mass tether. These forces are linearly related to the masses of the tether and the subsatellite and the distance of their centres of mass from the center of mass of the system, or, approximately from the centre of mass of the shuttle. Since the subsatellite has a larger mass (constant) compared to the mass of the tether (variable), it is expected that C_1, the linear part of the longitudinal displacement, will dominate the nonlinear part, C_2. (C_1 is nearly proportional to ℓ_0 while C_2 is mainly dependent on the distributed mass of the tether, which is roughly proportional to the square of ℓ_0.) When the tether is short, the effect of the distributed mass of the tether can be neglected compared to the mass of the subsatellite. In that case, the longitudinal displacements along the tether can be assumed to vary linearly with y_c (i.e., the longitudinal strain is constant).

5.2.2 The Effects of Eccentricity and Inclination of the Orbit on Quasi-Static Equilibrium State

The orbit may neither be circular nor be in the equatorial plane. In the former case eccentricity is used to denote the ellipticity of the orbit. In the latter case, inclination angle i describes the inclination of the orbital plane to the equatorial plane.

If the orbit is elliptical, a constant length tethered subsatellite will dive deep into the atmosphere sometimes while at other times it will rise far above the earth's surface. Obviously, the atmospheric drag will vary greatly with true anomaly θ. It is expected that the subsatellite will deviate from the vertical more when it is diving deep into the atmosphere because the corresponding density of atmosphere is larger.

If the orbit is inclined to the equatorial plane, then the oblateness of the earth will affect the altitude of the tethered subsatellite even when the orbit is circular. Strictly speaking, there is no static equilibrium configuration for these two cases as stated in the beginning of this chapter. However, the variation of atmospheric drag is very slow having a period of half the orbital period. Hence, one can assume that the rate terms of the variables are so small that they are negligible (this assumption is valid for vibrations but not so good for rotations). Thus, a quasi-static equilibrium configuration can be calculated at different θ for a given constant length ℓ_0.

In the following calculations, ℓ_0 and H are assumed to be 100 Km and 220 Km, respectively (see [2.8.7] for the definition of H). The system parameters used are the same as those used in Section 5.2.1. Three cases as listed below are considered:

Case	e	i	Purpose of investigation
1	0.001	0°	effect of e only
2	0	90°	effect of i only
3	0.001	90°	combined effects

Some results for the three cases are given in Tables 5.2, 5.3 and 5.4, respectively, while Figure 5.2 illustrates these results (with finer data points) in graphical form.

From the tables, the following observations can be made:

(a) If the orbit is in the equatorial plane, then out-of-plane rotation and transverse displacements are zero no matter what the eccentricity of the orbit is. This is expected because no atmospheric drag acts in the out-of-plane direction. On the other hand, the in-plane quantities $(\alpha-\pi)$, B_1 and B_2 change significantly over an orbital period. When $e = 0.001$, $\ell_0 = 100$ Km and $i = 0°$, α ranges from approximately 17° to 4°.

(b) If the orbit is not in the equatorial plane, the out-of-plane rotation and transverse displacements are non-zero. This is because due to the earth's rotation, there is a component of the atmospheric drag in the out-of-plane direction. However, these out-of-plane quantities are small, since the earth's rotation is much slower than the orbital rotation. As an example, the out-of-plane rotation γ is less than 1° for $e = 0$ and $i = \pi/2$. As for the in-plane quantities, $(\alpha-\pi)$, B_1 and B_2 are large and change significantly. For a polar circular orbit, the equilibrium deflections are small over the poles, since the corresponding altitudes are large.

(c) The longitudinal displacements are not affected by e and i significantly. These displacements are mainly governed by the gravity gradient and centrifugal forces which are strongly affected by the length ℓ_0 but not much by eccentricity e or orbital inclination i.

The static equilibrium configuration gives us some idea as to what the initial conditions are at the beginning of retrieval.

CHAPTER 6

NONLINEAR CONTROL OF ROTATIONAL DYNAMICS

Analysis of the SSTS system using the complete set of nonlinear equations describing the three-dimensional rotations as well as transverse and longitudinal vibrations is rather complex. Recognizing that inplane and out-of-plane rotations represent the most important variables of the problem, the rotational motion is studied first in the absence of vibrations. The rotations are allowed to be large and hence the equations are nonlinear.

The major difficulty lies in the control of out-of-plane rotations during retrieval. Linear length rate control laws or tension control laws proposed by previous investigators [16,24] based on linearized equations of motion do damp the inplane rotational motion but have no effect on the out-of-plane rotation during retrieval. This is due to the fact that change in length rate (or for that matter change in tether tension) has only a second order coupling with the out-of-plane rotation. Hence, to damp out-of-plane rotation, it is necessary to use the nonlinear equations.

In this chapter, a nonlinear length change law is developed to attain three-dimensional control of rotational motions during retrieval. As an extension, a nonlinear tension control law is proposed as well.

6.1 AN ANALYSIS OF ROTATIONAL MOTIONS

An analysis of the nonlinear rotational motion is necessary in order to find an appropriate length change law. Putting all the terms related to vibrations equal to zero in (4.2.14) and (4.2.15), one obtains

$$\alpha'' - F\alpha' - 2tg\gamma\gamma'(1+\alpha') + (1+\alpha')\eta'(2+\nu)/(1+\frac{1}{3}\nu)$$
$$+ 3s\alpha c\alpha/(1+e\ c\theta) = (P_\alpha + S_\alpha)/[(1+\frac{1}{3}\nu)c^2\gamma] \tag{6.1.1}$$

$$\gamma'' + \gamma'[(2+\nu)\eta'/(1+\frac{1}{3}\nu) - F] + \{(1+\alpha')^2 + 3c^2\alpha/(1+e\ c\theta)\}s\gamma c\gamma$$
$$= (P_\gamma + S_\gamma)/(1+\frac{1}{3}\nu) \tag{6.1.2}$$

Examining the above equations, the following features can be noted:

(i) The two equations are coupled by nonlinear terms;

(ii) Both equations are related to η'. However, there is some difference. α equation is coupled strongly to η' while γ equation depends weakly on η' since the product $\eta'\gamma'$ is usually small. Thus it is expected that α can be controlled easily if the form of η' is appropriate, but the same may not be true for γ.

Let us for a moment consider a very simplified case when the orbit is circular, the generalized forces and the control forces are absent, the motion is small and the mass of the tether is negligible compared to that of the subsatellite. This is being done to get some insight to the nature of the dynamics and possible form of control law. The actual numerical calculations, of course, are based on equations (6.1.1) and (6.1.2).

With the above assumptions, (6.1.1) and (6.1.2) reduce to

$$\alpha'' + 2\eta'(1 + \alpha') + 3\alpha = 0 \tag{6.1.3}$$

and

$$\gamma'' + 2\eta'\gamma' + 4\gamma = 0 \tag{6.1.4}$$

The two equations are now greatly simplified. One may note now the difference between deployment and retrieval. During deployment length ℓ_0 is always increasing, i.e., η' is positive, thus the equations involve positive damping and the motions are stable. On the other hand, during monotonic retrieval, length ℓ_0 is decreasing, η' is negative and the equations involve negative damping. Thus both α and γ are unstable. Physically, this can be explained in terms of Coriolis force. This force associated with pitch and roll is such that it is along a direction opposite to the velocity of the subsatellite during deployment thus making the motion stable. On the other hand, during retrieval this force is in the direction of the velocity of the subsatellite pushing it to instability.

Let us further assume that the length changes as follows:

$$\ell_0 = \ell_i \, e^{ct} \tag{6.1.5}$$

The length increases if $c > 0$ and reduces if $c < 0$. Clearly,

$$\eta' = \dot{\ell}_0/\ell_0 = c/\dot{\theta} = \tilde{c} \; . \qquad (6.1.6$$

$\tilde{c}$ is constant for a circular orbit under consideration.

The solutions of equations (6.1.3) and (6.1.4) are:

$$\alpha = Ae^{-\tilde{c}\theta}\cos[(3-\tilde{c}^2)^{\frac{1}{2}}\,\theta + B] \tag{6.1.7}$$

and

$$\gamma = Ce^{-\tilde{c}\theta}\cos[(4-\tilde{c}^2)^{\frac{1}{2}}\,\theta + D] \tag{6.1.8}$$

where A, B, C and D are constants of integration which are determined by the initial conditions.

From the solutions, we see that α and γ oscillate with increasing amplitudes during retrieval ($\tilde{c} < 0$). If $\tilde{c}$ is much smaller than 1, then the period of α is nearly $2\pi/\sqrt{3}$ and the period of γ is π. These estimations give us a rough picture of the rotational motions and will be used later. Returning to equations (6.1.3) and (6.1.4) now consider the case when η' is not only a function of θ but also involves state feedback. Integrating equation (6.1.3) with respect to α and equation (6.1.4) with respect to γ, one obtains what are essentially energy integrals. Defining Norm_α and Norm_γ as

$$\text{Norm}_\alpha = \left(\frac{1}{2}\,\alpha'^2 + \frac{3}{2}\,\alpha^2\right)^{\frac{1}{2}} \tag{6.1.9}$$

$$\text{Norm}_\gamma = \left(\frac{1}{2}\,\gamma'^2 + 2\gamma^2\right)^{\frac{1}{2}} \tag{6.1.10}$$

we get

$$\text{Norm}_\alpha^{\,2} - \text{Norm}_\alpha^{\,2}(0) = -2\int_0^\theta \eta'(\alpha'^2 + \alpha')d\theta \tag{6.1.11}$$

and

$$\text{Norm}_\gamma^{\,2} - \text{Norm}_\gamma^{\,2}(0) = -2\int_0^\theta \eta'\gamma'^2 d\theta \qquad (6.1.12)$$

Where $\text{Norm}_\alpha(0)$ and $\text{Norm}_\gamma(0)$ represent corresponding initial values, respectively. Norm_α and Norm_γ can be interpreted as the sum of gravitational potential energy and kinetic energy for α and γ degrees of freedom, respectively. If rotations α and γ are to be stable, energy input through length change (i.e., η') given by the RHS must be negative or zero; alternatively the integrals on the RHS must be positive or zero, i.e.,

$$\int_0^\theta \eta'(\alpha'^2 + \alpha')d\theta \geq 0 \qquad (6.1.13)$$

and

$$\int_0^\theta \eta'\gamma'^2\, d\theta \geq 0 \qquad (6.1.14)$$

must hold. Clearly, inequality (6.1.14) will never be satisfied if η' is negative all the time, i.e., if the length ℓ_0 is reduced monotonically.

For retrieval, we must have

$$\int_0^\theta \eta'\, d\theta < 0 \qquad (6.1.15)$$

Since γ'^2 is always positive, conditions (6.1.14) and (6.1.15) appear a bit contradictory, but actually they are not. η' need not be negative <u>all</u> the time. It may be positive sometimes and negative at other times in an approriate manner so as to satisfy both equations. This means that when the tether is being retrieved, it has to be released sometime to satisfy the stability requirements.

Let us investigate the α-motion first. Condition (6.1.13) may be rewritten as

$$- \int_0^\theta \eta' \alpha'^2 \, d\theta \leq \int_0^\theta \eta' \alpha' \, d\theta \qquad (6.1.16)$$

If $\alpha' > 0$, (6.1.16) is satisfied when $\eta' > 0$. Then the left hand side in (6.1.16) is negative while the right hand side is positive. The greater the difference between the two terms, more is the energy withdrawn from the tethered system. Similarly, if $\alpha' < 0$, the equation is still satisfied if one keeps $\eta' < 0$ (normally $|\alpha'| < 1$); but the difference between two sides is less than before since the signs are now the same.

Now a strategy of length change-rate can be deduced. Consider a cycle of oscillation shown in Fig. 6.1(a). When $\alpha' > 0$, one can make η' small and positive while when $\alpha' < 0$ one can let η' be large in magnitude and negative, so that on the average, tether is retrieved ($\int_0^\theta \eta' \, d\theta$ = total area = -ve) while the sign requirements specified above to guarantee stability are still satisfied.

Consider the form of η' given by

$$\eta' = -K_1 + K_2 \, \alpha' \qquad (6.1.17)$$

where K_1 and K_2 are two positive constants. This length rate is shown in Fig. 6.1(b). Most of the features of η' shown in Fig. 6.1(a) are retained in Fig. 6.1(b); hence the two inequalities (6.1.15) and (6.1.16) are likely to be satisfied. Substituting (6.1.17) into (6.1.16) and integrating over one period it can be shown that the stability is guaranteed if $K_1 \leq K_2$. The length rate presented by (6.1.17) is quite simple and involves linear pitch rate feedback.

In a similar manner, one can investigate inequality (6.1.14) associated with γ motion. This requirement is more challenging to satisfy in the light of (6.1.15). Note that γ'^2 is always positive. Let us approximate γ hence γ' as a harmonic oscillation (Fig. 6.2(a)). In order to retrieve the tether in an average sense in a stable manner, the following strategy is designed: when γ' is small, let η' be negative and large, which means retrieve the tether fast. When γ' is large, let η' be positive and small. Note that the total area under the η' curve is negative implying resultant retrieval. Referring to Fig. 6.2(b), it can be seen that $\eta'\gamma'^2$ can be such that stability requirement (6.1.14) is satisfied. η' shown in Fig. 6.2(b) corresponds to

$$\eta' = -K_3 + K_4\,\gamma'^2 \tag{6.1.18}$$

where K_3 and K_4 are positive constants. This length rate involves quadratic feedback of roll rate.

It is interesting to note that substituting (6.1.18) into (6.1.4) yields

$$\gamma'' - (2K_3\gamma' - 2K_4\gamma'^3) + 4\gamma = 0 \tag{6.1.19}$$

which is the familiar Rayleigh's equation (and can be converted to van der Pol's equation). It is well known that the solution is a limit cycle whose amplitude can be calculated to be $(4K_3/3K_4)^{(1/2)}$. This implies that length rate given by (6.1.18) can limit but not eliminate roll motion.

Combining equations (6.1.17) and (6.1.18), we get a convenient form of η' to control both α and γ:

$$\eta' = K_\theta[1 + K_\alpha \alpha' + K_\gamma \gamma'^2] \tag{6.1.20}$$

where K_α and K_γ are two negative constants. In general, K_θ is a negative function of θ during retrieval. For exponential retrieval, $K_\theta = \tilde{c}$, $\tilde{c} < 0$. The absolute values of K_α and K_γ depend on the initial conditions and the allowable values of α and γ. Roughly, the larger the values of K_α and K_γ, the smaller the ranges of oscillations of α and γ and the longer the time required to retrieve the subsatellite.

6.2 NUMERICAL RESULTS

Simulation of the three-dimensional rotational motion as described by (6.1.1) and (6.1.2) has been carried out using the retrieval law given by (6.1.20). The following parameters are used in the numerical calculations:

ℓ_i = starting length of the tether to be retrieved = 100 Km

ℓ_f = final length of the tether after retrieval = 100 m.

M_b = mass of the subsatellite = 150 Kg.

ρ_c = mass per unit length of the tether = 1.5 Kg/Km

d_c = tether diameter = 1 mm.

A_b = projected area of the subsatellite = 1 m^2

C_d = drag coefficient = 2 (assumed constant).

e = eccentricity of the orbit = 0.001

c = retrieval constant = -1×10^{-4} sec^{-1} to -3×10^{-4} sec^{-1}

$$[K_\theta = c/\dot{\theta} = c/E(\theta)]$$

θ_0 = argument of the perigee = 0

i = inclination of the orbit to the equatorial plane = 0 (unless otherwise stated).

The major axis of the earth = a_0 = 6378 Km

The minor axis of the earth = b_0 = 6357 Km

Figs. 6.3 and 6.4 show the length history and the rotational motion of the tethered system for two different values of c, one of which is -1×10^{-4} sec^{-1} and the other -2×10^{-4} sec^{-1}. For both the cases gains K_α and K_γ are -6 and -37, respectively, and the initial conditions are $\alpha-\pi = 5.7°$ (0.1 rad), $\gamma = 1.1°$ (0.02 rad), $\alpha' = \gamma' = 0$. Note that $\alpha-\pi$ reduces to about 2° within a short period of time while γ attains a limit cycle having an amplitude of approximately 7°. (Note that the simplified analysis predicts a limit cycles amplitude of $(4/3K_\gamma)^{(1/2)}$ rad or approximately 11°). The value of c has almost no effect on the amplitude of limit cycle, but has a strong effect on the time taken for retrieval. For the smaller value of c (numerically) the retrieval time is 46 orbits while for the large c it is only 28 orbits. Hence, a numerically large value of c must be used or the gains must be reduced. It must be realized that the tension in the tether may increase at the initial stage, due to the inertia force associated with the retrieval acceleration and in extreme cases the tether might break.

Analysis of the tether length history indicates that the retrieval at the beginning is quite rapid, but later the length changes rather slowly. To reduce the retrieval time, a revised length rate law can be proposed as follows:

$$\eta' = K_\theta(1 + K_L f)(1 + K_\alpha f\alpha' + K_\gamma f\gamma'^2) \qquad (6.2.1)$$

where

$$f = 1 - \ell_0/\ell_i \qquad (6.2.2)$$

and K_L is a constant. Initially $\ell_0 = \ell_i$ and $f = 0$; there is no control as the stability problem is not very serious. When the length becomes small, the feedback gains and the effective retrieval constant increase simultaneously. Fig. 6.5(a) and 6.5(b) compare the two length rate laws specified by (6.1.20) and (6.2.1), respectively. It may be noted that the retrieval time is shortened to about 15 orbits with this revised law without increasing the rotational motion significantly. Choice of a smaller value of K_α reduces the retrieval time but increases α. Further reduction in this retrieval time to about 2 orbits can be achieved by using thruster augmented control laws considered in Chapter 9.

Retrieval of the tether system corresponding to equatorial and polar orbits is compared in Fig. 6.6. The difference is negligible.

6.3 NONLINEAR TENSION CONTROL LAW

The linear tension control laws proposed by Baker, et al. [24] and Bainum and Kumar [16] are not very successful in controlling the rotational motions, especially the out-of-plane rotation during retrieval.

Similar to the nonlinear length change law proposed here, a nonlinear tension control law has been suggested by Modi, et al. [28]*. This nonlinear tension control law has the form

$$\Delta\tilde{T} = K_1\delta + K_2\delta' + K_\gamma\gamma'^2 \tag{6.3.1}$$

where K_1, K_2 and K_γ are a set of constants, $\Delta\tilde{T}$ is the difference between nondimensional, actual and equilibrium tension while δ is a nondimensional length defined by

$$\delta = (\ell - \ell_c) \quad , \tag{6.3.2}$$

Here ℓ and ℓ_c are instantaneous stretched length and commanded length of the tether respectively. If the tether is regarded to be inextensible, then

$$\ell = \ell_0 \tag{6.3.3}$$

It is clear that both nonlinear tension and length rate control laws are quite similar and both use the same kind of quadratic feedback term involving the roll rate. The nonlinear tension control law is as effective as the nonlinear length rate change law presented in this thesis. However, as is shown in the next chapter, when the extensibility of the tether is taken into account, the results differ from each other.

---

* The nonlinear tension control law was suggested after the nonlinear length rate law proposed here had been published.

CHAPTER 7

CONTROL OF LONGITUDINAL VIBRATIONS

Since the tether under consideration is very long (of the order of 100 Km), it has to be very thin from weight consideration. Its diameter is likely to be of the order of 1 mm only. Such a thin tether cannot be regarded as an inextensible string as was the case in Chapter 6. Due to the elasticity of the tether, longitudinal deformations occur when the gravity gradient and other forces act on the subsatellite as well as the tether. In addition, during deployment or retrieval, longitudinal vibrations are unavoidable. Unfortunately, these elastic vibrations are unstable during the retrieval stage and they may cause the tether to be slack when the length becomes small since then not much tension is available to the tether. Thus, these vibrations must be damped out.

In this chapter, the longitudinal vibrations are considered together with the rotational motions. But transverse vibrations are ignored. A nonlinear length change law to arrest instability is proposed for this case. The performance of this control law is compared with the tension control law proposed by Modi, et al. [28].

7.1 A CLOSE EXAMINATION OF LONGITUDINAL VIBRATIONS

To gain some insight as to how to damp the longitudinal vibrations using an appropriate length change law, a simplified case is considered first. The following assumptions are made:

(i) There is no rotational motion. The rotations are very slow compared to longitudinal vibrations; several cycles of these vibrations may take place during a period when very small changes in α and γ have occurred.

(ii) It is assumed that the longitudinal strain is uniform along the tether. This is equivalent to taking only the first term, the most important one, in the expansion. Thus $\varepsilon = C_1$.

(iii) The mass of the tether is negligible compared to that of the subsatellite.

(iv) There are no transverse vibrations.

(v) Aerodynamic forces are ignored.

(vi) The orbit is assumed to be circular.

Based on these assumptions, only C_1 equation remains and it can be written in the form

$$C_1'' + 2\eta' C_1' + (EA/M_b \ell_0 \omega^2) C_1 = 3 - (\eta'' + \eta'^2) \tag{7.1.1}$$

On the right hand side the term 3 is the contribution of the equilibrium tension due to gravity gradient and centrifugal force while the term $-(\eta''+\eta'^2)$ is the inertial force associated with the subsatellite mass due to length change. It can be shown that

$$\eta'' + \eta'^2 = \ell_0''/\ell_0 \tag{7.1.2}$$

The solution for C_1 can be split into

$$C_1 = C_{1s} + C_{1d} \tag{7.1.3}$$

where

$$C_{1s} = (3M_b \ell_0 \omega^2/EA) \tag{7.1.4}$$

which is a quasi-static equilibrium strain and decreases during retrieval. Substituting (7.1.3) and (7.1.4) into (7.1.1)

$$(C_{1s}+C_{1d})''+2\eta'(C_{1s}+C_{1d})'+(EA/M_b\ell_0\omega^2)C_{1d} = -(\eta''+\eta'^2) \qquad (7.1.5)$$

Using the definition of η given by (4.2.10)

$$\ell_0 = \ell_{ref}\, e^{\eta}$$

Thus from (7.1.4)

$$C'_{1s} = (3M_b\ell_{ref}\omega^2/EA)[\eta'\, e^{\eta}] \qquad (7.1.6)$$

and

$$C''_{1s} = (3M_b\ell_{ref}\omega^2/EA)[\eta''+\eta'^2]e^{\eta} \qquad (7.1.7)$$

Substituting (7.1.6) and (7.1.7) in (7.1.5)

$$C''_{1d} + 2\eta'C'_{1d}+(EA/M_b\ell_0\omega^2)C_{1d}= -(1+\delta_c)\eta''-(1+3\delta_c)\eta'^2 \qquad (7.1.8)$$

where

$$\delta_c = (3M_b\ell_{ref}\omega^2/EA) \qquad (7.1.9)$$

Considering typical values of M_b = 170 Kg, ℓ_{ref} = 100 Km, ω = 1.18 x 10^{-3} sec^{-1}, E = 2.1 x 10^{11} Newton/m^2 and d_c = 0.325 mm,

$$\delta_c \approx 10^{-3} << 1$$

Hence, approximately

$$C''_{1d}+2\eta'C'_{1d}+(EA/M_b\ell_0\omega^2)C_{1d} \approx -(\eta''+\eta'^2) \qquad (7.1.10)$$

If an exponential retrieval procedure is used $\eta' = \tilde{c} < 0$. Thus the second term implies negative damping and C_{1d} becomes unstable even though the stiffness is increasing. Our goal is to damp C_{1d}, the longitudinal vibration during retrieval.

If the retrieval is exponential, (7.1.10) becomes

$$C_{1d}'' + 2\,\tilde{c}\,C_{1d}' + (EA/M_b\,\ell_{ref}\,\omega^2)e^{-\tilde{c}\theta} = -\tilde{c}^2 \tag{7.1.11}$$

An analytical solution to the homogeneous part* of (7.1.11) can be found as follows:

Define a new independent variable

$$u = [(12/\delta_c\,\tilde{c}^2)e^{-\tilde{c}\theta}]^{\frac{1}{2}} \tag{7.1.12}$$

Then the homogeneous part of equation (7.1.11) transforms to

$$\frac{d^2}{du^2}C_{1d} + (3/u)\frac{d}{du}C_{1d} + C_{1d} = 0 \tag{7.1.13}$$

Further define a new dependent variable F such that

$$C_{1d} = u^4 F \tag{7.1.14}$$

Then equation (7.1.13) becomes

$$\frac{d^2F}{du^2} + \left(\frac{1}{u}\right)\frac{dF}{du} + F = 0 \tag{7.1.15}$$

---

* The particular integral of (7.1.11) reduces during retrieval. Thus, if homogeneous solution is stabilized the total solution remains stable.

This is Bessel's equation of order zero, the solution to which is

$$F = A_1 J_0 (u) + B_1 Y_0 (u) \tag{7.1.16}$$

where A_1, B_1 are constants of integration and J_0, Y_0 are zero order Bessel functions of first and second kind, respectively. Therefore, from (7.1.12), (7.1.14) and (7.1.16)

$$C_{1d} = (12/\delta_c \tilde{c}^2)^2 e^{-2\tilde{c}\theta} \{A_1 J_0[(12/\delta_c \tilde{c}^2)^{\frac{1}{2}} e^{\frac{-\tilde{c}\theta}{2}}] + B_1 Y_0[(12/\delta_c \tilde{c}^2)^{\frac{1}{2}} e^{\frac{-\tilde{c}\theta}{2}}]\} \tag{7.1.17}$$

From (7.1.17), it can be seen that C_{1d} is unstable because $e^{-2\tilde{c}\theta}$ increases with θ much faster ($\tilde{c} < 0$), than reduction of amplitude of oscillation of J_0 and Y_0. The $e^{-2\tilde{c}\theta}$ term represents the effect of negative damping while decreasing J_0, Y_0 terms correspond to the increase of stiffness, which gives some help towards stability.

The unstable longitudinal vibration C_{1d} may cause the slackness of the tether sometime during the retrieval. At the beginning of the retrieval, generally C_{1s} is relatively large compared to C_{1d}. During retrieval, C_{1s} is reduced; if the amplitude of C_{1d} grows it will catch up with C_{1s}. Thus slackness of the tether will occur sooner or later. Hence, the longitudinal vibration C_{1d} must be damped.

Now let η', the nondimensional length rate be dependent on C_{1d} as follows

$$\eta' = \tilde{c}\,[1 - K_c\, C_{1d}] \tag{7.1.18}$$

where K_c is a positive constant. Differentiating η' with respect to θ, one obtains

$$\eta'' = -K_c \tilde{c} C'_{1d} \qquad (7.1.19)$$

Substituting (7.1.18) and (7.1.19) in (7.1.10), one obtains

$$C_{1d}'' + 2\tilde{c}(1-K_c C_{1d})C_{1d}' + (EA/M_b \ell_0 \omega^2)C_{1d}$$

$$= -\tilde{c}^2(1-K_c C_{1d})^2 + K_c \tilde{c} C_{1d}' \qquad (7.1.20)$$

The dynamical strain C_{1d} is usually much smaller than 10^{-2}. If K_c is not chosen to be very large, then (7.1.20) may be approximated as

$$C_{1d}'' + \tilde{c}(2 - K_c)C_{1d}' + (EA/M_b \ell_0 \omega^2)C_{1d} \approx 0 \qquad (7.1.21)$$

Thus, if K_c is chosen greater than 2, the second term yields positive damping and C_{1d} becomes stable.

The feedback form of (7.1.18) or (7.1.19) has very clear physical meaning. This just means using the inertial force acting on the mass of the subsatellite due to the length acceleration judiciously, nothing else. On the right hand side of equation (7.1.10), the term $-(\eta'' + \eta'^2)$ represents this nondimensional inertial force. If η' is varying according to the form of (7.1.18), then a viscous type restoring force is produced to damp the longitudinal vibration C_{1d}.

This length rate law (7.1.18) is quite efficient. Again K_c can be chosen in a wide range without affecting the length rate η' too much since C_{1d} is very small. If η' is assumed as

$$\eta' = \tilde{c}(1 - K_c C_1) \qquad \tilde{c} < 0 \qquad (7.1.22)$$

it still works, but since C_1 is much larger than C_{1d}, K_c now cannot be chosen very large especially at the beginning of retrieval. The length rate change law (7.1.22) tends to pull C_1 back to zero, which is an overcorrection.

One can rewrite (7.1.18) in terms of C_1

$$\eta' = \tilde{c}[1 - K_c(C_1 - C_{1s})]$$

$$= \tilde{c}\{1 - K_c[C_1 - (3M_b \ell_0 \omega^2/EA)]\} \qquad (7.1.23)$$

The difference between (7.1.22) and (7.1.23) is obvious.

Considering rotational motions α and γ as well and a general elliptic orbit, corresponding form of η' may be written as

$$\eta' = \tilde{c}\{1 - K_\alpha \alpha' - K_\alpha \gamma'^2 - K_c[C_1 - (3M_b \ell_0 \dot{\theta}^2/EA)]\} \qquad (7.1.24)$$

7.2 NUMERICAL RESULTS

It must be emphasized that the numerical calculations are carried out based on unsimplified α, γ, C_1 and C_2 equations once the control law is obtained through the simplified analysis. Also note that in the expression of longitudinal displacement, two terms are retained, therefore the restrictive assumption of uniform strain in the tether is relaxed. Thus $v(y_c, \theta)$ has the form

$$v/\ell_0 = C_1(y/\ell_0) + C_2(y/\ell_0)^3 \qquad (7.1.25)$$

Since we have the C_2 term now, the strain along the tether is allowed to vary.

The mass of the subsatellite used in the numerical computations is assumed to be 170 Kg which is the same as that used by Baker, et al. [16]. The diameter of the tether is 0.325 mm. Note that even for this small diameter, the tether is strong enough not to break.

The initial conditions are $\alpha(0) = 15°$, $\gamma(0) = 3°$, $\alpha'(0) = \gamma'(0) = 0$, $C_1 = 4.7 \times 10^{-3}$ and $C_2 = 2.5 \times 10^{-4}$. Fig. 7.1 shows the motion when only α and γ are controlled using length rate law (6.1.20). Note how the longitudinal vibration C_1 increases resulting in slackness of the tether.

Corresponding motion including control of longitudinal vibrations by using (7.1.24) is described in Fig. 7.2 and Fig. 7.3 with the different retrieval constants $c = -2 \times 10^{-4} S^{-1}$ and $-4 \times 10^{-4} S^{-1}$, respectively. Note that α and γ are quite stable and confined within 3° and 8°, respectively. C_1 and C_2 approach zero in a stable manner and C_1 remains positive. The longitudinal displacement is positive everywhere along the tether at anytime, i.e., the tether is in tensile state all the time. Numerical calculations are carried out until the length of the tether is 50 m. The tension at the two ends of the tether are different at the beginning but with the retrieval they approach each other since C_2 reduces quite fast. The results in Figs. 7.2 and 7.3 show that the length rate control law (7.1.24) is quite effective.

7.3 COMPARISON BETWEEN LENGTH CHANGE LAW AND TENSION CONTROL LAW

As cited in the literature review, several tension control laws have been proposed. Out of them, two are effective during retrieval if out-of-plane motion is considered [28,30]. It may be interesting to compare the former to the present length change law. (Comparison of the latter is postponed until we consider thruster augmented control.)

If longitudinal stretch is ignored, i.e., the tether is regarded as having an infinite Young's modulus, then both results are good. The rotational motions α and γ are within the same small range and the retrieval time is nearly the same no matter which control law is used. On the other hand, if the tether material is considered to be elastic thus causing a longitudinal stretch of the tether, then the vibrational results are different. The result using the tension control law shows $\zeta < 0$ sometimes, i.e., the tether becomes slack.

From the view of practical use, these two types of control laws are different as follows:

(i) The tension control law in [28] does not rely on α' since α motion is stabilized through its coupling with longitudinal motion which is controlled. α' need not be measured. On the other hand, for length change law, α' is required and must be measured.

(ii) The length change law is direct to the reel mechanism. Specifying the length rate is equivalent to specifying the rotational rate of the reel mechanism or the speed of the tension reel motion. Tension control law appears indirect and more difficult to implement.

In any case, the tension varies along the length of the tether while tension control laws proposed are based on uniform tension.

(iii) For the length change law, the reel mechanism "knows" whether to roll in or out. Once T, α', γ' are measured η' is known; $\eta' > 0$ implies rolling out and $\eta' < 0$ involves rolling in. For tension control law, the picture is not so clear. If measured ΔT is larger than zero, which means the actual tension is larger than equilibrium tension, should the reel mechanism roll in or out? This question only can be answered after all measured ΔT, L_c, γ', L etc. are put into the tension control law (6.3.1) to get ℓ_0'.

From this comparison, the author feels that the length change control law may be superior to the tension control law.

CHAPTER 8

NONLINEAR VIBRATIONS OF THE TETHER

Although transverse vibrations of the tether were not considered in Chapter 7, in practice they cannot be ignored. If the tether is deployed downwards and is fairly long, the aerodynamic forces are quite large in the plane of the orbit. These forces not only push the subsatellite away from the vertical, they also act on the tether in the transverse direction making it curved. Furthermore, if the tether is moving axially during deployment or retrieval, the Coriolis forces can also give rise to transverse displacements of the tether. The stiffness of the tether arises due to the tension caused by the gravity gradient and centrifugal forces. All these forces vary during deployment and retrieval (and to some extent during stationkeeping), thus making the elastic tether vibrate in the transverse direction along with the longitudinal motion discussed earlier.

It may be recalled from Chapter 4 that the longitudinal and transverse vibrations are strongly coupled especially at the terminal phase of retrieval. On one hand, the transverse vibrations are governed by the tension along the tether which is proportional to the longitudinal strain. On the other hand, the longitudinal strain is dependent on the transverse displacements through nonlinear terms in the strain-displacement relation. Clearly, the two types of vibrations are intimately related and must be controlled together.

This chapter first considers the nonlinear vibrations by themselves and subsequently general rotational as well as vibrational motions.

8.1 EQUATIONS GOVERNING VIBRATIONS IN THE ABSENCE OF ROTATIONAL MOTION

The equations of vibrations, both longitudinal and transverse, have been derived in Chapter 2 and discretized in Chapter 4. If rotations are ignored, i.e., α, γ and their time derivatives are set to zero in (4.2.20), the corresponding B_1 equation is

$$\begin{aligned}
&B_1''+(3\eta'-F)B_1'-\frac{8}{3}B_2'+[\frac{3}{2}(\eta''-F\eta')+(2-\pi^3/3)\eta'^2]B_1 \\
&-[(3/4)(\eta''-F\eta')+(76/9)\eta'^2]B_2+4K\eta'-KF+2K\{C_1' \\
&+[(\pi^2-6)/\pi^2](C_2'-2\eta'C_2)\}+\pi^2\Omega^2\{B_1[C_1+(1+3/2\pi^2)C_2] \\
&-(20/9\pi^2)B_2C_2+\pi^2[(3/4)B_1^3+(3/4)B_1A_1^2+6B_1B_2^2+4B_2A_1A_1 \\
&+(2B_1A_2^2]\}=P_{B_1}+S_{B_1}
\end{aligned} \tag{8.1.1}$$

Equation (8.1.1) is still quite complicated. In order to grasp some important features of vibrational motion, the following assumptions are introduced:

(i) The orbit is assumed to be circular.

(ii) Aerodynamic forces are ignored (at terminal phase of retrieval, they are small anyway).

(iii) C_2 is ignored compared to C_1.

(iv) Mass ratio ν is ignored compared to unity.

Based on the above assumptions, (8.1.1) simplifies to

$$\begin{aligned}
&B_1''+3\eta'B_1'-(8/3)B_2'+2K[2\eta'+C_1']+\pi^2\Omega^2\{B_1C_1 \\
&+\pi^2[(3/4)B_1^3+(3/4)B_1A_1^2+6B_1B_2^2+4B_2A_1A_2+2B_1A_2^2]\}=0
\end{aligned} \tag{8.1.2}$$

Similarly C_1, A_1, A_2 and B_2 equations are

$$C_1''+2\eta'C_1'+\omega_\varepsilon^2\{C_1+(\pi^2/2)(A_1^2+4A_2^2+B_1^2+4B_2^2)\} = 3-(\eta''+\eta'^2) \tag{8.1.3}$$

$$A_1''+3\eta'A_1'-(8/3)A_2'+\pi^2\Omega^2\{A_1C_1+\pi^2[(3/4)A_1^3+(3/4)A_1B_1^2 + 6A_1A_2^2+4A_2B_1B_2+2A_1B_2^2]\} = 0 \tag{8.1.4}$$

$$A_2''+3\eta'A_2'+(8/3)A_1'+4\pi^2\Omega^2\{A_2C_1+\pi^2[(3/2)A_1^2A_2+3A_2^3 + A_1B_1B_2+3A_2B_2^2+0.5A_2B_1^2]\} = 0 \tag{8.1.5}$$

$$B_2''+3\eta'B_2'+(8/3)B_1'-KC_1'+4\pi^2\Omega^2\{B_2C_1+\pi^2[(3/2)B_1^2B_2 + 3B_2^3+B_1A_1A_2+3B_2A_2^2+ (1/2)B_2A_1^2]\} = 0 \tag{8.1.6}$$

where

$$\omega_\varepsilon^2 = EA/M_b\, \ell_0\, \omega^2 \tag{8.1.7}$$

and ω^2 is given by (4.2.17).

Recall that the longitudinal strain ε is given by

$$\varepsilon = \varepsilon_1 + \varepsilon_2 \tag{2.5.1}$$

where

$$\varepsilon_1 = \partial v/\partial y_c$$

and

$$\varepsilon_2 = \frac{1}{2}\left[\left(\frac{\partial u}{\partial y_c}\right)^2 + \left(\frac{\partial w}{\partial y_c}\right)^2\right]$$

The term $(\pi^2/2)(A_1{}^2+4A_2{}^2+B_1{}^2+4B_2{}^2)$ in Equation (8.1.3) is simply $\frac{1}{\ell_0}\int_0^{\ell_0} \varepsilon_2 \, dy_c$ and represents the contribution of nonlinearity in an average sense.

If nonlinear strain term ε_2 is ignored, then the corresponding C_1, A_1, A_2, B_1 and B_2 equations are

$$C_1''+2\eta'C_1'+\omega_\varepsilon{}^2C_1 = 3-(\eta''+\eta'^2) \tag{8.1.8}$$

$$A_1''+3\eta'A_1'-(8/3)A_2''+\pi^2\Omega^2A_1C_1 = 0 \tag{8.1.9}$$

$$A_2''+3\eta'A_2'+(8/3)A_1'+4\pi^2\Omega^2A_2C_1 = 0 \tag{8.1.10}$$

$$B_1''+3\eta'B_1'-(8/3)B_2'+\pi^2\Omega^2B_1C_1+2KC_1' = -4K\eta' \tag{8.1.11}$$

and

$$B_2''+3\eta'B_2'+(8/3)B_1'+4\pi^2\Omega^2B_2C_1-KC_1' = 0 \tag{8.1.12}$$

Equations (8.1.8-8.1.12) govern 'linear' vibrations. Note that there are terms like A_1C_1, A_2C_1, etc. in these equations which are nonlinear. However C_1 can be solved independently from (8.1.8) at least in principle. Once this solution is substituted in (8.1.9-8.1.12) the equations become linear in A_1, A_2, B_1, B_2 and their derivatives.

8.2 COMPARISON OF LINEAR AND NONLINEAR VIBRATIONS IN THE ABSENCE OF ROTATIONAL MOTION

In order to verify the importance of the nonlinear strain term, numerical simulations are carried out for both cases of linear and nonlinear strain modelling, using the same initial conditions and same physical parameters. The shuttle is assumed to be in an equatorial circular orbit at an altitude of 220 Km. To start with, a constant length tether (ℓ_0 = 1 Km) is considered. A short length is chosen because most of the difficulties during retrieval of the subsatellite are associated with small tether lengths and in addition, nonlinearity is more significant at these lengths.

Both nonlinear and linearized sets of equations are integrated with the same initial conditions: $A_1 = B_1 = 0.5 \times 10^{-3}$, $A_2 = -B_2 = -0.1 \times 10^{-3}$, $C_1 = 0.45 \times 10^{-3}$ and $A_1' = A_2' = B_1' = B_2' = C_1' = 0$. In Fig. 8.1, nonlinear results for A_1, B_1, C_1 and ε are compared with corresponding linear ones. ε for the linear case is given by the dashed curve in C_1 graph. It may be noted that the periods for linear transverse vibrations are slightly higher, i.e., nonlinear vibrations have higher frequencies indicating that the nonlinearity is of a hardening type. Nonlinearity has a small effect on the magnitudes of oscillations in the case of transverse vibrations, at least for these initial conditions. Note that the linear strain in this simulation is given by C_1 while the nonlinear strain is a function of C_1, A_1, B_1, A_2, B_2 and y_c,

$$\varepsilon = C_1+\pi^2\{[\sum_{i=1}^{2} A_i \; i \; c(i \; \pi y_c/\ell_0)]^2+[\sum_{i=1}^{2} B_i \; i \; c(i \; \pi y_c/\ell_0)]^2\} \qquad (8.2.1)$$

The difference between linear and nonlinear results increases if the tether length is reduced further.

Vibrations of the tether during gradual reduction of its length are considered next. Fig. 8.2 shows the behaviour of the out-of-plane transverse modal coordinates A_1 and A_2 during exponential reduction of length from 1 Km (equation (6.1.6), $c = -2 \times 10^{-4}\ S^{-1}$). Note that A_1, A_2 increase quite fast if linearized equations are used, while the stiffening nature of the nonlinearity causes a much more modest rate of growth.

Inplane transverse vibrations during retrieval using feedback of C_1 term alone are shown in Fig. 8.3. The length rate law is simply given by (7.1.22)

$$\eta' = \tilde{c}(1-K_c C_1),\ K_c = 300,\ c = -2 \times 10^{-4}\ S^{-1} = (\tilde{c}\omega) \tag{8.2.2}$$

As the coupling between transverse and longitudinal vibrations is weak in the linearized case, the feedback of C_1 has no effect on B_1 and B_2. However, when the nonlinearity is taken into account, control of longitudinal strain can arrest the growth of B_1 and B_2 to a certain extent, although it cannot eliminate the growth completely.

The effects of nonlinear strain on the vibrations are greatly dependent on the initial conditions. The larger the magnitude of the transverse vibrations, the greater the effects of the nonlinear strain. On one hand, this kind of coupling between longitudinal and transverse vibrations may help to suppress the transverse vibrations. On the other hand, these transverse vibrations may excite large longitudinal vibrations. This merely suggests that the control of longitudinal and transverse vibrations must be considered together.

8.3 FEASIBILITY ANALYSIS OF CONTROLLING TRANSVERSE VIBRATIONS

In the simplified equations (8.1.8-8.1.12), the following features may be observed:

(i) Transverse vibrations are inherently unstable during retrieval just as are the longitudinal vibrations. If η' is negative, each equation involves a negative damping term.

(ii) Transverse vibrations are coupled with longitudinal vibrations through the stiffness term.

(iii) All vibrations are coupled to η' or η''.

However, the coupling is stronger for longitudinal vibrations due to the presence of the term $(\eta'' + \eta'^2)$ on the right hand side of C_1 equation (i.e., 8.1.8). Even among the transverse vibrational equations, there is some difference. B_1 equation, containing a term $-4K\eta'$ on the right hand side, is more strongly dependent on η' compared to A_1, A_2 and B_2 equations. Physically speaking, the tether is retrieved axially; thus the inertial force due to the length change is mainly along the longitudinal direction. Hence, longitudinal vibrations (characterized by C_1) are greatly affected by the length rate. Inplane transverse vibrations are affected by η' because of the Coriolis effect. For B_1 degree of freedom, the result is the $-4K\eta'$ while for B_2 the net effect is zero due to the deflection shape.

From the observations above, one may expect that control of transverse vibrations using length change laws may be difficult, since so many modal coordinates depend on η' weakly.

As shown in Chapter 7, the dynamic part C_{1d} of the longitudinal vibrations can be controlled if

$$\eta'' + \eta'^2 = K_c\, C_{1d}' \qquad (8.3.1)$$

In that case, C_1 gradually approaches the quasi-static value C_{1s} (see equation (8.1.8)).

$$C_1 \approx C_{1s} = [3-(\eta''+\eta'^2)]/\omega_\varepsilon^2 = (3-K_c\, C_{1d}')/\omega_\varepsilon^2 \tag{8.3.2}$$

If the length change law involves feedback of only longitudinal vibrations, the transverse vibrations obtained from numerical integration of the unsimplified equations grow. This is shown in Fig. 8.4(b). Therefore, the length change law must have feedback of the transverse vibrations as well. Let

$$\eta'' + \eta'^2 = K_c\, C_{1d}' + f(A_1, A_1', \ldots) \tag{8.3.3}$$

where f is feedback of transverse vibrations in a functional form and is to be determined. Therefore from (8.3.2) approximately,

$$C_1 \approx (3-K_c\, C_{1d}'-f)/\omega_\varepsilon^2 \tag{8.3.4}$$

Clearly, f must not be larger than 3, because C_1 represents the strain in the tether which must remain positive.

Substituting (8.3.4) into equations (8.1.9-8.1.12), we have

$$B_1''+3\eta'B_1'-(8/3)B_2'+(\pi^2/\nu)[3-K_c\, C_{1d}'-f]B_1+2K\, C_1' = -4K\eta' \tag{8.3.5}$$

$$B_2''+3\eta'B_2'+(8/3)B_1'+(4\pi^2/\nu)[3-K_c\, C_{1d}'-f]B_2-K\, C_1' = 0 \tag{8.3.6}$$

$$A_1''+3\eta'A_1'-(8/3)A_2'+(\pi^2/\nu)[3-K_c\, C_{1d}'-f]A_1 = 0 \tag{8.3.7}$$

$$A_2''+3\eta'A_2'+(8/3)A_1'+(4\pi^2/\nu)[3-K_c\, C_{1d}'-f]A_2 = 0 \tag{8.3.8}$$

where the following relation has been used:

$$\Omega^2/\omega_\varepsilon^{\,2} = \nu^{-1} \tag{8.3.9}$$

This is obvious from equations (4.2.17) and (8.1.7). Moreover, the longitudinal vibrational equation (7.1.10) for C_{1d} can be rewritten using (8.3.3) as

$$C_{1d}'' + (K_c + 2\eta')C_{1d}' + \omega_\varepsilon^{\,2}\, C_{1d} = -f \tag{8.3.10}$$

The remaining task is to determine the feedback function f so that A_1, A_2, B_1, B_2 and C_{1d} are all stable. Multiplying (8.3.5) by B_1' , (8.3.6) by B_2', etc., adding and integrating from θ to $\theta + \Delta\theta$, one can obtain an energy integral from equations (8.3.5-8.3.10). Here $\Delta\theta$ is a small orbital angle but still large enough compared with periods of these vibrations. We then have

$$\begin{aligned}
&\frac{1}{2}\left[(A_1'^2+A_2'^2+B_1'^2+B_2'^2+C_{1d}'^2)\Big|_{\theta}^{\theta+\Delta\theta}\right] \\
&+ \left[\int_\theta^{\theta+\Delta\theta} \frac{1}{2}\{\pi^2\nu^{-1}(3-K_cC_{1d}')\frac{d}{d\theta}(A_1^2+4A_2^2+B_1^2+4B_2^2)\right. \\
&\left.+\,\omega_\varepsilon^{\,2}\frac{d}{d\theta}(C_{1d}^2)\}d\theta\right] = \int_\theta^{\theta+\Delta\theta} -\eta'[3(A_1'^2+A_2'^2+B_1'^2+B_2'^2)+4K\,B_1'+2C_{1d}'^2]d\theta \\
&+ \int_\theta^{\theta+\Delta\theta} f[\pi^2\nu^{-1}(A_1A_1'+4A_2A_2'+B_1B_1'+4B_2B_2')-C_{1d}']d\theta \\
&-K\int_\theta^{\theta+\Delta\theta}(C_{1s}'+C_{1d}')(2B_1'-B_2')d\theta - K_c\int_\theta^{\theta+\Delta\theta} C_{1d}'^2 d\theta = F
\end{aligned} \tag{8.3.11}$$

On the left hand side, the two terms represent kinetic and potential energy associated with the vibrations, respectively. The vibrations are damped if F, which represents the remaining integrals, is negative.

Recalling that $C_{1s} = 3M_b \ell_0 \omega^2/EA$, (7.1.4), we have

$$C_{1s}' = 3M_b \ell_0' \omega^2/EA = (3M_b \ell_0 \omega^2/EA)(\ell_0'/\ell_0)$$
$$= C_{1s} \eta' \quad (8.3.12)$$

Substituting (8.3.12) in (8.3.11),

$$F = \int_{\theta}^{\theta+\Delta\theta} -\eta'[3(A_1'^2+A_2'^2+B_1'^2+B_2'^2)+4KB_1'$$
$$+ 2C_{1d}'^2+KC_{1s}(2B_1'-B_2')]d\theta + \int_{\theta}^{\theta+\Delta\theta} f[\pi^2\nu^{-1}(A_1A_1'$$
$$+ 4A_2A_2'+B_1B_1'+4B_2B_2')-C_{1d}']d\theta - K\int_{\theta}^{\theta+\Delta\theta} C_{1d}'(2B_1'-B_2')d\theta$$
$$- K_c \int_{\theta}^{\theta+\Delta\theta} C_{1d}'^2 d\theta \quad (8.3.13)$$

The integral $\int f\, C_{1d}' d\theta$ over several cycles will vanish. Furthermore, since C_{1d} has a frequency that is different from those of A_1, A_2, B_1 and B_2, in the long run the term $-K\int_{\theta}^{\theta+\Delta\theta} C_{1d}'(2B_1'-B_2')d\theta$ will tend to zero. For simplicity, it is negelcted here.

The term $K_c \int_{\theta}^{\theta+\Delta\theta} C_{1d}'^2 d\theta$ plays a helpful role in withdrawing energy from the system, essentially making the longitudinal vibration C_{1d} stable. However the term $\int_{\theta}^{\theta+\Delta\theta} -3\eta'(A_1'^2+A_2'^2+B_1'^2+B_2'^2)d\theta$ is greater than zero (since η' is negative for retrieval) and plays an adverse role adding energy into the transverse vibrations. Note that this term is due to the negative damping in the A_1, A_2, B_1, B_2 equations. Examining (8.3.10) and (3.3.13), the sufficient conditions to make both longitudinal and transverse vibrations stable are

$$K_c > -2\eta' \qquad (8.3.14)$$

and

$$f[\pi^2\nu^{-1}(A_1A_1'+4A_2A_2'+B_1B_1'+4B_2B_2')]$$
$$< \eta'[3(A_1'^2+A_2'^2+B_1'^2+B_2'^2)+4KB_1'$$
$$+ KC_{1s}(2B_1'-B_2')] \qquad (8.3.15)$$

Thus, one chooses

$$f = -K_{AB}(A_1A_1'+4A_2A_2'+B_1B_1'+4B_2B_2'), \qquad (8.3.16)$$

where $K_{AB} > 0$ and sufficiently large. Then the term on the left hand side of (8.3.15) is negative all the time and large enough in magnitude to satisfy the inequality (8.3.15).

Examining (8.3.3) and (8.3.16) the length change law to control both transverse and longitudinal vibrations may be written as

$$\eta''+\eta'^2 = K_cC_{1d}'-K_{AB}(A_1A_1'+4A_2A_2'+B_1B_1'+4B_2B_2')$$
$$= K_cC_{1d}'-\frac{1}{2}K_{AB}\frac{d}{d\theta}[(A_1^2+B_1^2)+4(A_2^2+B_2^2)] \qquad (8.3.17)$$

The analysis is based on linear strain model. However, the computer simulation will use the unsimplified nonlinear equations (8.1.1) etc.

Physically, the form f chosen in equation (8.3.16) "asks" the changing length to produce a tension having appropriate components along the transverse directions thus stabilizing them. However, these forces are very weak unless K_{AB} is chosen reasonably large. Note that K_{AB} cannot be indefinitely large since f must be smaller than 3.

If K_c and K_{AB} are zero in equation (8.3.17), i.e., the retrieval is uncontrolled, then

$$\eta'' + \eta'^2 = 0 \tag{8.3.18}$$

This has a solution

$$\eta' = \tilde{c}/(1+\tilde{c}\theta) \tag{8.3.19}$$

where $\eta'(0) = \tilde{c}$; $\tilde{c}$ is negative during retrieval. Recalling that

$$\eta' = \ell_0'/\ell_0 \quad ,$$

$$\ell_0 = \ell_i(1+\tilde{c}\theta) \quad , \tag{8.3.20}$$

where $\ell_i = \ell_0(0)$.

Clearly, $\ell_0' = \tilde{c}\,\ell_i$ ($\tilde{c} < 0$ during retrieval).

This represents a constant velocity retrieval. Hence the length change law given in equation (8.3.17) is basically a modulation of constant velocity retrieval. Exponential retrieval can be modulated similarly.

The length change law (8.3.17) can be rewritten in length rate form (approximately and somewhat more generally) as

$$\eta' = K_a/\{1+K_a\theta+K_bC_{1d}+[K_1(A_1{}^2+B_1{}^2)+K_2(A_2{}^2+B_2{}^2)]\} ,$$

$$K_a < 0, \quad K_b, K_1 > 0 \tag{8.3.21}$$

The analysis is based on linear strain model. However, the computer simulation will use the unsimplified nonlinear equation (8.1.1) and similar equations obtained from (4.2.16), (4.2.19), (4.2.21) and (4.2.2) after putting α and γ terms to zero.

The dynamics during retrieval of the subsatellite from 1 Km is shown in Figure 8.5, where $K_b = 300$, $K_1 = 10^5$, $K_2 = -4$ while K_a is is calculated from $\eta'(0) = \tilde{c}$. Note that all the vibrations are reasonably stable.*

8.4 AN EXAMINATION OF FAST RETRIEVALS

When the tether becomes shorter during retrieval, the strain or tension in the tether becomes smaller. Examining the tension carefully in Figure 8.4(b), it can be seen that the tensions at both ends have vibratory components even though they are quite small. This is not desirable as vibrations may subsequently cause the tether to become slack. The question arises as how to maintain a certain amount of tension in the tether so that this can be avoided. Probably, the tether should be retrieved fast at the terminal phase of retrieval, so that the inertial force produced from the fast accelerating retrieval will add to the tension in the tether.

---

* Examining (8.3.17) one notes the $K_2 = 4$ should arrest the growth of transverse vibrations; however, in numerical simulations this was not the case. On the other hand $K_2 = -4$ works. The reason still remains unclear to the author.

Recall that the quasi-static equilibrium strain is given by

$$C_{1s} = [3-(\eta''+\eta'^2)](M_b \ell_0 \omega^2/EA) \tag{8.3.2}$$

If we let

$$\eta'' + \eta'^2 = \begin{cases} 0 & \ell_0 > \ell_{fr} \\ 3-3(\ell_{fr}/\ell_0) & \ell_0 < \ell_{fr} \end{cases} \tag{8.4.1}$$

where the constant ℓ_{fr} stands for the length at which the fast retrieval begins, then

$$C_{1s} = (3M_b \ell_{fr} \omega^2/EA) = \text{const for } \ell_0 < \ell_{fr} \tag{8.4.2}$$

With (8.4.1), the strain is continuous at $\ell_0 = \ell_{fr}$ and remains constant for $\ell_0 < \ell_{fr}$.

Using the definition of η in (4.2.10), i.e.,

$$e^{\eta} = \ell_0/\ell_{ref} \quad ,$$

the second part of (8.4.1) can be rewritten as

$$e^{\eta}(\eta''+\eta'^2)=3e^{\eta}-3(\ell_{fr}/\ell_{ref}) \tag{8.4.3}$$

the solution to which is

$$e^{\eta} = A\text{sh}\sqrt{3}\theta+B\text{ch}\sqrt{3}\theta +(\ell_{fr}/\ell_{ref}) \tag{8.4.4}$$

where A and B are constants. If the fast retrieval starts from $\theta = \theta_{fr}$, then

$$\ell_0(\theta_{fr}) = \ell_{fr} \tag{8.4.5}$$

and

$$\eta'(\theta_{fr}) = \tilde{c}\ ,\ \tilde{c} < 0 \tag{8.4.6}$$

Thus (8.4.4) becomes

$$\eta = \ell n[(\ell_{fr}/\ell_{ref})(1+(\tilde{c}/\sqrt{3})\text{sh}\sqrt{3}(\theta-\theta_{fr})] \tag{8.4.7}$$

and

$$\eta' = \tilde{c}\ \text{ch}\sqrt{3}(\theta-\theta_{fr})/[1+(\tilde{c}/\sqrt{3})\text{sh}\sqrt{3}(\theta-\theta_{fr})] \tag{8.4.8}$$

for $\theta > \theta_{fr}$. Since

$$\eta' = \ell_0'/\ell_0\ ,$$

we have

$$\ell_0' = \ell_0\ \eta' = \ell_{ref}\ e^{\eta}\ \eta' \tag{8.4.9}$$

Substituting (8.4.7) and (8.4.8) in (8.4.9),

$$\ell_0' = \ell_{fr}\ \tilde{c}\ \text{ch}\sqrt{3}(\theta-\theta_{fr})\quad ,\quad \theta > \theta_{fr} \tag{8.4.10}$$

From (8.4.10) it is clear that the retrieval velocity is increasing with θ.

The effect of this fast terminal retrieval on the vibrations in the absence of rotational motions is tested by integrating the nonlinear vibrational equations numerically. The retrieval starts from

1 Km and ℓ_{fr} is set to 250 m. Corresponding vibrational behaviour is represented by Figure 8.6. Note that in the first phase the retrieval speed is constant while in the second phase after $\ell_0 < \ell_{fr} = 250$ m, it is speeding up and the tension is maintained approximately to a constant value. Some artificial viscous damping in the longitudinal direction has been introduced ($\xi \cong 0.8$). Notice that A_1 and B_1 increase only slightly, the actual displacements $\ell_0 A_1$ etc. of course, reduce.

Figure 8.7 describes the vibratory behaviour during reduction of the tether length given by

$$\eta'' = \begin{cases} 0 & 250 \leq \ell_0 \leq 1000 \\ -\eta'^2 - 3(1000-\ell_0)/\ell_0 & \ell_0 < 250 \end{cases} \tag{8.4.11}$$

where ℓ_0 is in meters. The longitudinal viscous damping is the same as in the previous case. $\eta'' = 0$ corresponds to exponential retrieval. Thus the first phase is a slow exponential retrieval, but the second phase corresponds to even a faster retrieval (compared to the case in Fig. 8.6) with a strong jump in acceleration at $\ell_0 = 250$ m. This is designed to raise the tension in the tether, hence forcing the transverse vibrations to smaller amplitudes. From the results, it may be seen that the tensions at both ends of the tether jump to higher levels and the transverse vibrations are bounded to small values. It should be mentioned here that the scale in the plots of transverse vibrations are 10 times smaller than the scale used in Figure 8.6.

Fast retrieval can only be performed at the very end of retrieval. When it starts, it must be maintained until the end of retrieval. Otherwise the slowdown could cause tether slackness.

8.5 CONTROL OF GENERAL DYNAMICS INCLUDING BOTH ROTATIONS AND VIBRATIONS

So far this chapter has examined the nonlinear vibrations at the terminal phase of retrieval ignoring the rotational motions. This section brings the rotational oscillations and vibrations (both longitudinal and transverse) together and the investigation is from the very beginning of retrieval. The length change law uses feedback from rotational as well as vibrational state variables.

8.5.1 Numerical Results using Linear Strain Model

At first, the linear strain dynamic model is used for the numerical simulation. In Section (8.5.2), nonlinear strain model is used.

It has been shown in Chapter 6 that pitch and roll behaviour of the system can be stabilized during retrieval of the subsatellite using

$$\eta' = \tilde{c}(1-\alpha'-9\gamma'^2),\ c = \tilde{c}\omega = -2\times10^{-4}s^{-1} \qquad (8.5.1)$$

The vibrational behaviour using the same length rate is shown in Figure 8.8. The longitudinal oscillation grows rather fast and the transverse vibrations also build up slowly. Numerical integration was stopped when the longitudinal oscillation became too large. This clearly shows the importance of including vibrational feedback in the length rate.

Figure 8.9 shows the response of the system when the length rate is

$$\eta' = \tilde{c}(1-\alpha'-9\gamma'^2-K_c\ C_1),\quad K_c = 30 \tag{8.5.2}$$

The value of $\tilde{c}$ is the same as before. Longitudinal vibrations are more or less eliminated. The vibratory displacements $\tilde{A}_1$, $\tilde{A}_2$, $\tilde{B}_1$, $\tilde{B}_2$ and the resultant transverse deflection of the mid-point of the tether denoted by R are small towards the end of retrieval. However, the nondimensional transverse displacements represented by A_1, A_2, B_1, B_2 grow slowly.

Using a length rate

$$\eta' = \tilde{c}(1-\alpha'-9\gamma'^2-K_{B_1}\ B_1') \tag{8.5.3}$$

with $K_{B_1} = 10$ and employing a viscous damper to provide a force proportional to C_1', one obtains the system response shown in Fig. 8.10. This response is very similar to that in Fig. 8.9, except that the transverse vibrations are slightly smaller. The retrieval dynamics up to a tether length of 250 m using (8.5.2) is described in Fig. 8.11. K_c is 30 for $\ell_0 > 1.2$ Km but is 300 for $\ell_0 < 1.2$ Km. It is noted that again the actual displacements $\tilde{A}_1$ etc. remain small. The nondimensional transverse displacements, however, increase slightly.

The linear strain model is not very good during the terminal phase of retrieval even though the transverse vibrations may have small amplitudes. This is because the strain in the tether approaches zero during the retrieval. Noting that in Fig. 8.9 A_1, B_1 are of the order of 0.01, while C_1 is of the order of 10^{-5} at 1 Km, the nonlinear strain term calculated from A_1^2, B_1^2 etc. is larger than the linear term C_1. This merely suggests that the nonlinear strain has to be considered in the dynamical modelling.

8.5.2 Numerical Results Using Nonlinear Strain Model

Figure 8.12 shows the dynamical response represented by C_1, A_1, A_2, B_1 and B_2 during retrieval of the subsatellite from 100 Km using the length change law

$$\eta' = \tilde{c}[1-5\alpha'-18\gamma'^2-1.5\,\omega_\varepsilon\, C_{1d}], \quad \tilde{c} = c/\omega \tag{8.5.4}$$

The retrieval constant c is $-2 \times 10^{-4}S^{-1}$, the same as before. So are the initial conditions of A_1, A_2, B_1, B_2 and C_1. Comparing the length change laws (8.5.4) and (8.5.2), they are basically of the same kind. However, the gains for α' and γ'^2 feedback have been changed from 1 and 9 to 5 and 18, respectively. Also, the feedback that η' gets from longitudinal vibration has been altered from C_1 to C_{1d}. All these changes have been made to make α, γ and C_1 more stable. One can see from Fig. 8.12 that C_1 is stable. However, A_1, B_1 are building up. It is obvious that C_1 is affected by A_1 and B_1, resulting in high frequency oscillations. This is due to the nonlinear strain term. The strong coupling between longitudinal and transverse vibrations also advances the occurrence of the slackness of the tether as can be seen from the tension σ shown in Fig. 8.12. This fact merely shows that transverse vibrations could also make the tether slack just as longitudinal vibrations if they are not damped out. Unfortunately, modal coordinate B_1 associated with transverse vibrations is quite large at the beginning of the retrieval because of the aerodynamic and Coriolis forces. Thus damping transverse vibrations during retrieval is quite challenging.

Although the transverse vibrations excite longitudinal vibrations and vice versa, the requirements to control these two types of vibrations are somewhat conflicting. This is depicted in Fig. 8.13. At first, retrieval from 100 Km is carried out using feedback of longitudinal and transverse vibrations, i.e.,

$$\eta'' = \tilde{c}\{-2\alpha''-36\gamma'\gamma''-\omega_\varepsilon C_{1d}'+(1/2)K_{AB}\frac{d}{d\theta}[(A_1{}^2+B_1{}^2)+4(A_2{}^2+B_2{}^2)]\}$$

and

$$\eta'(0) = \tilde{c} \tag{8.5.5}$$

After four orbits, when the length has reduced to 17 Km, feedback of longitudinal vibration alone is used, i.e.,

$$\eta'' = \tilde{c}\{-2\alpha''-36\gamma'\gamma''-\omega_\varepsilon C_{1d}'\} \tag{8.5.6}$$

where K_{AB}, $c\,(=\tilde{c}\omega)$ are taken as 5×10^4 and $-0.5 \times 10^{-4} S^{-1}$, respectively. The initial conditions are $\gamma = 1°$, $\alpha-180° = 15°$, $A_1 = -5 \times 10^{-4}$, $A_2 = 5 \times 10^{-4}$, $B_1 = -0.16 \times 10^{-2}$, $B_2 = 0.28 \times 10^{-3}$, $C_1 = 0.49 \times 10^{-2}$, $C_2 = -0.28 \times 10^{-3}$, $\alpha' = \gamma' = A_1' = A_2' = B_1' = B_2' = C_1' = C_2' = 0$. From 8.13(a) it is clear that the gains used for α' and γ'^2 are adequate to confine the rotations to small range. The transverse vibration B_1 is damped during the first four orbits while there is no appreciable growth in A_1, A_2, B_2. However C_1 is affected adversely, resulting in large oscillations. If the feedback of transverse vibrations is dropped, it is clearly seen that C_1 becomes stable. However B_1, A_1 steadily increase henceforth. From the plot of tension σ (Fig. 8.13(b)), it may be noted that during the second phase, there is a small oscillatory component of tension due to the transverse vibrations (C_1 has negligible oscillatory component).

The results above suggest that control of nonlinear vibrations from the very beginning of retrieval until the end is a difficult task if only length change strategies are used. The fact is that the tension in the tether weakens during retrieval while there are too many degrees of freedom to be taken care of. Probably, if the retrieval is carried out very slowly so that the material damping is larger than the negative damping associated with the retrieval process, then stable retrieval might be achieved. However, this will imply quite a long time to retrieve the subsatellite, which may not be acceptable in the practical sense. Based on the above reasoning, this very slow retrieval is not examined.

It might be interesting to note that under certain circumstances, the internal resonance between longitudinal and transverse vibrations can be used to absorb the transverse vibrational energy (although not completely) through damping of longitudinal vibrations. This requires reducing the frequency of longitudinal vibration C_{1d} to a value closer to the frequency associated with the modal coordiante A_1 (or B_1).

From equation (7.1.10), if η'' is chosen as

$$\eta'' = a(EA/M_b \, \ell_0 \, \omega^2)C_{1d}', \quad a = \text{const.}, \tag{8.5.7}$$

then C_{1d} has a frequency of oscillation

$$\omega_\varepsilon \approx \{[1-(a^2/4)](EA/M_b \, \ell_0 \, \omega^2)\}^{1/2} \tag{8.5.8}$$

From equations (8.3.7) or (8.3.8), the frequency associated with A_1 or B_1 is approximately

$$\omega_{A1} \approx (3\pi^2 M_b/\rho_c\, \ell_0)^{1/2} \tag{8.5.9}$$

It may be noted that both frequencies ω_c and ω_{A1} are proportional to $(\ell_0)^{-1/2}$. To make these two frequencies approximately equal, i.e.,

$$\omega_\varepsilon \approx \omega_{A1} \tag{8.5.10}$$

we must have

$$[1-(a^2/4)] \approx 3\pi^2 M_b{}^2 \omega^2/\rho_c\, EA \tag{8.5.11}$$

The term on the right hand side is a constant while a can be chosen arbitrarily. Consider typical parameters as follows

$$M_b = 170 \text{ Kg} \tag{8.5.12a}$$

$$d_c = 0.325 \times 10^{-3} \text{m} \tag{8.5.12b}$$

$$A = \pi d_c{}^2/4 \tag{8.5.12c}$$

$$E = 2.1 \times 10^{11} \text{ N/m}^2 \tag{8.5.12d}$$

$$\rho_c = 7.8 \times 10^3 \text{ A Kg/m} \tag{8.5.12e}$$

$$\omega = 1.1 \times 10^{-3} \text{S}^{-1} \tag{8.5.12f}$$

a can be determined as

$$a = 1.7889 \tag{8.5.13}$$

In the numerical simulation, a is taken to be 1.8. Consider the length change law

$$\eta'' = \tilde{c}[\,-5\alpha''-36\gamma'\gamma''] + a(EA/M_b\,\ell_0\,\omega^2)C_{1d}'$$

$$+10^4(B_1B_1' + A_1A_1') \tag{8.5.14}$$

Figures 8.14 and 8.15 show the dynamic response during the retrieval of the subsatellite from 100 Km under the same initial conditions and physical parameters except that a is taken as 1.5 and 1.8, respectively. (The retrieval constant c is -1 x $10^{-4}S^{-1}$ and the initial conditions are the same as given in Fig. 8.13 except γ = 0.5°.)

There is no internal resonance between longitudinal and transverse vibrations for a = 1.5 while there is for a = 1.8. Clearly, the behaviour of modal coordinates A_1 and B_1 is quite different in the two cases. For a = 1.5, transverse vibrations A_1, B_1 are quite large while they are small for a = 1.8. However, C_1 has a larger variation at the beginning of retrieval in the case of a = 1.8. Since A_1 and B_1 are maintained small in the case of internal resonance, the tensions at both ends of the tether rapidly approach the same value during retrieval.

Although this resonance does not absorb the transverse vibrational energy completely, it still does some good. In the next chapter, which deals with the thruster augmented active control, a mixed control strategy will be used. At first, this kind of resonance can be employed to retrieve the subsatellite from 100 Km to a shorter length, say 20 Km. Since transverse vibrational energy is absorbed partially, it helps the thruster augmented control that follows. It may be pointed out that the relatively large variation of C_1 at the beginning of the retrieval is not a problem because at that moment, C_1 is large enough to keep the tether taut in spite of the variation.

CHAPTER 9

THRUSTER AUGMENTED ACTIVE CONTROL

As the length of the tether reduces to a small value during the retrieval of the subsatellite, the equilibrium tension in the tether approaches zero and during a dynamical situation the tether may become slack. It has been seen earlier in this thesis that the rotational motion of the shuttle supported tethered subsatellite system as well as the longitudinal and transverse vibrations of the tether are inherently unstable during the retrieval phase. If only a length change or tension control law is used, it is difficult to control all the motions during the terminal phase of retrieval when the condition of very weak tension prevails. This is especially true if one wants to control the objectionable transverse vibrations.

To alleviate this difficulty, Banerjee and Kane [30] proposed to use a set of thrusters (in addition to a torque control law) to control the retrieval dynamics. The results presented in their paper are quite promising; however, the transverse vibrations of the tether were neglected in their dynamical model implying that the tether always remained straight. The objective of this chapter is to remove this restriction and to present thruster augmented control schemes that are effective in the presence of transverse vibrations of the tether. The nonlinear equations of motion, developed in Chapter 4 are used for examining the proposed thruster augmented control schemes. At first, active control of the system dynamics by using thrusters alone is considered. This is followed by a mixed control strategy involving the thrusters in conjunction with a length change control law, with an objective of saving the thruster fuel. In order to determine an appropriate functional form of the thrust an approximate analysis of the equations of motion is carried out; however, the final results are obtained numerically considering the original equations.

9.1 ARRANGEMENT OF THE THRUSTERS

Consider three thrusters placed on the subsatellite which can fire along local x_c, y_c, z_c directions, respectively (Fig. 9.1). The task of the thrust T_c, which is along the direction of the tetherline, is to control the longitudinal vibrations and to provide extra tension in the tether when the tether is retrieved to a short length. The function of T_α, acting in the orbital plane along z_c, i.e., approximately in the direction of flight, is to provide a torque to control inplane rotational motion α as well as the inplane vibrations of the tether. Probably this thrust can be called inplane thrust for better physical appreciation. Finally, T_γ applied along the x_c direction perpendicular to the orbital plane (approximately), similarly produces a torque to control out-of-plane rotational motion γ as well as the out-of-plane vibrations. It can be termed out-of-plane thrust.

Note that T_α and T_γ not only control the appropriate rotational motions but also are used for arresting the growth of corresponding transverse vibrations. It is not difficult to visualize that the rotational motions can be controlled quite easily through the thruster forces T_α and T_γ. All that is required is that T_α and T_γ act along directions opposing the rotational motions α and γ at all times.

However, it is not so obvious how at the same time, T_α and T_γ can control the inplane and out-of-plane vibrations. Hence, an approximate analysis of the equations of motion is made at first.

9.2 ANALYSIS TO DERIVE THRUST CONTROL LAWS

9.2.1 Generalized Forces due to the Thrusters

When the thrusters T_α, T_γ and T_c act on the subsatellite, the equations of motion will include the corresponding generalized forces caused by these thrusters. Clearly, the total thrust $\vec{T}$ acting on the subsatellite can be expressed as

$$\vec{T} = T_\gamma \vec{i}_c + T_c \vec{j}_c + T_\alpha \vec{k}_c \tag{9.2.1}$$

The position vector of the subsatellite relative to the center of the earth E is

$$\begin{aligned} \vec{R}_{EB} &= \vec{R}_0(\theta) + \vec{R}_b \\ &= \vec{R}_0(\theta) + [\ell_0(t) + v(\ell_0,t)]\vec{j}_c\,(\alpha,\gamma) \\ &= \vec{R}_0(\theta) + [1 + C_1 + C_2]\ell_0\,\vec{j}_c \end{aligned} \tag{9.2.2}$$

Therefore, the generalized forces due to thrust $\vec{T}$ are:

$$QT_{C_1} = \vec{T}\cdot(\partial\vec{R}_{EB}/\partial C_1) = T_c\,\ell_0 \tag{9.2.3a}$$

$$QT_{C_2} = \vec{T}\cdot(\partial\vec{R}_{EB}/\partial C_2) = T_c\,\ell_0 \tag{9.2.3b}$$

$$QT_\alpha = \vec{T}\cdot(\partial\vec{R}_{EB}/\partial\alpha) = (1 + C_1 + C_2)\ell_0\ \vec{T}(\partial\vec{j}_c/\partial\alpha)$$

Since from (2.9.6) $(\partial\vec{j}_c/\partial\alpha) = c\gamma\ \vec{k}_c$, we have

$$QT_\alpha = (1 + C_1 + C_2)T_\alpha\ \ell_0\ c\gamma = T_\alpha\ \ell\ c\gamma \tag{9.2.3c}$$

where ℓ is the stretched length of the tether. Similarly, using $(\partial\vec{j}_c/\partial\gamma) = -\vec{i}_c$

$$QT_\gamma = -(1 + C_1 + C_2)T_\gamma\ \ell_0 = -T_\gamma\ \ell \tag{9.2.3d}$$

It may be noted that QT_α and QT_γ are merely torques associated with α and γ rotations.

Considering the α, γ and C_γ equations (4.2.14), (4.2.15) and (4.2.22), which have been nondimensionalized through a division by $M_b\ \ell_0{}^2\ \dot\theta^2$, corresponding nondimensional generalized forces S_α, S_γ, S_{C_1} are

$$S_\alpha = QT_\alpha/M_b\ \ell_0{}^2\ \dot\theta^2 = (1 + C_1 + C_2)T_\alpha\ c\gamma/M_b\ \ell_0\ \dot\theta^2, \tag{9.2.4a}$$

$$S_\gamma = -(1 + C_1 + C_2)T_\gamma/M_b\ \ell_0\ \dot\theta^2\ , \tag{9.2.4b}$$

and

$$S_{C_1} = (1 + C_1 + C_2)T_c/M_b\ \ell_0\ \dot\theta^2 \tag{9.2.4c}$$

Noticing that the modified C_2 equation (4.2.23) is obtained by subtracting the original C_2 equation from the C_1 equation, one can show that

$$S_{C_2} = 0 \qquad (9.2.4d)$$

Defining nondimensional forces $\tilde{T}_\alpha$, $\tilde{T}_c$ and $\tilde{T}_\gamma$ as

$$\tilde{T}_\alpha = T_\alpha / M_b \ell_0 \dot{\theta}^2 \qquad (9.2.5a)$$

$$\tilde{T}_\gamma = T_\gamma / M_b \ell_0 \dot{\theta}^2 \qquad (9.2.5b)$$

and

$$\tilde{T}_c = T_c / M_b \ell_0 \dot{\theta}^2 \qquad (9.2.5c)$$

one obtains

$$S_\alpha = (1 + C_1 + C_2)\tilde{T}_\alpha \, c\gamma \approx \tilde{T}_\alpha \, c\gamma \qquad (9.2.6a)$$

$$S_\gamma = -(1 + C_1 + C_2)\tilde{T}_\gamma \approx -\tilde{T}_\gamma \qquad (9.2.6b)$$

$$S_{C_1} = (1 + C_1 + C_2)\tilde{T}_c \approx \tilde{T}_c \qquad (9.2.6c)$$

$$S_{C_2} = 0 \qquad (9.2.6d)$$

9.2.2 Simplified Equations

The discretized equations of motion (4.2.14), (4.2.15), (4.2.17), (4.2.19) - (4.2.23) are very complicated and it is difficult to determine the required control thrusts T_α, T_γ and T_c from these equations. Hence, these equations are simplified solely for the purpose of obtaining these thrusts. To do so, the following assumptions are made:

(i) The orbit is assumed to be circular.

(ii) The nonlinear strain term is neglected.

(iii) C_2 is ignored compared with C_1.

(iv) Some insignificant terms in the equations are neglected; for example in A_1 equation $[\frac{3}{2}(\eta''-F\eta')+(2-\frac{\pi^2}{3})\eta'^2]A_1$ is insignificant compared with $\pi^2\Omega^2\{...\}$ term, because Ω^2 is a very large term.

(v) Equations are linearized.

(vi) Aerodynamic forces are not considered.

(vii) Mass ratio ν is small compared to 1.

With the above assumptions and substituting (9.2.6) into corresponding α,γ, C_1 equations (4.2.14), (4.2.15) and (4.2.17), we have the simplified equations as follows:

$$\alpha'' + 2\eta'(1+\alpha') + 3\alpha = \tilde{T}_\alpha \tag{9.2.7}$$

$$B_1''+3\eta'B_1'-(8/3)B_2'+4K\eta'(1+\alpha')+K\alpha''+3K\alpha+\pi^2\Omega^2B_1C_1= 0 \tag{9.2.8}$$

$$B_2''+3\eta'B_2'+(8/3)B_1'-\frac{1}{2}K\alpha''-(3/2)K\alpha+4\pi^2\Omega^2B_2C_1 = 0 \tag{9.2.9}$$

$$\gamma''+2\eta'\gamma'+4\gamma = -\tilde{T}_\gamma \tag{9.2.10}$$

$$A_1''+3\eta'A_1'-(8/3)A_2'-4K\eta'\gamma'-K\gamma''-4K\gamma+\pi^2\Omega^2A_1C_1 = 0 \tag{9.2.11}$$

$$A_2''+3\eta'A_2'+(8/3)A_1''+\frac{1}{2}K\gamma''+2K\gamma+4\pi^2\Omega^2A_2C_1 = 0 \tag{9.2.12}$$

$$C_1''+2C_1'\eta'+\omega_\varepsilon{}^2C_1 = 3-(\eta''+\eta'^2)+\tilde{T}_C \tag{9.2.13}$$

In the simplified equations above, it may be noted that $\tilde{T}_\alpha$, $\tilde{T}_\gamma$ and $\tilde{T}_c$ appear in α, γ and C_1 equations but not in A_1, A_2, B_1 and B_2 equations. Thus, it might appear that these transverse vibrations may not be controllable by the thrusts T_α, T_γ and T_c. However, this is not true. The out-of-plane transverse modal coordinates A_1 and A_2 are coupled with γ equation; so are the inplane transverse modal coordinates B_1 and B_2 with α equation. Therefore A_1 and A_2 are affected by T_γ as are B_1 and B_2 by T_α. This is shown in the following sections.

9.2.3 Derivation of a Suitable Form of $\tilde{T}_\gamma$

The inplane and out-of-plane motions are coupled very weakly. Hence, corresponding equations are investigated separately for simplicity. The equations governing γ, A_1 and A_2 (9.2.10) - (9.2.12) can be written in matrix form as

$$\begin{bmatrix} 1 & 0 & 0 \\ -K & 1 & 1 \\ K/2 & 0 & 0 \end{bmatrix} \begin{Bmatrix} \gamma'' \\ A_1'' \\ A_2'' \end{Bmatrix} + \begin{bmatrix} 2\eta' & 0 & 0 \\ -4K\eta' & 3\eta' & -(8/3) \\ 0 & (8/3) & 3\eta' \end{bmatrix} \begin{Bmatrix} \gamma' \\ A_1' \\ A_2' \end{Bmatrix}$$

$$+ \begin{bmatrix} 4 & 0 & 0 \\ -4K & \omega_1{}^2 & 0 \\ 2K & 0 & 4\omega_1{}^2 \end{bmatrix} \begin{Bmatrix} \gamma \\ A_1 \\ A_2 \end{Bmatrix} = - \begin{Bmatrix} 1 \\ 0 \\ 0 \end{Bmatrix} \tilde{T}_\gamma \qquad (9.2.14)$$

where

$$\omega_1{}^2 = \pi^2\Omega^2 C_1$$

Inverting the matrix coefficient of the accelerations, we have

$$\begin{Bmatrix} \gamma'' \\ A_1'' \\ A_2'' \end{Bmatrix} + \begin{bmatrix} 2\eta' & 0 & 0 \\ -2K\eta' & 3\eta' & -(8/3) \\ -K\eta' & (8/3) & 3\eta' \end{bmatrix} \begin{Bmatrix} \gamma' \\ A_1' \\ A_2' \end{Bmatrix} + \begin{bmatrix} 4 & 0 & 0 \\ 0 & \omega_1^2 & 0 \\ 0 & 0 & 4\omega_1^2 \end{bmatrix} \begin{Bmatrix} \gamma \\ A_1 \\ A_2 \end{Bmatrix}$$

$$= - \begin{Bmatrix} 1 \\ K \\ -K/2 \end{Bmatrix} \tilde{T}_\gamma \qquad (9.2.15)$$

Equation (9.2.15) indicates that A_1, A_2 are affected by $\tilde{T}_\gamma$. This fact can be explained from physical consideration. When $\tilde{T}_\gamma$ acts on the subsatellite, it produces a torque around the system centre of mass, thus changing the rotational acceleration $\ddot{\gamma}$. This change in acceleration $\ddot{\gamma}$ introduces distributed forces along the tether in the transverse out-of-plane direction. Thereby, transverse vibrations A_1 and A_2 are indirectly affected by $\tilde{T}_\gamma$.

Now, it is not difficult to see of what form $\tilde{T}_\gamma$ must be. In order to make γ, A_1 and A_2 motions stable, $\tilde{T}_\gamma$ must produce rate dependent terms to overcome the negative damping represented by the second term of the left hand side of equation (9.2.15). This suggests a form of $\tilde{T}_\gamma$ as

$$\tilde{T}_\gamma = (-K_\gamma \gamma' - K_{A_1} A_1' + K_{A_2} A_2')\eta' \qquad (9.2.16)$$

where K_γ, K_{A_1} and K_{A_2} are positive numbers greater than 2, 3/K and 6/K, respectively. The coefficients of A_1' and A_2' in (9.2.16) have different signs since the effects of $\tilde{T}_\gamma$ on the two motions as given in (9.2.15) have opposite signs.

9.2.4 Derivation of a Suitable Form of $\tilde{T}_\alpha$

Following an analysis similar to that for $\tilde{T}_\gamma$, one can get a simplified matrix equation for inplane motion as

$$\begin{Bmatrix} \alpha'' \\ B_1'' \\ B_2'' \end{Bmatrix} + \begin{bmatrix} 2\eta' & 0 & 0 \\ 2K\eta' & 3\eta' & (-8/3) \\ K\eta' & (8/3) & 3\eta' \end{bmatrix} \begin{Bmatrix} (1+\alpha') \\ B_1' \\ B_2' \end{Bmatrix}$$

$$+ \begin{bmatrix} 3 & 0 & 0 \\ 0 & \omega_1{}^2 & 0 \\ 0 & 0 & 4\omega_1{}^2 \end{bmatrix} \begin{Bmatrix} \alpha \\ B_1 \\ B_2 \end{Bmatrix} = \begin{Bmatrix} 1 \\ -K \\ K/2 \end{Bmatrix} \tilde{T}_\alpha \qquad (9.2.17)$$

Through the coupling between pitch rotation and the vibrations, $\tilde{T}_\alpha$ can influence B_1 and B_2.

To make inplane motion stable, $\tilde{T}_\alpha$ must depend on α', B_1' and B_2' as follows:

$$\tilde{T}_\alpha = (2+K_\alpha\alpha'-K_{B_1}B_1'+K_{B_2}B_2')\eta' \qquad (9.2.18)$$

where K_α, K_{B_1} and K_{B_2} are positive numbers greater than 2, 3/K and 6/K, respectively (note that $\eta' < 0$ during retrieval).

It should be mentioned that the orbital rotational rate has an effect on inplane rotation α. In equation (9.2.17), the term $(1+\alpha')$ includes the contribution of the orbital rotation (1 added to the pitch rate). During the retrieval process, orbital rotation tends to push the subsatellite away from the vertical. Thus, α usually has a certain amount of steady value which is dependent on how large η' is. Dimensionless thrust $\tilde{T}_\alpha$ given in equation (9.2.18) involves a $2\eta'$ term just to cancel this steady rotation. Thus α is expected to return to the vertical position. Clearly, $\tilde{T}_\alpha$ required is much larger than $\tilde{T}_\gamma$. This will be seen in the numerical results presented later.

9.2.5 Derivation of an Appropriate Form of $\tilde{T}_c$

$\tilde{T}_c$ acting along the direction of tetherline has two functions. One is to damp the longitudinal vibrations, i.e., control the unstable generalized coordinate C_1. The other is to provide a certain amount of tension in the tether during the terminal phase of retrieval.

This second function of $\tilde{T}_c$ is very important. Very small tension in the tether is always instrumental in inducing slackness of the tether. Theoretically, when ℓ_0 goes to zero, the tension in the tether approaches zero as well (except when the retrieval process is gradually speeding up). Any longitudinal vibrations could make the tether slack.

The question arises as to what minimum tension must be maintained in the tether. Obviously, the larger the thrust T_c the greater the tension provided, thus making it more likely to prevent slackness of the tether. However, more fuel is consumed that way. Since the tension is fairly large when the tether is long, the second function of $\tilde{T}_c$ could be performed at the terminal phase of retrieval.

Observing the C_1 equation (9.2.13) it is not difficult to find an appropriate form of $\tilde{T}_c$ to damp the unstable longitudinal vibration. $\tilde{T}_c$ is designed as

$$\tilde{T}_c = \begin{cases} -K_c\omega_\varepsilon(C_1') \quad , & \ell_i \geq \ell_0 \geq \ell_T \\ -K_c\omega_\varepsilon C_1'+3(\ell_T-\ell_0)/\ell_0, & \ell_0 < \ell_T \end{cases} \tag{9.2.19}$$

where ℓ_T is a preset value of the length below which the thruster fires additionally to maintain a certain amount of tension. The term $3(\ell_T-\ell_0)/\ell_0$ in (9.2.19) causes the tension in the tether to remain approximately constant when ℓ_0 is reduced below ℓ_T. Referring to equation (8.4.5), one may notice that this term is almost the same as that on the right hand side of (8.4.5).

The larger the conditional value of length ℓ_T, the larger is the tension maintained in the tether although more fuel is consumed. The choice of the value of ℓ_T is limited by the maximum thrust provided by the thruster.

9.3 NUMERICAL RESULTS FOR THRUSTER CONTROL

Once the control laws for $\tilde{T}_\alpha$, $\tilde{T}_\gamma$ and $\tilde{T}_c$ have been obtained through a simplified analysis, their effectiveness is examined through computer simulation. The equations used to obtain the numerical results are no longer the simplified ones but the original more complicated ones, i.e., equations (4.2.14), (4.2.15), (4.2.17), (4.2.19) - (4.2.23).

Both Figs. 9.2 and 9.3 use the same physical parameters as in the case of Fig. 8.15, the retrieval constant $c = \tilde{c}\omega = -4 \times 10^{-4}S^{-1}$ and the initial conditions are $(\alpha-\pi) = 15°$, $\gamma = 1°$, $C_1 = 0.47 \times 10^{-2}$, $C_2 = -0.19 \times 10^{-3}$, $A_1 = 0.5 \times 10^{-4}$, $A_2 = -0.5 \times 10^{-4}$, $B_1 = -0.16 \times 10^{-2}$, $B_2 = 0.48 \times 10^{-3}$ and $A_1' = A_2' = B_1' = B_2' = C_1' = C_2' = \alpha' = \gamma' = 0$. Since the thrusters are used to control all the motions from the beginning of retrieval to the end, retrieval length rate is not modulated by the state variables and is assumed to follow the exponential retrieval law, i.e., $\eta' = \tilde{c}$.

Figure 9.2 shows the dynamical response during retrieval when an attempt is made to maintain the tension in the tether at the initial level, i.e., in equation (9.2.19) $\ell_T = 100$ Km. The control thrusts then are given by

$$\tilde{T}_\alpha = 2c^2\gamma(1+\nu/2)[1+\alpha']\eta'-2\alpha'+10(B_1'-0.5B_2')$$

$$\tilde{T}_\gamma = -2(1+\nu/2)\gamma'\eta'+2\gamma'-10(A_1'-0.5A_2')$$

$$\tilde{T}_c = -\omega_\varepsilon(C_1'+C_2')+3[(\ell_T-\ell_0)/\ell_0] \qquad (9.3.1)$$

Equation (9.3.1) makes a little modification to the already derived thrust forms from the simplified analysis since the original equations are used now. It is not difficult to see that the first term on the right hand side of either $\tilde{T}_\alpha$ or $\tilde{T}_\gamma$ expression is just to balance the identical term in α or γ equation.

It can be seen from Fig. 9.2 that the thruster active control law (9.3.1) is quite successful. α rotation rapidly goes to zero from an initial deviation of 15° away from the vertical. So does γ rotation from an initial value of 1°. All the transverse vibrations A_1, A_2, B_1, B_2, as well as the longitudinal variable C_2 are also rapidly damped to zero. On the other hand, C_1 approaches a constant level. The tensions at the two ends gradually approach the same constant value.

The drawback of this scheme is that a large thruster impulse is required, especially for the tether-aligned thruster. T_c gradually increases to 70 N during retrieval. The reason is that an unnecessarily high tension level is maintained in the tether. It may not be practical to provide that kind of thrust. In any case, it is not necessary to do so. A small tension maintained in the tether is good enough to prevent slackness of the tether. Thus, henceforth we reduce ℓ_T and put a limitation on the maximum thrust provided by the thrusters.

Figure 9.3 shows the dynamical behaviour of the system when the control thrusts are provided according to (9.3.1) with ℓ_T = 3 Km. The maximum thrust provided by any of the thrusters is ±5 N. Note that all the motions are well controlled during the retrieval process. For tether length less than 3 Km, the tension is maintained at a low level (approximately 2 N, Fig. 9.3(e)). Thus, much smaller thrusts compared to Fig.9.2 are required. The ±5 N limitation on the thrusters yielding T_c and T_α is clearly visible in Fig. 9.3(d). Again from Fig. 9.3(d), it can be estimated that the total thruster impluse is about 50000 N.s. It may also be noted that the thruster providing T_α works hard at the beginning, spending more thruster fuel than that providing T_c. The time of retrieval from a length of 100 Km to 250 m is approximately 2.8 orbits (4.2 hours). The numerical simulation was terminated at ℓ_0 = 250 m to limit computational costs; the same trend is likely to continue when ℓ_0 < 250 m.

Although the results shown in Fig. 9.3 are quite good, they can be improved. There are two aspects: one is further saving of the thruster fuel; the other is to reduce the retrieval time. The next section considers means to attain these improvements.

9.4 A MIXED CONTROL STRATEGY

In this section, a mixed control strategy using thrusters as well as a length change control law is proposed. The retrieval process is divided into two parts: one is from an initial length of 100 Km to 20 Km, while the other is from 20 Km to the end of retrieval. For the first part, a length change law is used to control the motions; this is followed by a retrieval process using a thruster augmented active control law to control the motions and maintain a certain amount of tension in the tether. Below ℓ_0 = 10 Km, a constant velocity retrieval is used instead of exponential retrieval for reducing the retrieval time.

As mentioned earlier, the thruster impulse used in the case shown in Fig. 9.3 is still considerably large. There are two reasons for this. One is that the thrusters start to fire from the beginning of retrieval and last for a long time. The second reason is that the retrieval is too slow at the terminal phase when an exponential retrieval is used all the time. The thrusters keep on firing even through the retrieval process turns to a snail's pace. Observing the plots of T_α, T_γ and T_c in Fig. 9.3(d) carefully, one can note the following:

(i) At the beginning, all the thrusters, especially that yielding T_α work very hard. T_α is maintained for about 1.2 hours at a maximum level of 5 N. The reason is that $(\alpha-\pi)$ is quite big (approximately 15°) at the beginning of retrieval. Bringing the tether back to the local vertical ($\alpha=\pi$, for the tether deployed downward) requires large thrust acting for a long time. A lot of thruster fuel, of course, is spent.

(ii) At the terminal phase of retrieval, thrust T_c must be maintained at a nonzero value since a certain amount of tension is required. If the retrieval is exponential, it lasts for a fairly long time. Thus a lot of thruster fuel is spent too.

Possible improvements are clearly indicated by the above discussion. Firstly, the thrusters need not fire so early from the beginning of retrieval. Just let the length change control law do its job. After 20 Km (say), fire the thrusters. To choose 20 Km as the starting point of firing the thrusters is somewhat arbitrary. However, if it is chosen too small, the tether might be already slack when the firing of the thrusters starts. From 20 Km to 10 Km, exponential retrieval is continued. Beyond that a constant velocity retrieval instead of the exponential retrieval is carried out, mainly to reduce the retrieval time.

9.4.1 Laws for Mixed Control Strategy

From 100 Km to 20 Km, a control law taking advantage of the internal resonance property is used. Since B_1 is the largest among the transverse vibrations, the coupling term involves the state variable B_1 alone. The length change law thus is

$$\eta'' = -\tilde{c}K_\alpha\alpha''-2\tilde{c}K_\gamma\gamma'\gamma''+1.8\omega_\varepsilon C_{1d}'-10^4B_1B_1' \qquad (9.4.1)$$

with the initial condition

$$\eta'(0) = \tilde{c}, \quad \tilde{c} < 0 \tag{9.4.2}$$

Note that (9.4.1) is equivalent to

$$\eta' = \tilde{c}\{1-K_\alpha\alpha'-K_\gamma\gamma' +(1.8/\tilde{c})\omega_\varepsilon C_{1d}-(5 \times 10^3/\tilde{c})[B_1{}^2-B_1{}^2(0)]\} \tag{9.4.3}$$

From 20 Km to 10 Km, an exponential retrieval is used, i.e., all the gains in (9.4.1) are zero and

$$\eta'' = 0 \tag{9.4.4a}$$

From 10 Km onwards, a constant velocity retrieval is employed, i.e.,

$$\eta'' + \eta'^2 = 0 \tag{9.4.4b}$$

Care is taken so that η' is continuous at both $\ell_0 = 20$ Km and $\ell_0 = 10$ Km.

The thrusters start firing when the length reaches 20 Km. The thrusts are given by

$$\tilde{T}_\alpha = 2\eta'(1+\alpha')-2\alpha'+[10-(3/K)\eta'](B_1'-2B_2') \tag{9.4.5a}$$

$$\tilde{T}_\gamma = -2\eta'\gamma'+2\gamma'+[10-(3/K)\eta'](A_1'-2A_2') \tag{9.4.5b}$$

and

$$T_c = \begin{cases} -5\omega_\varepsilon(C_1'+C_2') & \ell_0 \geq \ell_T \\ -5\omega_\varepsilon(C_1'+C_2')+3(\ell_T-\ell_0)/\ell_0 & \ell_0 < \ell_T \end{cases} \tag{9.4.5c}$$

where ℓ_T depends on the steady tension to be maintained for small tether lengths. In the numerical simulation ℓ_T was chosen as either 3 Km or 10 Km. In addition, a ±5 N limit is put on T_α, T_γ and T_c. (The relations between T_α and $\tilde{T}_\alpha$, etc. are given in the equations (9.2.5 a - c) etc. earlier).

The thrusts given in (9.4.5) are slightly different from those given in (9.3.1). Firstly, ν appearing in (9.3.1) has been ignored in (9.4.5) since it is very small. Secondly, for $\tilde{T}_\alpha$ and $\tilde{T}_\gamma$, a term $(-3/K)\eta'$ has been added to 10. The reason for doing so is quite obvious. Since from 10 Km onwards the retrieval is a constant velocity retrieval, η' becomes larger and larger in absolute value giving rise to higher negative damping. The added term is just to balance this in the transverse vibrational equations. If an exponential retrieval is used all the time, η' is a constant $(=\tilde{c})$, and the correction term is not required.

9.4.2 Numerical Results for Mixed Control Strategy

Numerical results using the mixed control strategy are shown in Figs. 9.4 - 9.6. The dynamical response and the thrusts are plotted with respect to θ. The initial conditions for these three figures are the same and are $(\alpha-\pi) = 15°$, $\gamma = 1°$, $C_1 = 0.47 \times 10^{-2}$, $C_2 = -0.25 \times 10^{-3}$, $A_1 = 0.5 \times 10^{-4}$, $A_2 = -0.5 \times 10^{-4}$, $B_1 = -0.16 \times 10^{-2}$, $B_2 = 0.48 \times 10^{-3}$, and $A_1' = A_2' = B_1' = B_2' = C_1' = C_2' = \alpha' = \gamma' = 0$.

Figure 9.4 shows the system dynamics when $\tilde{T}_\alpha$ and $\tilde{T}_\gamma$ get no feedback from the transverse vibrations, i.e., for $\ell_0 < 20$ km

$$\tilde{T}_\alpha = 2\eta'(1+\alpha')-2\alpha'$$

$$\tilde{T}_\gamma = -2\eta'\gamma'+2\gamma' \qquad (9.4.6)$$

$$\tilde{T}_c = -5\omega_\varepsilon(C_1'+C_2')+3(\ell_T-\ell_0)/\ell_0, \quad \ell_T = 3 \text{ Km}$$

The importance of getting feedback from the transverse vibrations for $\tilde{T}_\alpha$ and $\tilde{T}_\gamma$ is clearly seen from Fig. 9.4(b). The transverse vibrations continue to grow although the rotations α and γ approach zero in Fig. 9.4(a). This causes the tension at both ends of the tether to oscillate rapidly (Fig. 9.4(d)). C_1 also is affected by the transverse vibrations due to the nonlinear coupling (Fig. 9.4(c)). When ℓ_0 is about 6 Km, C_1 becomes zero, which shows that there is slackness somewhere along the tether. The computer calculation is then terminated.

The results in Fig. 9.5 use $c(=\tilde{c}\omega) = -2 \times 10^{-4} S^{-1}$ and $\ell_T = 10$ Km while in Fig. 9.6, $c = -4 \times 10^{-4} S^{-1}$ and $\ell_T = 3$ Km. Thus, the retrieval is faster in Fig. 9.6. Numerical simulation was stopped at $\ell_0 = 250$ m to reduce computational costs. The behaviour is likely to be similar when ℓ_0 decreases further. In both cases, α and γ go to zero. So do the transverse vibrations as well as longitudinal vibrational variable C_2. C_1 is maintained at certain finite value during the terminal phase of retrieval. Thus the overall dynamical response is quite satisfactory.

In Fig. 9.5, the time required to retrieve the subsatellite to 250 m is about 3 orbits (4.5 hours), while it is only about 1.3 orbits (2 hours) in Fig. 9.6. The total thruster impulse used is approximately 20,000 N.s. in Fig. 9.5 and 10,000 N.s in Fig. 9.6. These are much smaller compared to 50,000 N.s (estimated from Fig. 9.3) consumed during retrieval using the thrusters alone (i.e., no length change control).

CHAPTER 10

CONCLUSION

10.1 CLOSING REMARKS

Throughout this thesis, the main objective of the investigation has been the dynamical modelling of the Shuttle Supported Tethered Subsatellite System (SSTS) and control of the motion during retrieval of the subsatellite. Both dynamical analysis and control of the SSTS system are very complex problems, the latter being more difficult than the former. The two problems are closely related. A good dynamical model of the SSTS system lays the foundation for the control analysis. An oversimplified model may lead to incorrect control procedure.

Rather than presenting a massive amount of data, the emphasis has been on the physical understanding of the problem and on the methods to control the motions during retrieval. A set of partial differential equations governing the vibrations of the tether and a set of ordinary differential equations describing the rotations of the system have been derived. The partial differential equations have been discretized using Galerkin's method.

Approximate analytical procedures have been developed to gain an insight to the dynamics of the tethered satellite systems and to devise control laws. The control laws thus obtained have been validated by numerical analysis of the unsimplified equations of motion. Steps have been taken to improve the efficiency of numerical schemes. The important conclusions based on the study are summarized below.

Dynamical Aspects:

(i) The dynamical model of the SSTS system must consider the vibrations of the tether. Both longitudinal as well as transverse vibrations of the tether tend to grow during retrieval of the sub-satellite. They could make the tether slack during the terminal phase of retrieval when the strain or the tension is very small. This results in loss of control.

(ii) Aerodynamic drag is significant when the subsatellite dives into the earth's atmosphere. The oblateness of the earth can have an important effect on the density of the atmosphere and thus on the aerodynamic forces acting on the subsatellite and the tether. This effect must be taken into account in the dynamical model.

(iii) Longitudinal and transverse vibrations of the tether are strongly coupled specifically at the terminal phase of retrieval. On one hand, the transverse vibrations are governed by the tension along the tether which is proportional to the longitudinal strain. On the other hand, the longitudinal strain is dependent on the transverse displacements. The dynamical model must consider the nonlinear strain term caused by transverse vibrations since there can be significant differences between the linear and nonlinear results. The tension (or strain) in the tether is affected marginally by the transverse vibrations through the nonlinear strain term when the length of the tether is very long. However, during the retrieval process, the tension (or strain) becomes weaker and weaker and the nonlinear strain term becomes more and more significant.

Control Aspects:

(i) Unlike in the case of deployment or station-keeping, all the motions are inherently unstable during retrieval of the subsatellite. Hence, the control of motion during retrieval is comparatively more difficult.

(ii) A nonlinear length rate feedback control law has been developed to control successfully the unstable pitch and roll rotations. Since the pitch motion is strongly coupled to the length rate, its growth can be arrested rather easily and it can be made as small as desired. The roll, on the other hand, can only be confined to a finite amplitude limit cycle by using quadratic feedback of the roll rate.

(iii) During retrieval, the subsatellite moves mainly in the axial direction of the tether. The longitudinal vibrations are strongly affected by the acceleration of the subsatellite caused by the length change. Hence, the unstable longitudinal vibrations can be controlled very well by using an appropriate length change control law.

(iv) It is quite difficult to control the unstable transverse vibrations by using a length change feedback control law since the transverse vibrations and length change are weakly coupled. Material damping of the tether is not sufficient to overcome the negative damping associated with retrieval of the subsatellite if the retrieval is reasonably fast. Transverse vibrations can be suppressed by a nonlinear length change law that produces forces along transverse directions. However, in the meantime, longitudinal vibrations are adversely affected.

(v) In order to avoid slackening of the tether during the terminal phase of retrieval, the control strategy must be able to maintain a certain amount of tension in the tether. This can be achieved by speeding up the retrieval towards the end or using thrusters.

(vi) Thruster augmented control is a very promising means to arrest the growth of motion at the terminal phase of retrieval. The trouble taken in equipping the subsatellite with thrusters gets rewarded by the short retrieval time and safety of retrieval.

(vii) A mixed control strategy which at first uses a length change control law and follows it up with a thruster augmented control law is quite effective. This appears to be a very promising way of retrieving the subsatellite. The subsatellite not only can be retrieved from a distance of 100 Km to 250 m within approximately two hours in a safe manner, but the method also saves a lot of thruster fuel compared to a control scheme using thrusters alone.

10.2 SUGGESTIONS FOR FURTHER WORK

There are numerous possibilities for extension of the present investigation. Only some of the important ones are mentioned below:

(i) Investigation of the effect of using multiple tethers [42] on the dynamics of the system may be of some interest. One possibility is to use two or more tethers to link the subsatellite to the shuttle. If two tethers are attached at different locations on the shuttle, it might help in controlling the motion during the terminal phase of retrieval. This is because there may be then more flexibility in varying the tension. The second way is to use an extra pulley which supports the subsatellite and the tether at the subsatellite end moves on that pulley (see diagram below). One end of the tether is fixed to

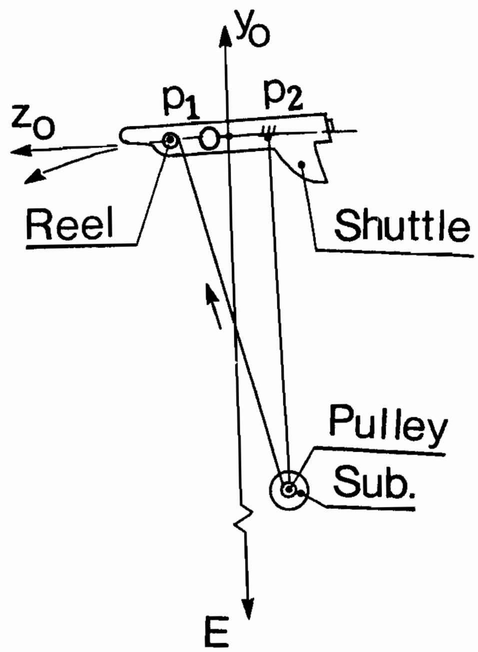

a point on the shuttle while the other end of the tether winds around the drum of the reel mechanism. Turning the reel mechanism will retrieve the subsatellite at approximately half the speed of the tether. During the terminal phase of retrieval, this might be more effective in controlling the motions.

There may be another feasible way to retrieve the subsatellite, that is by using several thinner tethers. During the retrieval process, the tethers are disconnected from the subsatellite one by one when the length becomes shorter and shorter. Suppose that the initial length of the tethers at the beginning of retrieval is 100 Km and the subsatellite is linked by ten tethers having smaller cross-sectional area than the one tether case. When the subsatellite is retrieved to a distance of 90 Km, disconnect one. When the length is 80 Km, disconnect another and so on, until the length is 10 Km and only one tether remains connected to the subsatellite. In doing so, the strain in the uncut tethers does not drop substantially with the retrieval process. When the strain in the tethers does not change drastically, the slackening of the tethers may be avoided and the transverse vibrations will probably not be objectionably high. It should be mentioned that the gravity gradient force is proportional to the length of the tethers. Even one thin tether will be sufficient to support the subsatellite when the tether is not very long.

(ii) The rotation of the subsatellite around the tether is not considered in the present dynamical model. Probably it may induce twist of the tether. Further research should include this degree of freedom as well.

(iii) This research may be extended to a "dumbbell system", with the two bodies connected by the tether having the same order of mass. The center of mass of the system is then no longer very close to that of one of the bodies.

(iv) The study may also be extended to an electrodynamic tether, in which case the electromagnetic forces have to be considered.

(v) Methods similar to those in this thesis can be used to study dynamics and control of deployment of structures other than tethers. These structures may be beam type appendages, solar panels, etc.

(vi) The proposed control laws must be verified by experiments. Although NASA will test the SSTS system in space soon, experimental simulation on the ground should prove useful. The difficulty involved in simulating the real environment on the ground might be very challenging.

(vii) The operation of the SSTS system is dependent on the reliability of the tether. Unfortunately such long and thin tethers are very difficult to manufacture. Careful checking of the tether is very important to guarantee that it has no cracks and defects so that the tether will not break while in use. The material aspect of the tether must be investigated further.

(viii) Material damping tests should be carried out in low-g condition to provide an accurate value of damping in the tether material. This might be done in a free fall simulation.

(ix) The dynamics of the system when the tether is partially slack,or the motion of the subsatellite when the tether breaks are interesting problems to investigate.

STATEMENT OF ORIGINALITY AND CONTRIBUTION TO KNOWLEDGE

Original contributions to the knowledge of Shuttle Supported Tethered Satellite System through this investigation may be cited as follows:

(i) A fairly detailed dynamical model of the SSTS system characterizing its features has been proposed and the corresponding analytical and numerical procedures have been developed.

(ii) All the vibrations of the tether have been brought into consideration for the first time.

(iii) A nonlinear length rate control law has been presented to control the rotational motions of the system as well as longitudinal vibrations of the tether during the retrieval of the subsatellite.

(iv) Thruster augmented control laws have been obtained to control all the motions during the entire retrieval process and to prevent the tether from becoming slack at the terminal phase of retrieval. Furthermore, a mixed control strategy using first a length change control followed by thruster augmented control has been developed. This saves the retrieval time and thruster fuel significantly.

REFERENCES

[1] Eades, J.B. and Wolf, H., "Tethered Body Problems and Relative Motion Orbit Determination", Final Report, Contract NASA S-21453, Analytical Mechanics Associates, Inc., August, 1972.

[2] Starly, W.H. and Adlhock, R.W., "Study of the Retrieval of an Astronaut from an Extra-Vehicular Assignment", TMC Report No. S-356, November 1963.

[3] Perrine, B.S., "A Method for Soft Tether Stationkeeping", NASA TMX-53643, July 1967.

[4] Lang, D.L. and Nolting, R.K., "Operations with Tethered Space Vehicles", NASA SP-138, Gemini Summary Conference, February, 1967.

[5] Colombo, G., et al., "Shuttle-Borne 'Skyhook': A New Tool for Low-Orbital-Altitude Research", Smithsonian Institution, Astrophysical Observatory, September 1974.

[6] Gilruth, R.R., "Why Space Stations?" Astronautics and Aeronautics, Vol. 6, No. 11, 1967, pp. 54-60.

[7] Bekey, I., "Tethers Open New Space Options", Astronautics and Aeronautics, April 1983, Vol. 21, No. 4, 1983, pp. 32-40.

[8] Rupp, C.C., et al., "Shuttle/Tethered Satellite System Conceptual Design Study", NASA TMX-73365, December 1976.

[9] Laue, J.H. and Manarini, F., "The Tethered Retreivable Platform Concept and Utilization", 33rd Congress of the International Astronautical Federation, Paris, September 1982, Paper No. 82-13.

[10] Modi, V.J. and Misra, A.K., "Orbital Perturbations of Tethered Satellite Systems", The Journal of Astronautical Sciences, Vol. 25, No. 3, 1977, pp. 271-278.

[11] Rupp, C.C., "A Tether Tension Control Law for Tethered Sub-satellites Deployed Along Local Vertical", NASA TMX-64963, September 1975.

[12] Misra, A.K. and Modi, V.J., "Dynamics and Control of Tethered Connected Two-Body System - A Brief Review", 33rd Congress of International Astronautical Federation, Paris, September 1982, Paper No. 82-315.

[13] Chobotov, V.A., "Gravity-Gradient Excitation of a Rotating Cable-Counterweight Space Station in Orbit", Journal of Applied Mechanics, Vol 30, No. 4, 1963, pp. 547-554.

[14] Bainum, P.M. and Evans, K.S., "The Effect of Gravity-Gradient Torques on the Three Dimensional Motion of a Rotating Space Station-Cable-Counterweight System", AIAA 13th Aerospace Sciences Meeting, Pasadena, California, 1975, Paper No. 75-157.

[15] Tai, C.L. and Loh, M.M.H., "Planar Motion of a Rotating Cable-Connected Space Station in Orbit", Journal of Spacecraft and Rockets, Vol. 2, No. 6, 1965, pp. 889-894.

[16] Baker, W.P., Dunkin, J.A., Galaboff, Z.J., Johnston, K.D., Kissel, R.R., Rheinfurth, M.H. and Siebel, M.P.L., "Tethered Subsatellite Study", NASA TMX-73314, 1976.

[17] Buckens, F., "On the Motion Stability of Tethered Satellites Configurations", Proceedings of the 12th International Symposium on Space Technology and Science, Tokyo, Editor:H. Nagasu, 1977, pp. 351-358.

[18] Modi, V.J. and Misra, A.K., "On the Deployment Dynamics of Tether Connected Two-Body Systems", Acta Astronautica, Vol. 6, No. 9, 1979, pp. 1183-1197.

[19] Kalaghan, P.N., Arnold, D.A., Colombo, G., Grossi, M.D., Kirschner, L.R. and Orringer, O., "Study of the Dynamics of a Tethered Satellite System (Skyhook)", Final Report, Contract NAS8-32199, Smithsonian Institution, Astrophysical Observatory, March, 1978.

[20] Modi, V.J., and Misra, A.K., "Deployment Dynamics of a Tethered Satellite System", AIAA/AAS Astrodynamics Conference, Palo Alto, California, August 1978, Paper No. 78-1398.

[21] Kohler, P., Maas, W., Wehrli, R., Weber, R. and Brauchli, H., "Dynamics of a System of Two Satellites Connected by a Deployable and Extensible Tether of Finite Mass", Contract Report, ESTEC Contract No. 2992/76/NL/Ak(SC), Vols. 1 and 2, October, 1978.

[22] Spencer, T.M., "Atmospheric Perturbation and Control of a Shuttle/Tethered Satellite", 8th IFAC Space Symposium, Oxford, U.K., July 1979, paper no. 79-165.

[23] Misra, A.K. and Modi, V.J., "A General Dynamical Model for the Space Shuttle Based Tethered Subsatellite System", Advances in the Astronautical Sciences, Vol. 40, Part II, 1979, pp. 537-557.

[24] Bainum, P.M. and Kumar, V.K., "Optimal Control of the Shuttle-Tethered System", Acta Astronautica, Vol. 7, No. 12, 1980, pp. 1333-1348.

[25] Banerjee, A.K. and Kane, T.R., "Tether Deployment Dynamics", The Journal of the Astronautical Sciences, Vol. 15, No. 4, 1982, pp. 347-366.

[26] Glaese, J.R. and Pastrick, H.L., "Modal Synthesis Simulation of the Shuttle Orbiter Tethered Satellite System", AIAA/AAS Astrodynamics Conference, San Diego, California, August 1982, Paper No. AIAA-82-1424.

[27] Kulla, P., "Stabilization of Tethered Satellites", ESTEC Report TMM/78-07/PK-avs., December 1977.

[28] Modi, V.J., Chang-Fu, G., Misra, A.K. and Xu, D.M., "On the Control of the Space Shuttle Based Tethered Systems", 32nd Congress of the International Astronautical Federation, Rome, Italy, September 1981.

[29] Misra, A.K. and Modi, V.J., "Deployment and Retrieval of Shuttle Supported Tethered Satellite", Journal of Guidance, Control and Dynamics, Vol. 5, No. 3, 1982, pp. 278-285.

[30] Banerjee, A.K. and Kane, T.R., "Tethered Satellite Retrieval with Thruster Augmented Control", AIAA/AAS Astrodynamics Conference, San Diego, California, August 1982, Paper No. AIAA-82-1421.

[31] Merovitich, L., Methods of Analytical Dynamics, McGraw-Hill, New York, 1970, pp. 408-493.

[32] Nayfeh, A.H. and Mook, D.T., Nonlinear Oscillations, John Wiley and Sons, New York, 1979, pp. 485-500.

[33] Crawley, E.F., Sarver, G.C. and Mohr, D.G., "Experimental Measurement of Passive Material and Structural Damping for Flexible Space Structures", 33rd Congress of the International Astronautical Federation, Paris, September 1982, Paper No. 82-380.

[34] Mughrabi, H., Wang, R. and Daffert, K., "Fatigue Crack Initiation by Cyclic Slip Irreversibilities in High-Cycle Fatigue", Fatigue Mechanisms: Advances in Quantitative Measurement of Physical Damage, ASTM STP 811, 1983, pp. 5-45.

[35] Baumeister, T., Editor-in-Chief, Mark's Standard Handbook for Mechanical Engineers, McGraw-Hill, New York, 1978, pp. 3-20.

[36] Vorlicek, P.L., "Material Damping of Aluminum and Graphite/ Epoxy in a Simulation Zero-Gravity Environment", M.I.T. Space System Lab. 1981, Report No. 13-8.

[37] Kane, T.R., Likins, P.W. and Levinson, D.A., Spacecraft Dynamics, McGraw-Hill, 1982.

[38] Geying, F.T. and Westerman, H.R., Introduction to Orbital Mechanics, Addison-Wesley Publishing Company, 1971.

[39] Stenman, L.H., "Free Molecule Flow Theory and Its Application to the Determination of Aerodynamic Forces", Lockheed Report LMSC 448514, Appendix C, October 1968.

[40] Bailey, A.B., "High Speed Sphere Drag in the Transition Flow Regime in an Aeroballistic Range", Rarefied Gas Dynamics, Supplement 4, Vol. 2, Academic Press, 1967, pp. 1127-1144.

[41] Lips, K.W. and Modi, V.J., "General Dynamics of a Large Class of Flexible Satellite Systems", Acta Astronautica, Vol. 7, No. 12, 1980, pp. 1349-1360.

[42] Misra, A.K. and Diamond, G.S., "On the Dynamics of a Subsatellite System Supported by Two Tethers", AIAA 22nd Aerospace Sciences Meeting, Reno, Nevada, January 1984, Paper No. 84-0062.

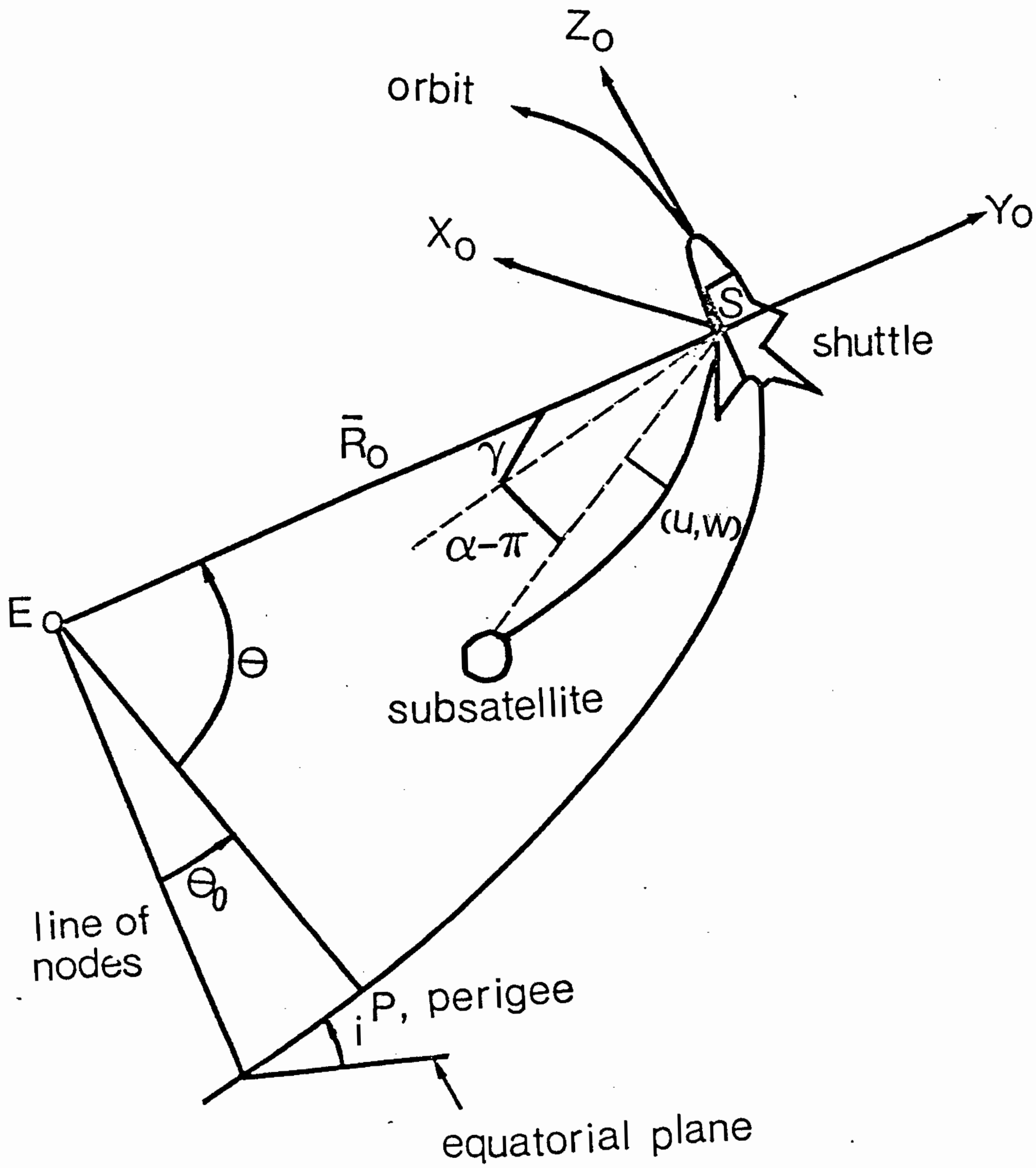

Fig. 1.1 Illustration of the SSTS system

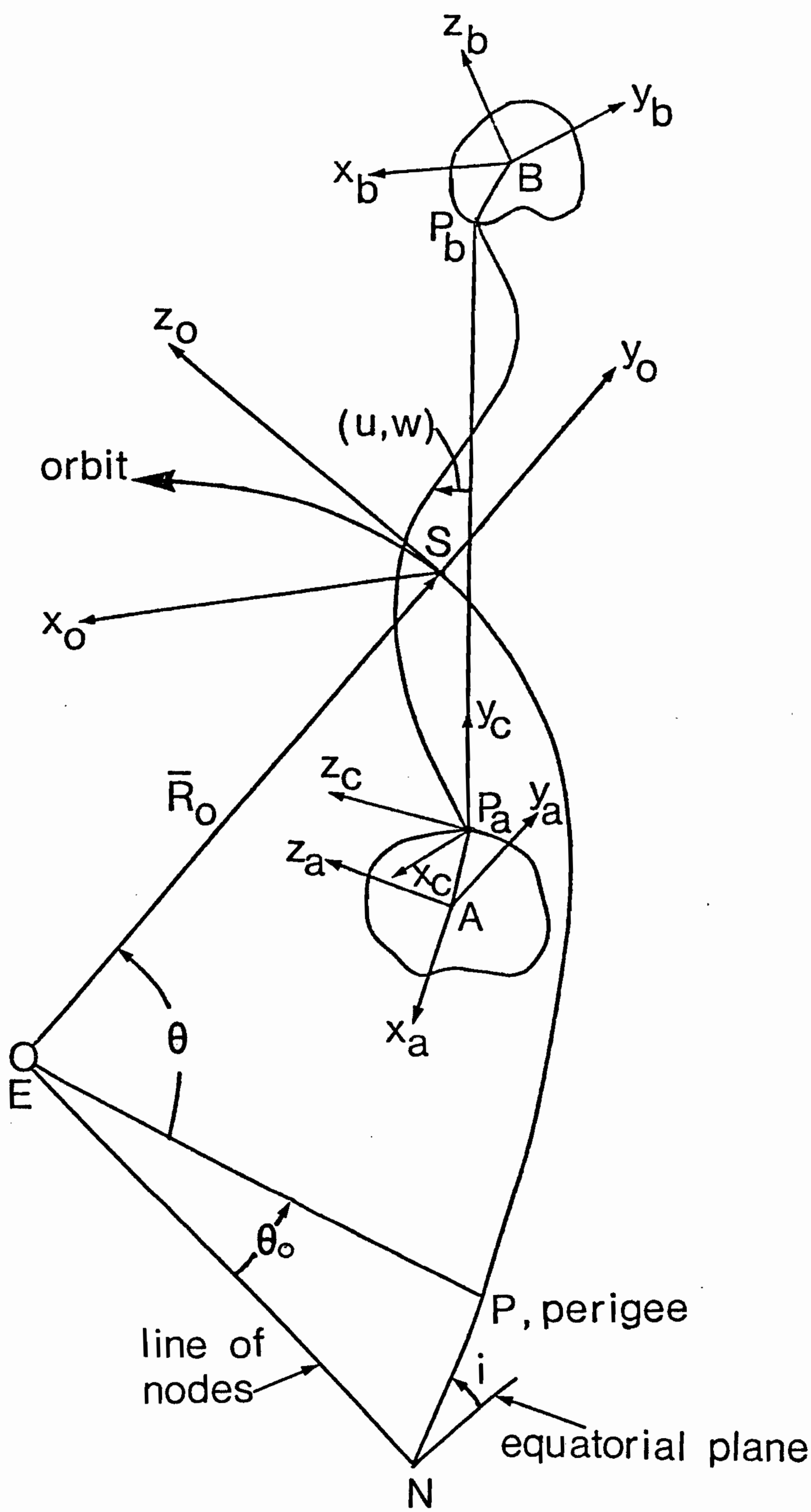

Fig. 2.1 Geometry of motion

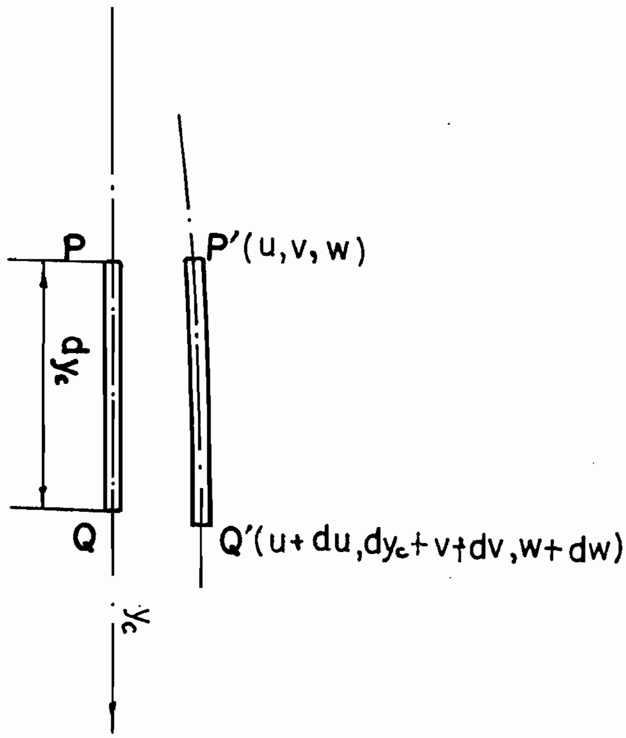

Fig. 2.2 Deformation of the tether

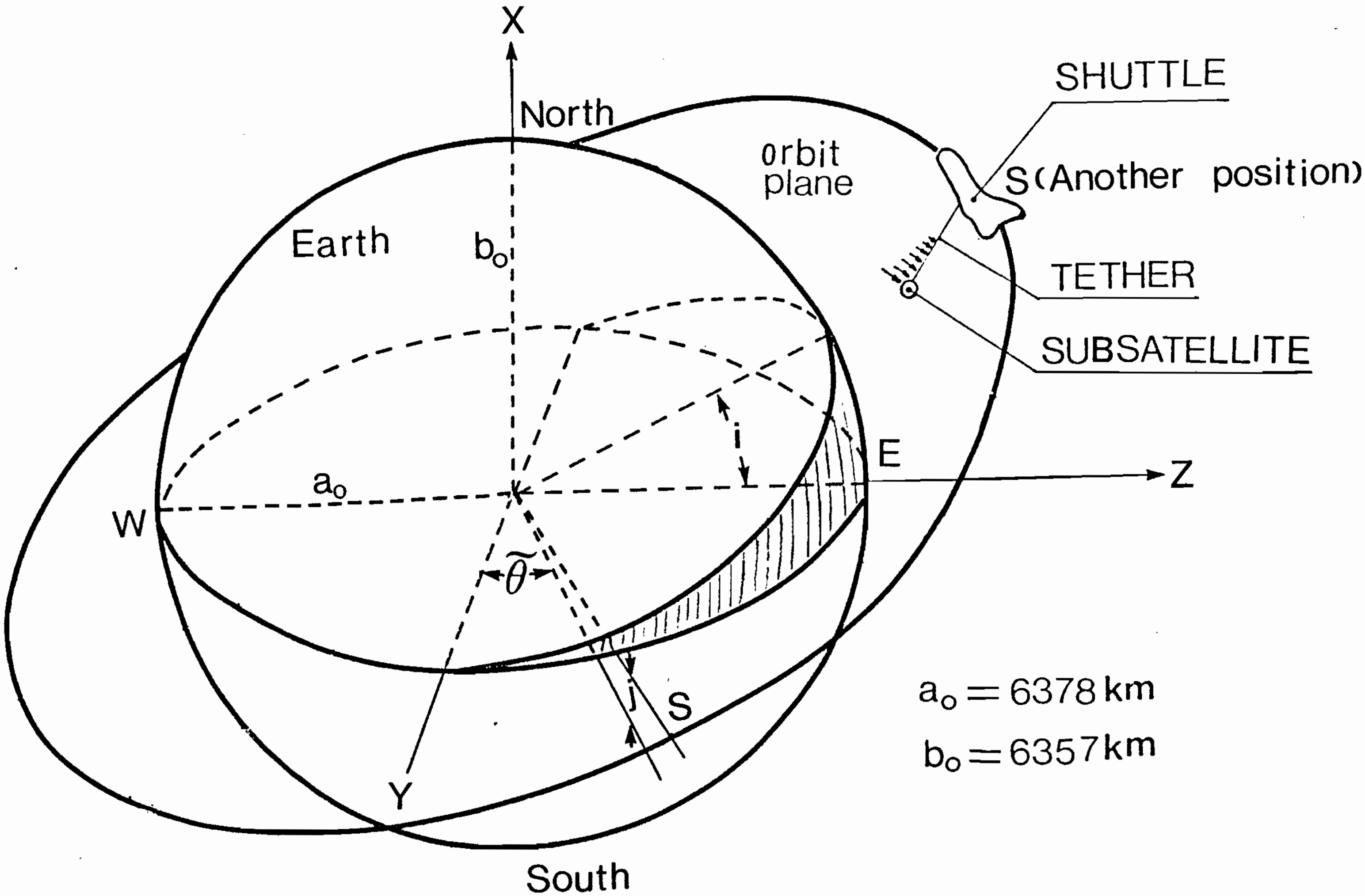

Fig. 3.1 The earth and the SSTS system

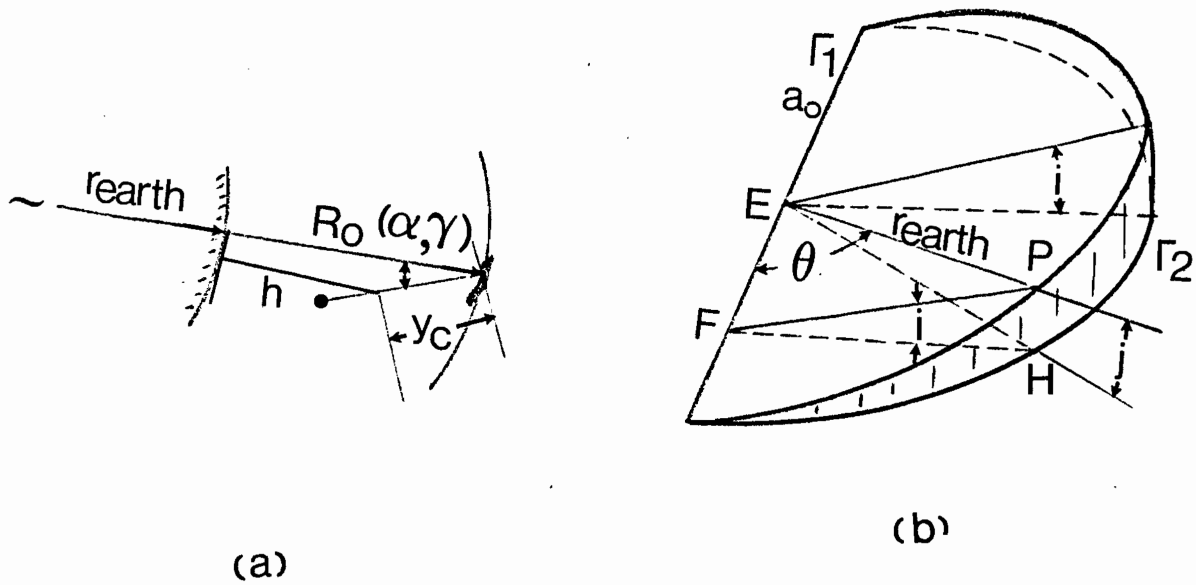

Fig. 3.2 Geometrical consideration of the oblateness of the earth

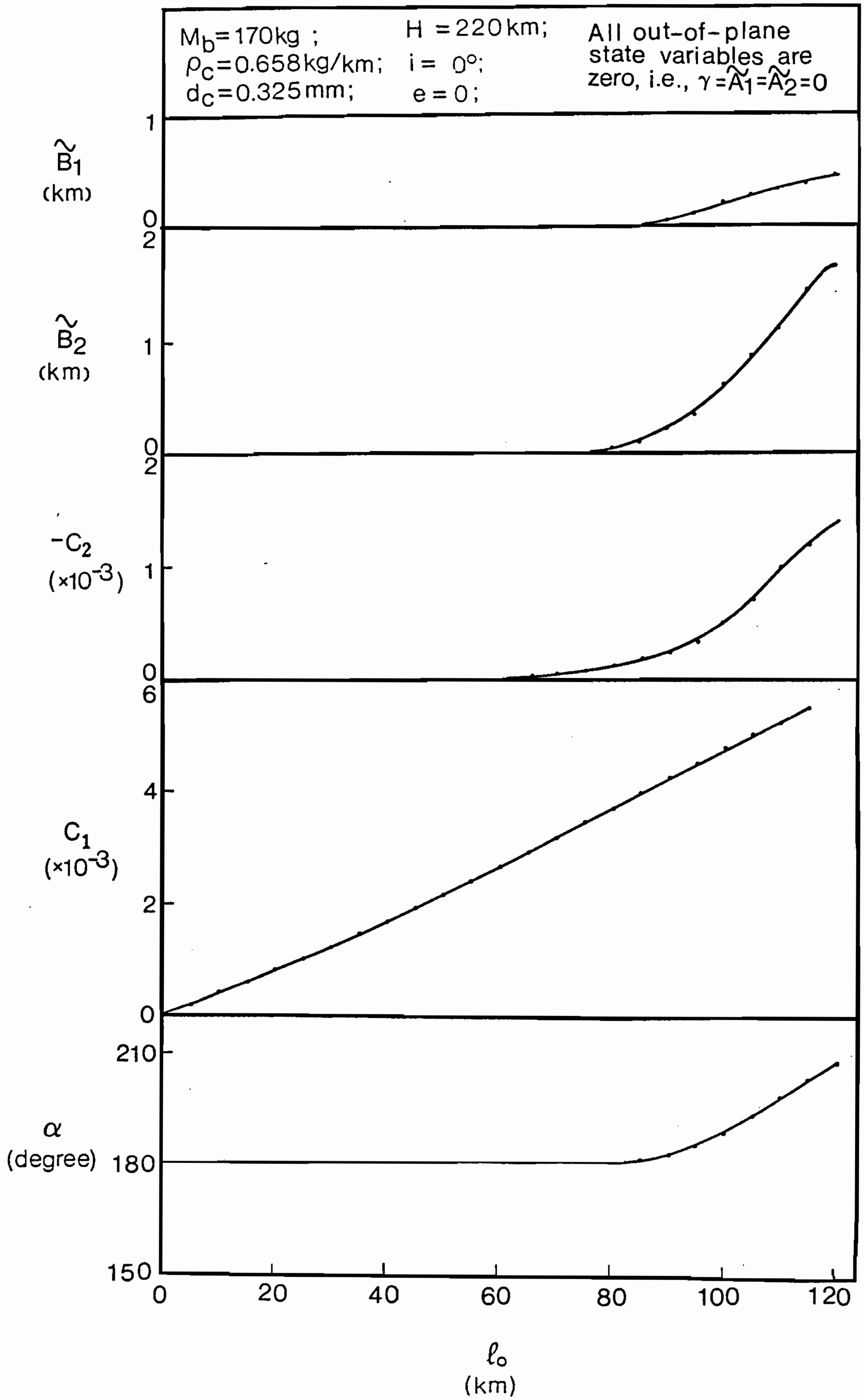

Fig. 5.1 Variation of equilibrium states with length ℓ_0

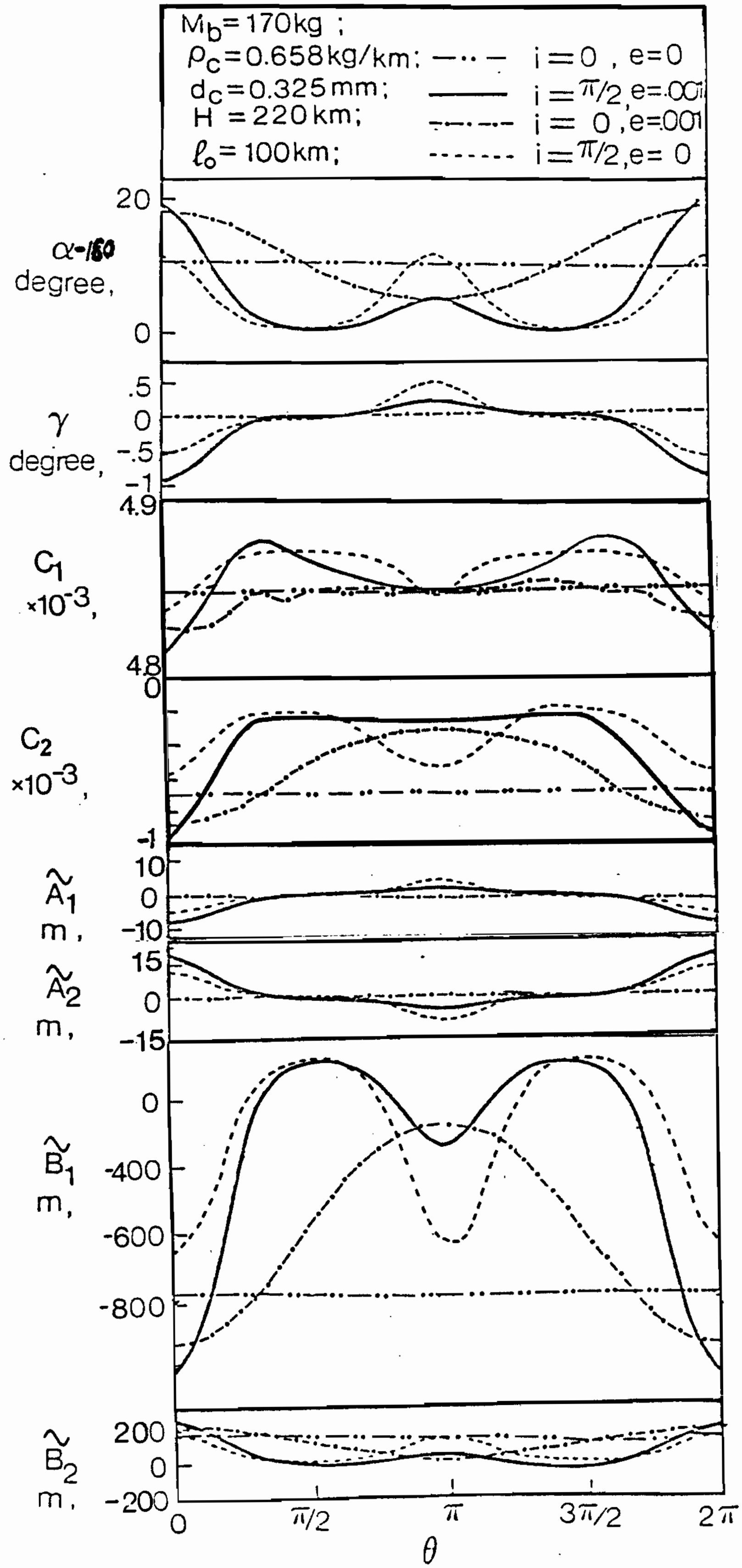

Fig. 5.2 Variation of quasi-equilibrium states with true anomaly θ at a given length ℓ_0 = 100 Km

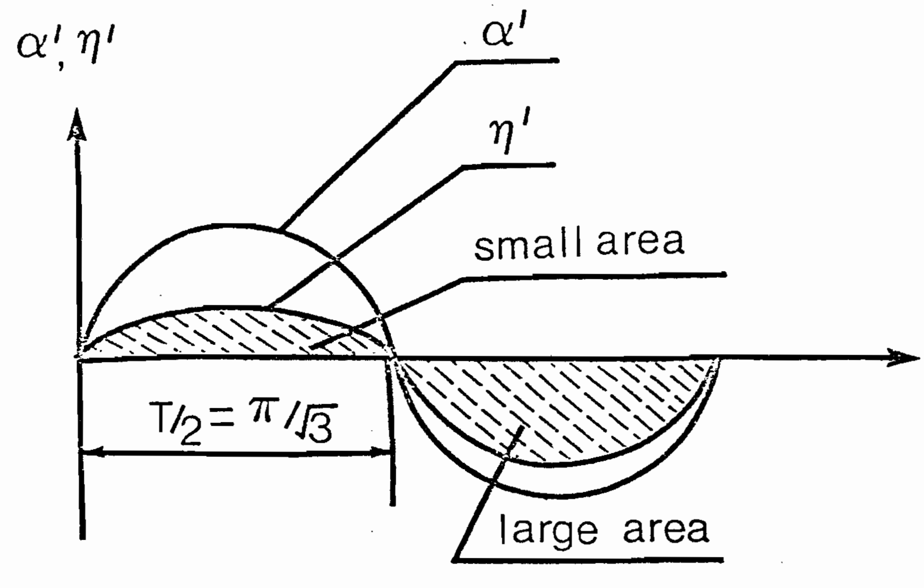

(a) Required nature of length rate η'

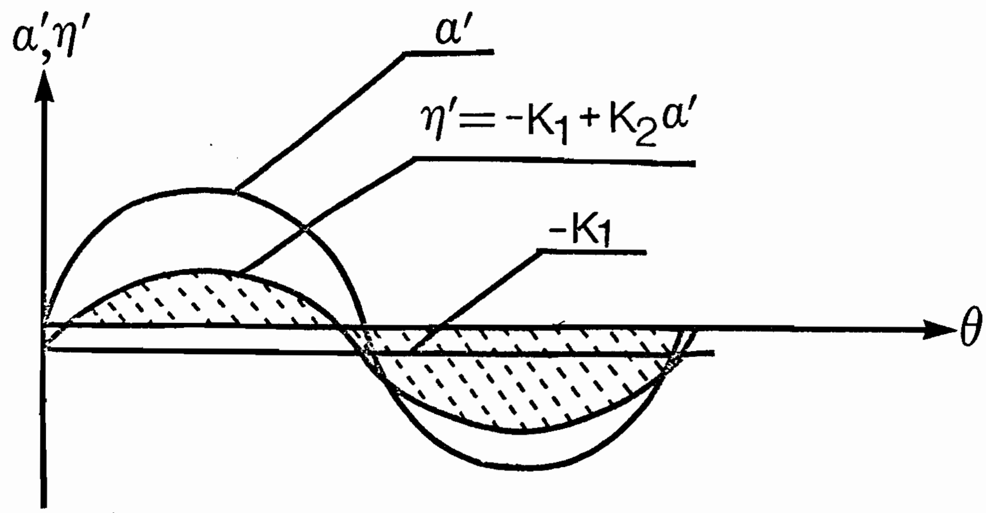

(b) A linear form of η'

Fig. 6.1 Examination of length rate to control inplane rotation

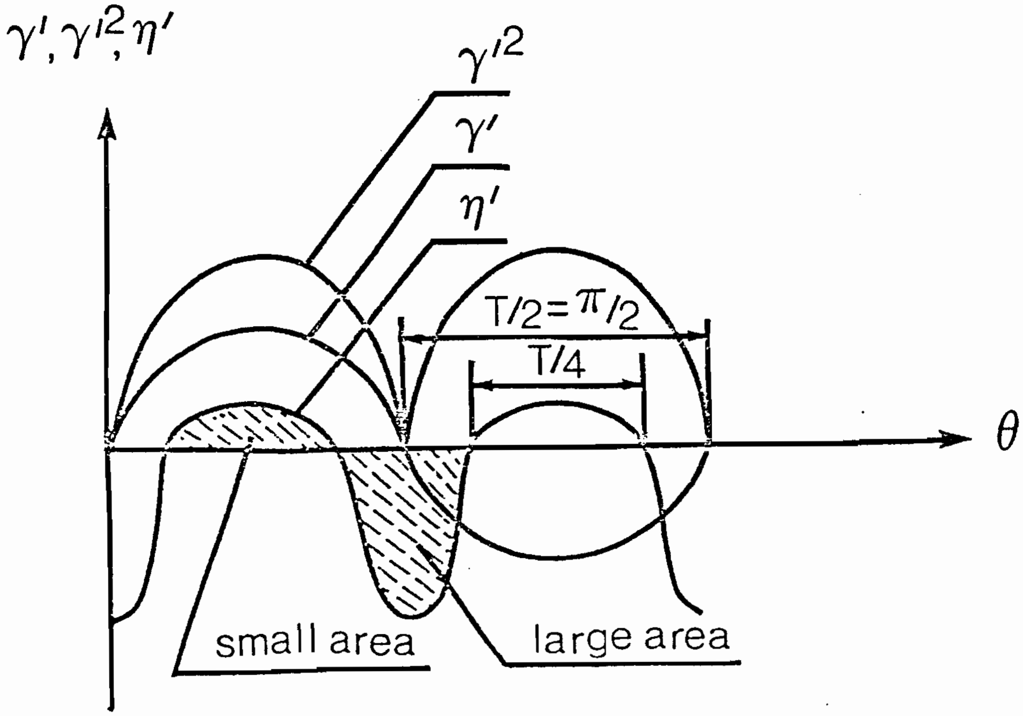

(a) Required nature of length rate η'

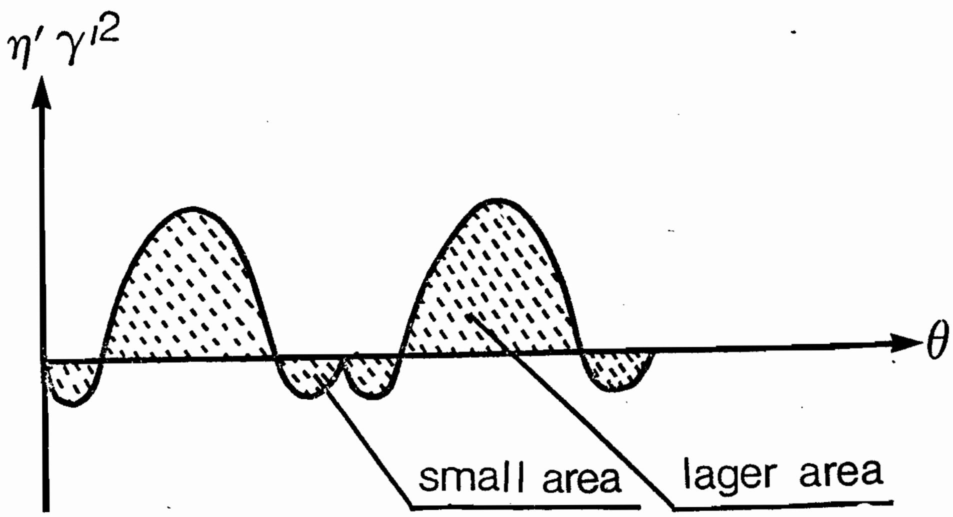

(b) A satisfactory quadratic form of η'

Fig. 6.2 Examination of length rate to control out-of-plane rotation

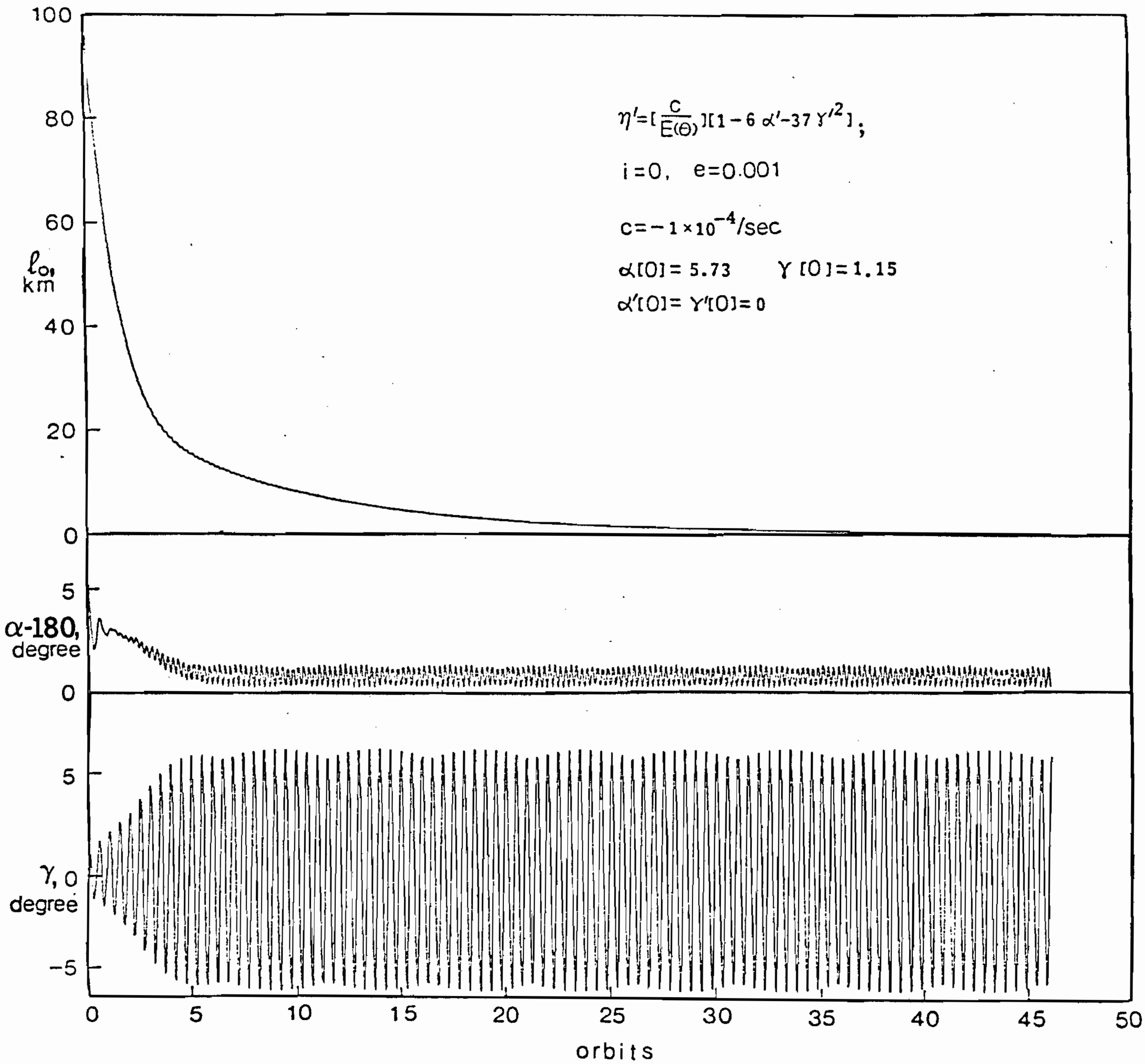

Fig. 6.3 Controlled rotational dynamics during retrieval with $C = -1 \times 10^{-4} s^{-1}$

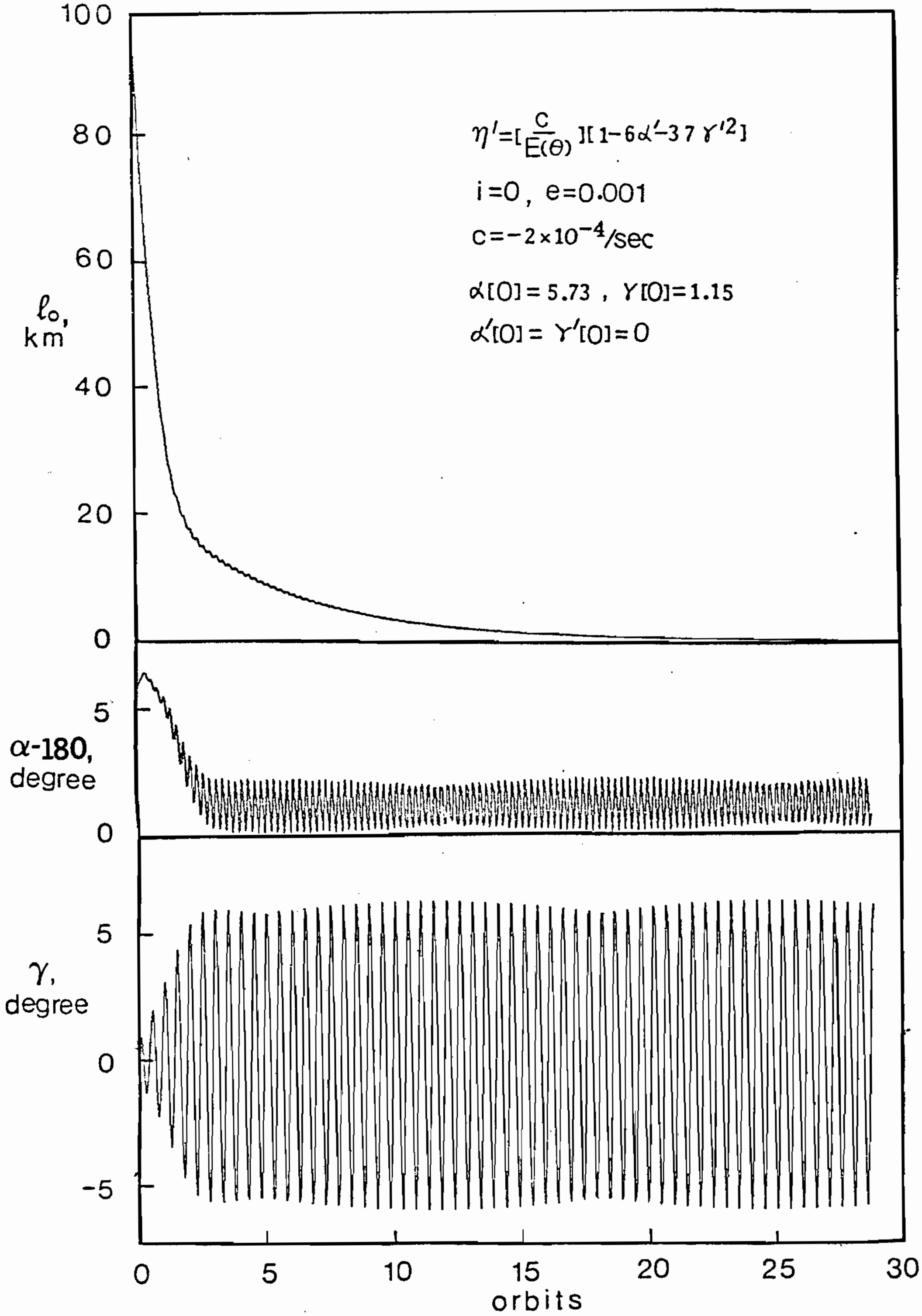

Fig. 6.4 Controlled rotational dynamics during retrieval with $C = -2 \times 10^{-4} S^{-1}$

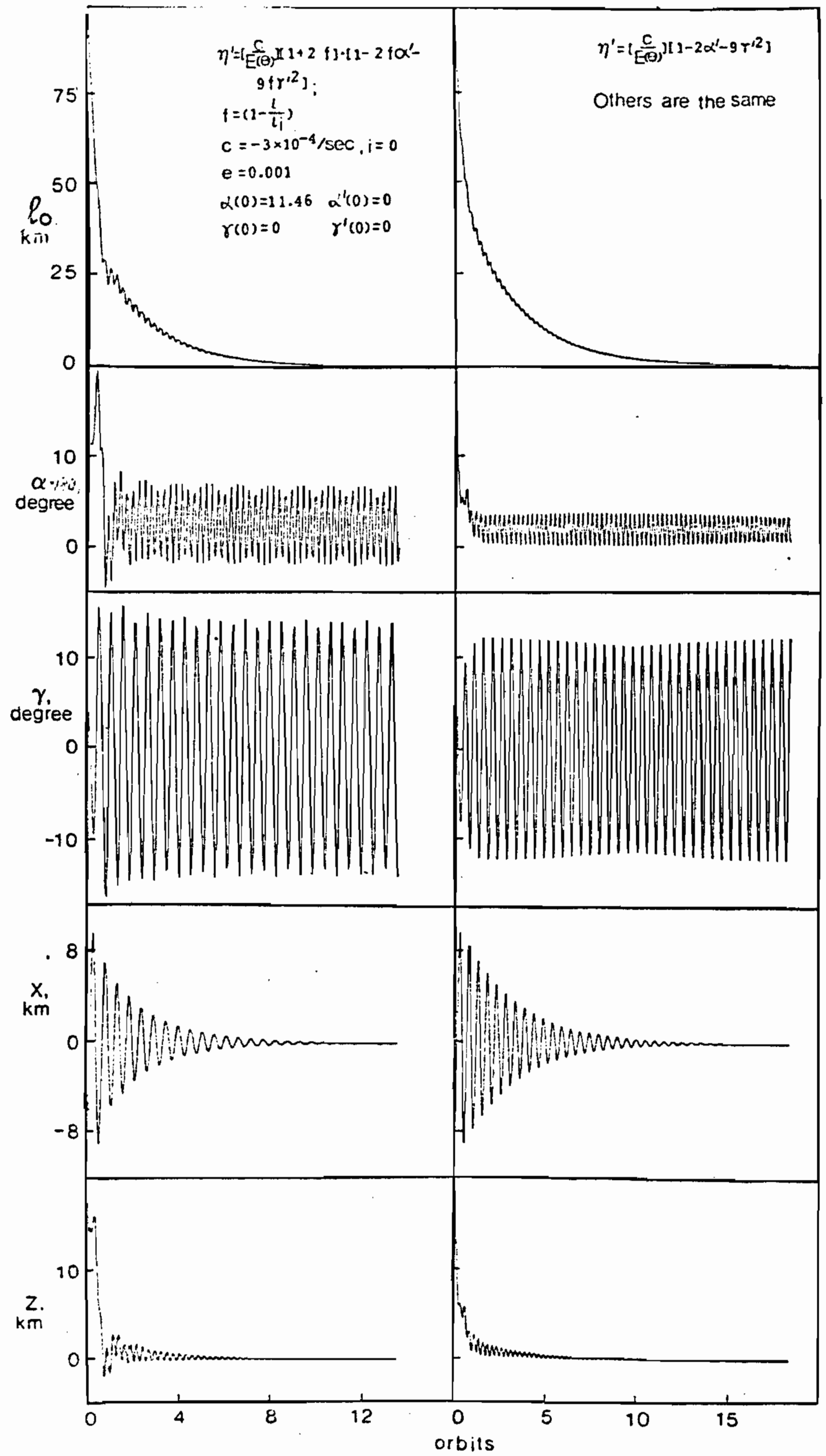

Fig. 6.5 Comparison of revised and unrevised length rate control.

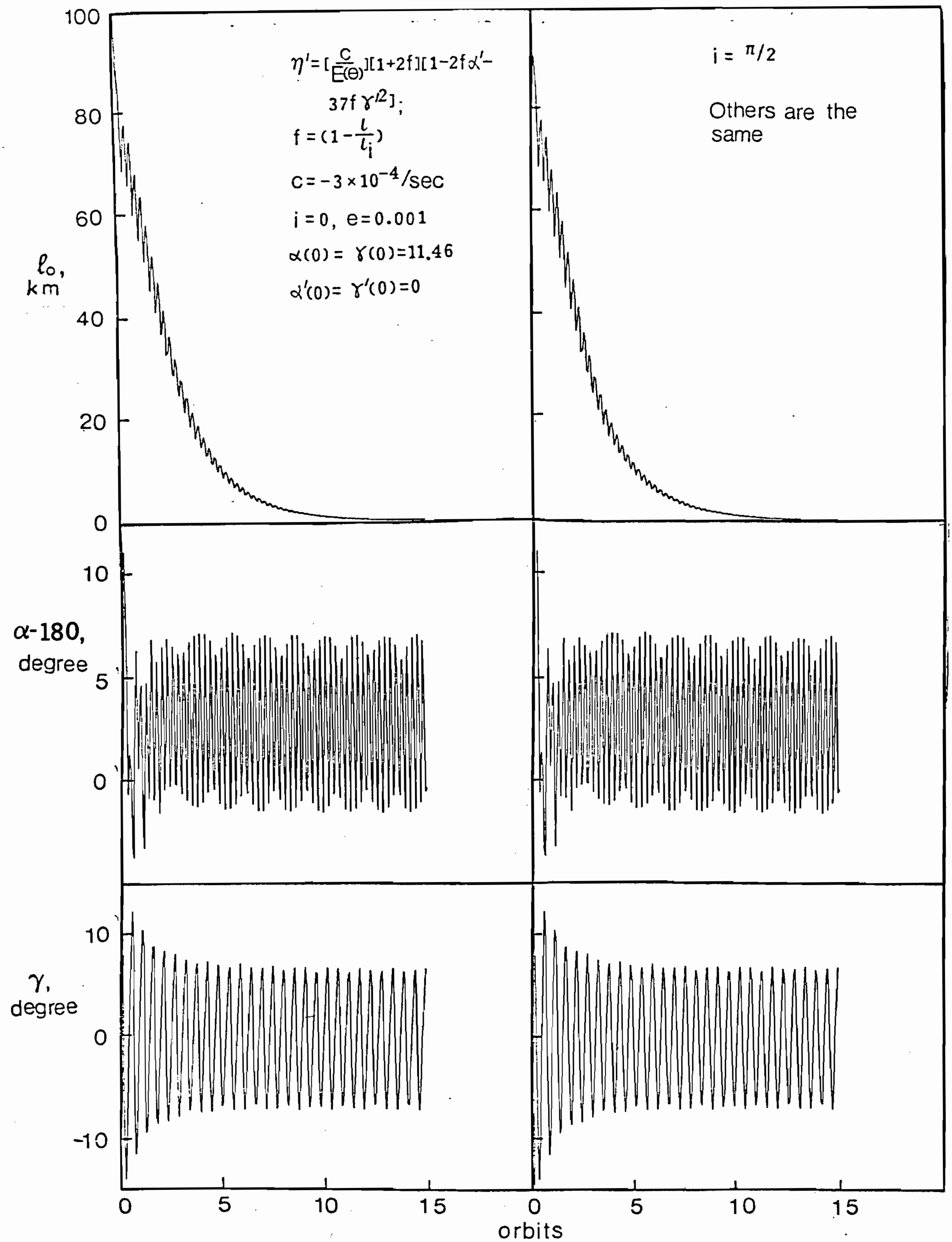

Fig. 6.6 Effect of inclination of the orbit on controlled retrieval.

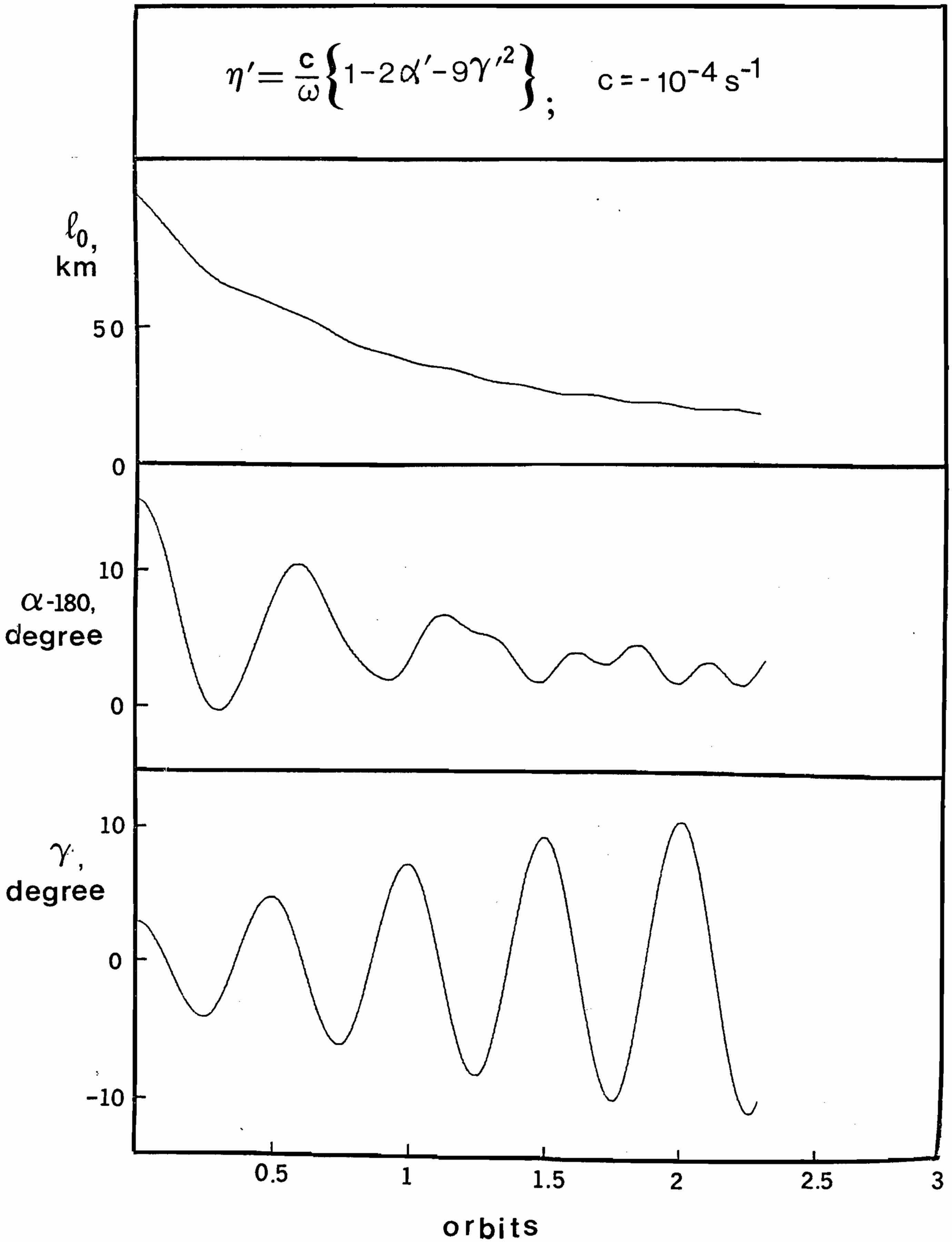

(a) Controlled rotations

Fig. 7.1 Uncontrolled longitudinal vibration if length rate gets feedback from rotations only

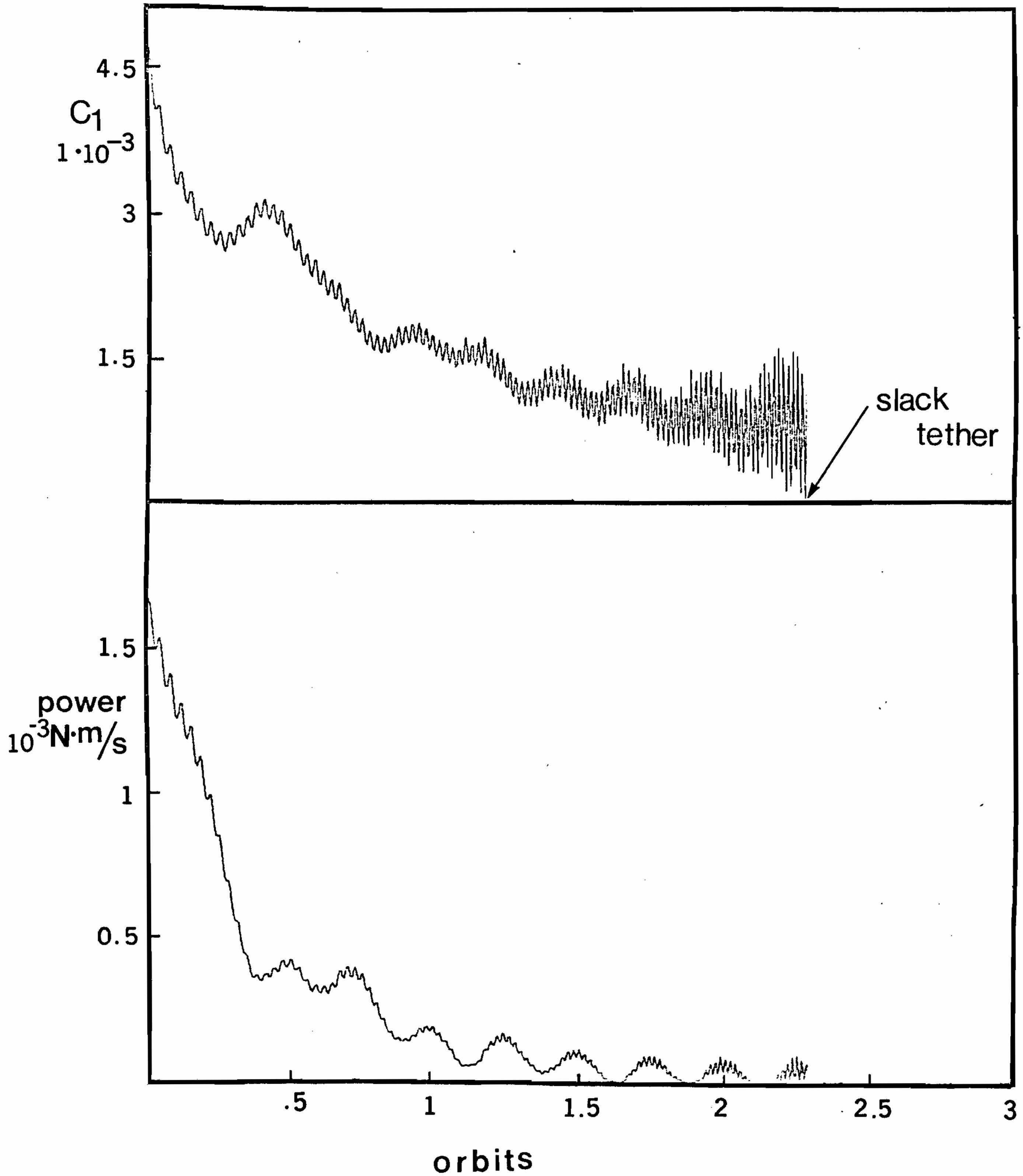

(b) Uncontrolled longitudinal vibration

Fig. 7.1 Uncontrolled longitudinal vibration if length rate gets feedback from rotations only

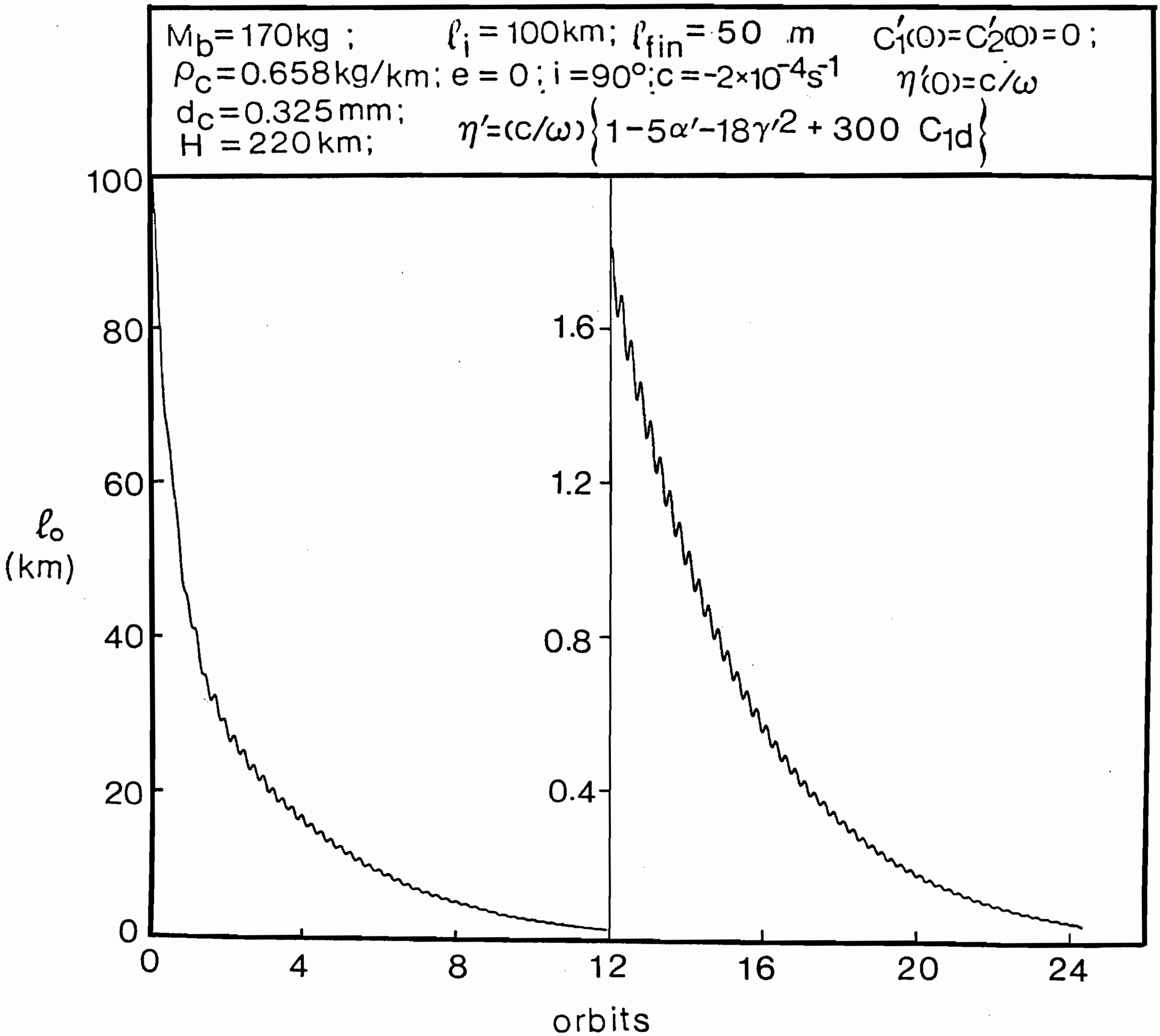

(a) Length history

Fig. 7.2 Dynamics during retrieval when the length rate involves feedback of both rotations and longitudinal vibration ($C = -2 \times 10^{-4} S^{-1}$)

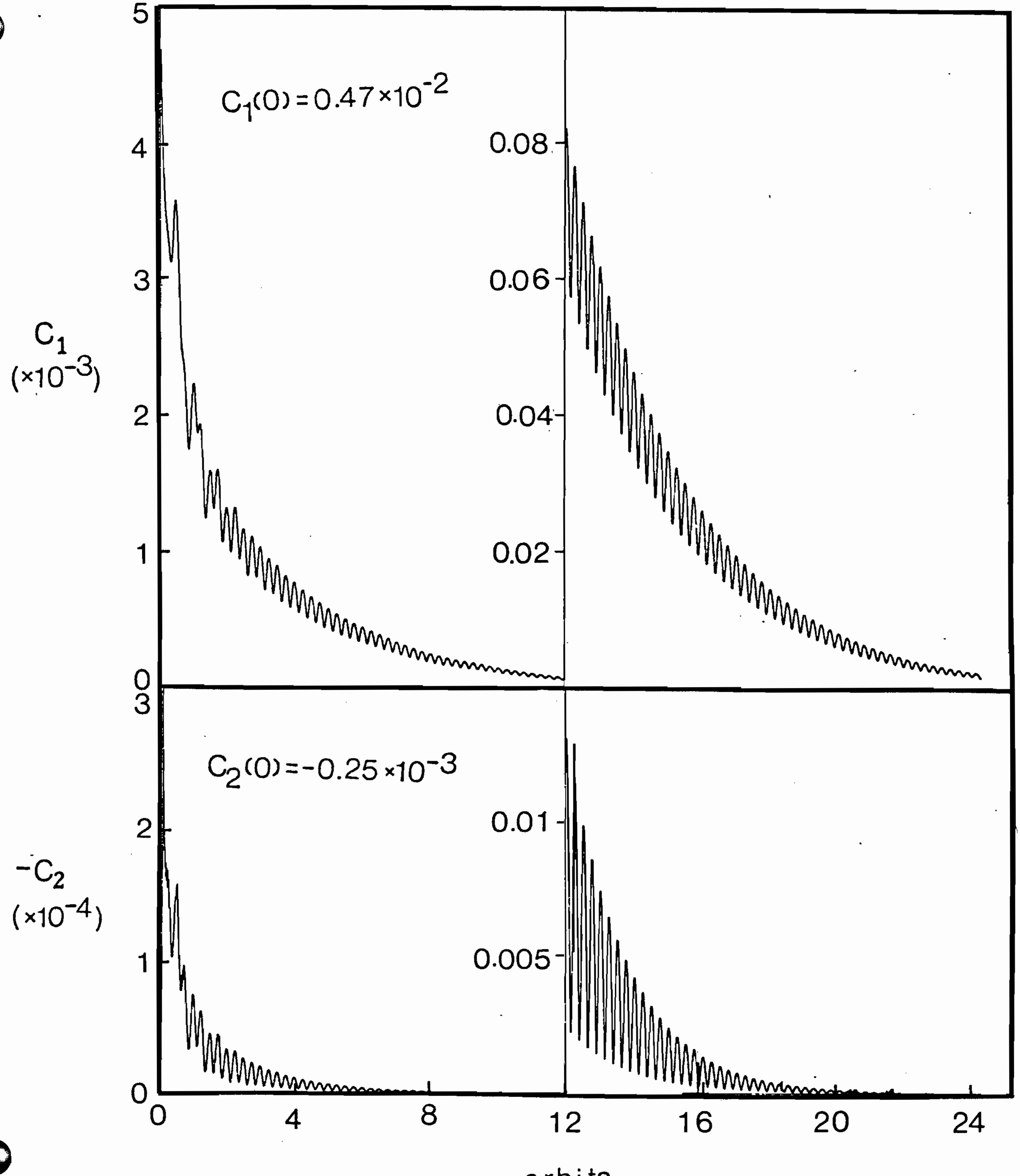

(b) Controlled longitudinal vibrations

Fig. 7.2 Dynamics during retrieval when the length rate involves feedback of both rotations and longitudinal vibration ($C = -2 \times 10^{-4} S^{-1}$)

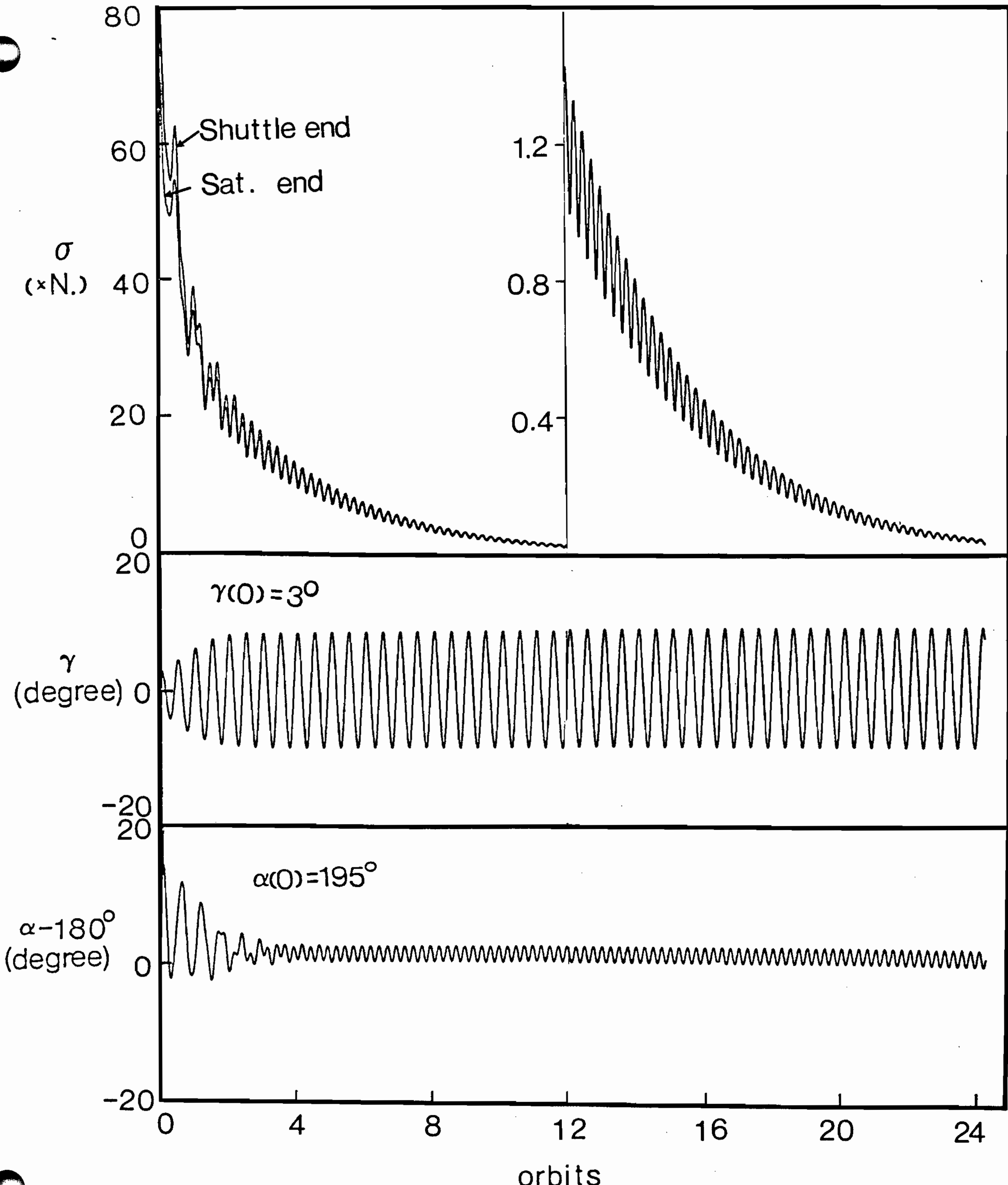

(c) Tension at both ends of the tether and controlled rotations

Fig. 7.2 Dynamics during retrieval when the length rate involves feedback of both rotations and longitudinal vibration ($C = -2 \times 10^{-4} s^{-1}$)

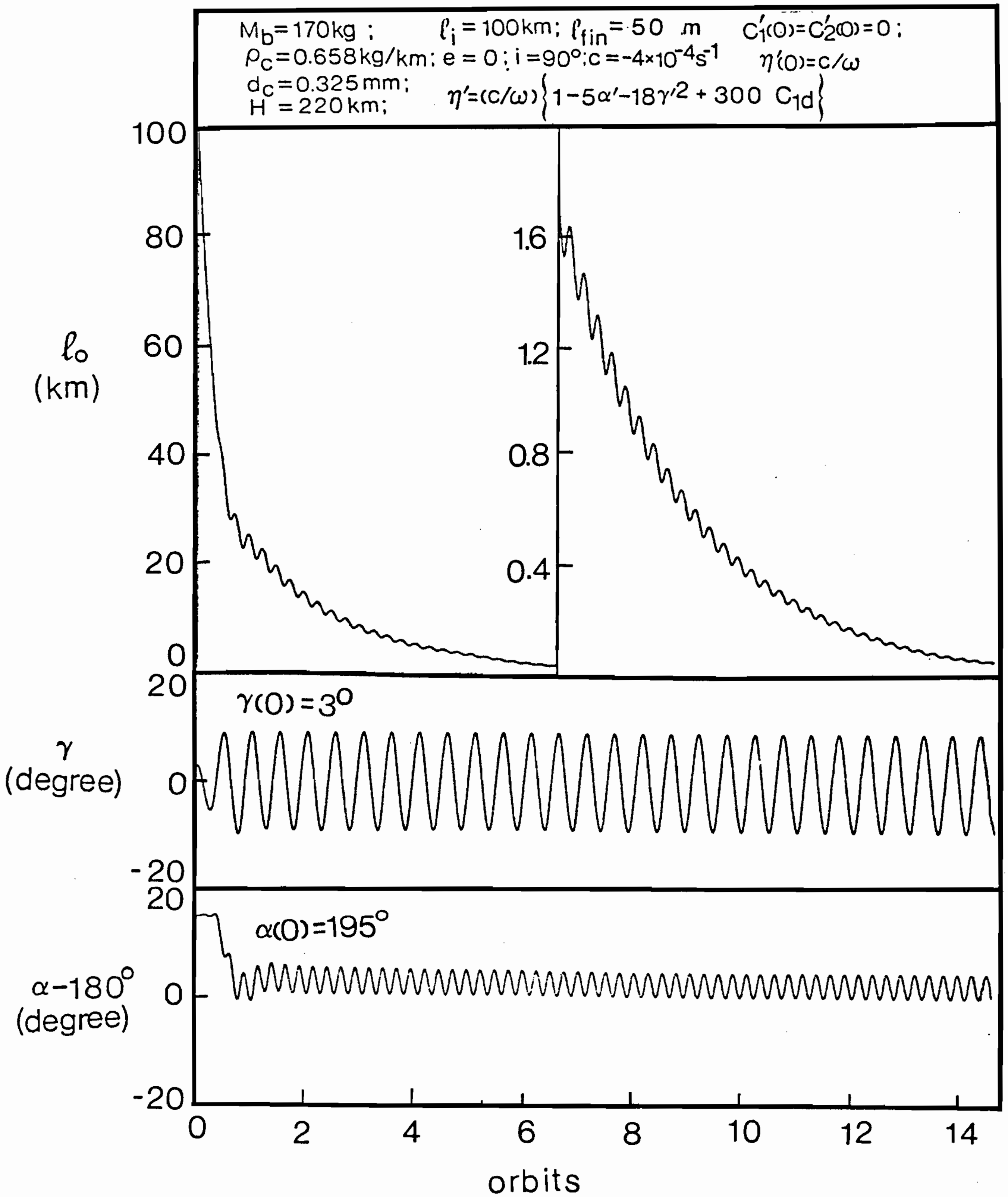

(a) Controlled rotations

Fig. 7.3 Dynamics during retrieval when the length rate involves feedback of both rotations and longitudinal vibration ($C = -4 \times 10^{-4}S^{-1}$)

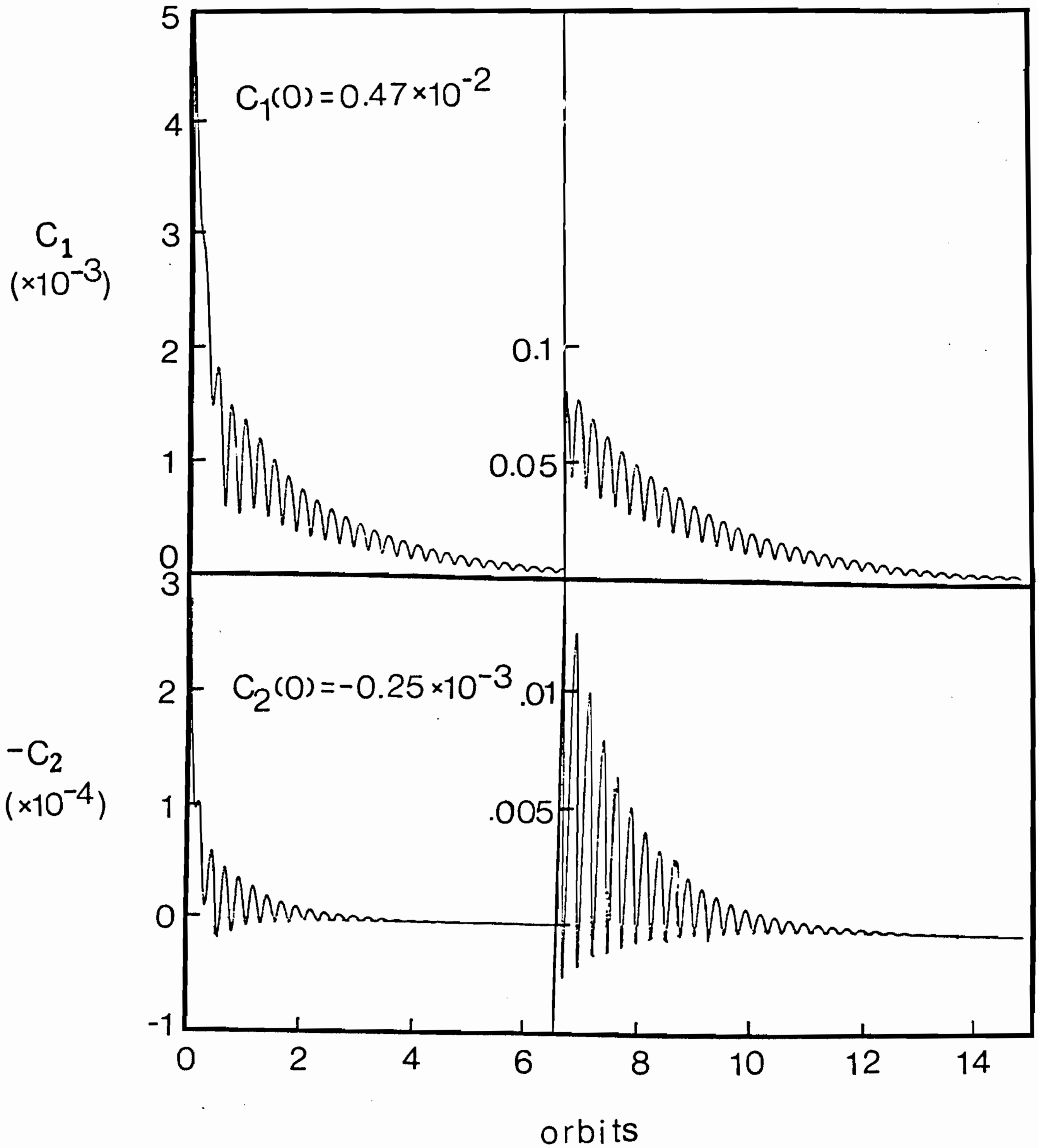

(b) Controlled longitudinal vibrations

Fig. 7.3 Dynamics during retrieval when the length rate involves feedback of both rotations and longitudinal vibration ($C = -4 \times 10^{-4} S^{-1}$)

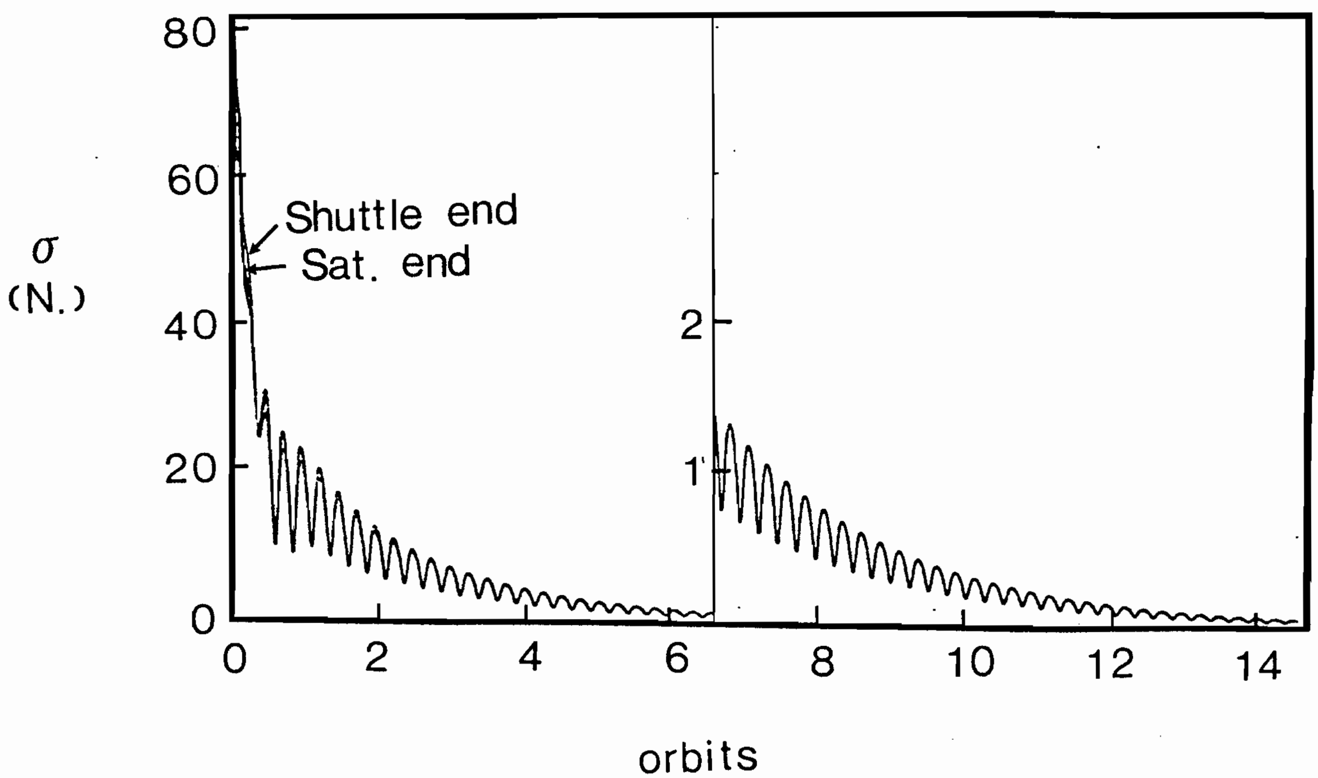

(c) Tensions at both ends of the tether

Fig. 7.3 Dynamics during retrieval when the length rate involves feedback of both rotations and longitudinal vibration ($C = -4 \times 10^{-4} S^{-1}$)

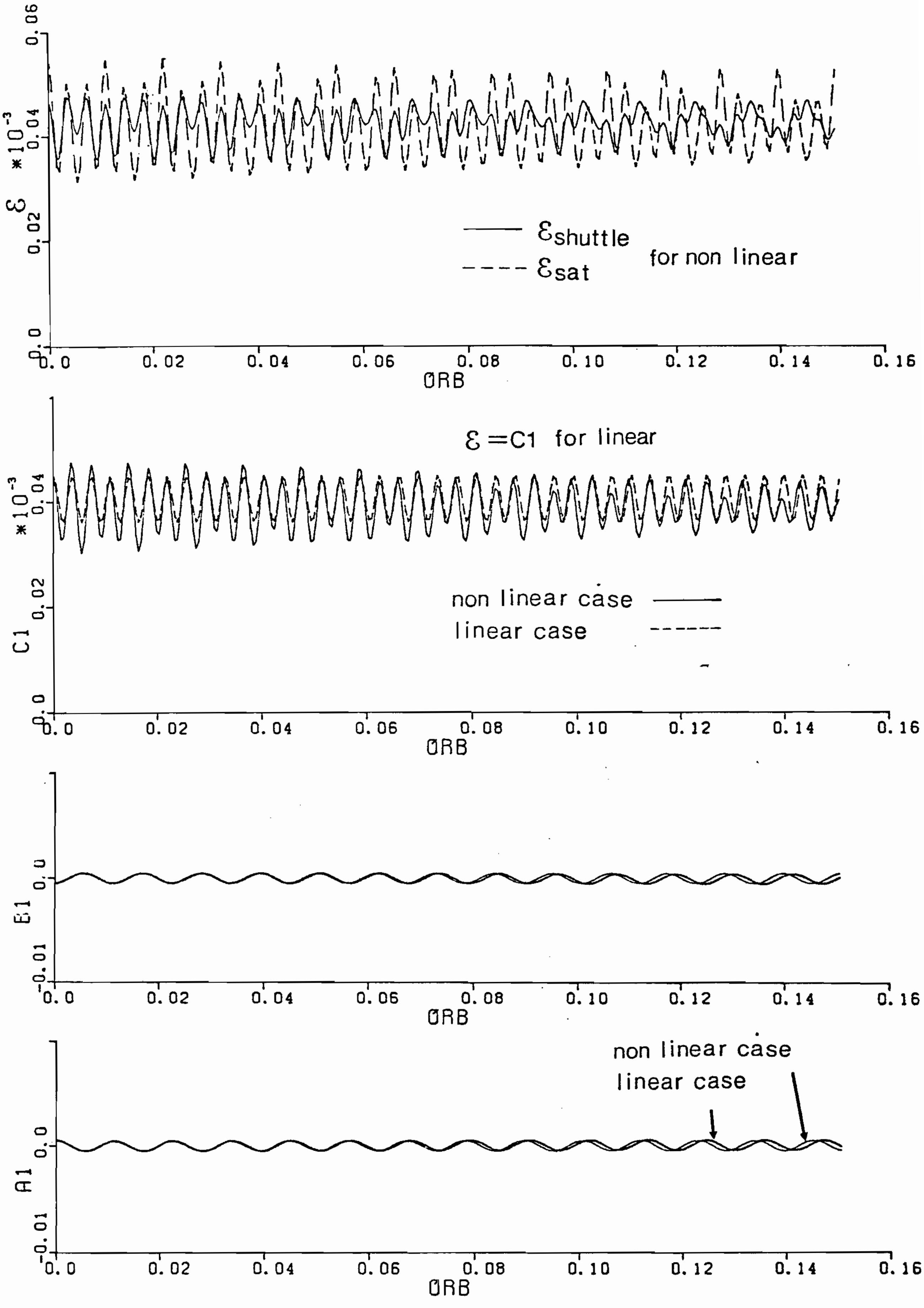

Fig. 8.1 Comparison of linear and nonlinear vibrations

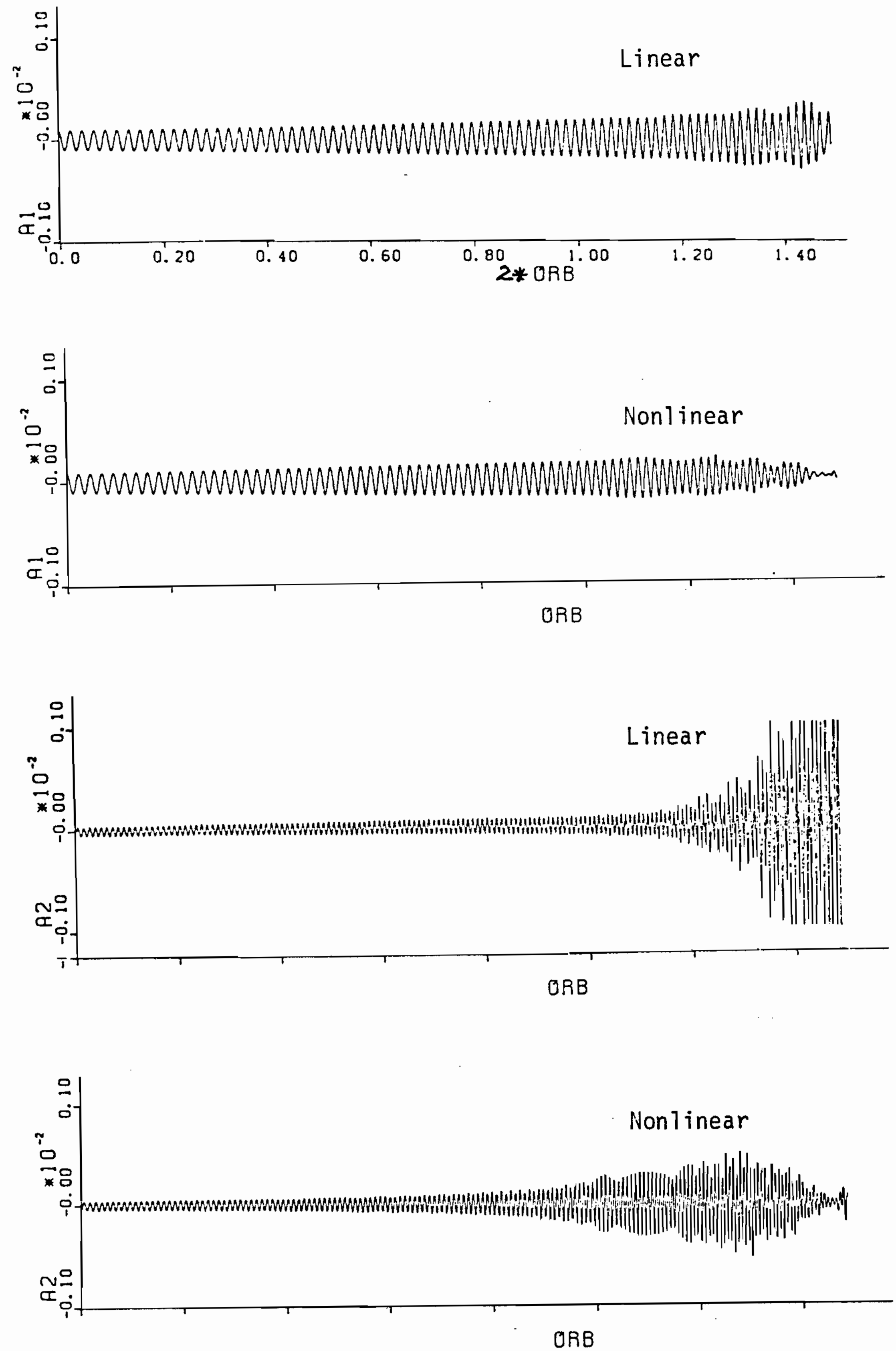

Fig. 8.2 Out-of-plane linear and nonlinear transverse vibrations during uncontrolled retrieval from 1 km.

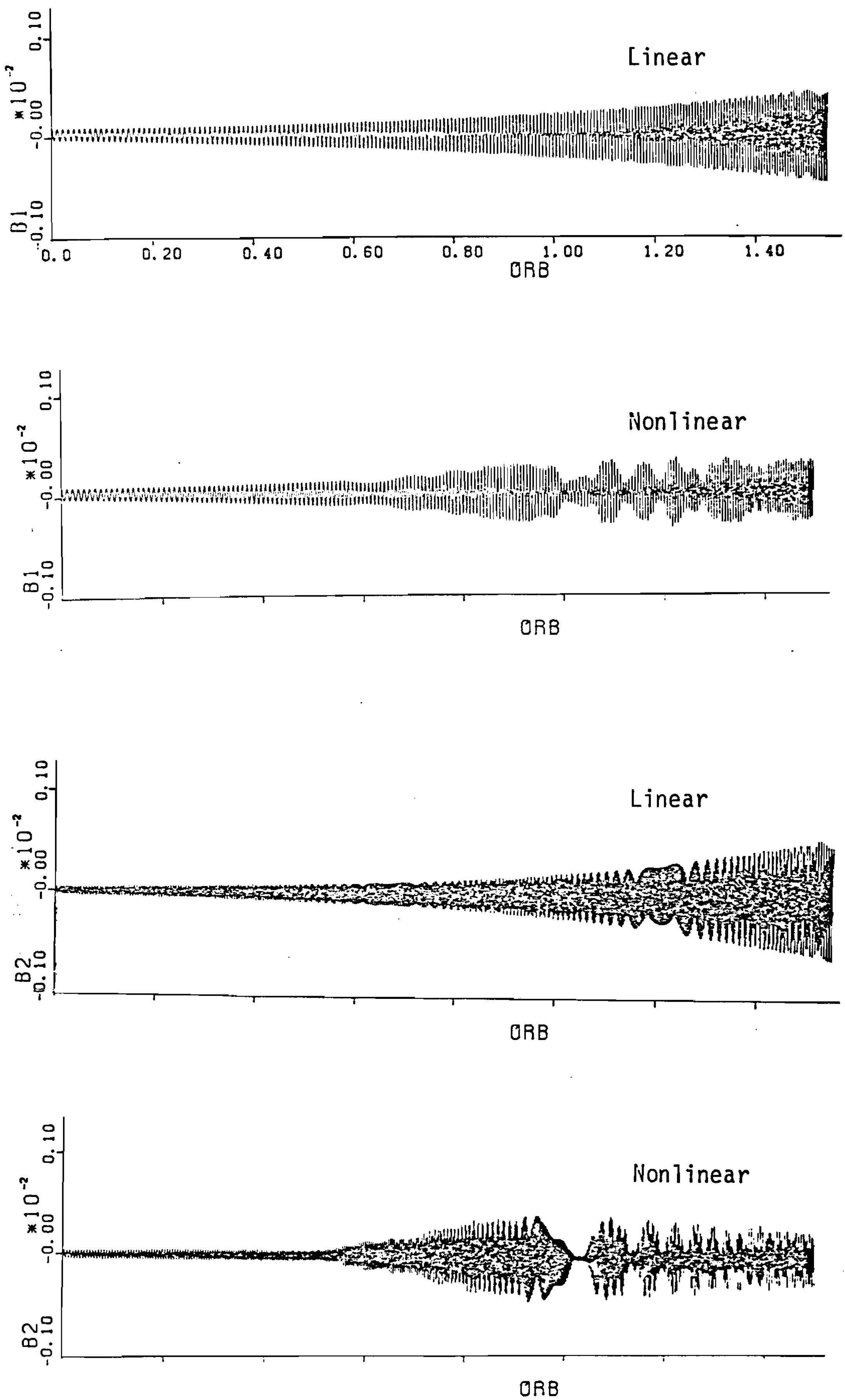

Fig. 8.3 Inplane linear and nonlinear transverse vibrations during retrieval from 1 km using longitudinal strain feedback.

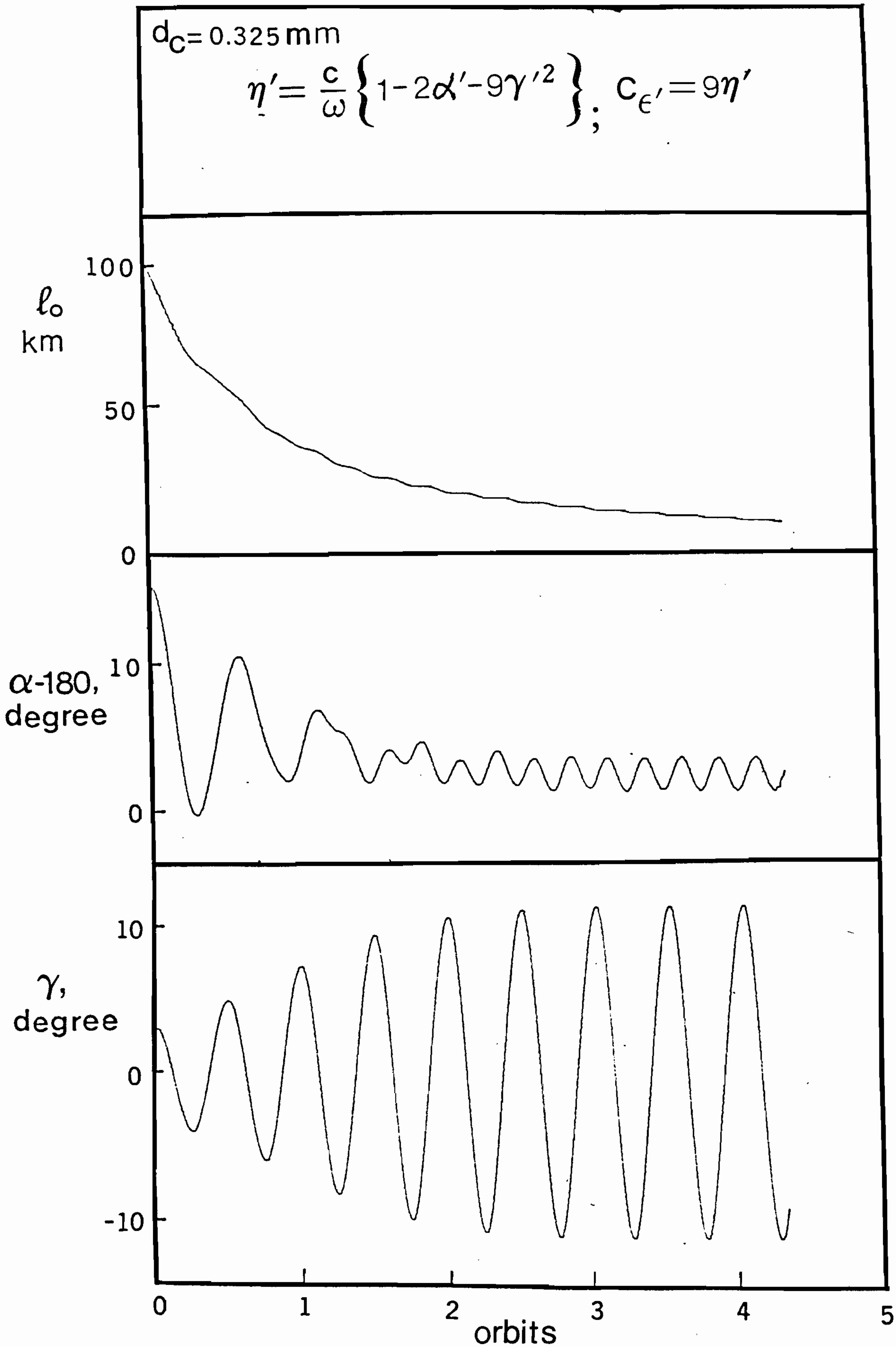

(a) Length ℓ_0, rotations α and γ

Fig. 8.4 Growth of uncontrolled transverse vibrations during retrieval from 100 Km if length rate does not get

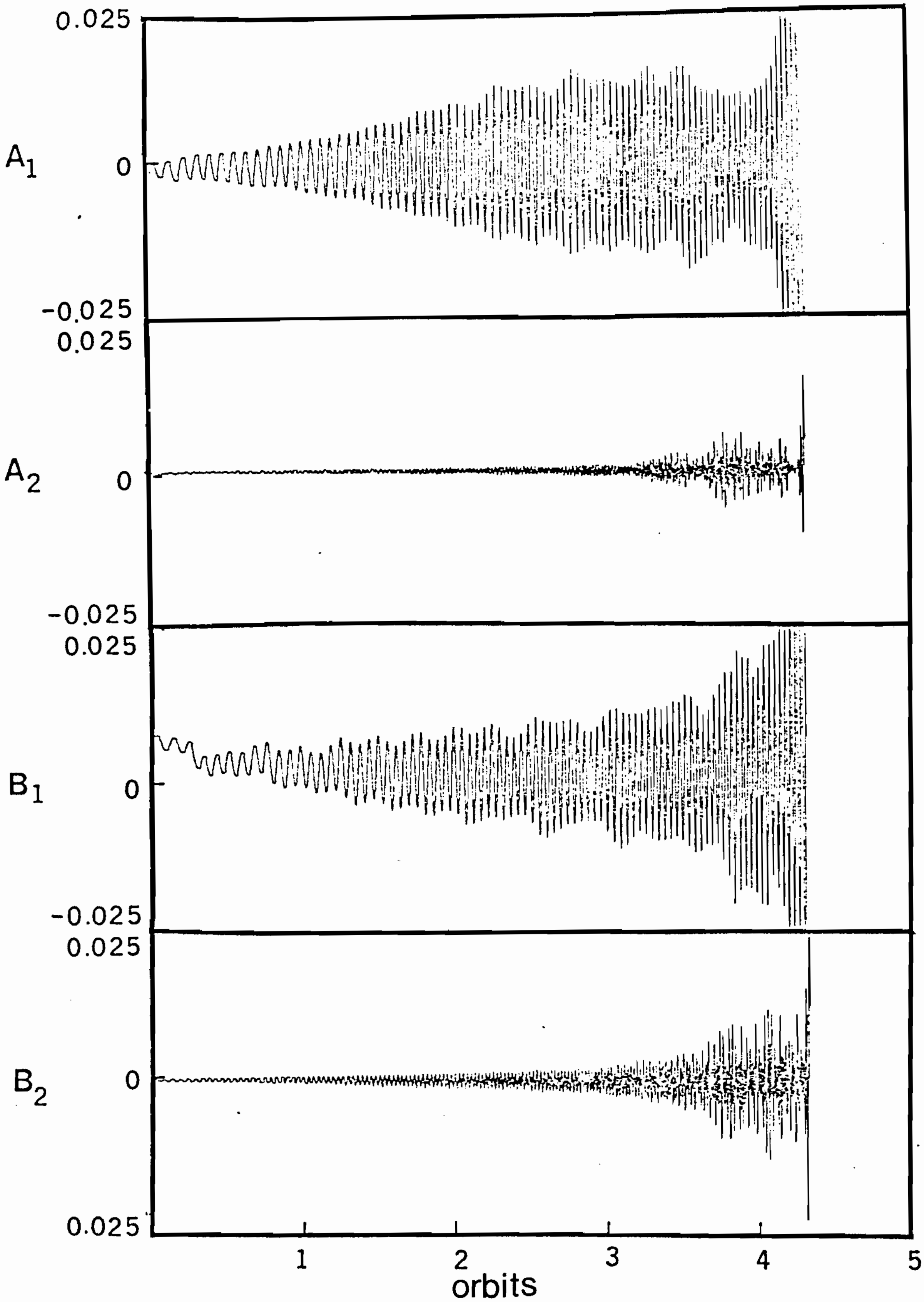

(b) Transverse vibrations A_1, A_2, B_1, B_2

Fig. 8.4 Growth of uncontrolled transverse vibrations during retrieval from 100 Km if length rate does not get feedback from them

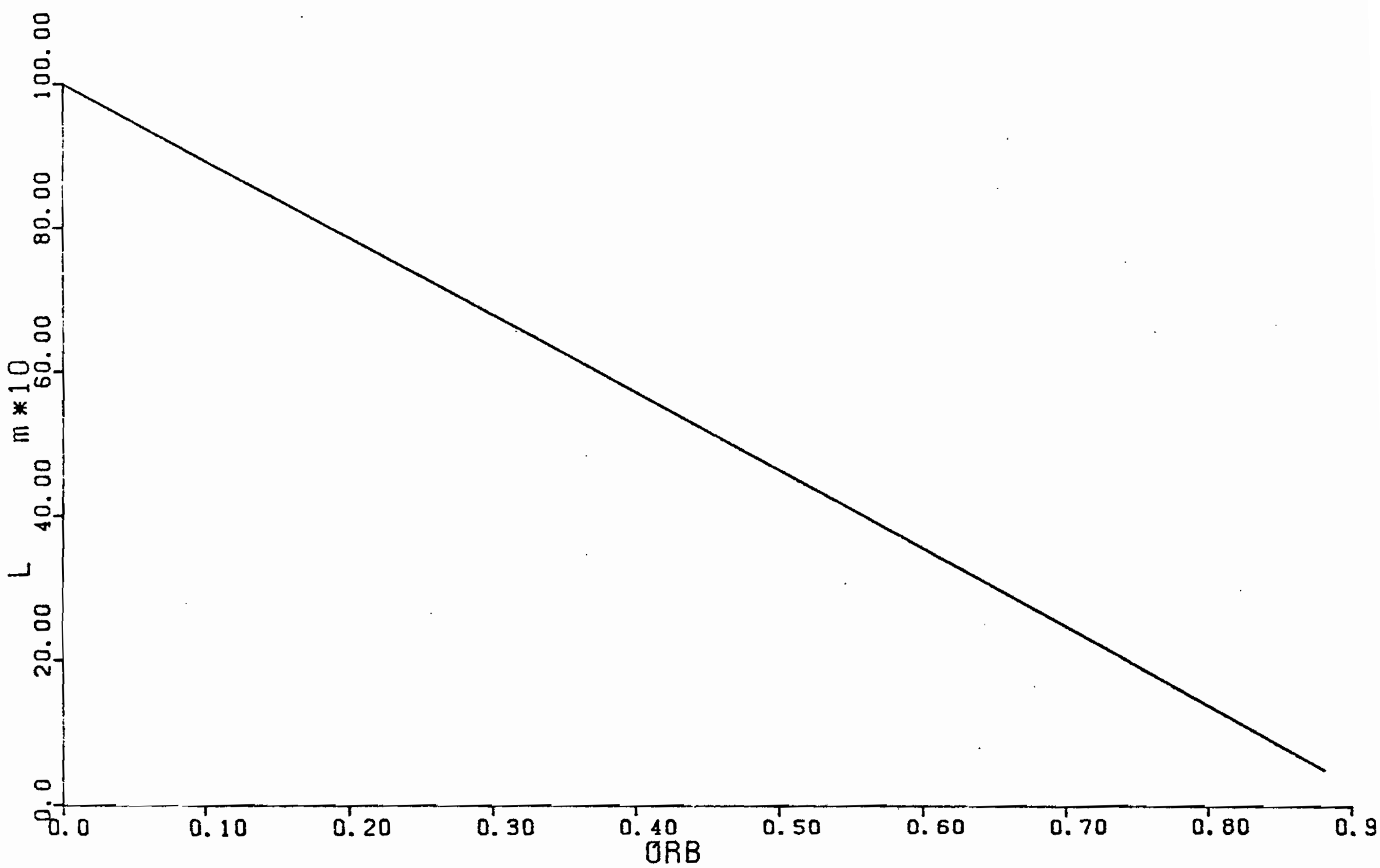

(a) Variation of length

Fig. 8.5 Vibrational response during retrieval from 1 Km using length rate law (8.3.21)

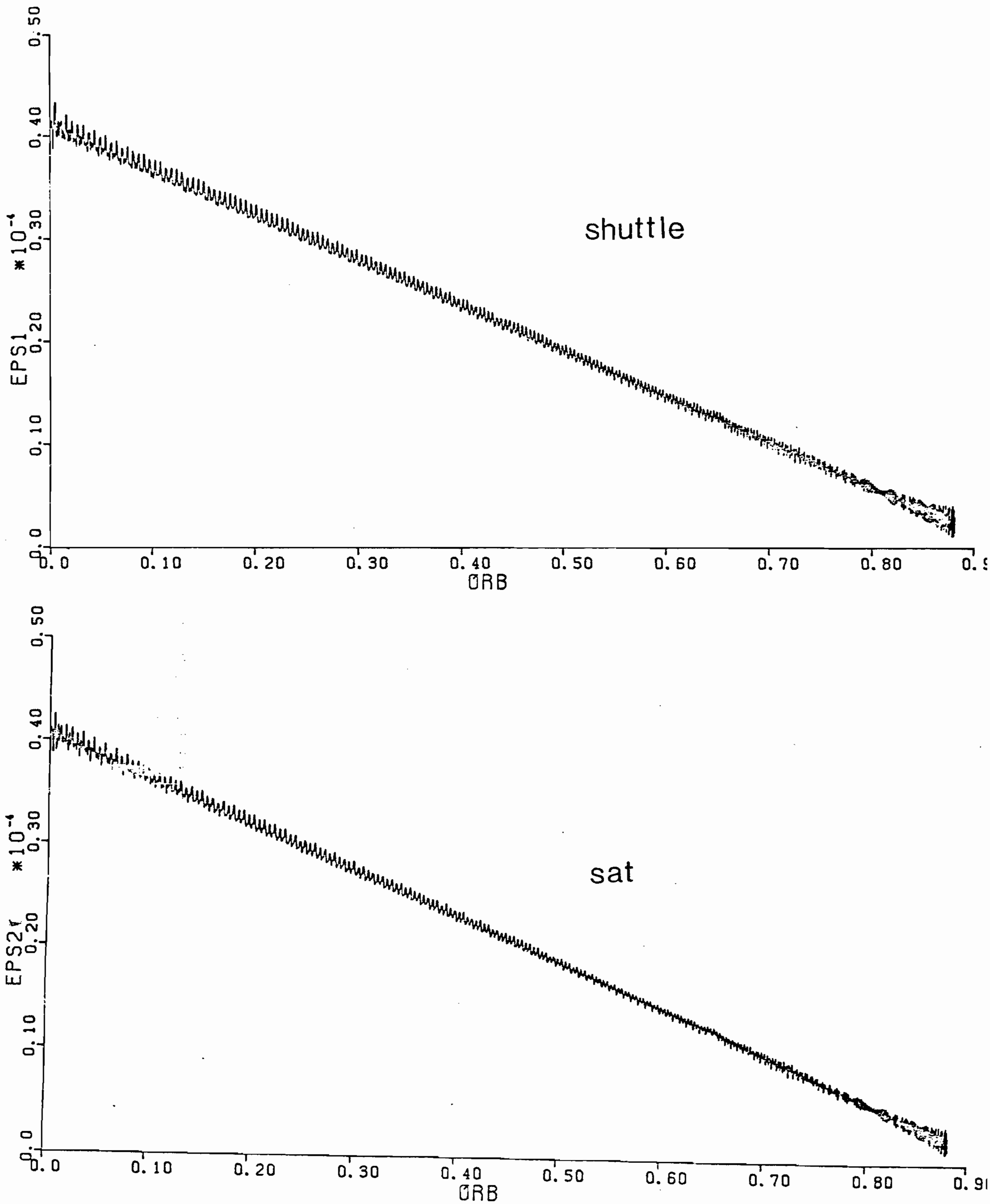

(b) Longitudinal strain

Fig. 8.5 Vibrational response during retrieval from 1 Km using length rate law (8.3.21)

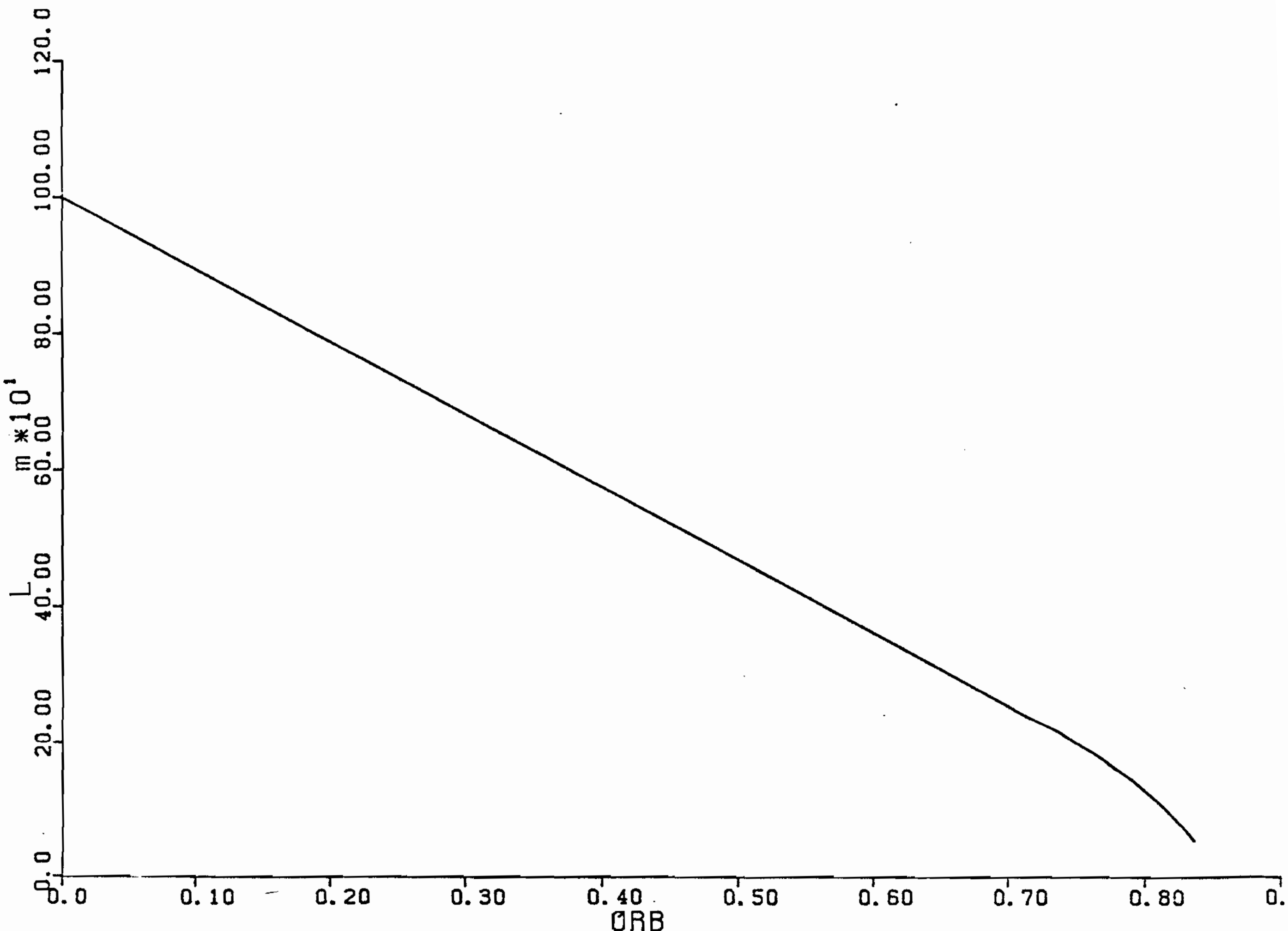

(a) Variation of length

Fig. 8.6 Vibrational response during retrieval from 1 Km using length change law (8.4.1)

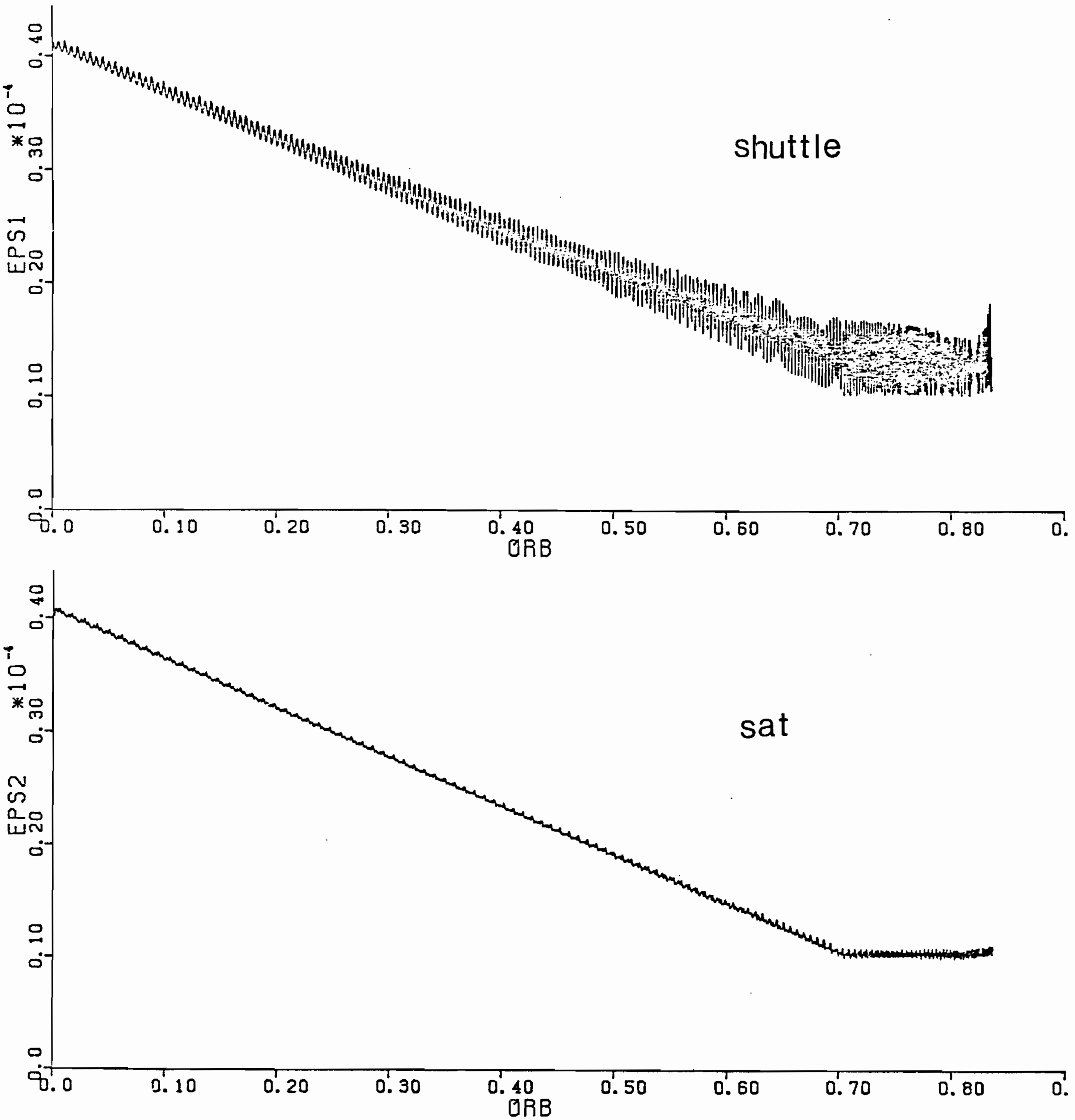

(b) Longitudinal strain

Fig. 8.6 Vibrational response during retrieval from 1 Km using length change law (8.4.1)

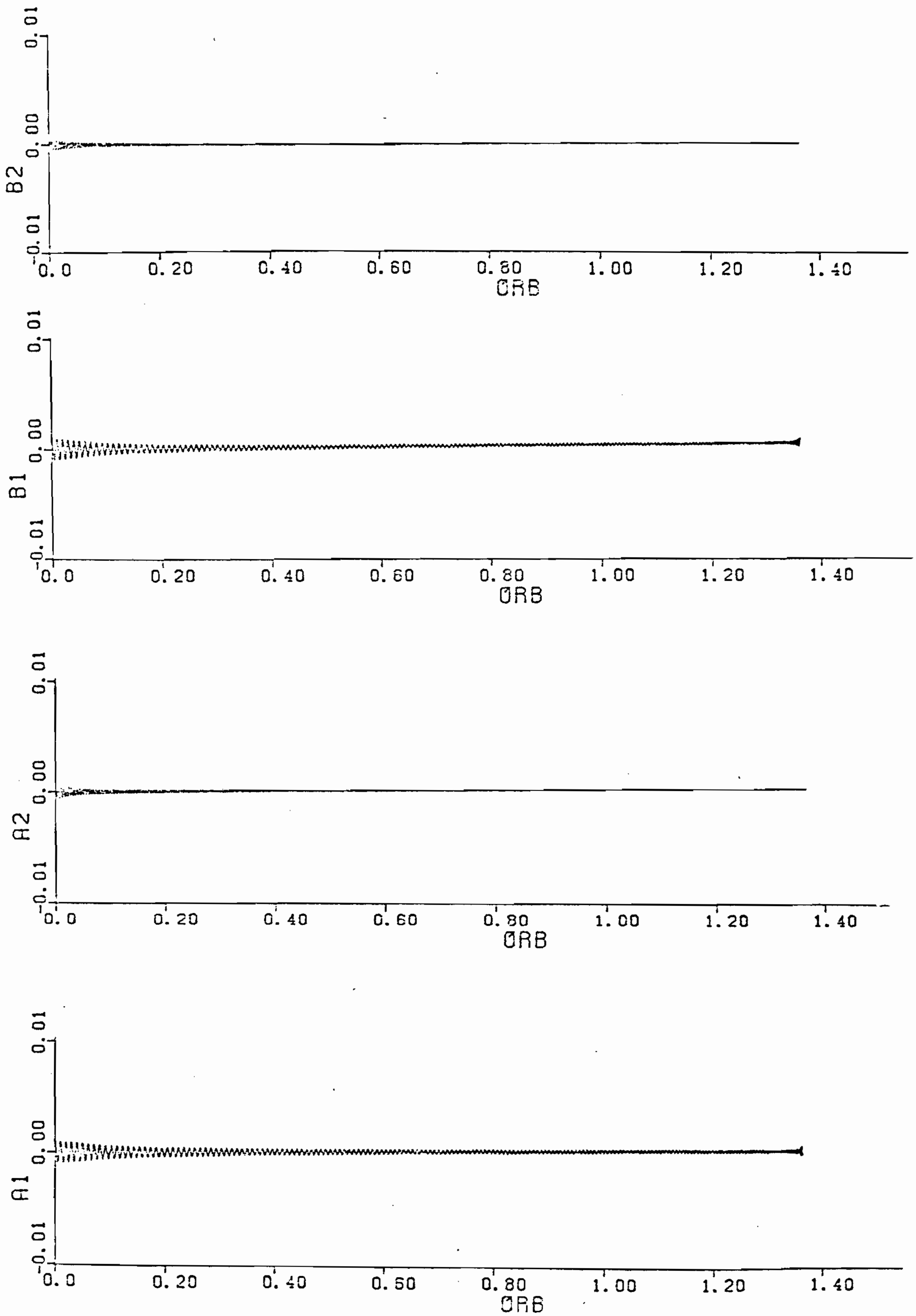

(c) Transverse vibrations

Fig. 8.6 Vibrational response during retrieval from 1 Km using length change law (8.4.1)

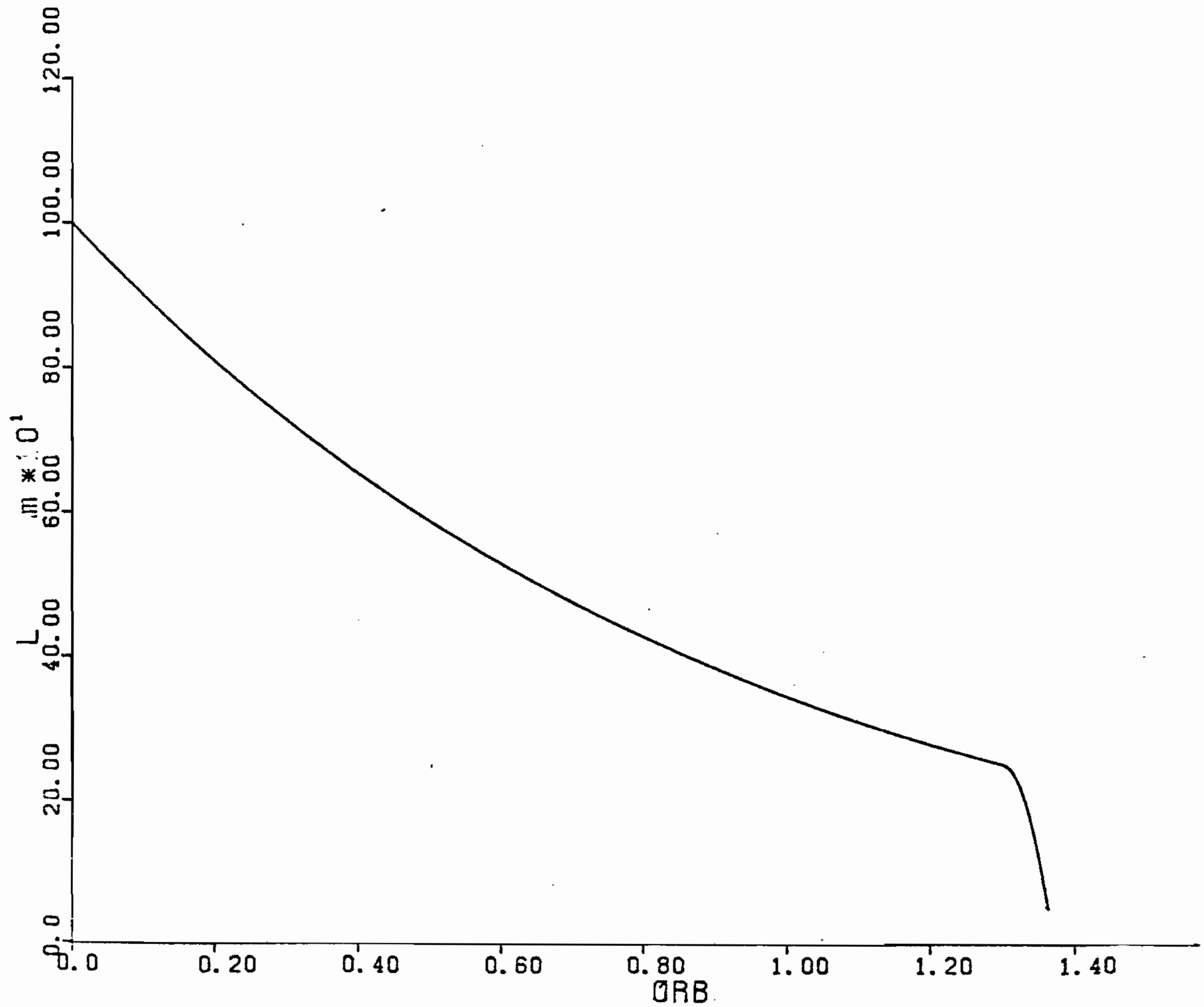

(a) Variation of length

Fig. 8.7 Vibrational response during retrieval from 1 Km using length change law (8.4.11)

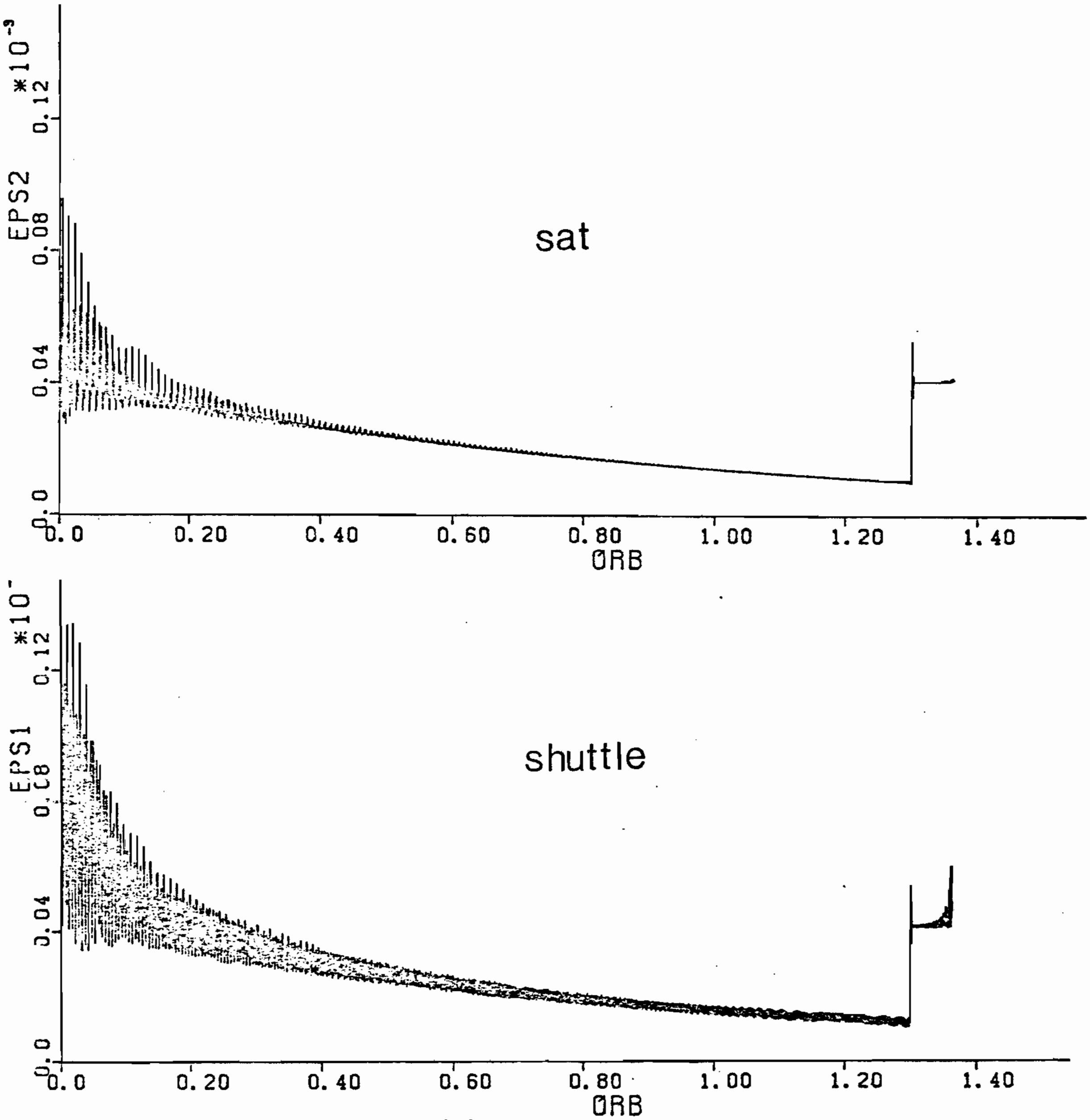

(b) Longitudinal strain

Fig. 8.7 Vibrational response during retrieval from 1 Km using length change law (8.4.11)

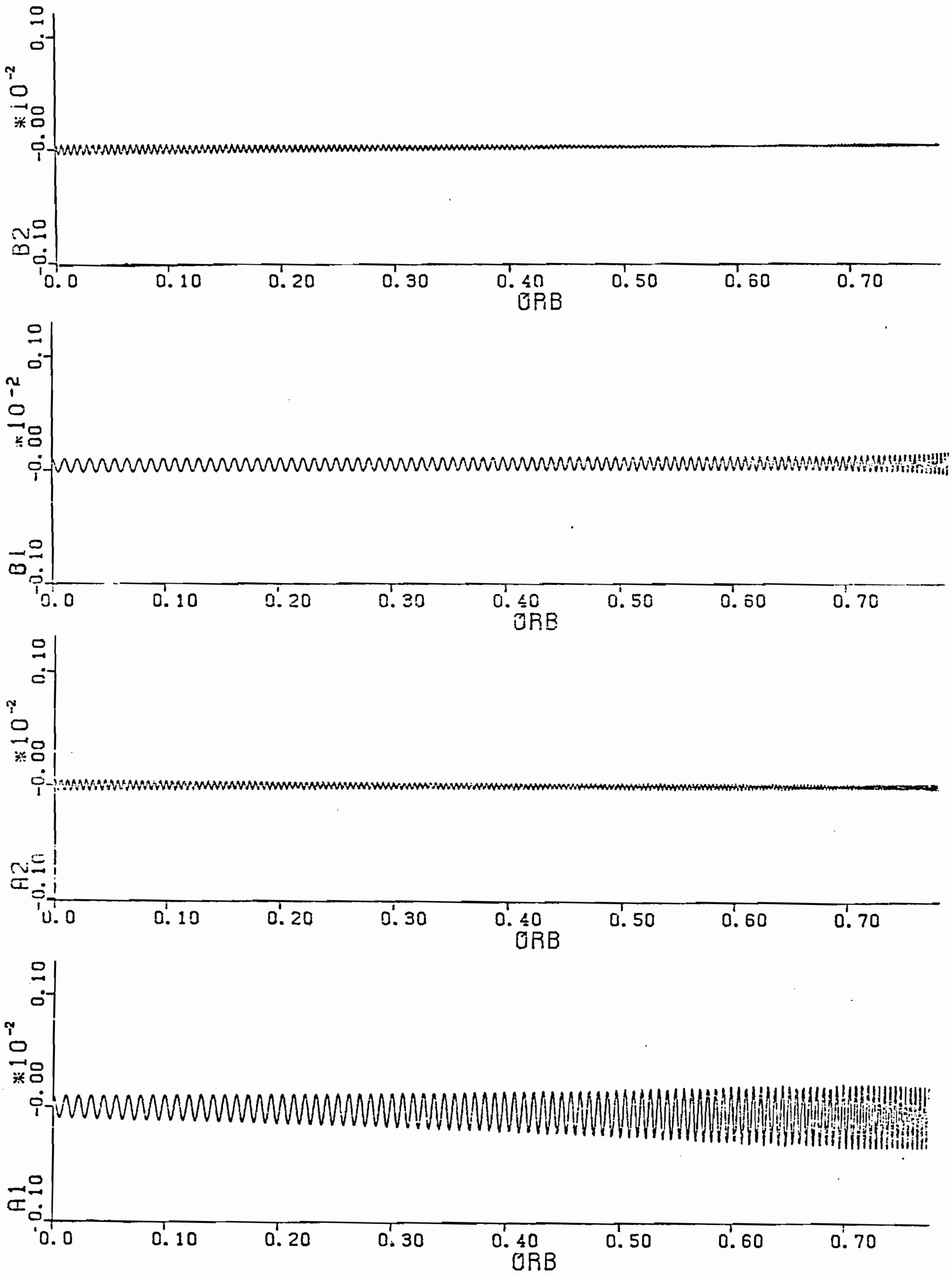

(c) Transverse vibrations

Fig. 8.7 Vibrational response during retrieval from 1 Km using length change law (8.4.11)

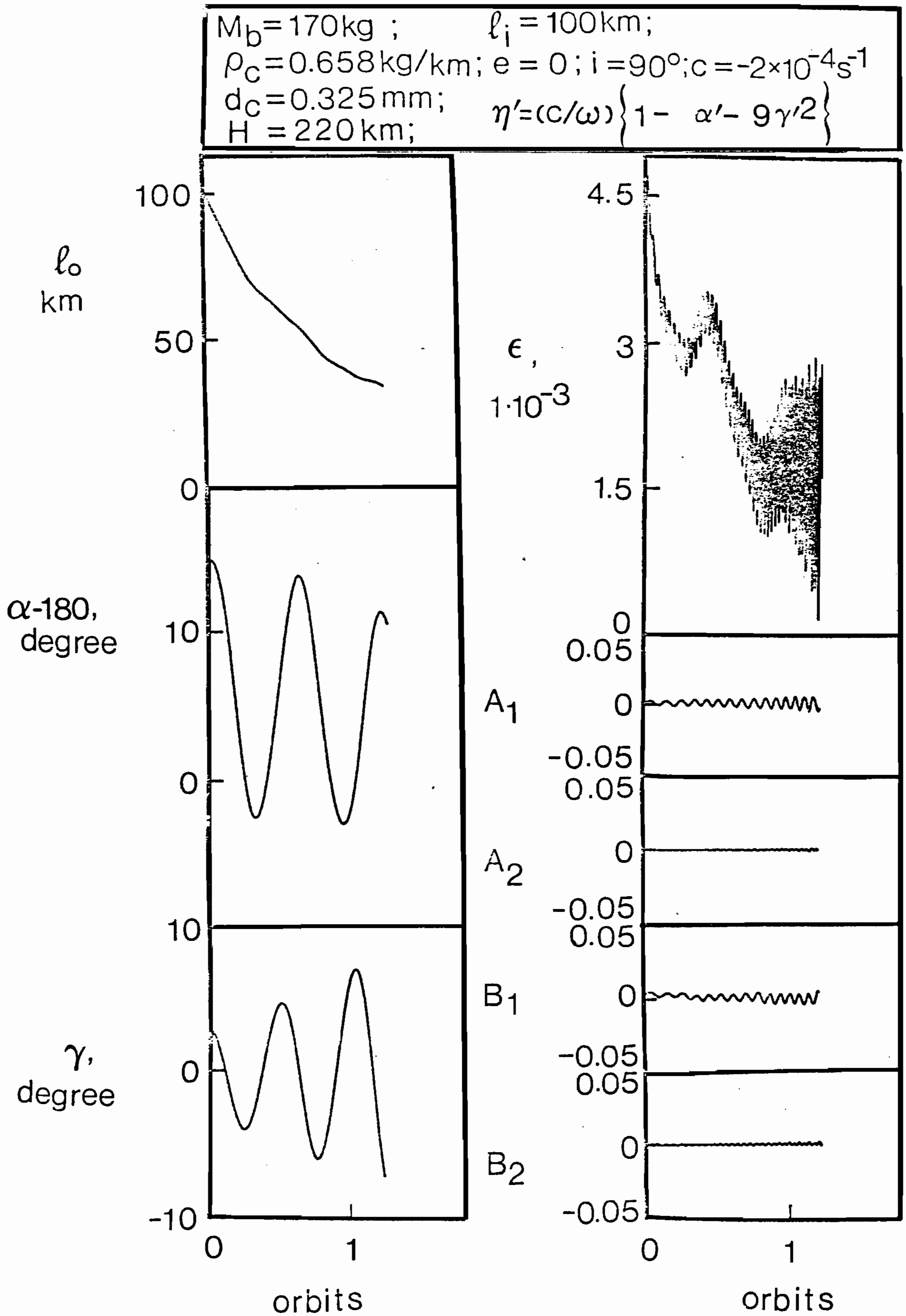

Fig. 8.8 Vibrational response during retrieval from 100 Km with the linear strain model and using length rate law (8.5.1)

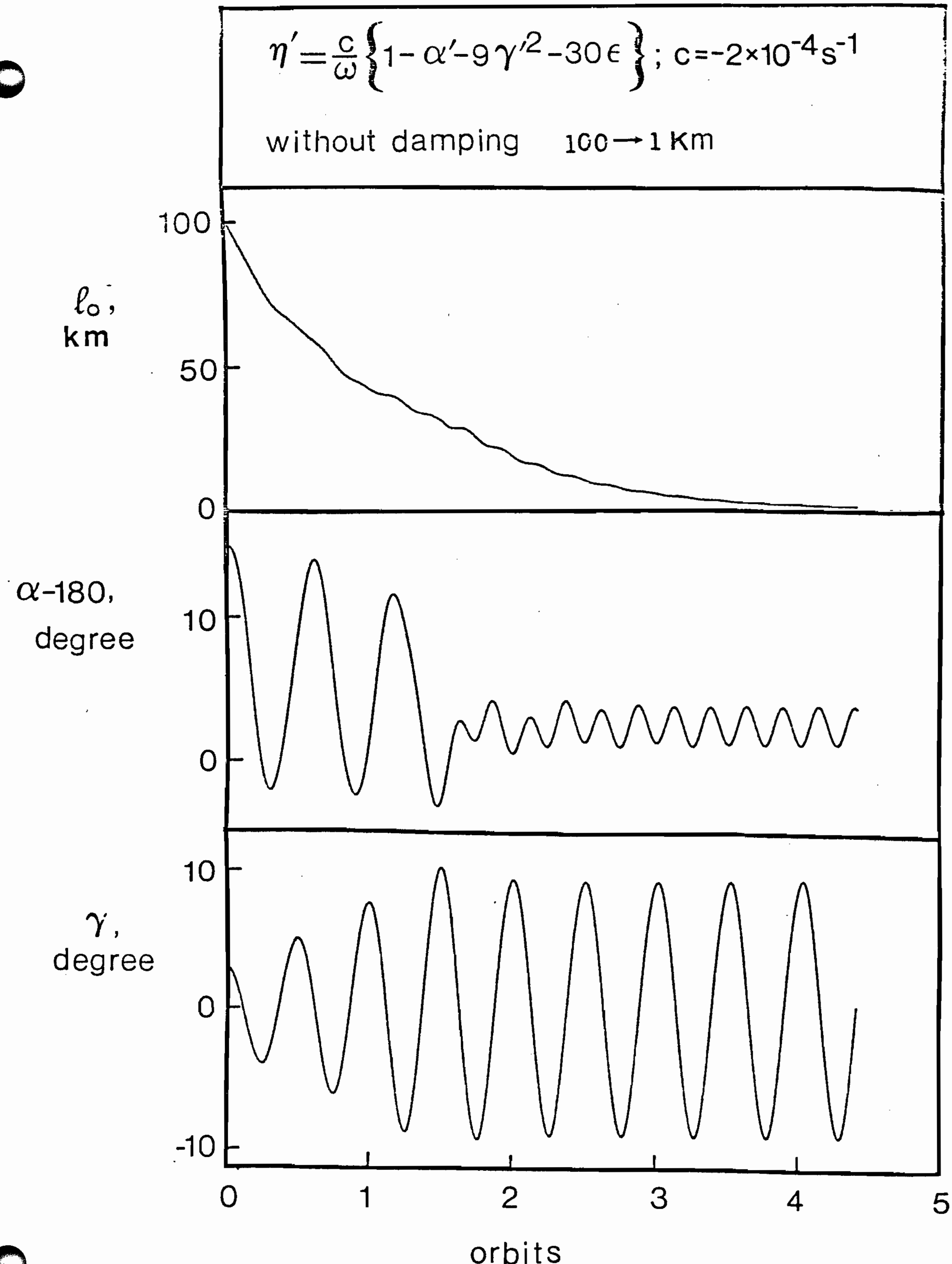

(a) Variation of length ℓ_0 and rotations α and γ

Fig. 8.9 Dynamical response (both rotations and vibrations during retrieval from 100 Km with the linear strain model and using length rate law (8.5.2)

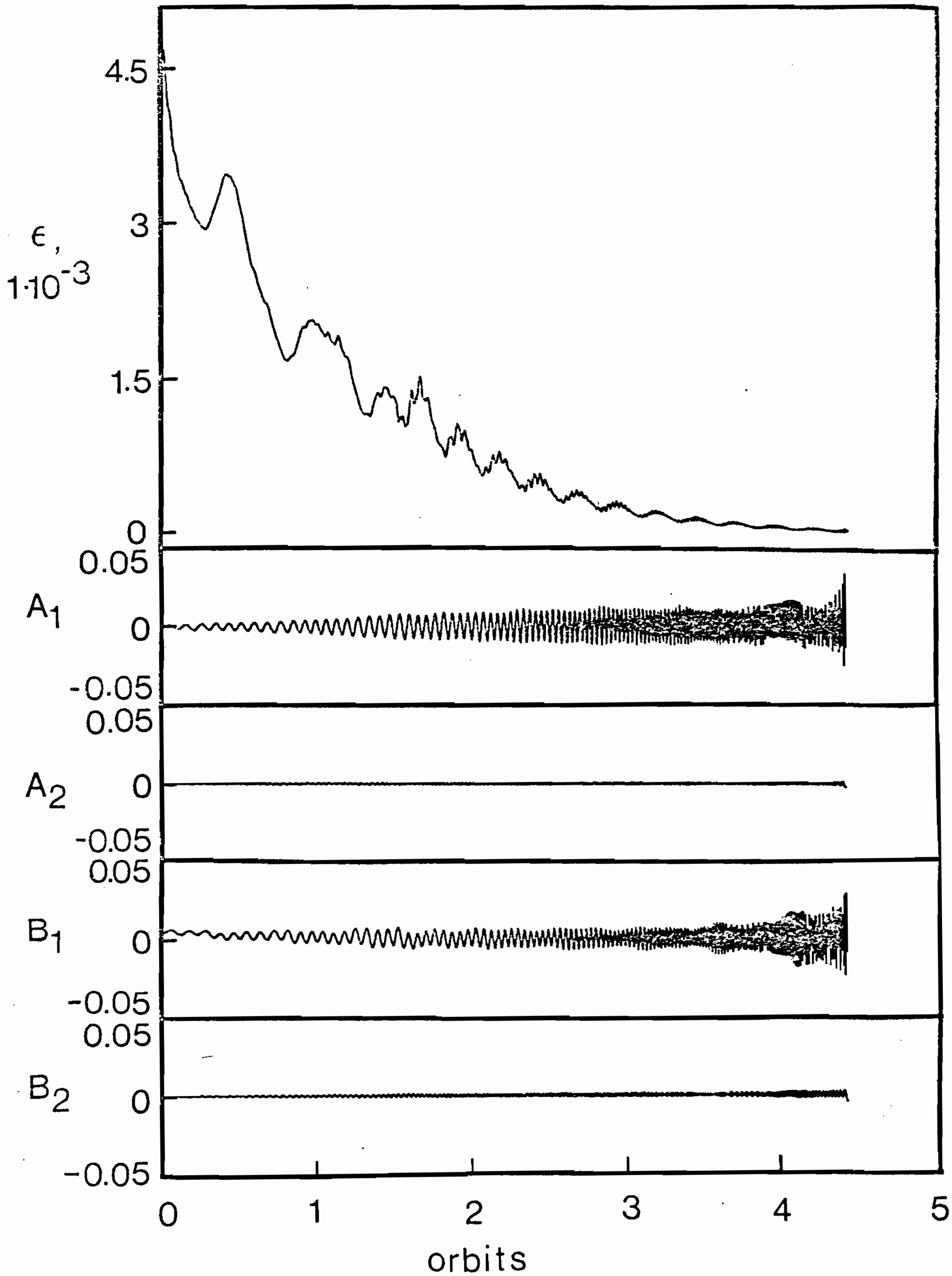

(b) Longitudinal strain and transverse modal coordinates A_1, A_2, B_1 and B_2

Fig. 8.9 Dynamical response (both rotations and vibrations during retrieval from 100 Km with the linear strain model and using length rate law (8.5.2)

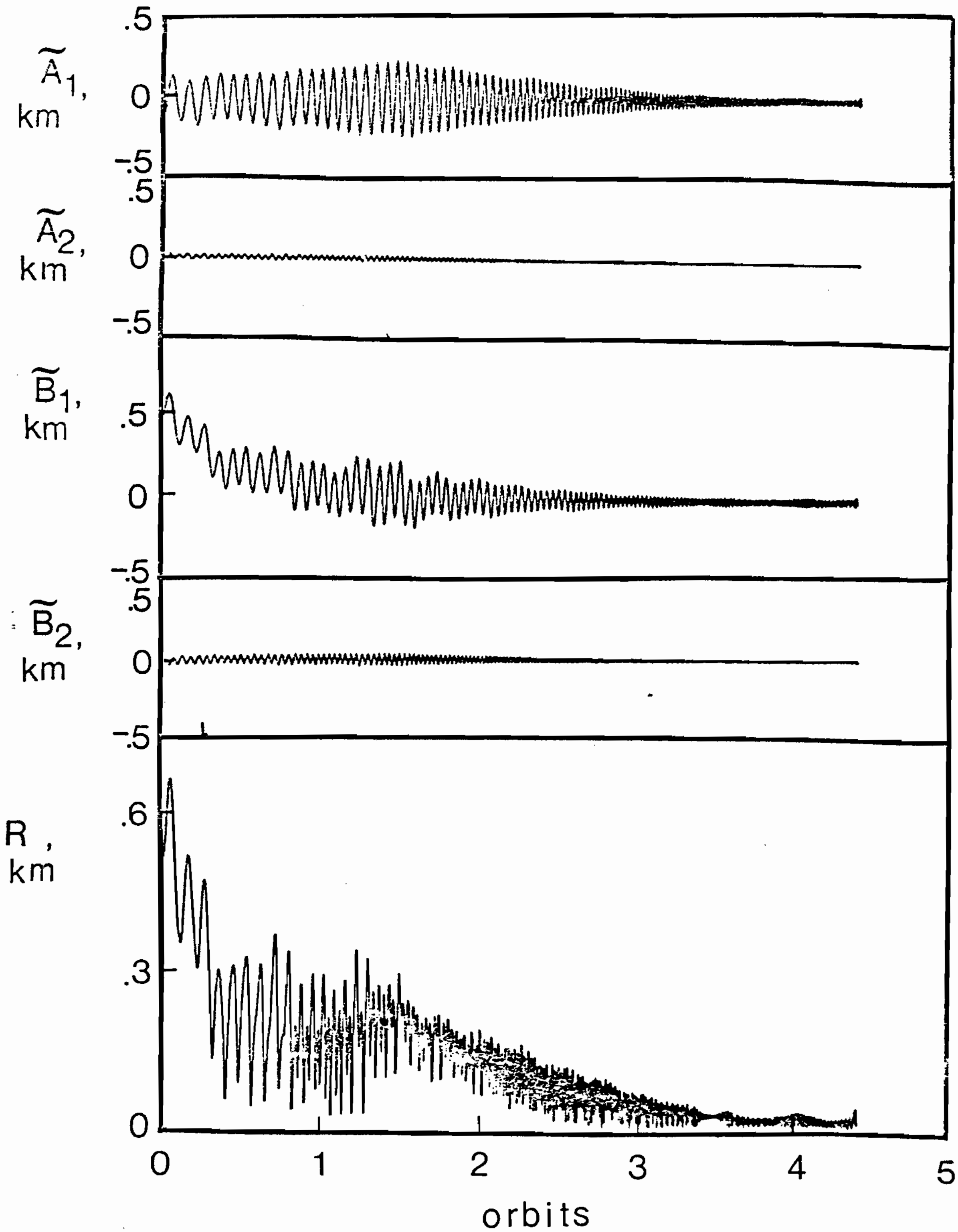

(c) Dimensional displacements $\tilde{A}_1$, $\tilde{A}_2$, $\tilde{B}_1$, $\tilde{B}_2$ and the transverse displacement R of the middle point of the tether

Fig. 8.9 Dynamical response (both rotations and vibrations) during retrieval from 100 Km with the linear strain model and

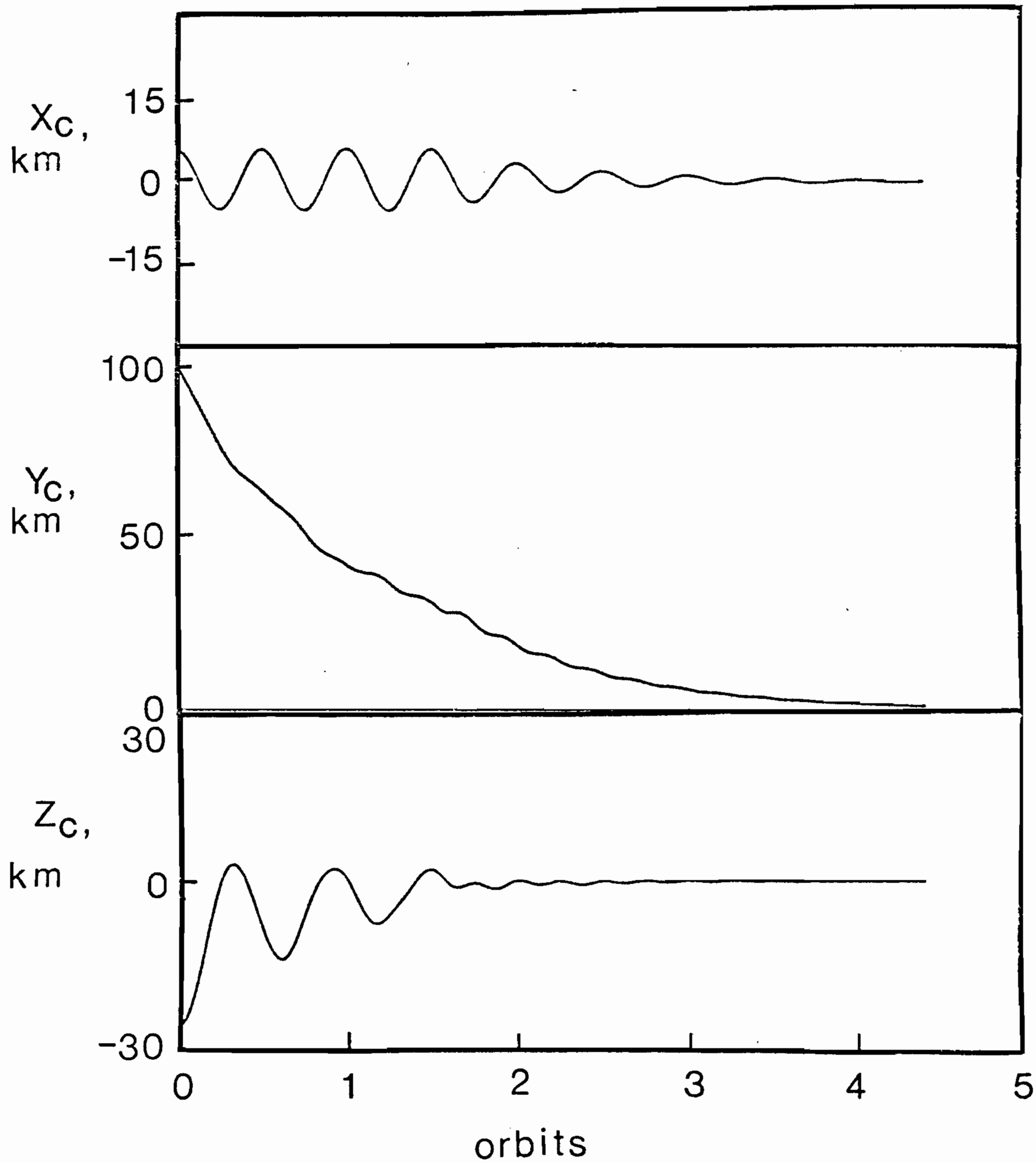

(d) Displacements of the middle point of the tether along x_c, y_c, z_c directions, respectively

Fig. 8.9 Dynamical response (both rotations and vibrations) during retrieval from 100 Km with the linear strain model and using lnegth rate law (8.5.2)

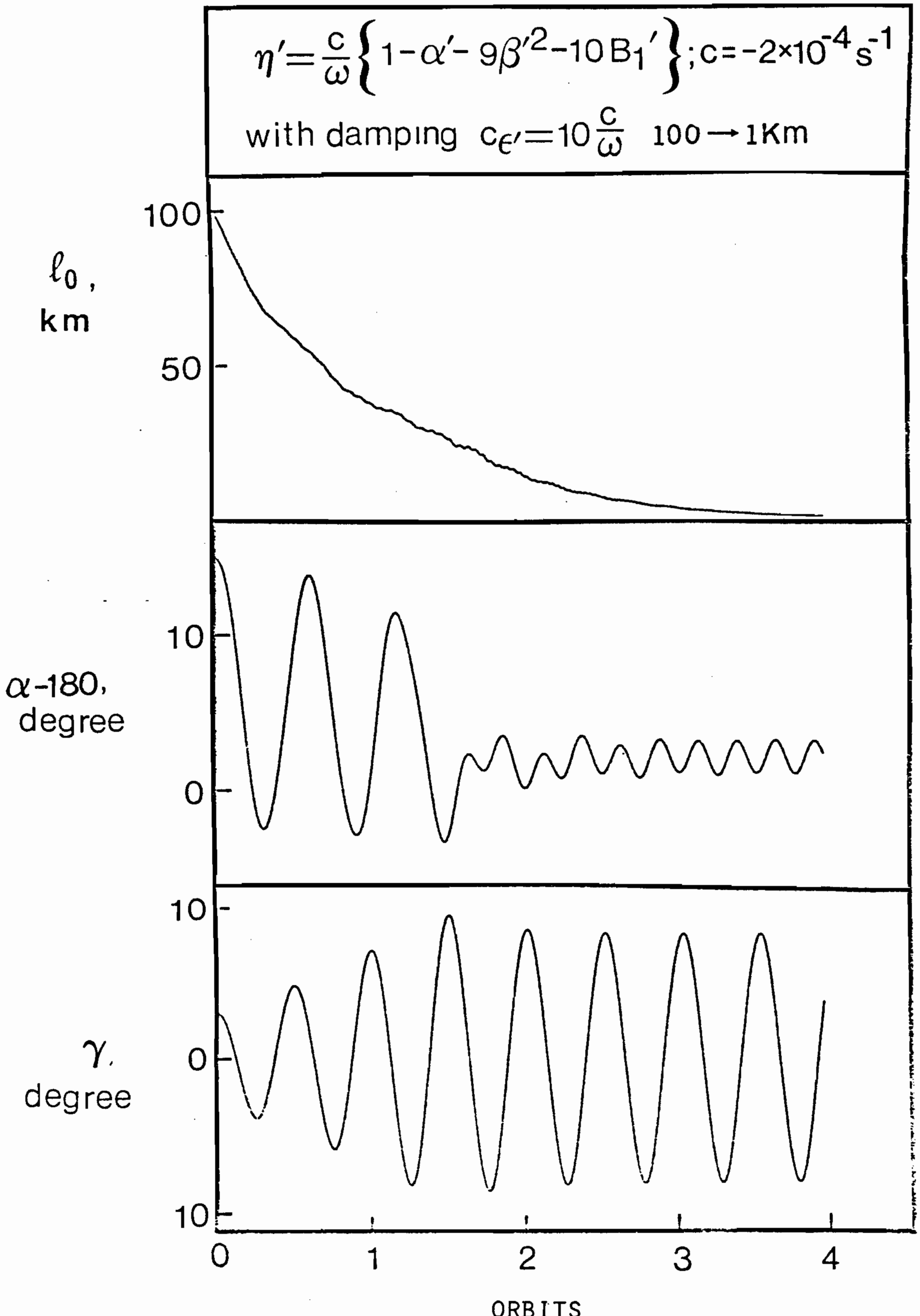

(a) Variations of length ℓ_0 and rotations α and γ

Fig. 8.10 Dynamical response (both rotations and vibrations) during retrieval from 100 Km with the linear strain model and using length rate law (8.5.3)

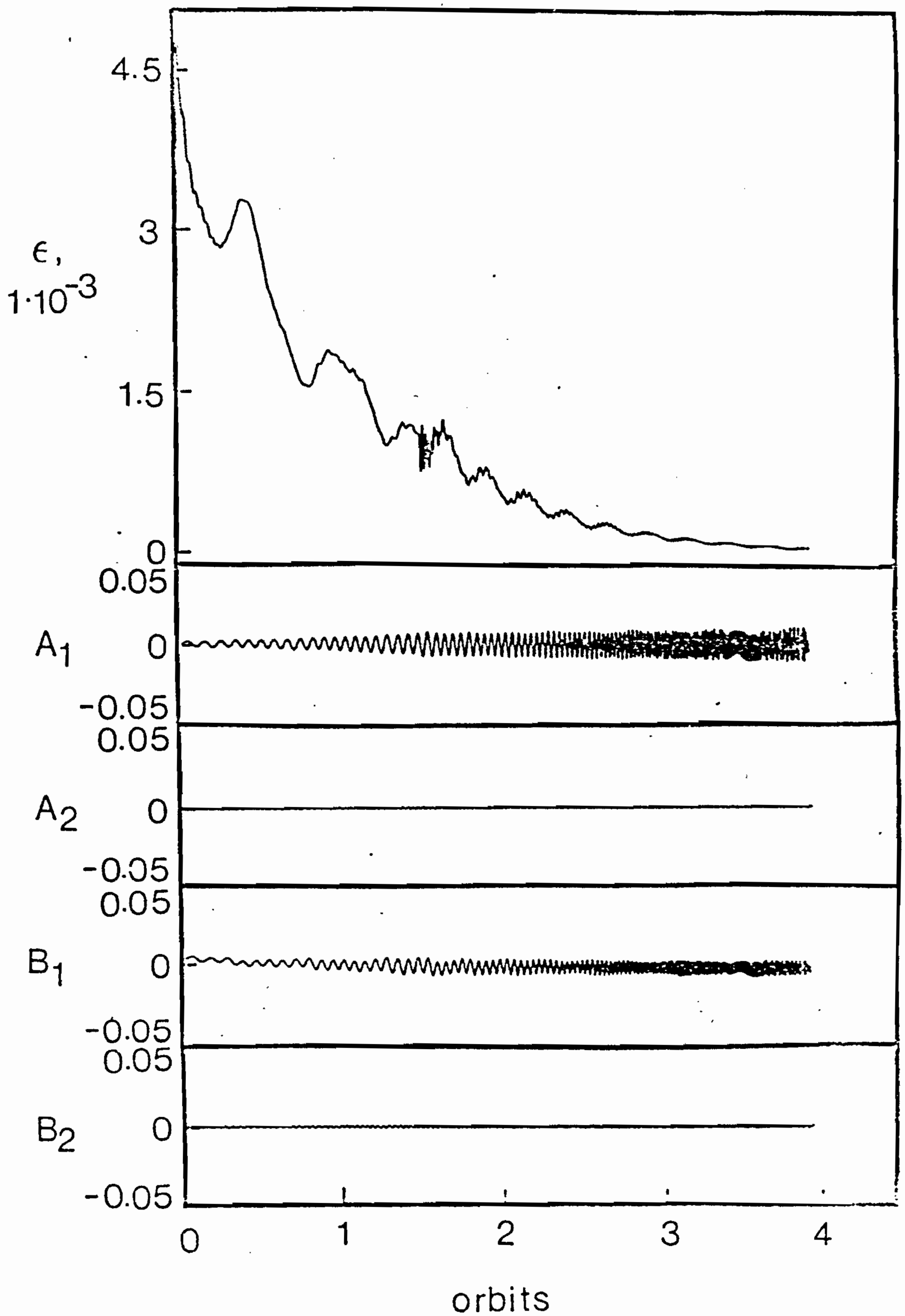

(b) Longitudinal strain and transverse modal coordinates A_1, A_2, B_1 and B_2

Fig. 8.10 Dynamical response (both rotations and vibrations) during retrieval from 100 Km with the linear strain model and using length rate law (8.5.3)

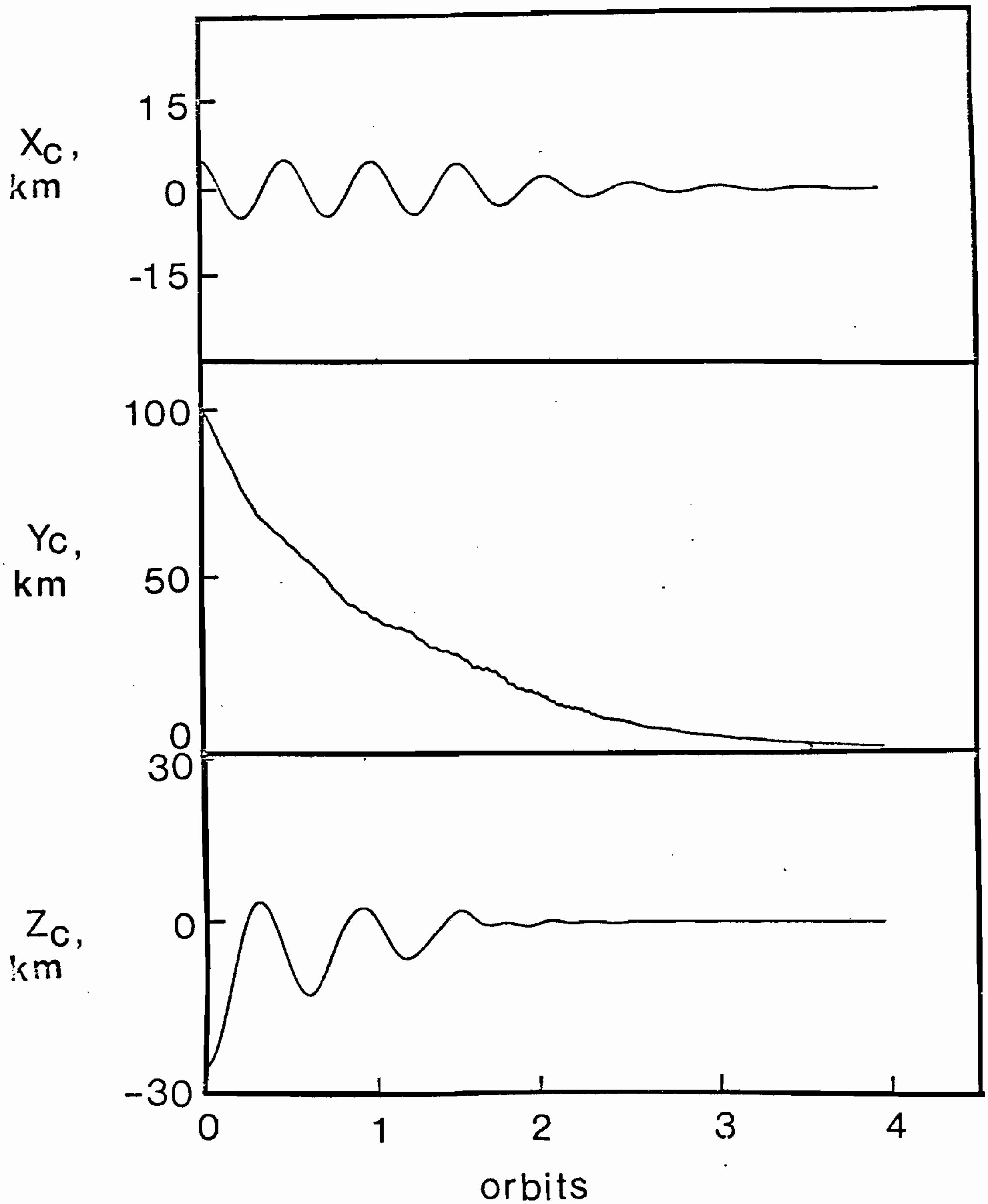

(c) Displacements of the middle point of the tether along x_C, y_C, z_C directions, respectively

Fig. 8.10 Dynamical response (both rotations and vibrations) during retrieval from 100 Km with the linear strain model and using length rate law (8.5.3)

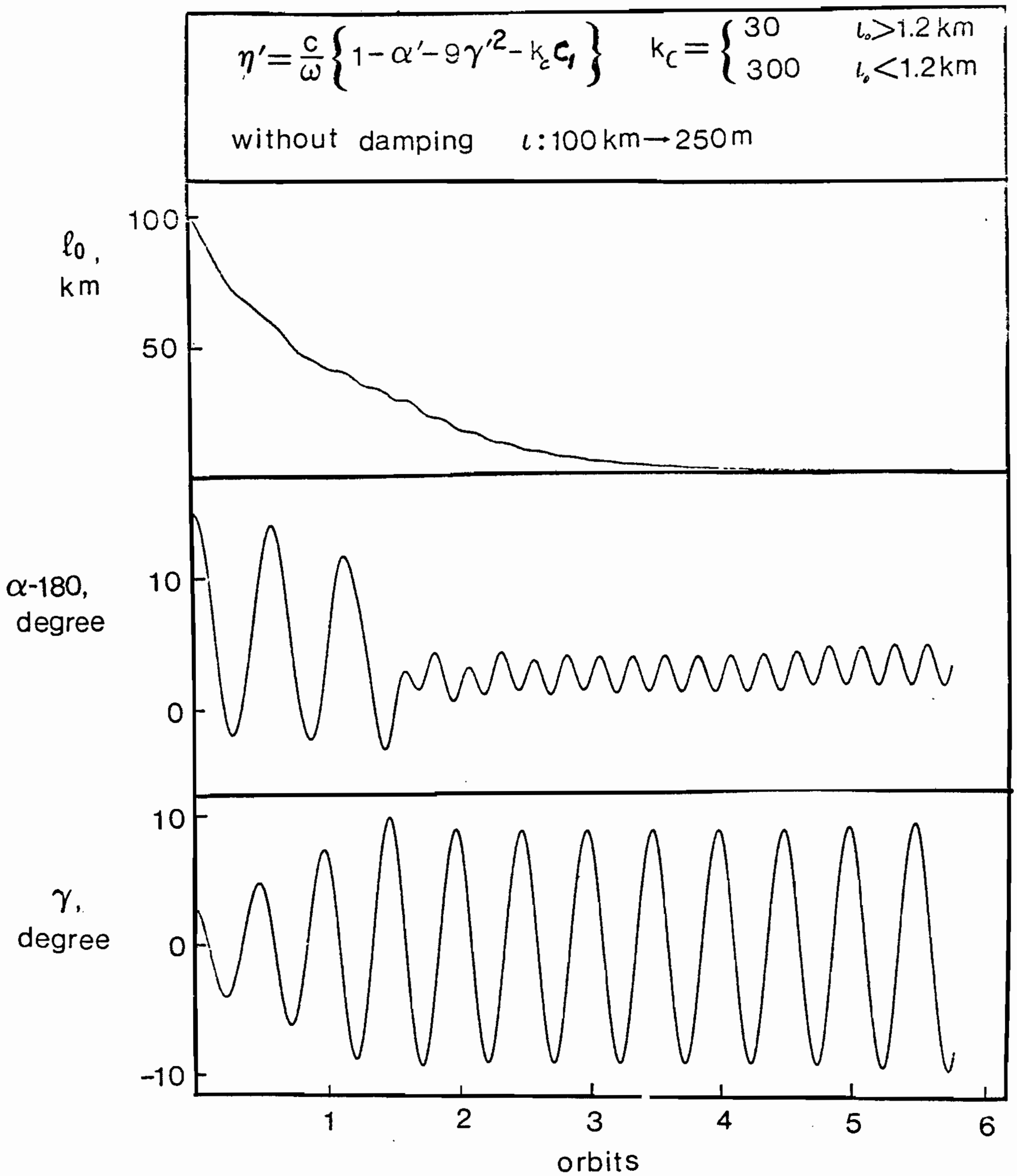

(a) Variations of length ℓ_0 and rotations α and γ

Fig. 8.11 Dynamical response (both rotations and vibrations) during retrieval from 100 Km with the linear strain model using length rate law (8.5.2)

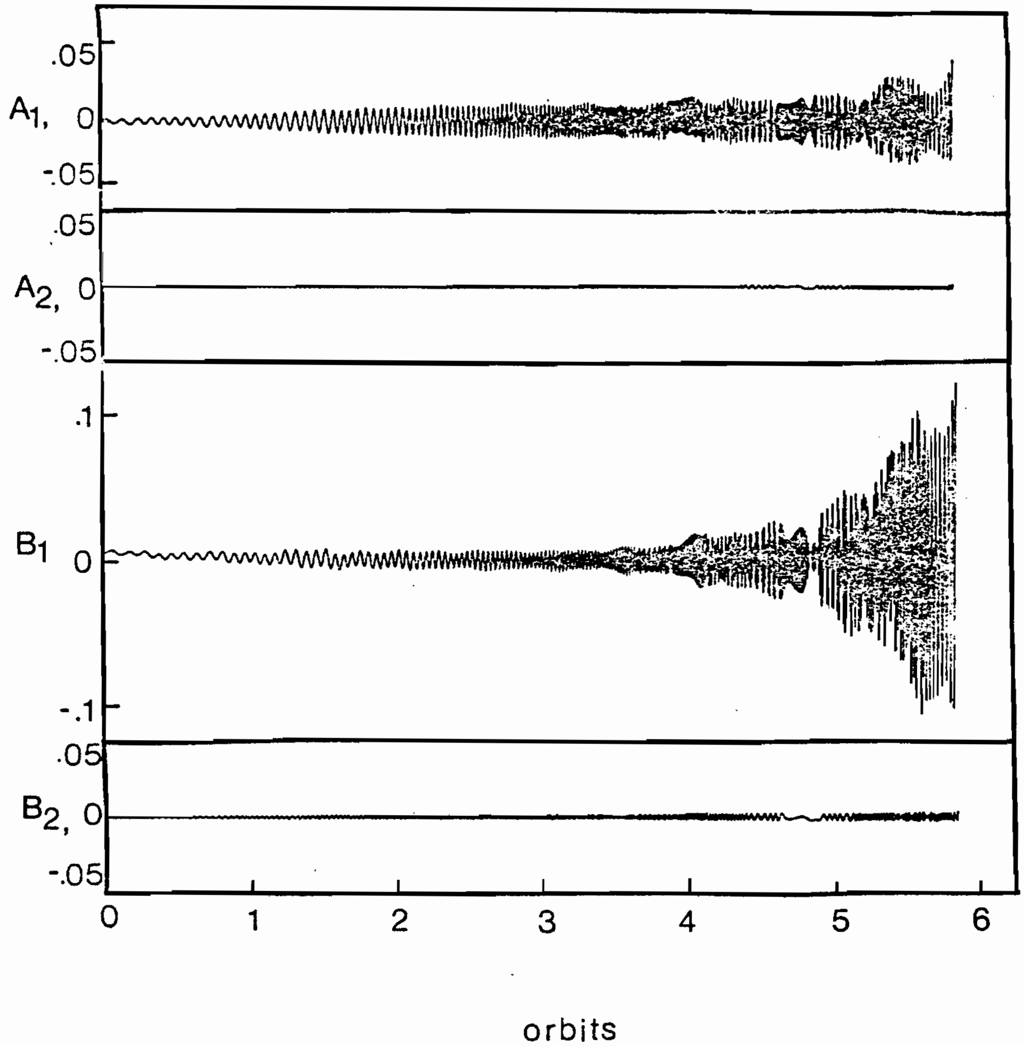

(b) Transverse modal coordinates A_1, A_2, B_1 and B_2

Fig. 8.11 Dynamical response (both rotations and vibrations) during retrieval from 100 Km with the linear strain model and using length rate law (8.5.2)

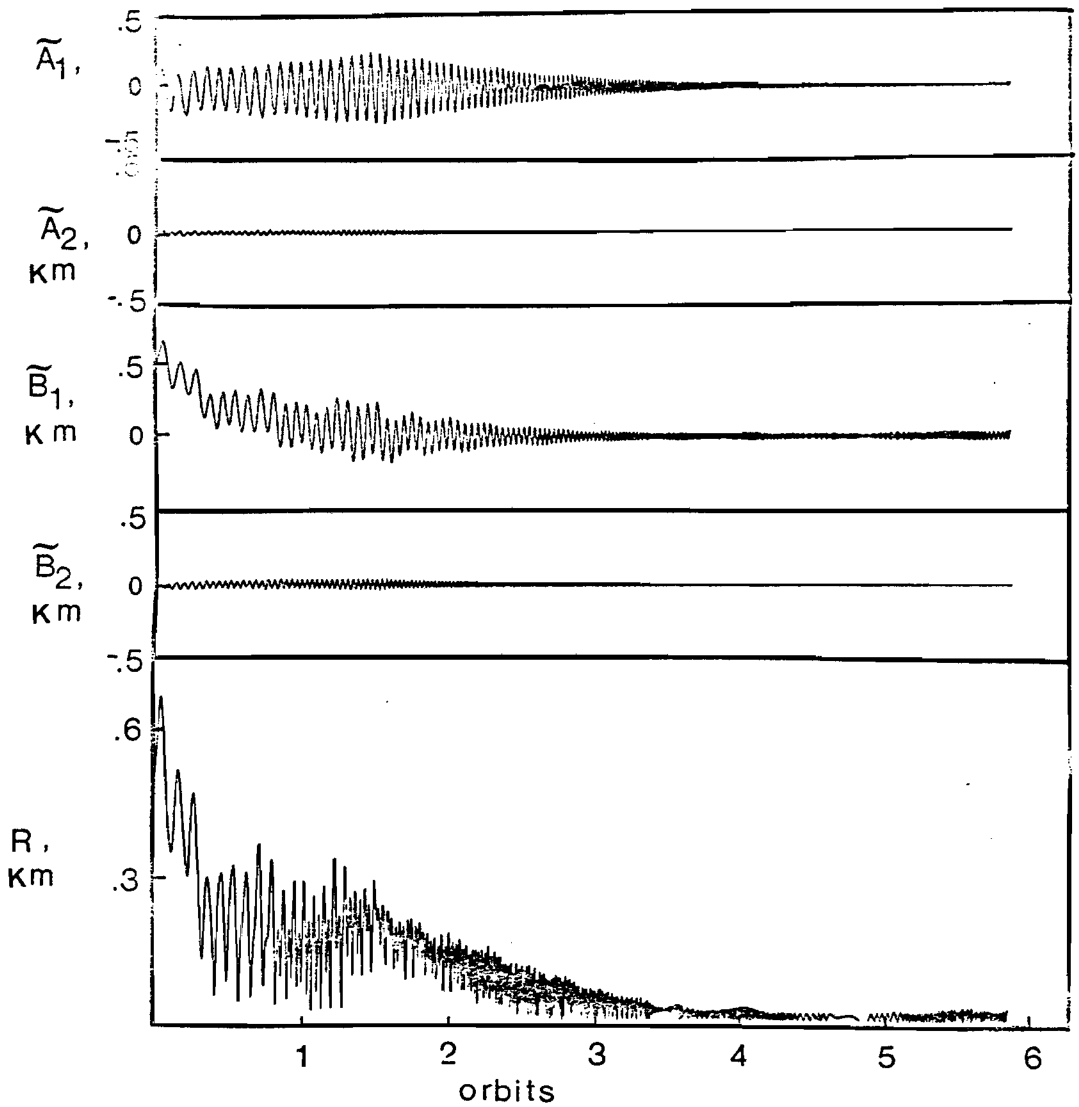

(c) Dimensional displacements $\tilde{A}_1$, $\tilde{A}_2$, $\tilde{B}_1$ and $\tilde{B}_2$ and the transverse displacement R of the middle point of the tether

Fig. 8.11 Dynamical response (both rotations and vibrations) during retrieval from 100 Km with the linear strain model and using length rate law (8.5.2)

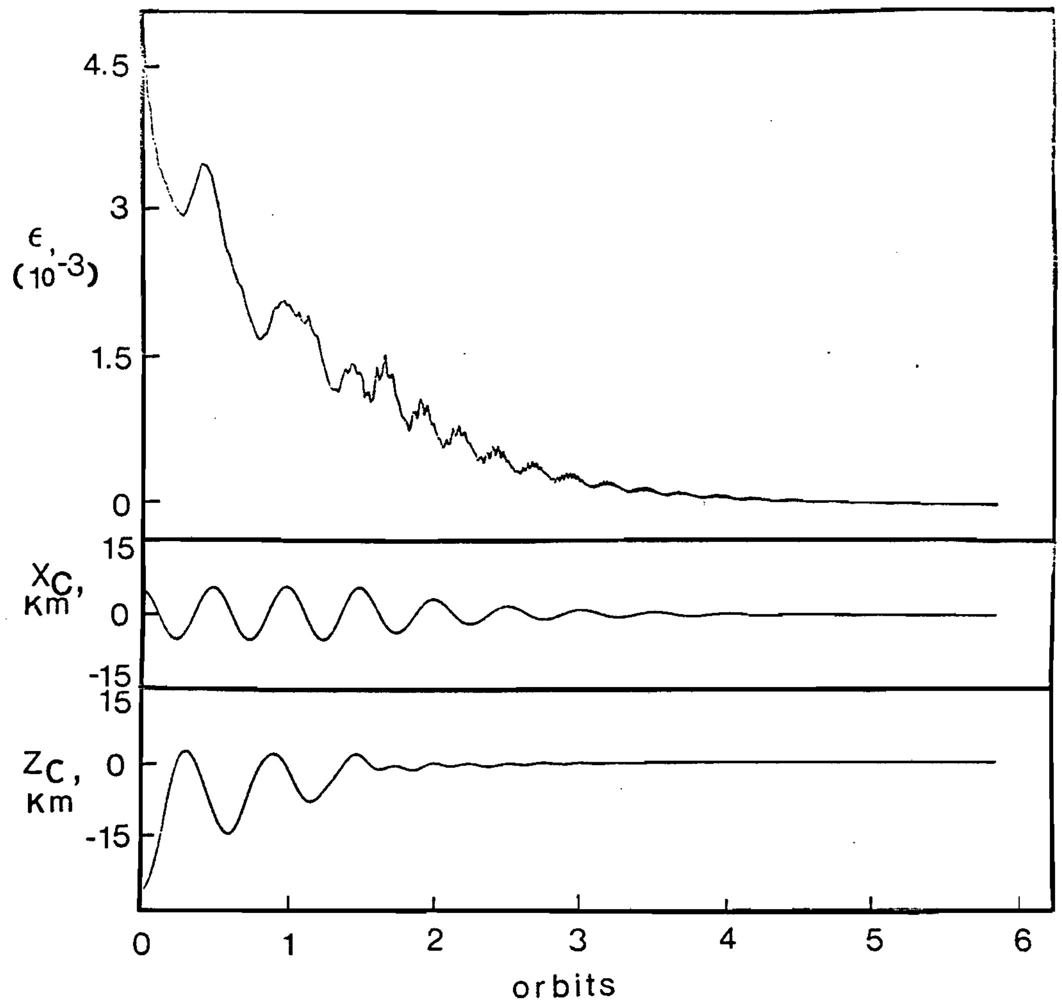

(d) Displacements of the middle point of the tether along x_c and z_c directions, respectively and the longitudinal strain

Fig. 8.11 Dynamical response (both rotations and vibrations) during retrieval from 100 Km with the linear strain model and using length rate law (8.5.2)

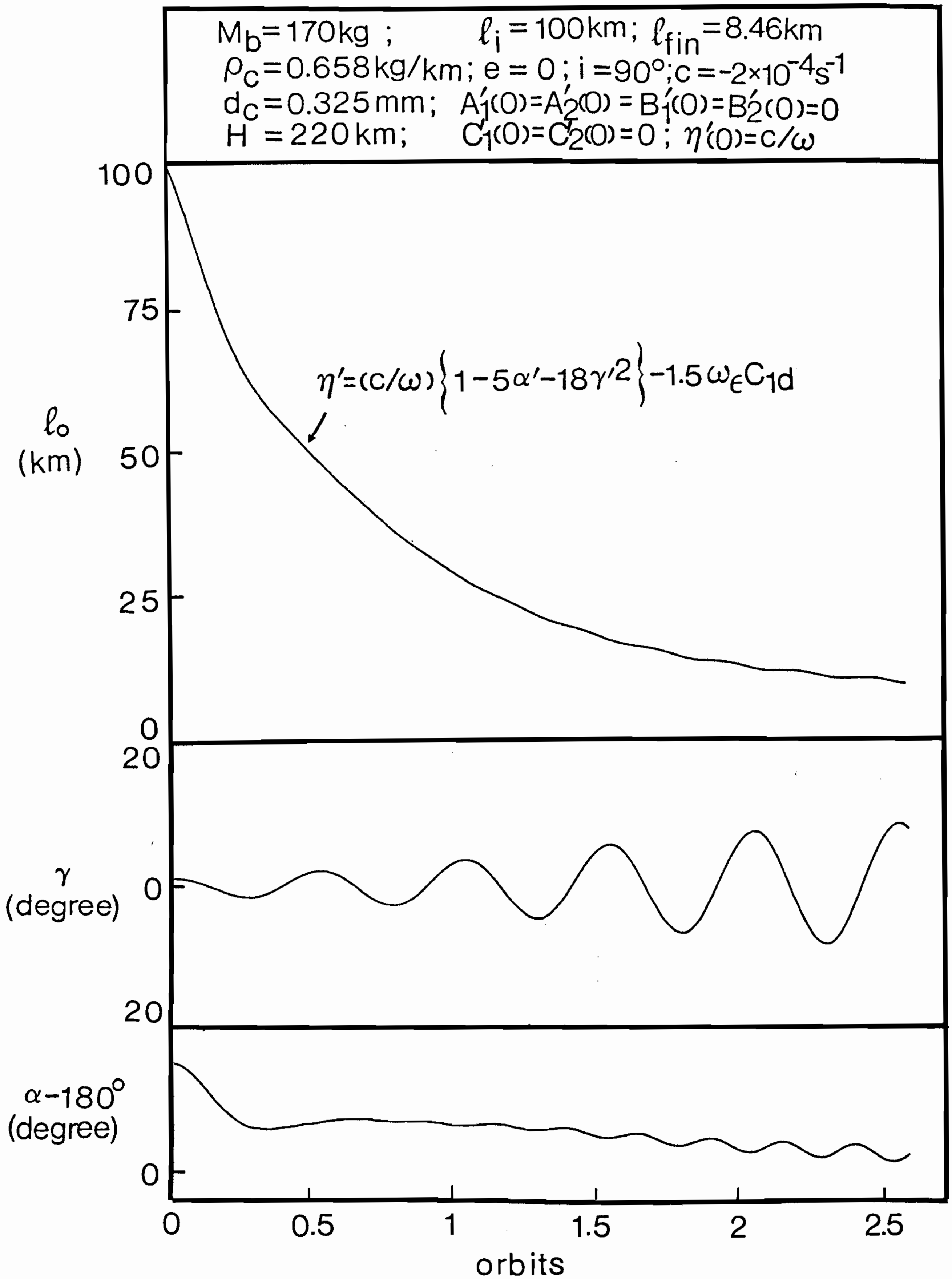

(a) Variation of length ℓ_0 and rotations α and γ

Fig. 8.12 Dynamical response (both rotations and vibrations) during retrieval from 100 Km with the nonlinear strain model and using length rate

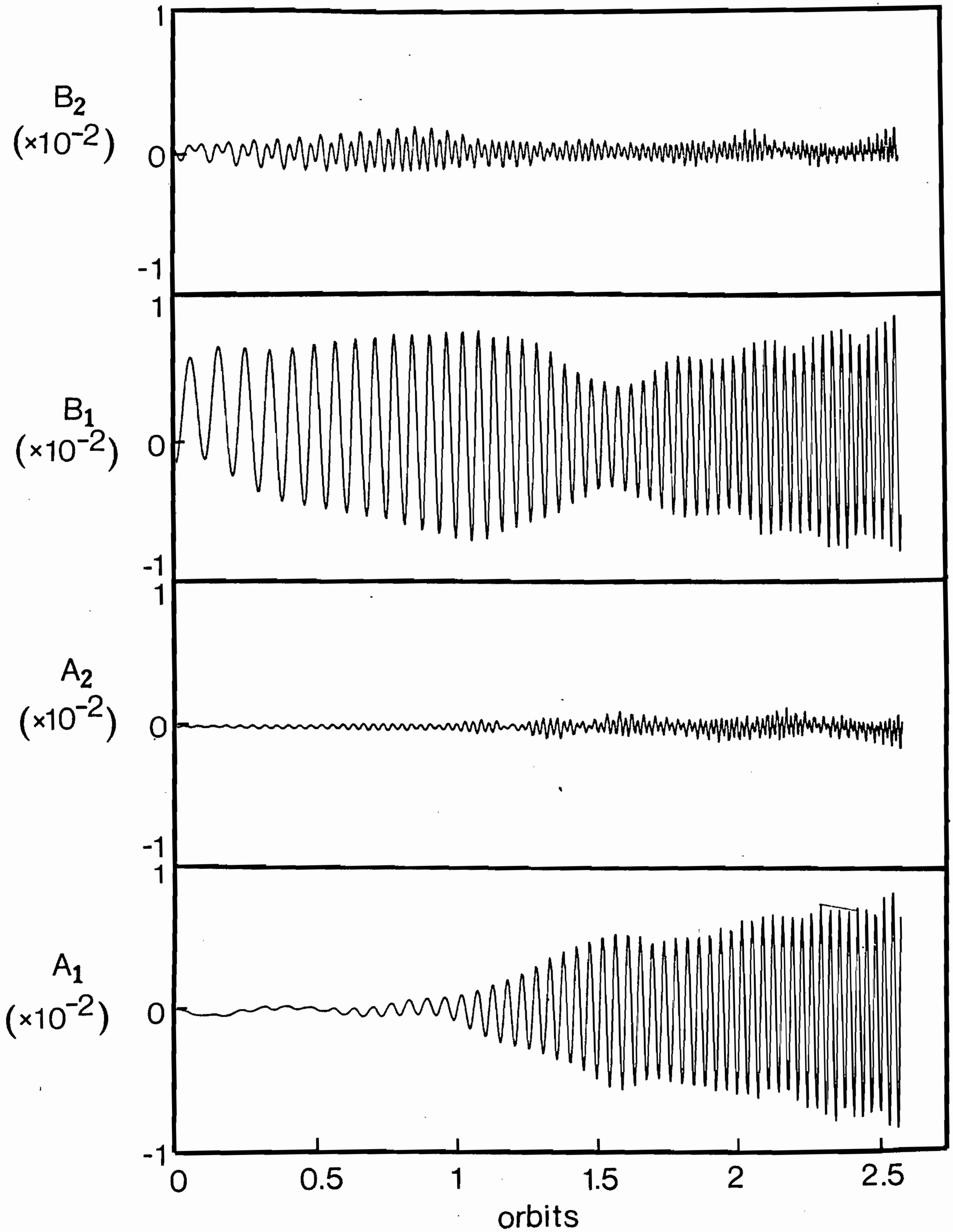

(b) Transverse modal coordinates A_1, A_2, B_1 and B_2

Fig. 8.12 Dynamical response (both rotations and vibrations) during retrieval

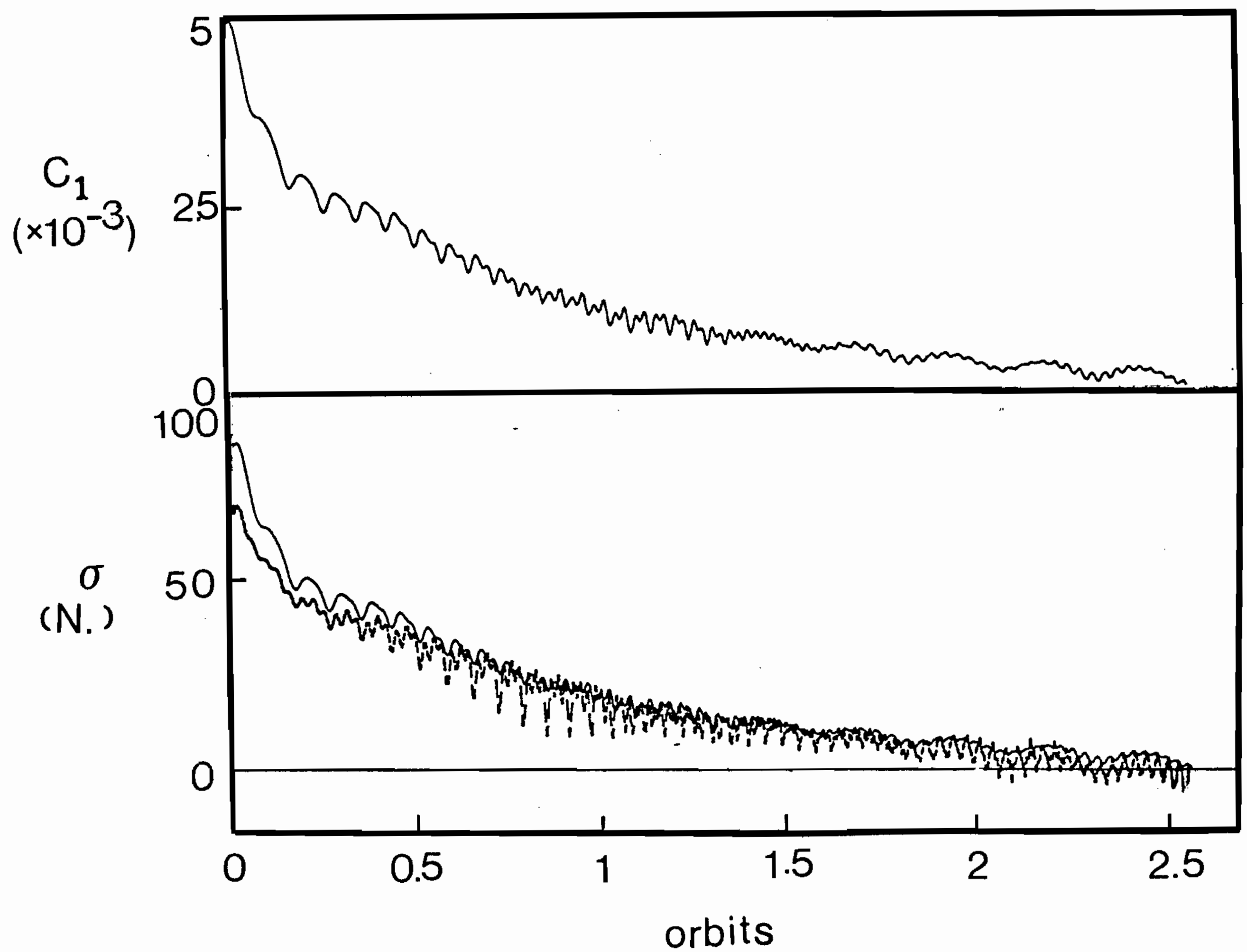

(c) Longitudinal vibrations C_1 and tension at both ends of the tether

Fig. 8.12 Dynamical response (both rotations and vibrations) during retrieval from 100 Km with the nonlinear strain model and using length rate control law (8.5.4)

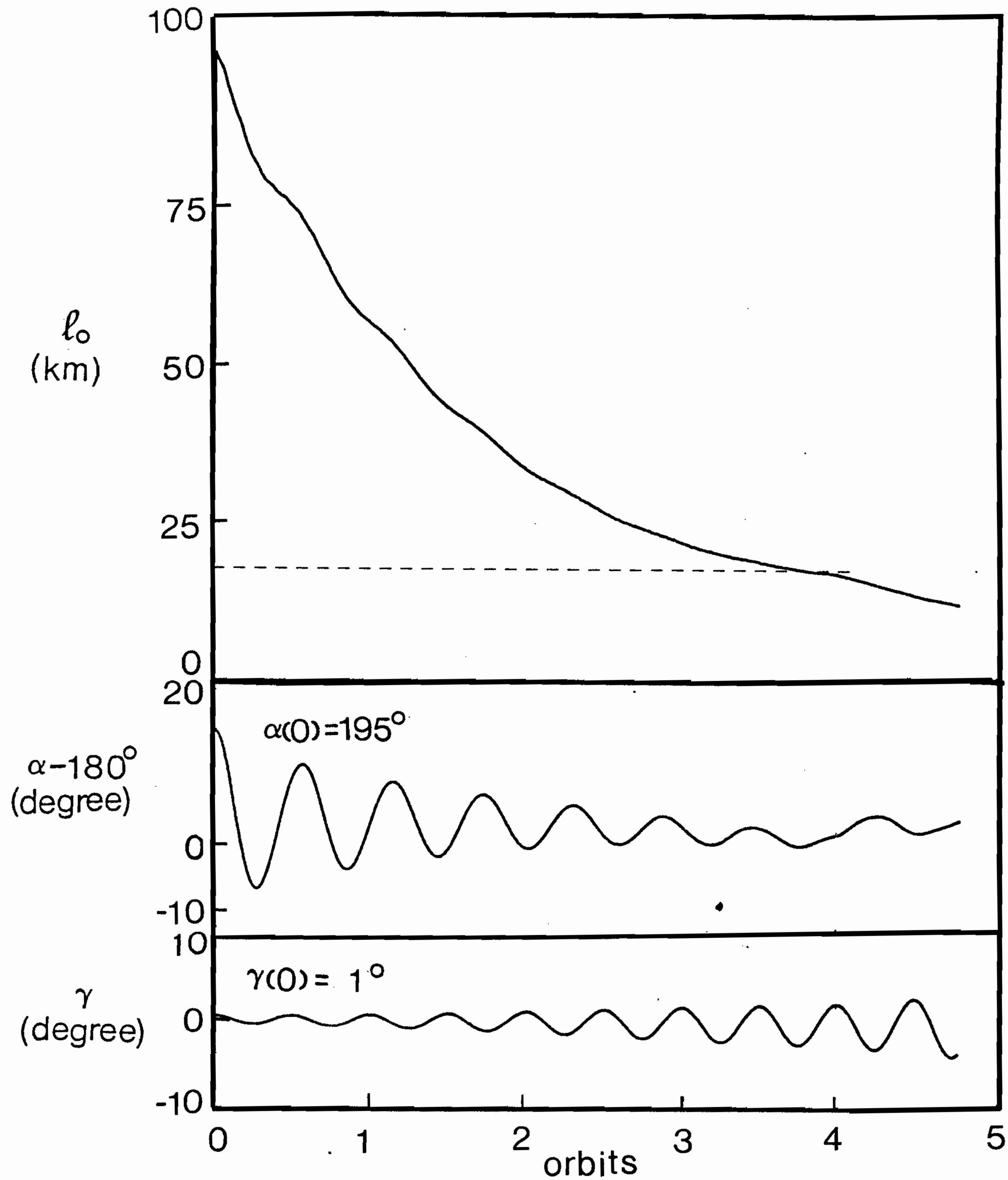

(a) Variation of length ℓ_0 and rotations α and γ

Fig. 8.13 General dynamics (both rotations and vibrations) during retrieval from 100 Km with the nonlinear strain model using length control law (8.5.5) and (8.5.6)

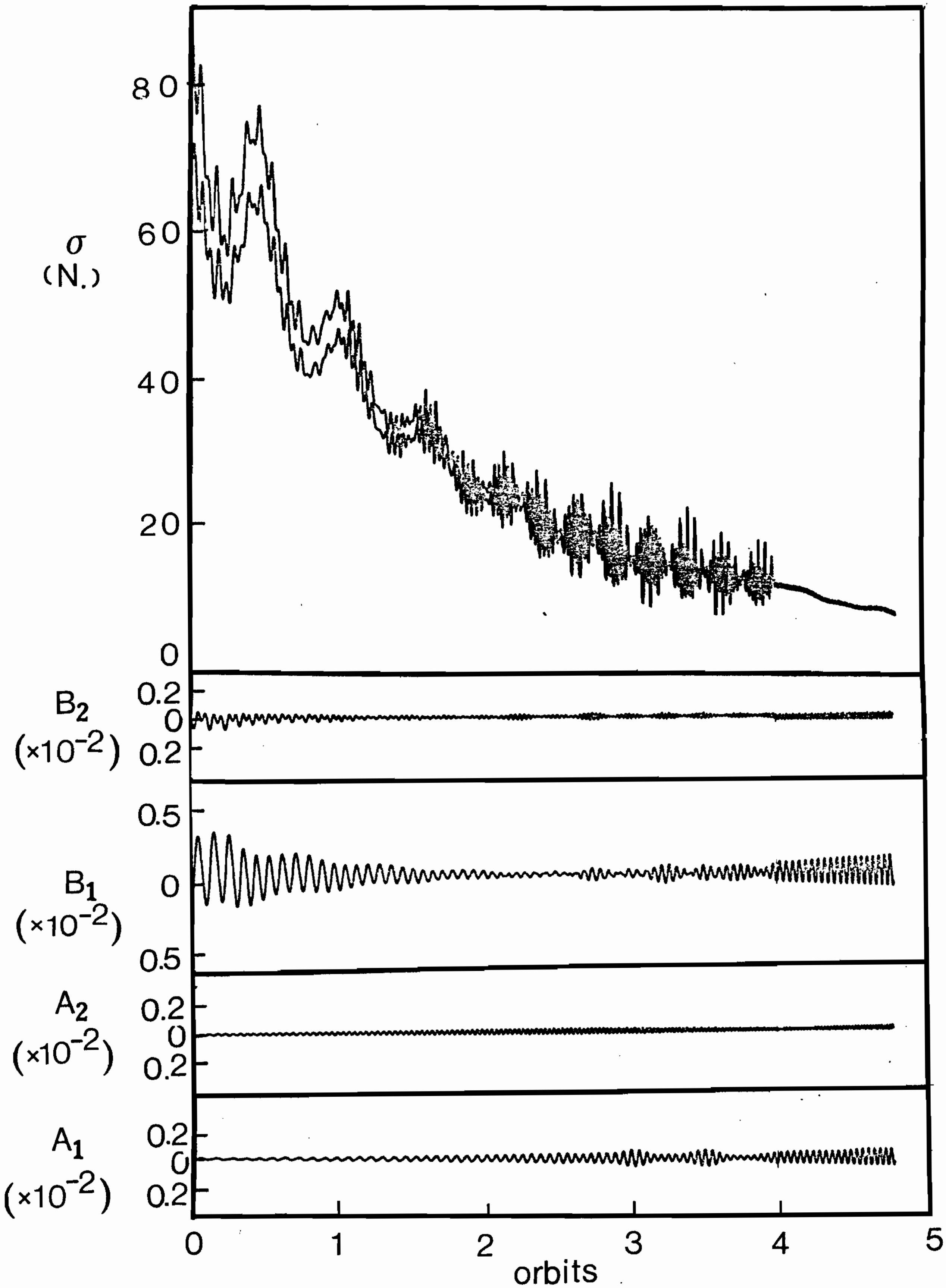

(b) Tension at both ends of the tether and transverse modal coordinates A_1, A_2, B_1, B_2

Fig. 8.13 General dynamics (both rotations and vibrations) during retrieval from 100 Km with the nonlinear strain model and using length rate control

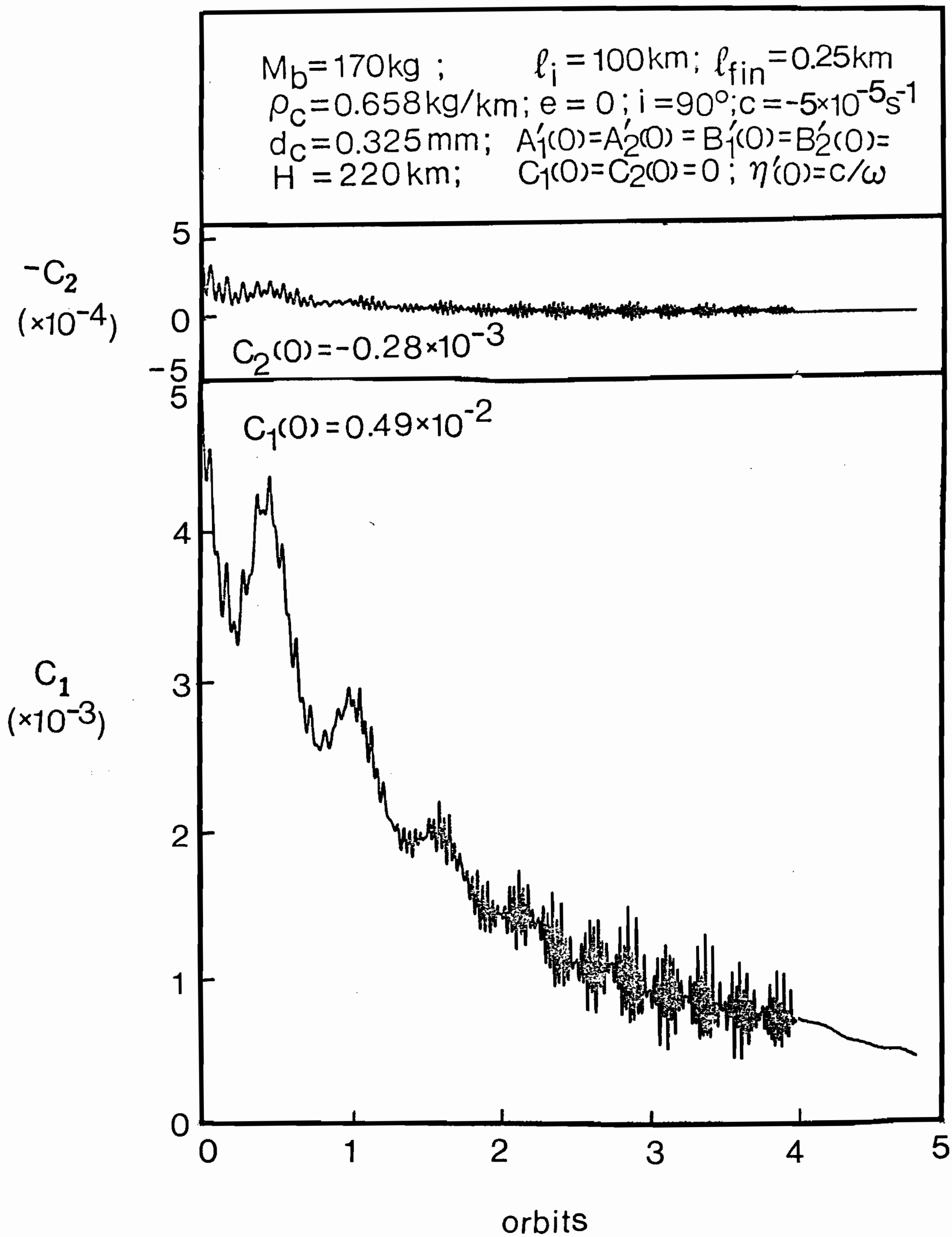

(c) Longitudinal generalized coordinates C_1 and C_2

Fig. 8.13 General dynamics (both rotations and vibrations) during retrieval from

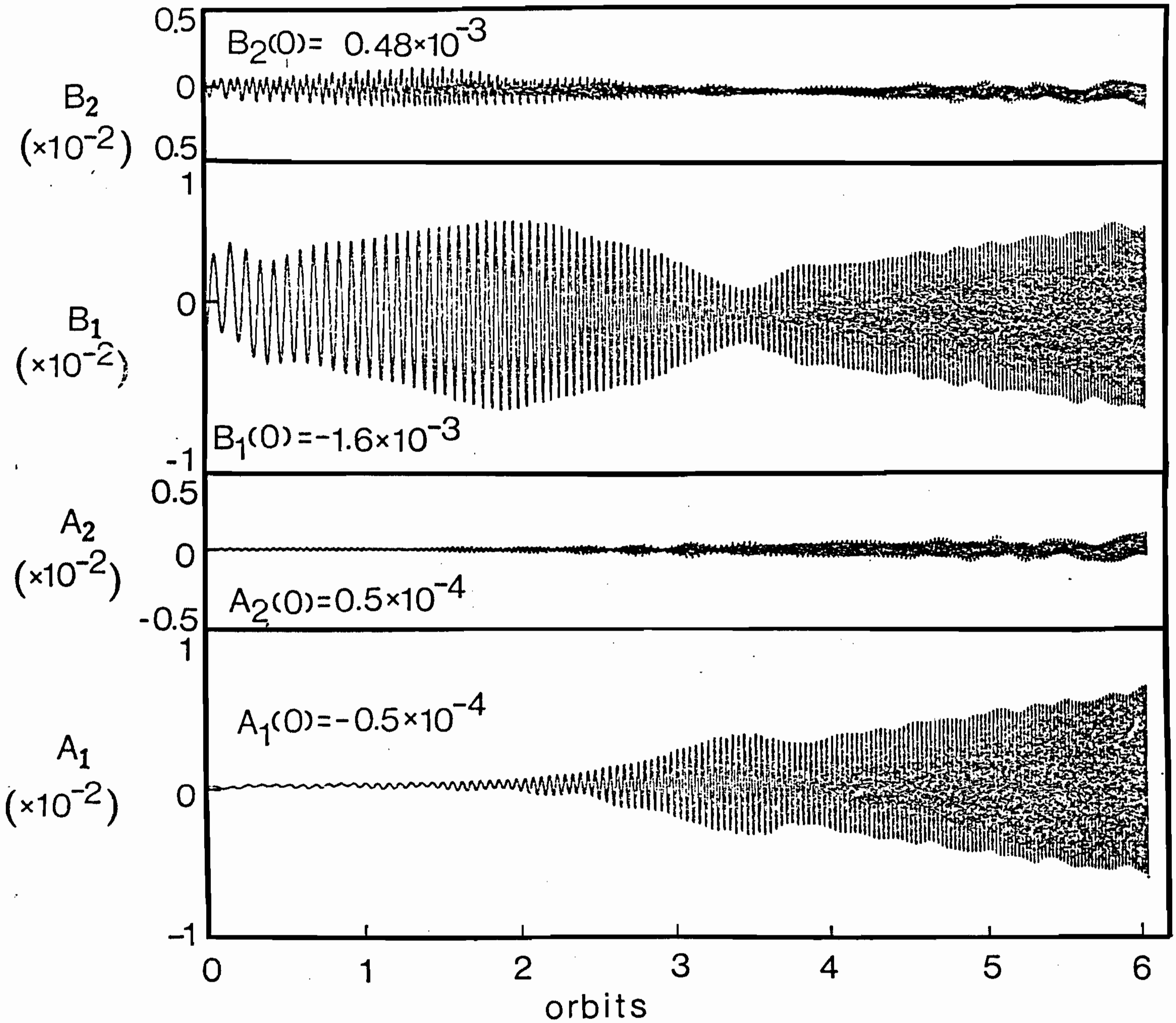

(a) Transverse modal coordinates A_1, A_2, B_1 and B_2

Fig. 8.14 Dynamical response (rotations and vibrations) during retrieval from 100 Km with the nonlinear strain model using a length control law not taking advantage of the internal resonance

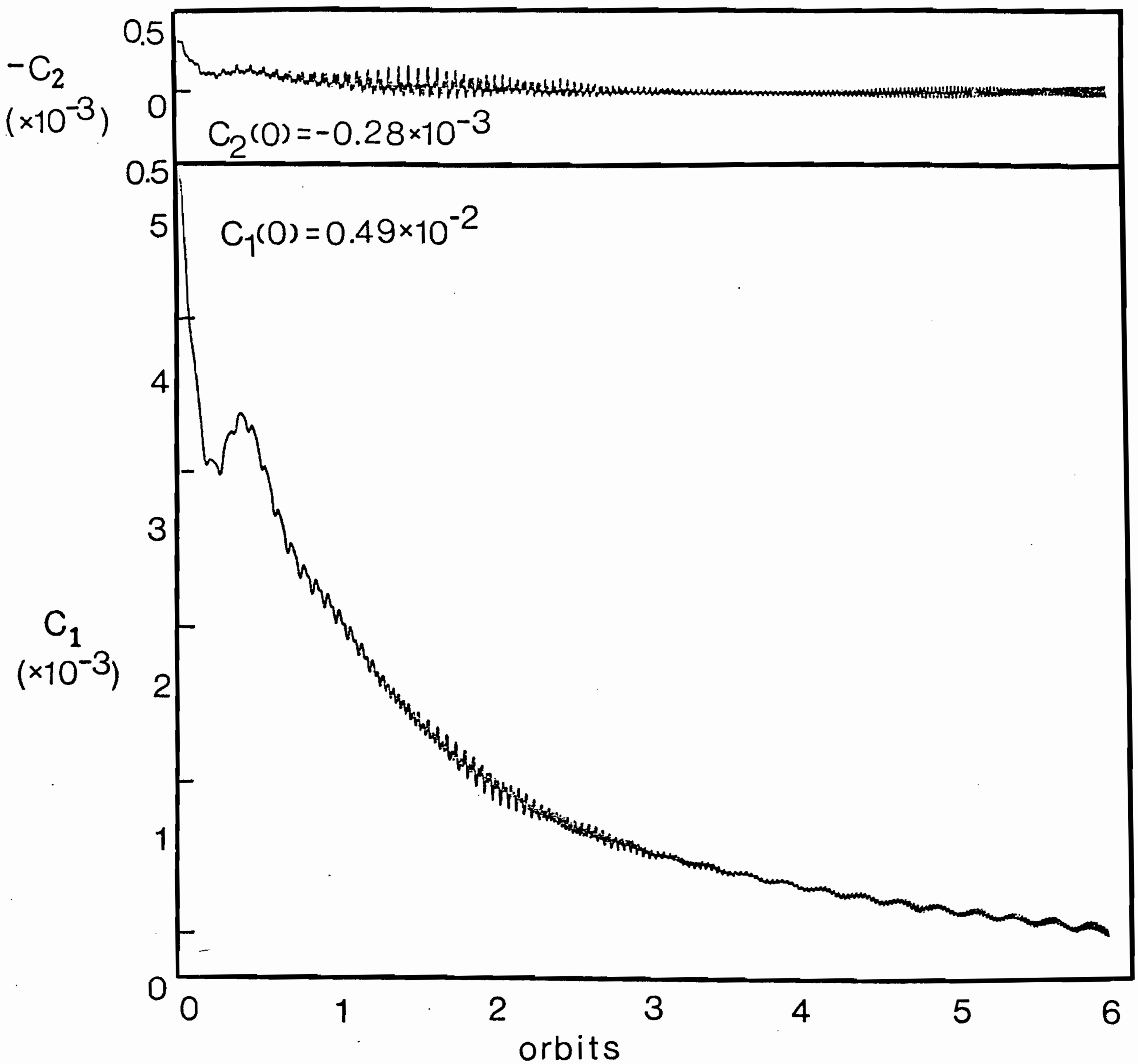

(b) Longitudinal generalized coordinates C_1 and C_2

Fig. 8.14 Dynamical response (rotations and vibrations) during retrieval from 100 Km with the nonlinear strain model using a length control law not taking advantage of the internal resonance

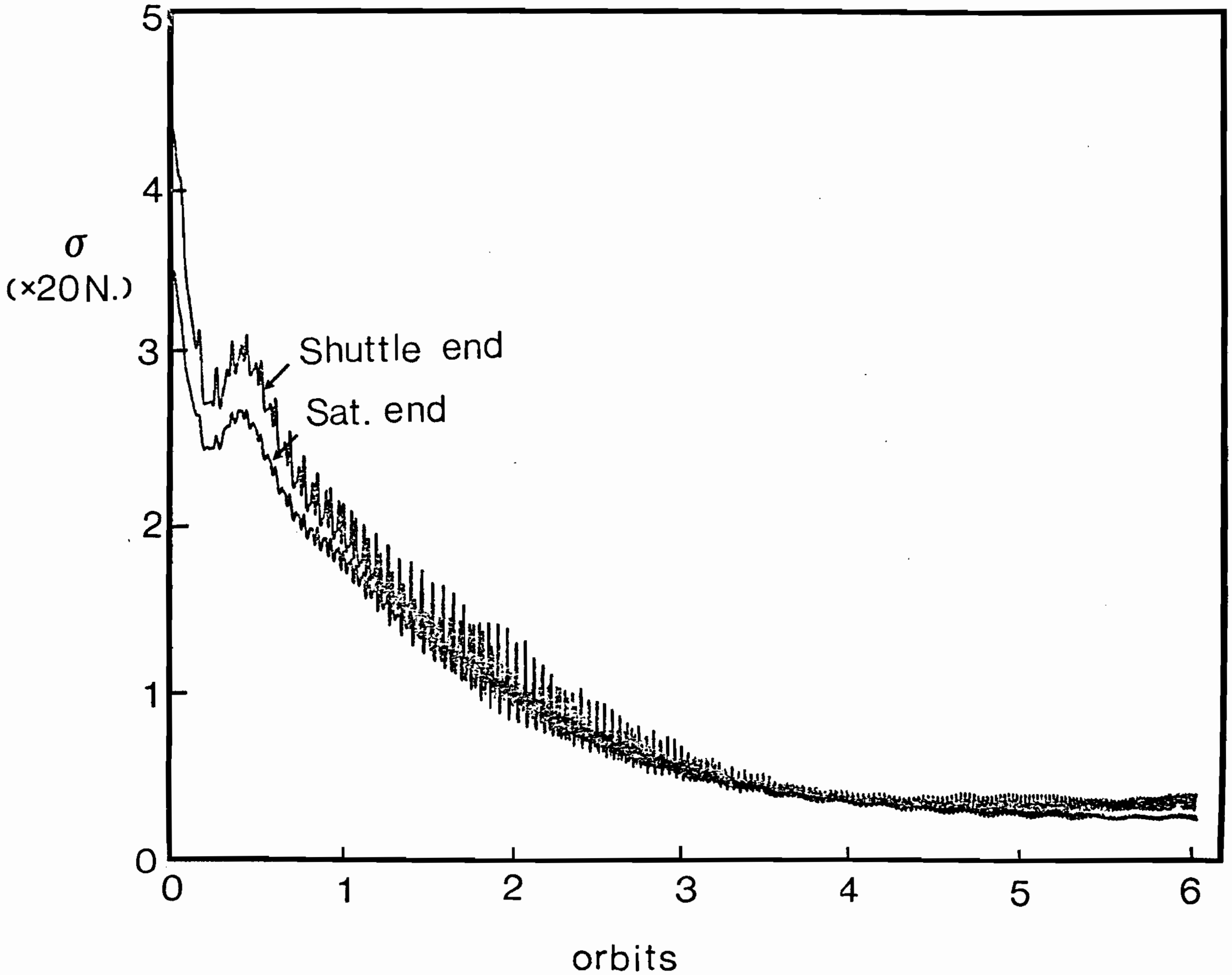

(c) Tension at both ends of the tether

Fig. 8.14 Dynamical response (rotations and vibrations) during retrieval from 100 Km with the nonlinear strain model using a length control law not taking advantage of the internal resonance

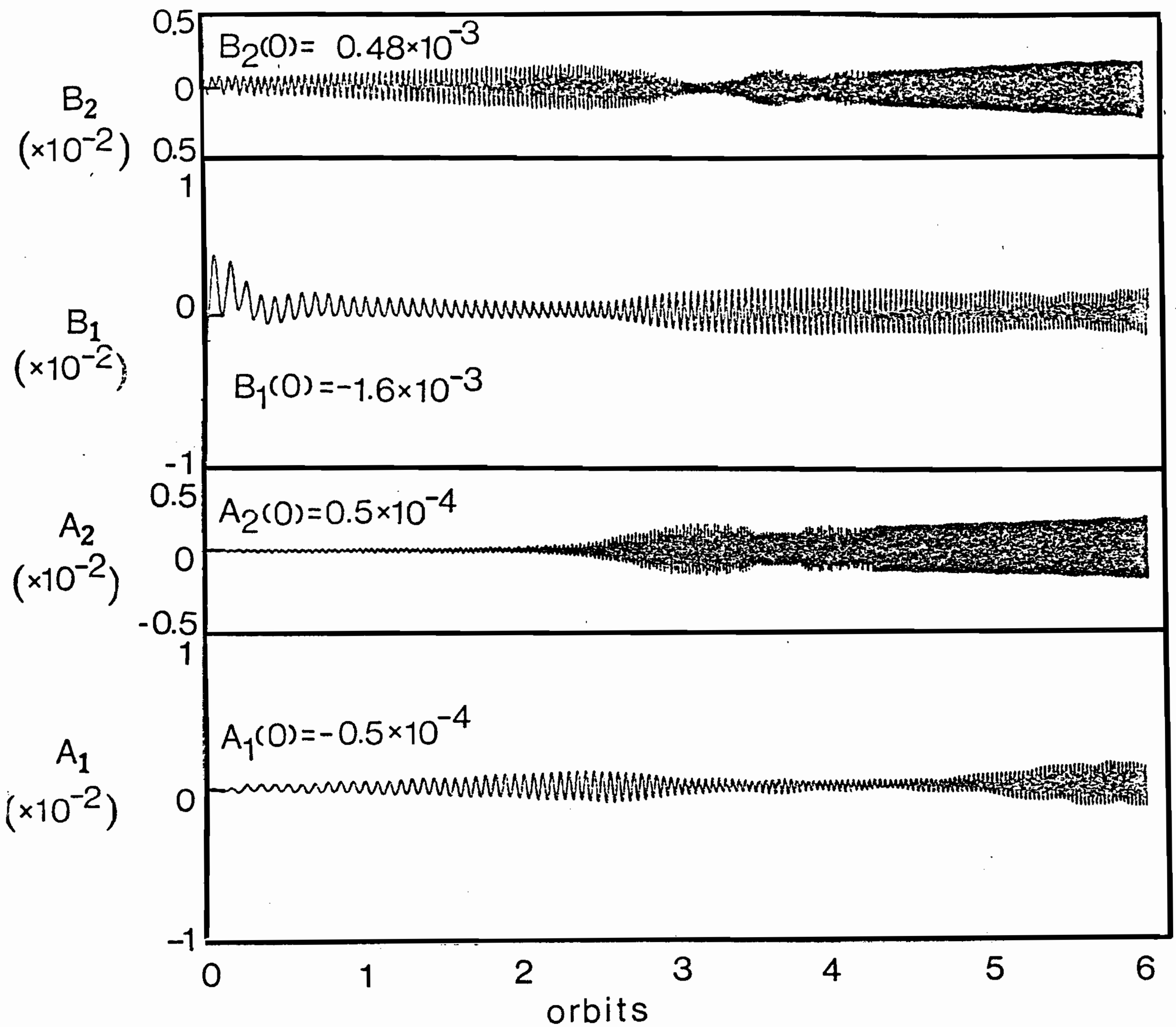

(a) Transverse modal coordinates A_1, A_2, B_1 and B_2

Fig. 8.15 Dynamical response (both rotations and vibrations) during retrieval from 100 Km with the nonlinear strain model using a length control law taking advantage of the internal resonance

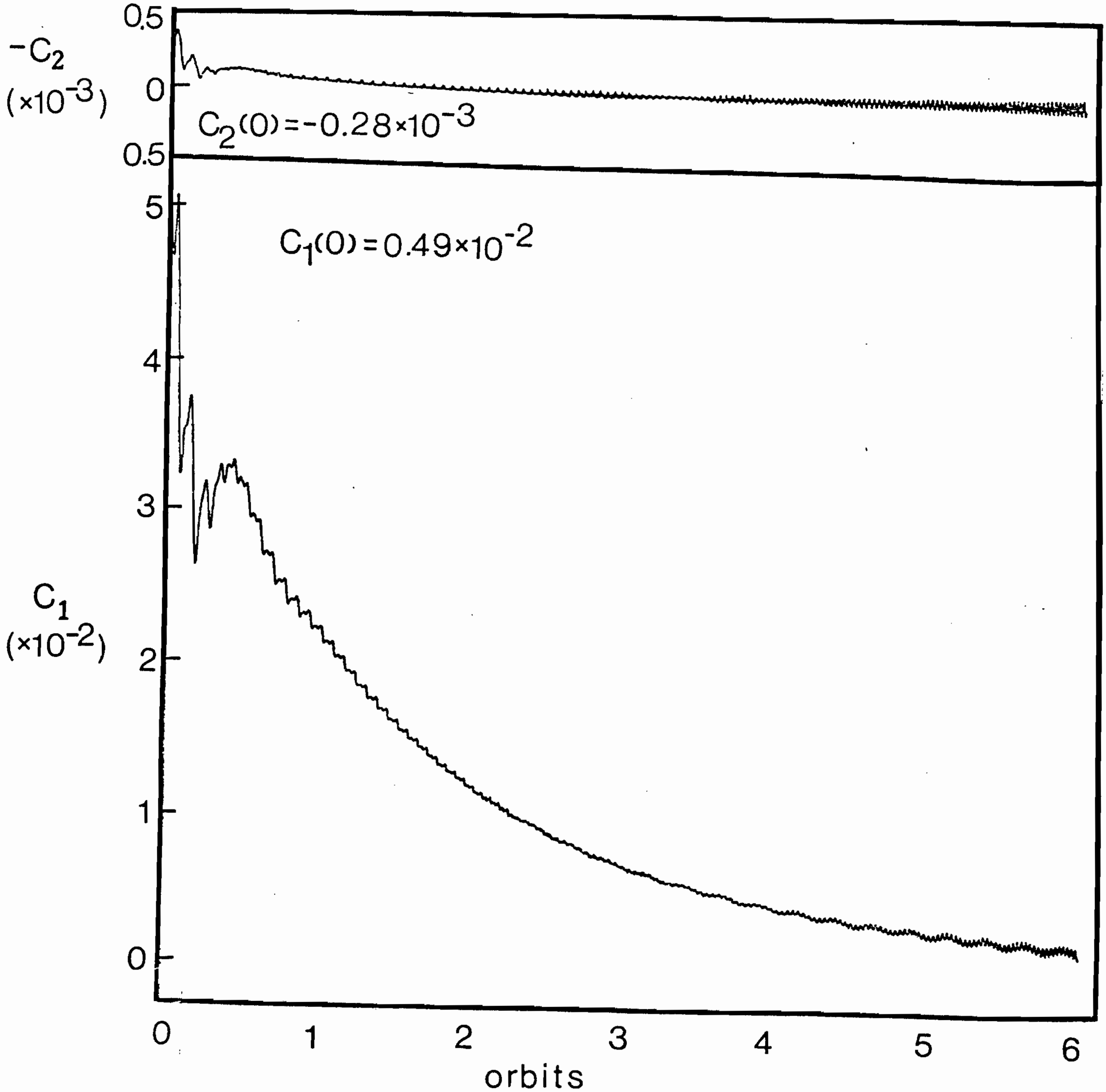

(b) Longitudinal generalized coordinates C_1 and C_2

Fig. 8.15 Dynamical response (both rotations and vibrations) during retrieval from 100 Km with the nonlinear strain model using a length control law taking advantage of the internal resonance

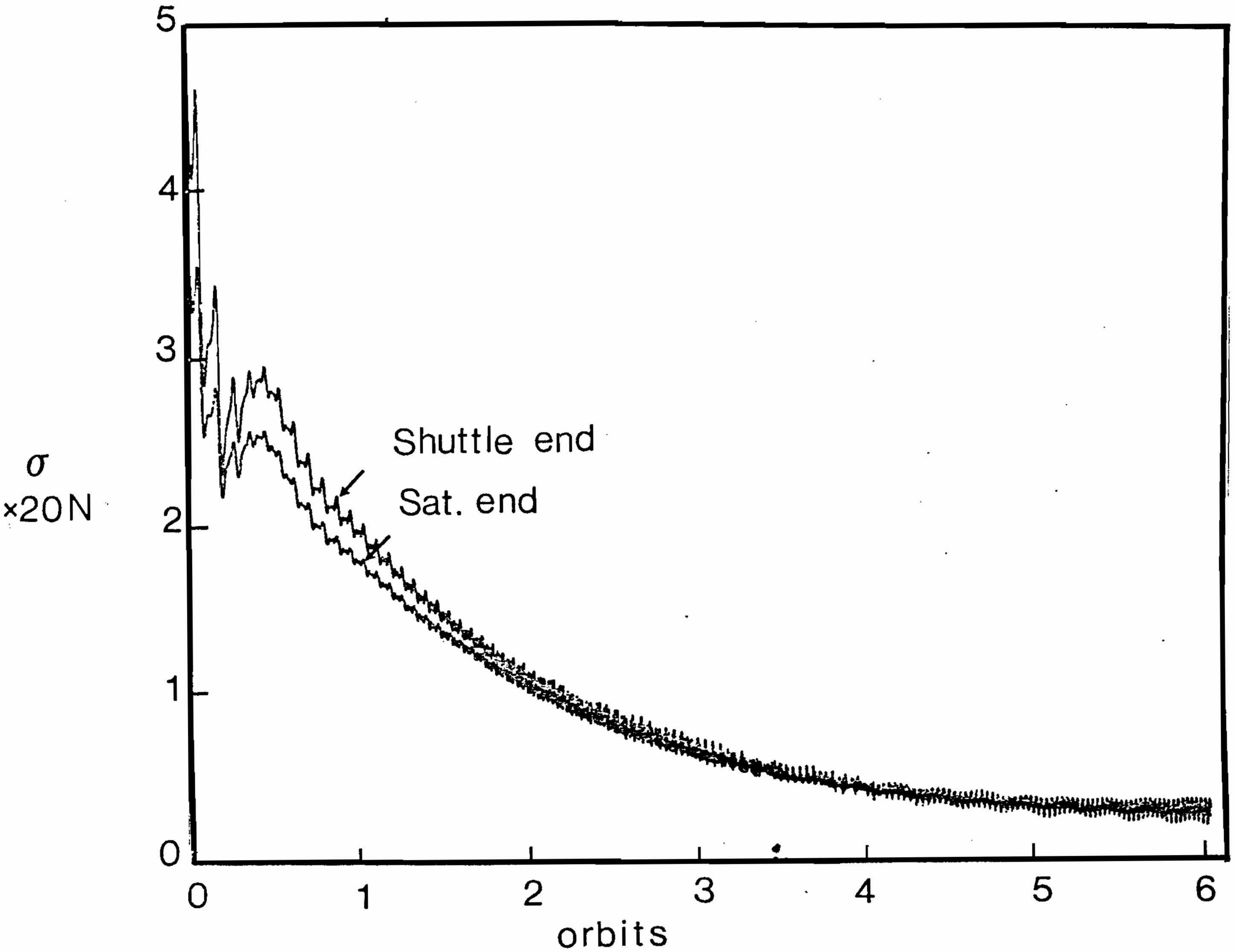

(c) Tension at both ends of the tether

Fig. 8.15 Dynamical response (both rotations and vibrations) during retrieval from 100 Km with the nonlinear strain model using a length control law taking advantage of the internal resonance

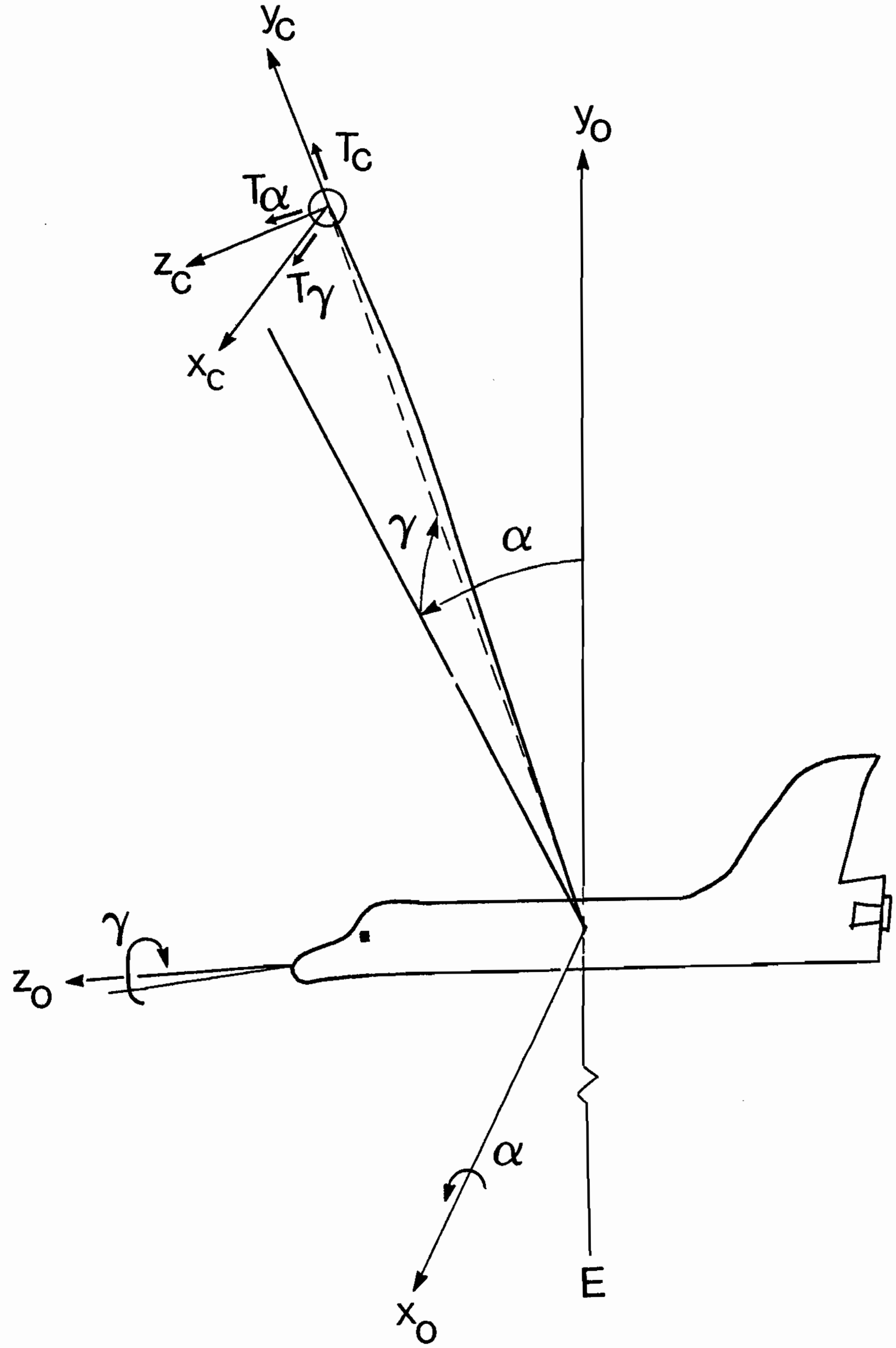

Fig, 9.1 Arrangement of the thrusters

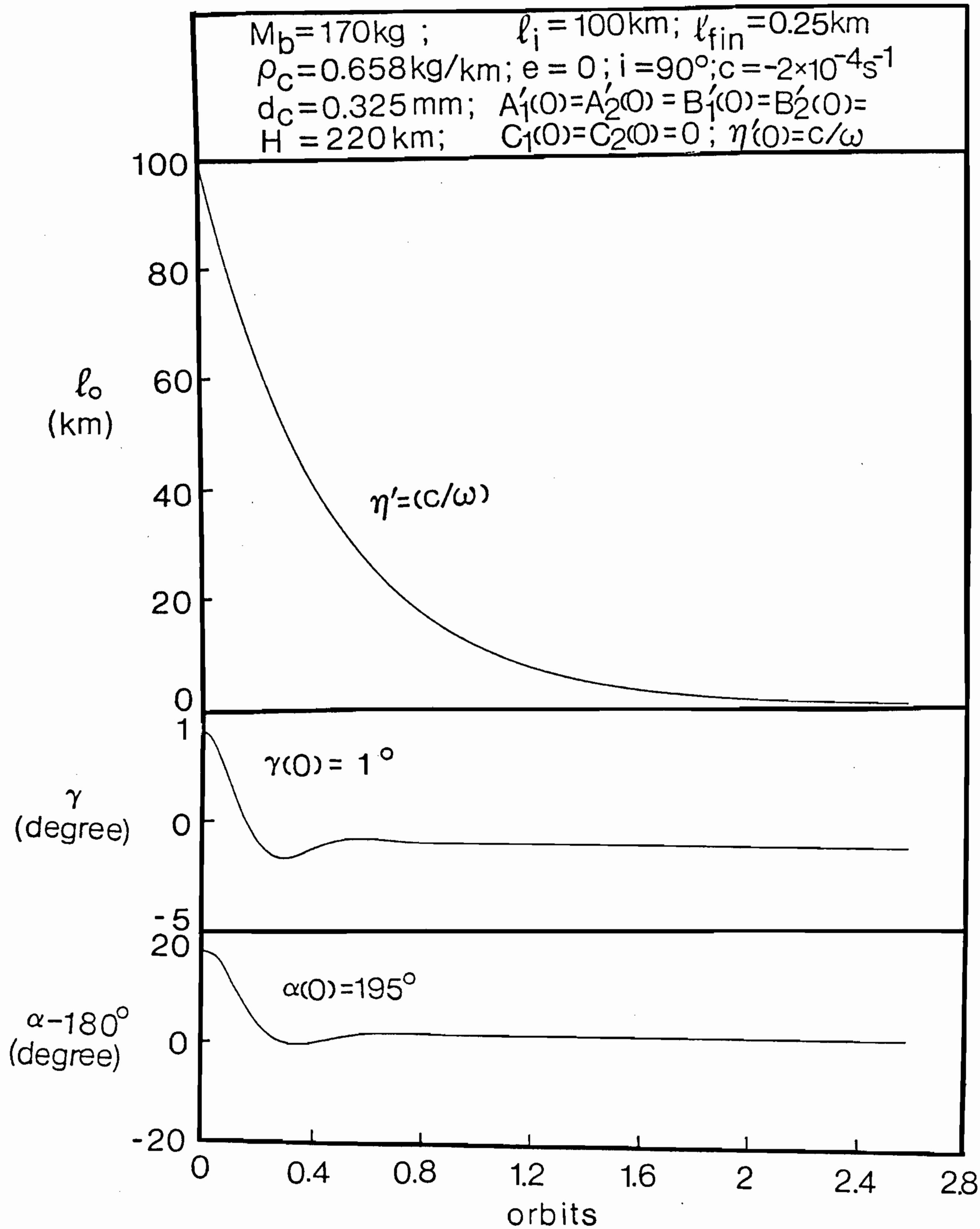

(a) Variation of length ℓ_0 and rotations α and γ

Fig. 9.2 Dynamical response during retrieval from 100 Km using thrusters

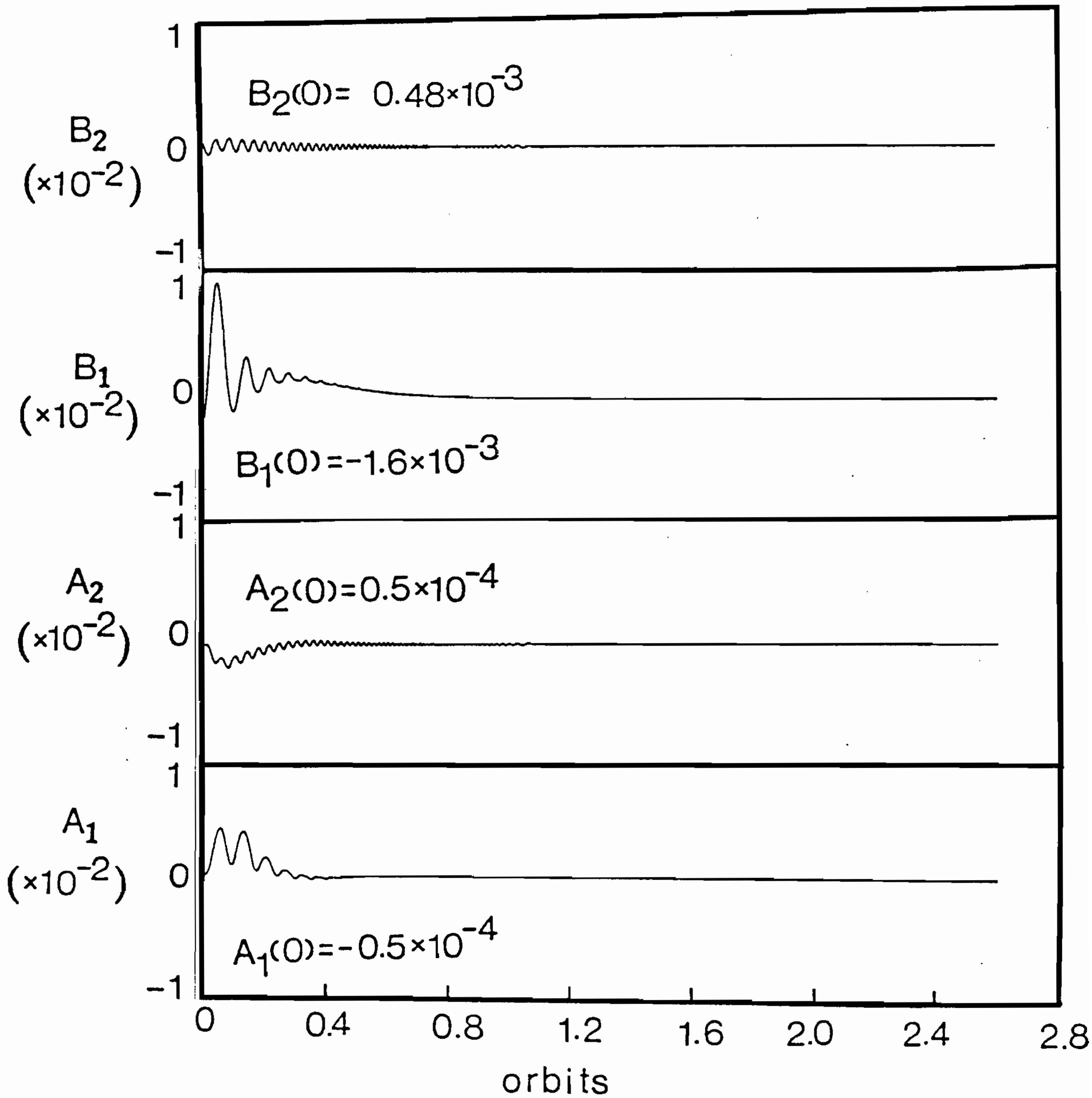

(b) Transverse modal coordinates A_1, A_2, B_1 and B_2

Fig. 9.2 Dynamical response during retrieval from 100 Km using thrusters and maintaining tensions at the initial level.

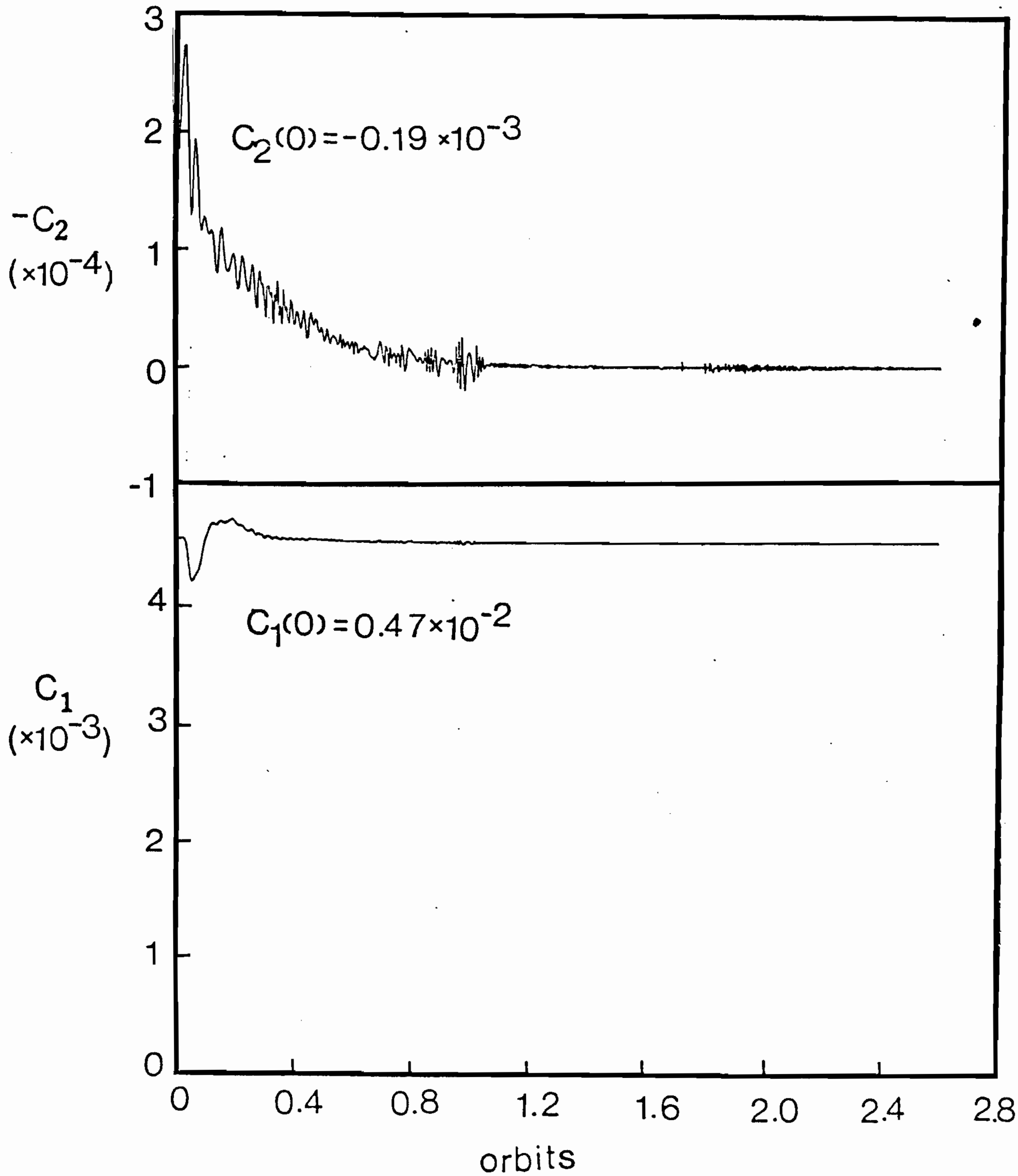

(c) Longitudinal generalized coordinates C_1 and C_2

Fig. 9.2 Dynamical response during retrieval from 100 Km using thrusters and maintaining tensions at the initial level

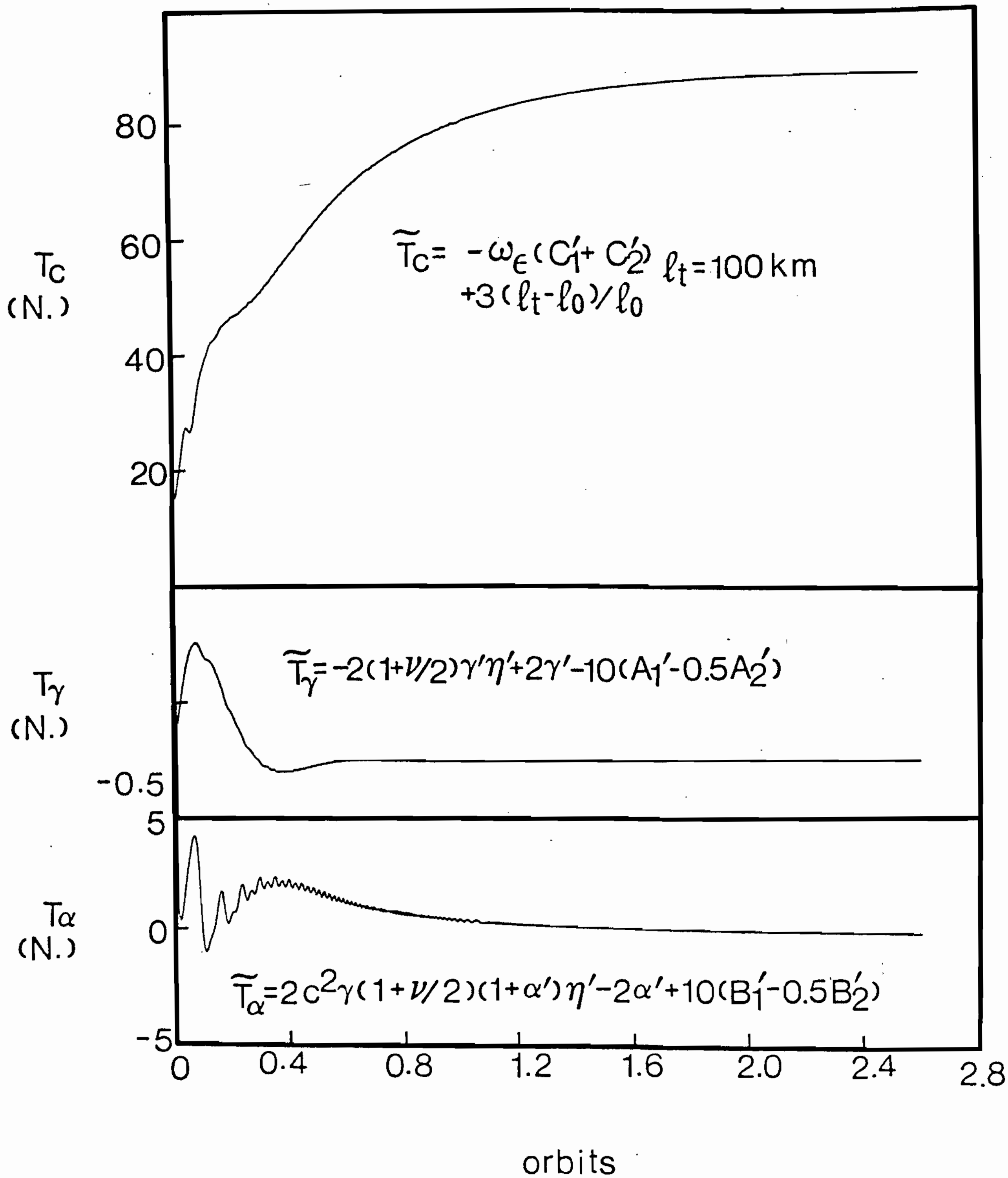

(d) Thruster forces T_α, T_γ and T_c

Fig. 9.2 Dynamial response during retrieval from 100 Km using thrusters and maintaining tensions at the initial level

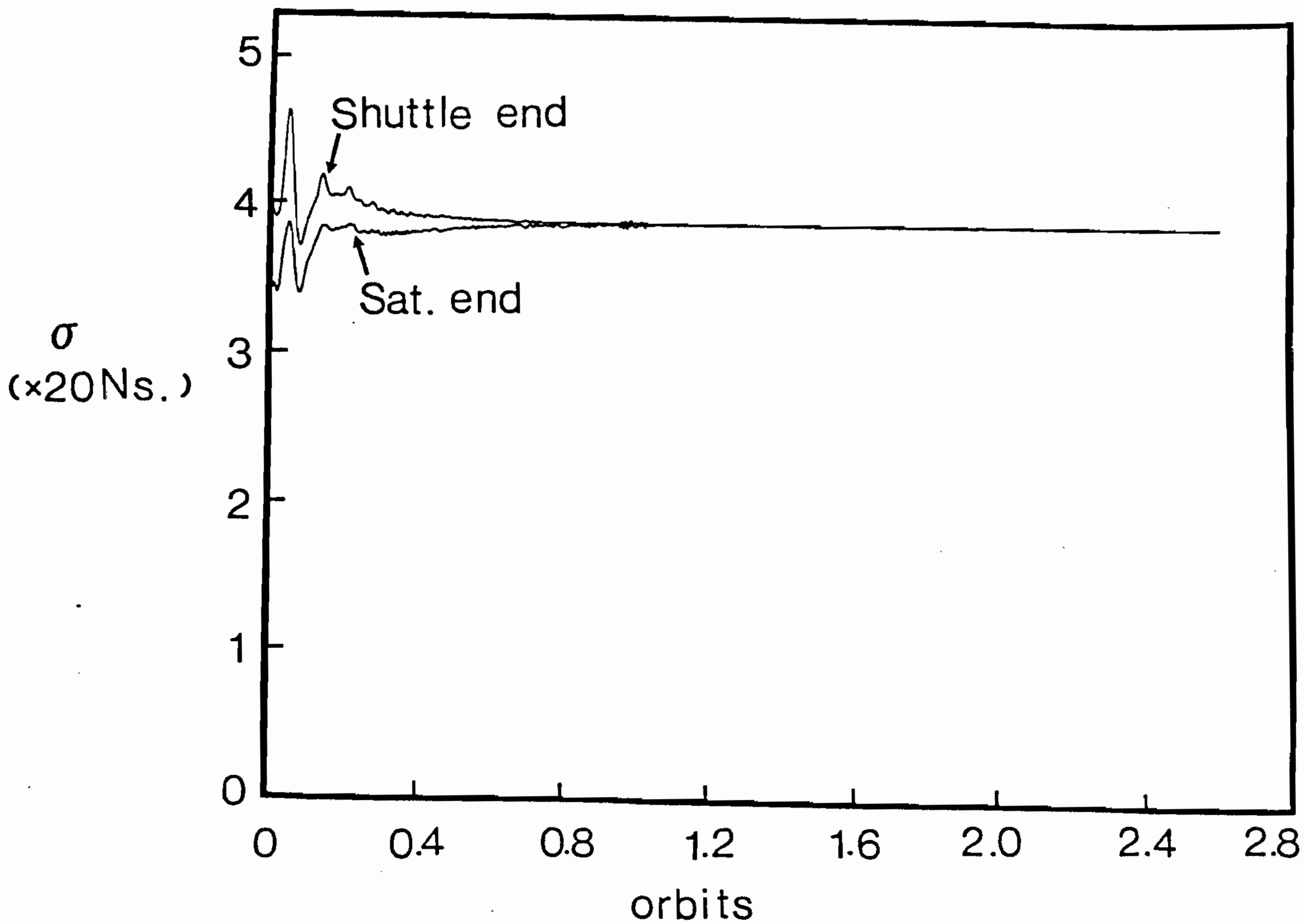

(e) Tension at both ends of the tether approaching the initial level

Fig. 9.2 Dynamical response during retrieval from 100 Km using thrusters and maintaining tensions at the initial level

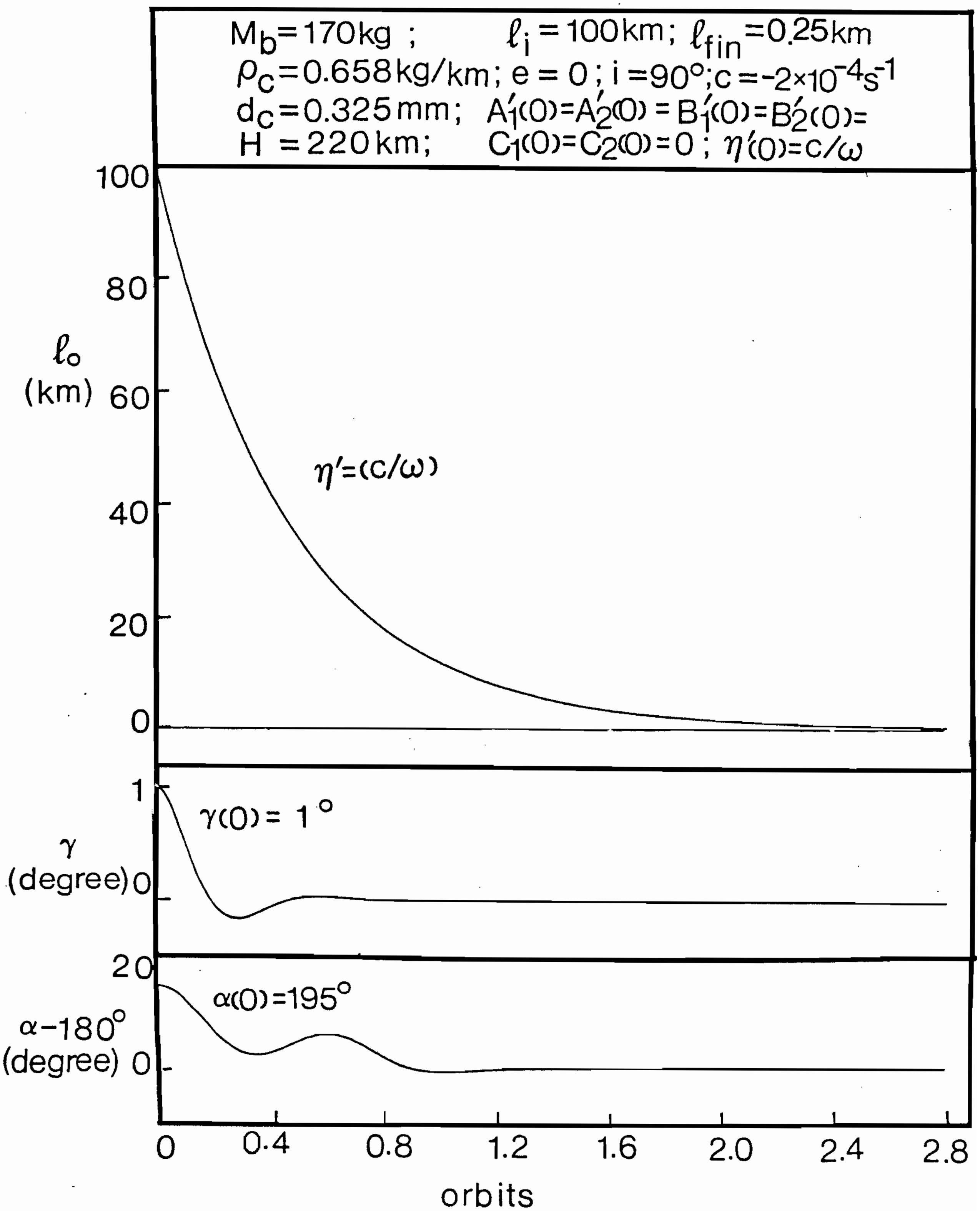

(a) Variation of length ℓ_0 and rotations α and γ

Fig. 9.3 Dynamical response during retrieval from 100 Km using thrusters and maintaining tension at a low level

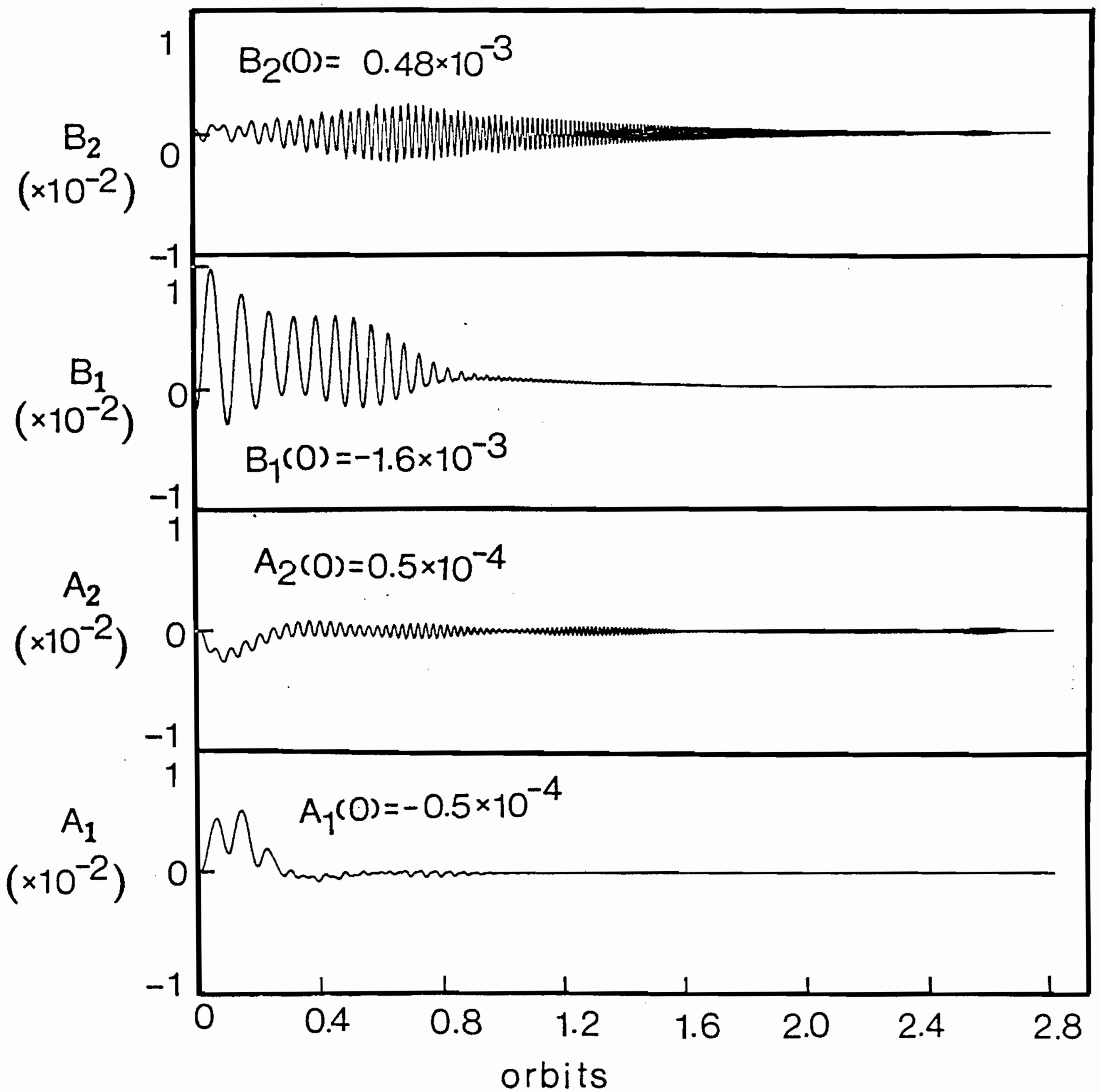

(b) Transverse modal coordinates A_1, A_2, B_1 and B_2

Fig. 9.3 Dynamical response during retrieval from 100 Km using thrusters and maintaining tension at a low level

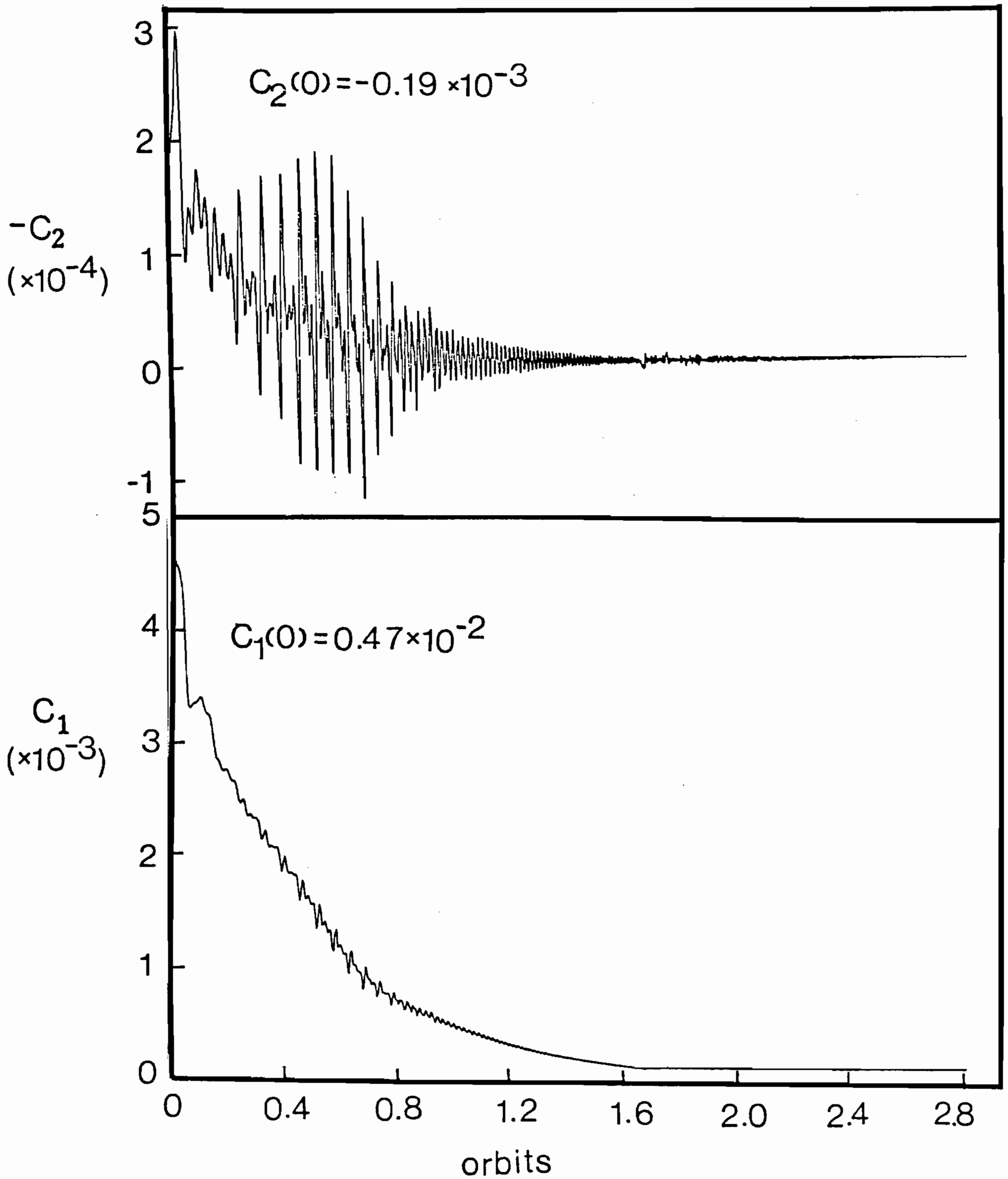

(c) Longitudinal generalized coordinates C_1 and C_2

Fig. 9.3 Dynamical response during retrieval from 100 Km using thrusters and maintaining tension at a low level

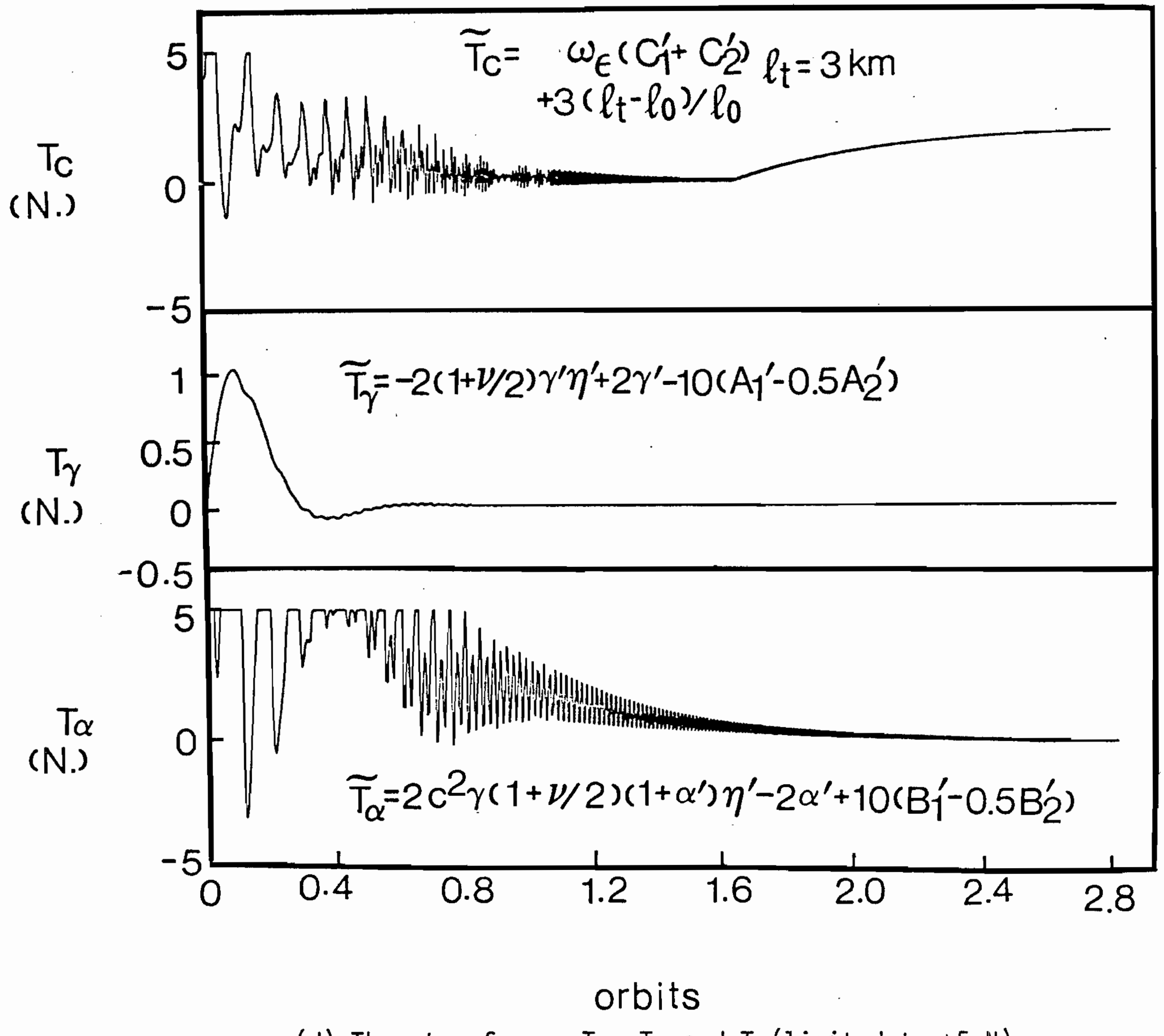

(d) Thruster forces T_α, T_γ and T_c(limited to ±5 N)

Fig. 9.3 Dynamical response during retrieval from 100 Km using thrusters and maintaining tension at a low level

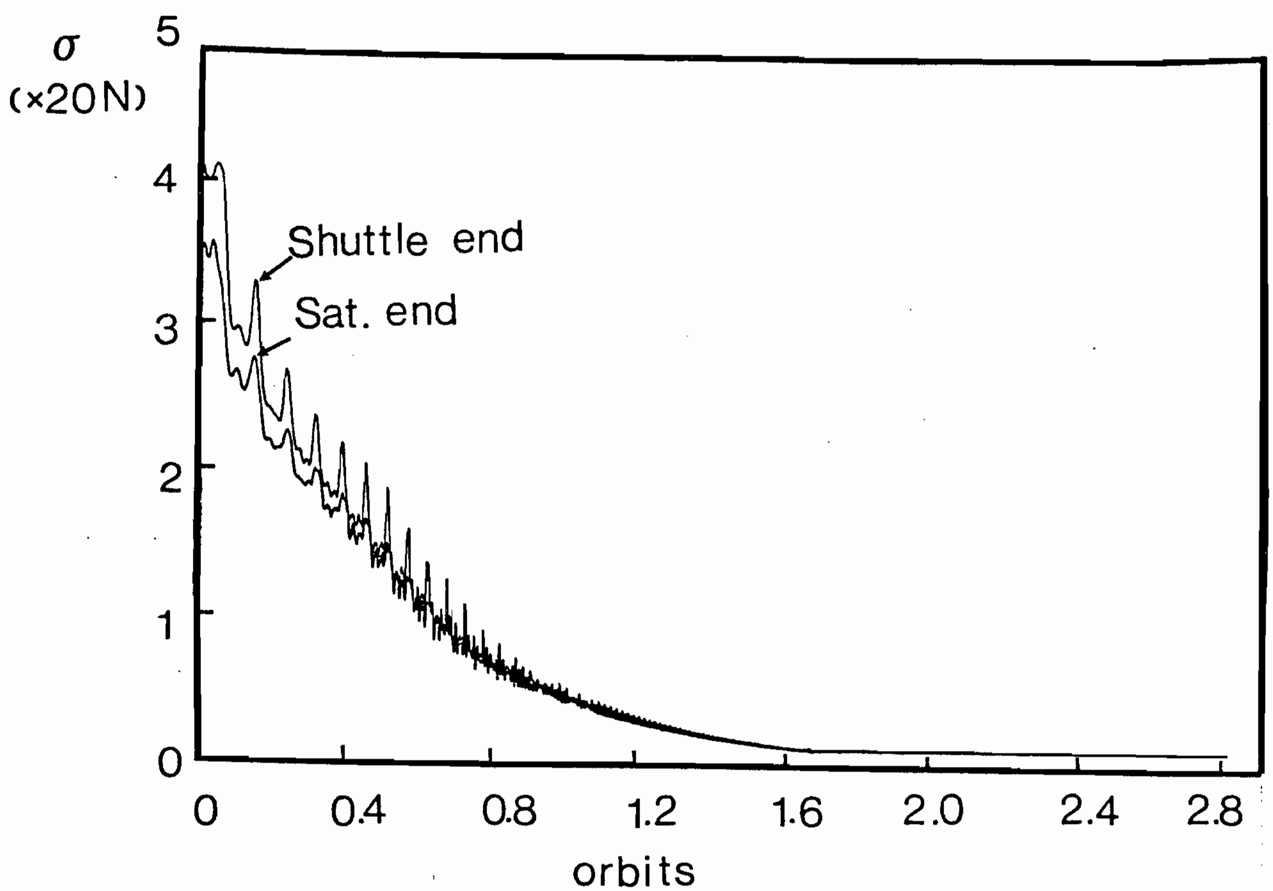

(e) Tension at both ends of the tether (approaching a low level)

Fig. 9.3 Dynamical response during retrieval from 100 Km using thrusters and maintaining tension at a low level

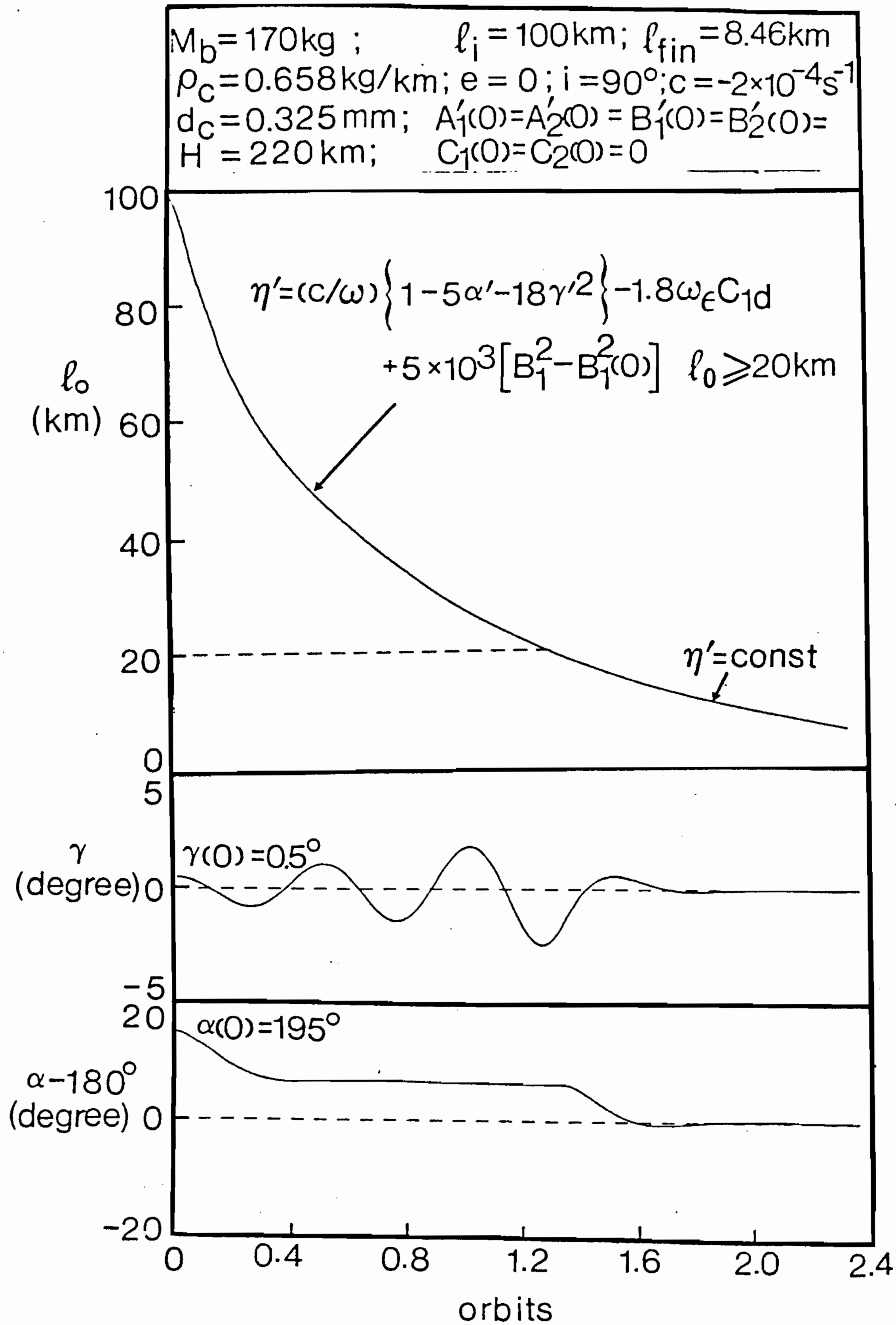

(a) Variation of length ℓ_0 and stable rotations α and γ

Fig. 9.4 Dynamical response during retrieval from 100 Km using a length

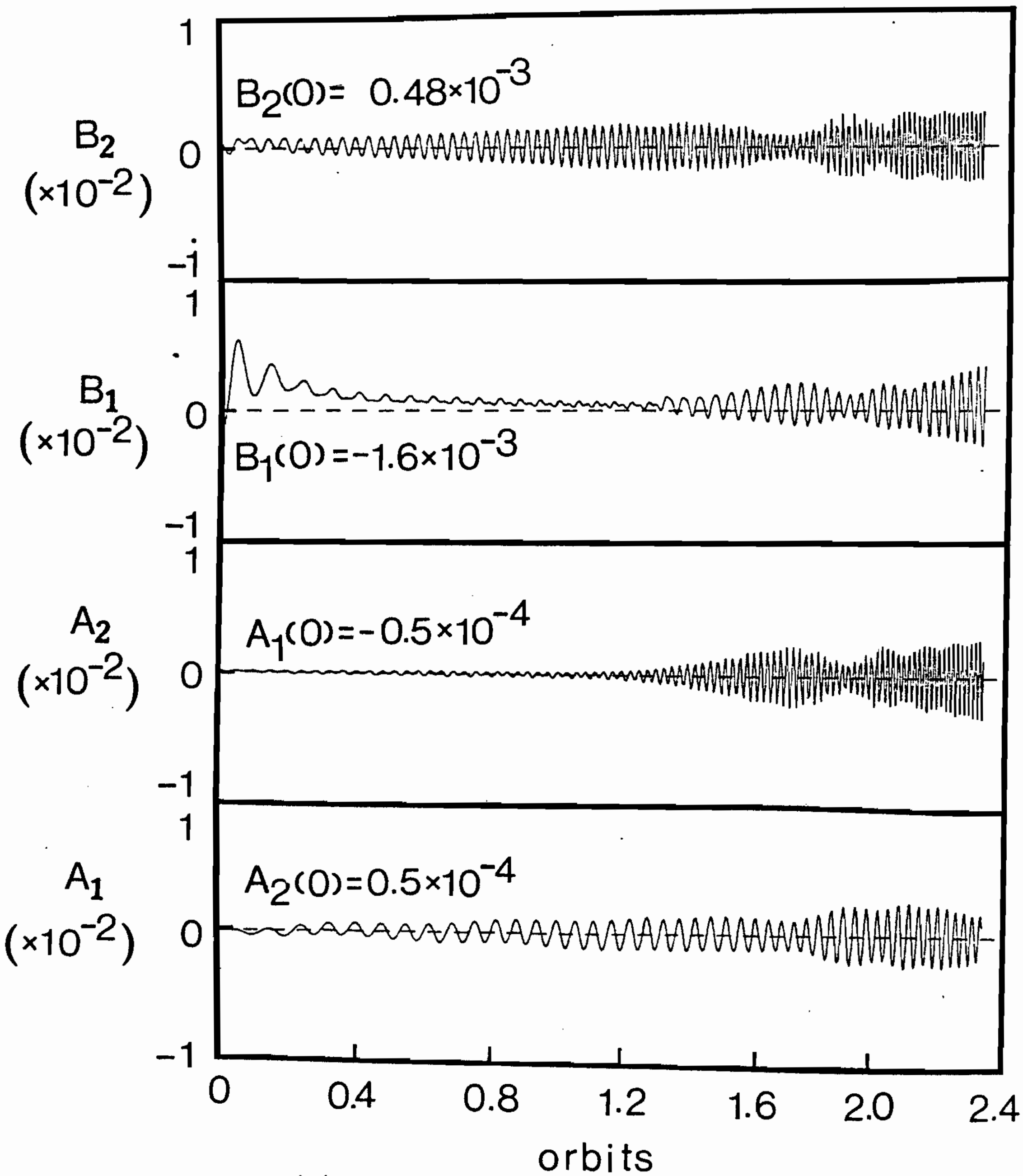

(b) Unstable transverse modal coordinates A_1, A_2, B_1 and B_2

Fig. 9.4 Dynamical response during retrieval from 100 Km using a length control law at first followed by thruster control without getting feedback from the transverse vibrations

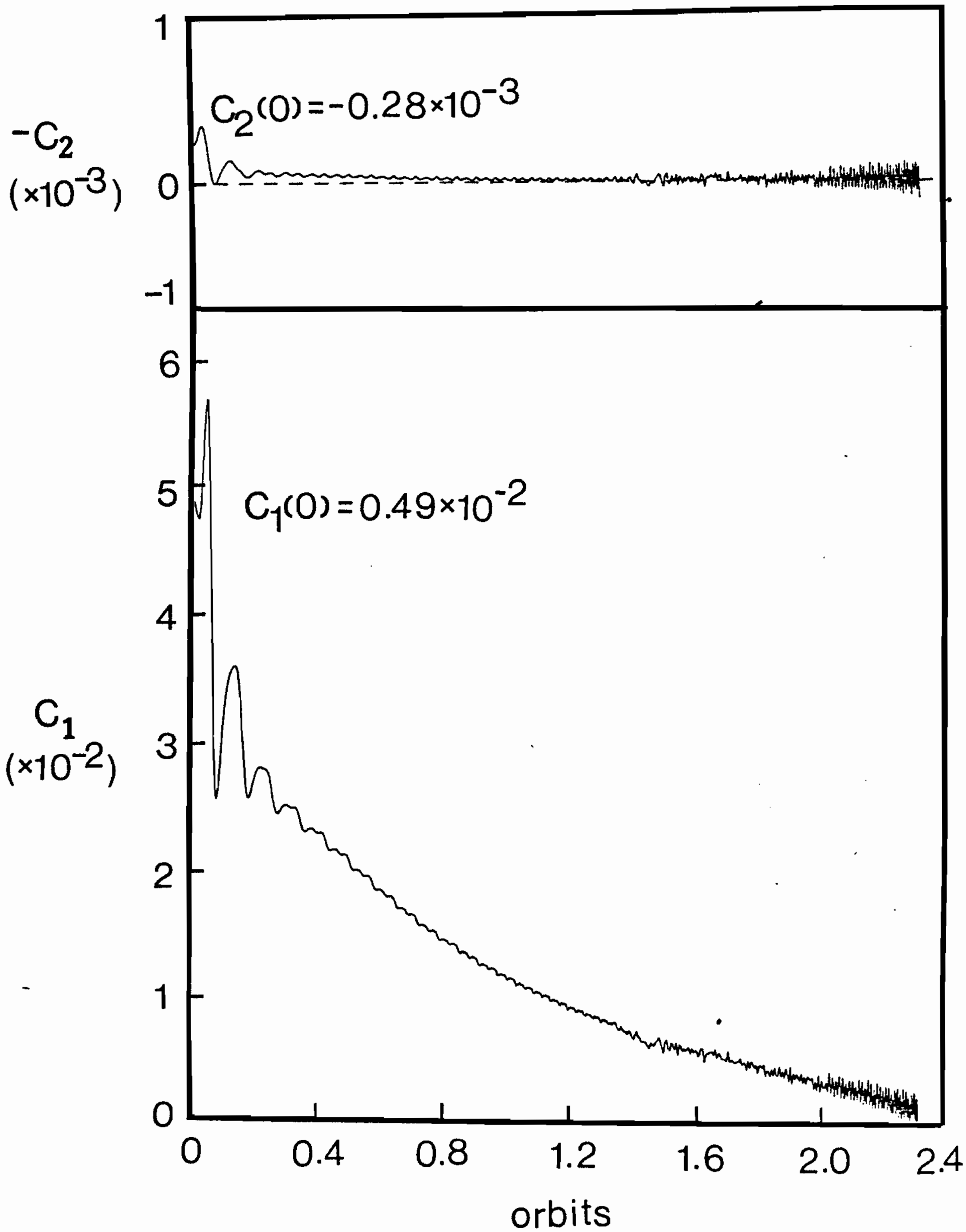

(c) Unstable longitudinal vibrations C_1 and C_2 (leading to slackening of the tether)

Fig. 9.4 Dynamical response during retrieval from 100 Km using a length control law at first followed by thruster control without getting feedback from the transverse vibrations

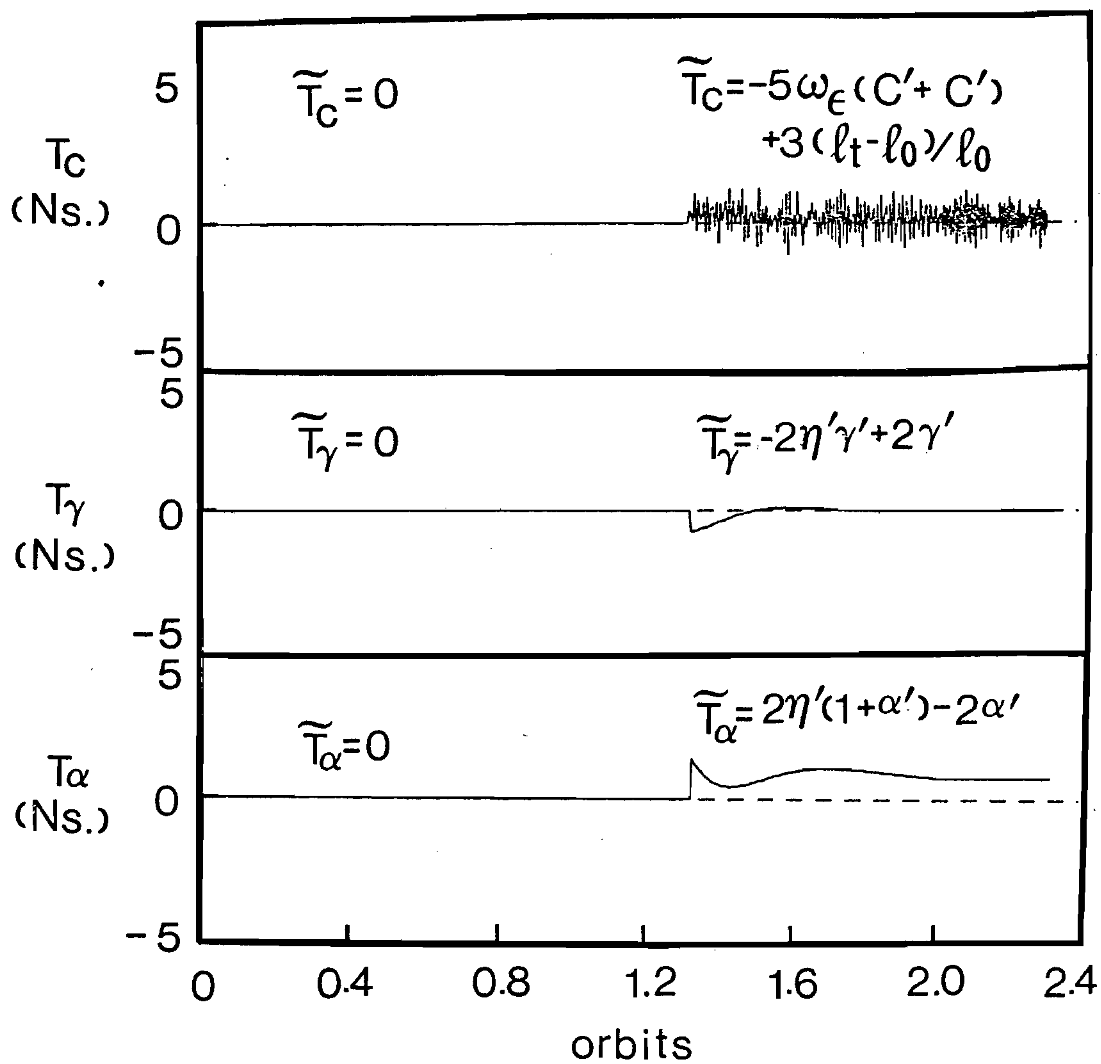

(d) Thruster forces T_α, T_γ and T_c

Fig. 9.4 Dynamical response during retrieval from 100 Km using a length control law at first followed by thruster control without getting feedback from the transverse vibrations

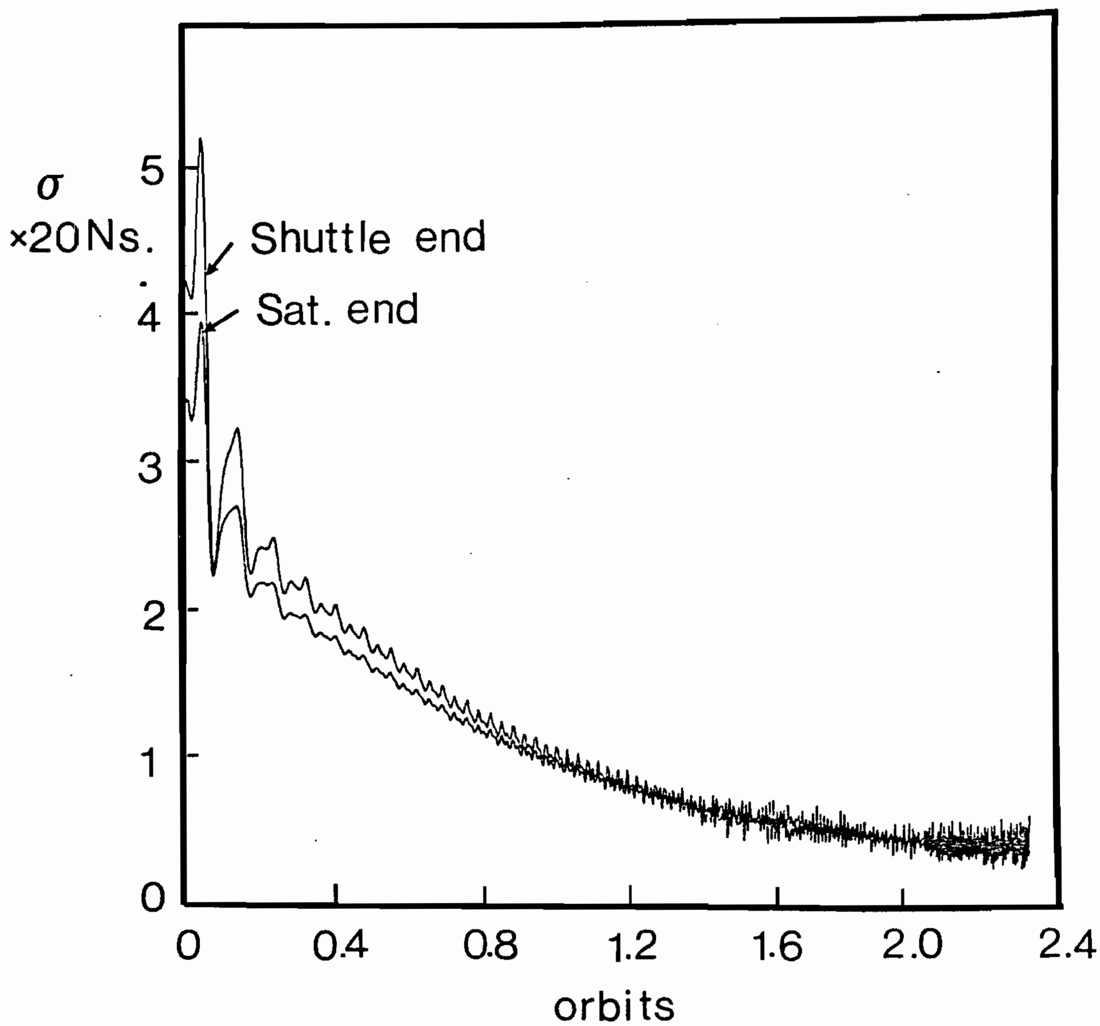

(e) Tension at both ends of the tether

Fig. 9.4 Dynamical response during retrieval from 100 Km using a length control law at first followed by thruster control without getting feedback from the transverse vibrations

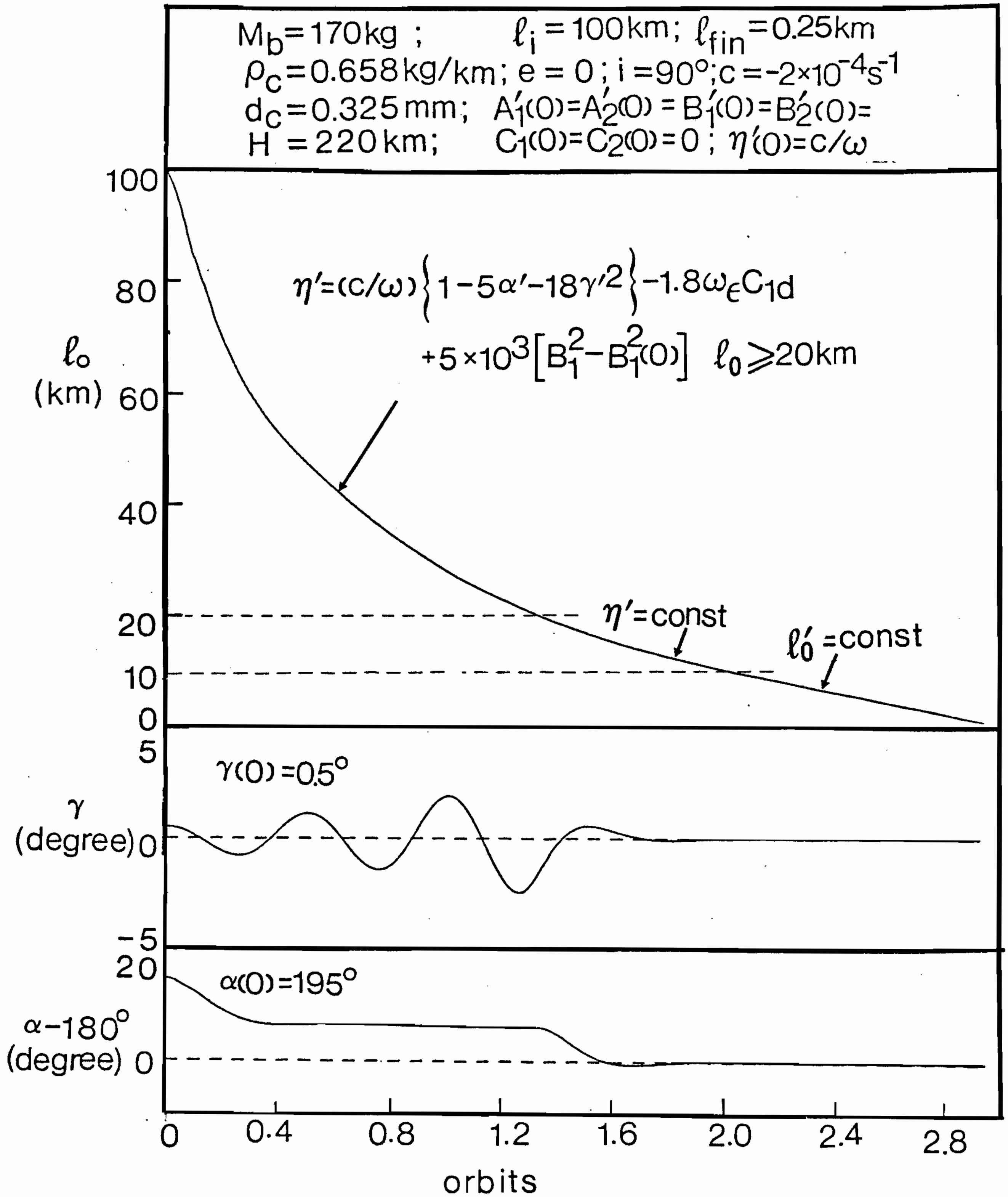

(a) Variation of length ℓ_0 and stable rotations α and γ

Fig. 9.5 Dynamical response during retrieval from 100 Km using a length control law at first followed by thruster control with feedback from transverse vibrations

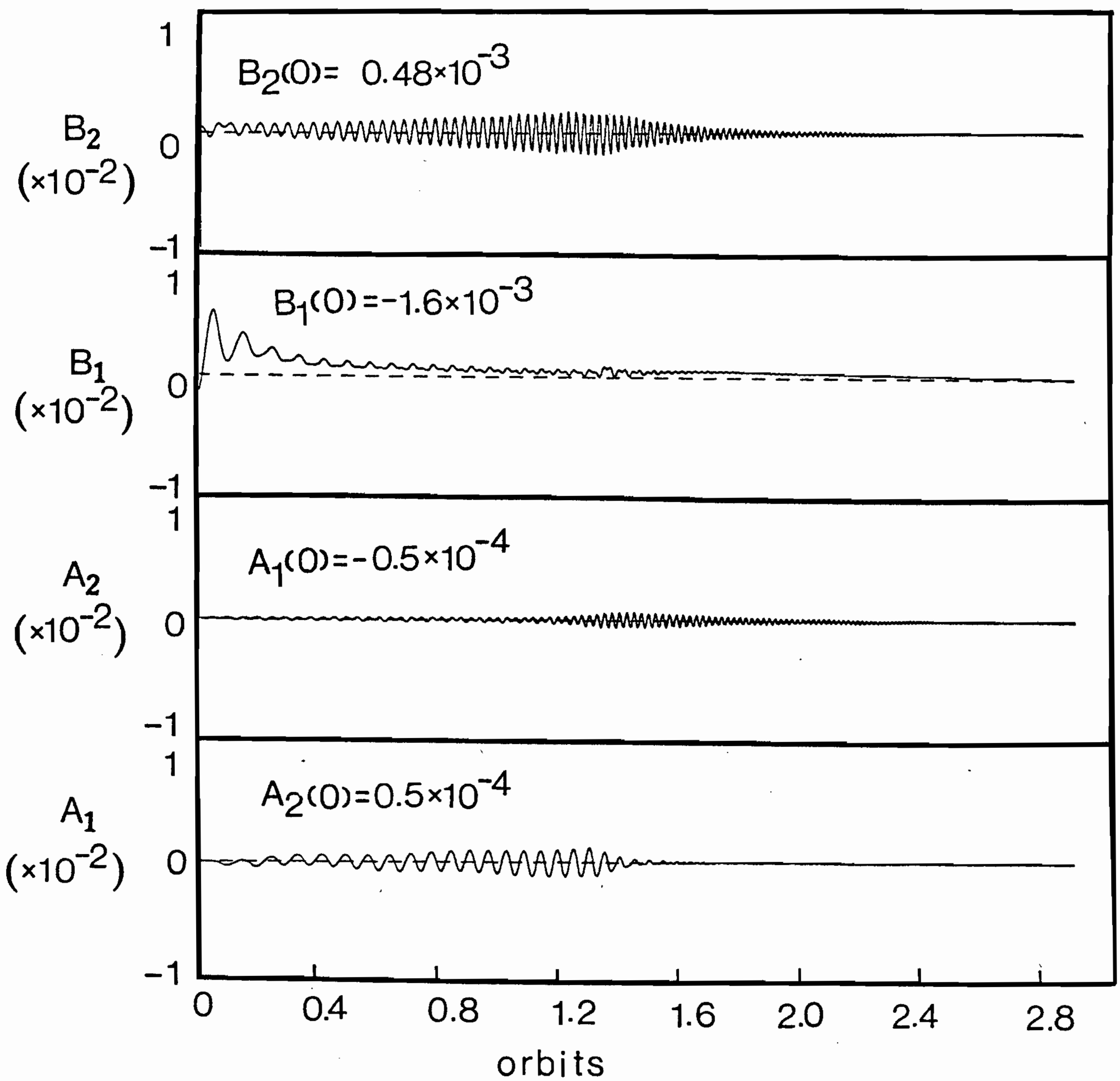

(b) Stable transverse modal coordinates A_1, A_2, B_1 and B_2

Fig. 9.5 Dynamical response during retrieval from 100 Km using a length control law at first followed by thruster control with feedback from transverse vibrations

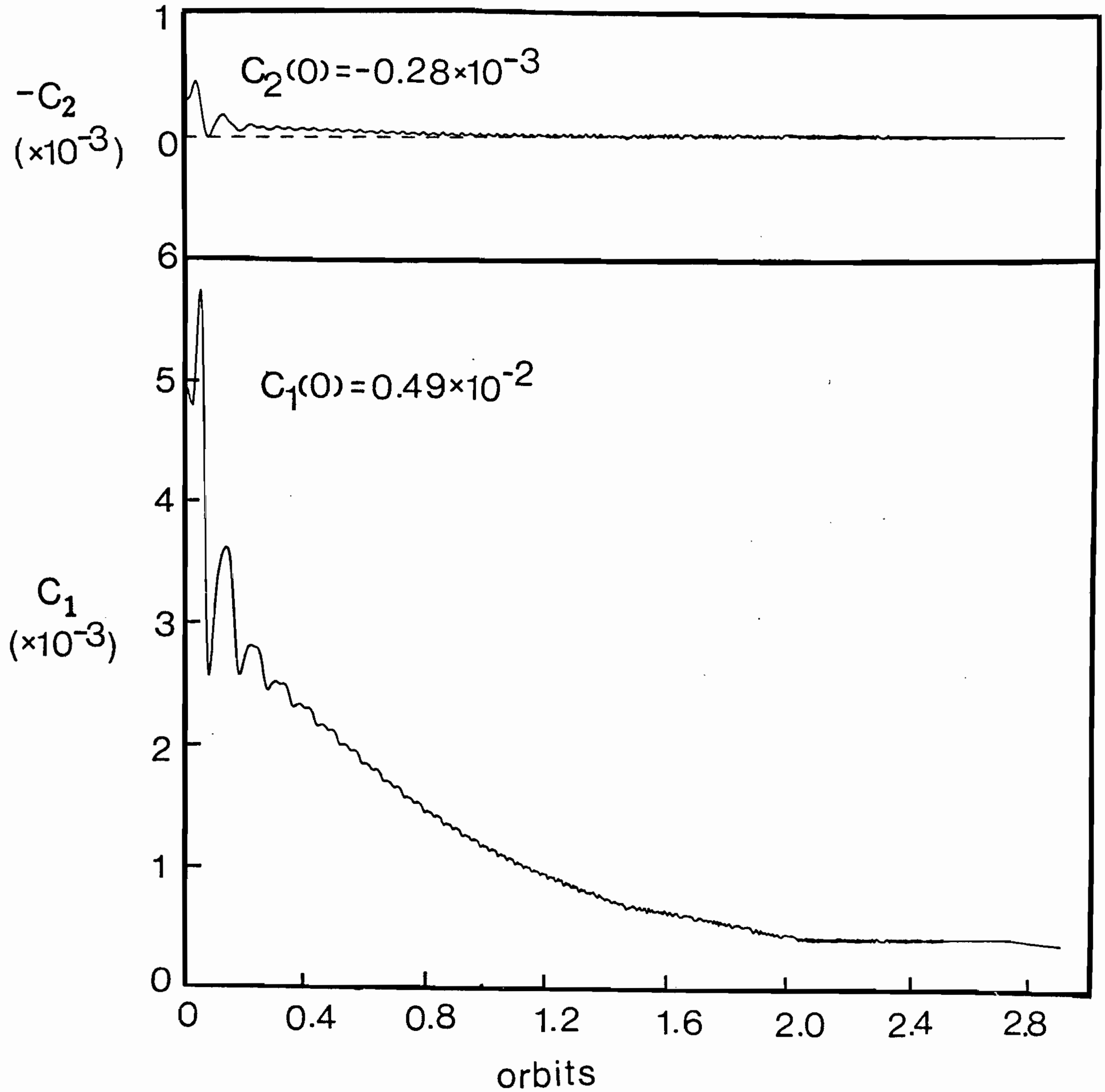

(c) Stable longitudinal vibrations C_1 and C_2

Fig. 9.5 Dynamical response during retrieval from 100 Km using a length control law at first followed by thruster control with feedback from transverse vibrations

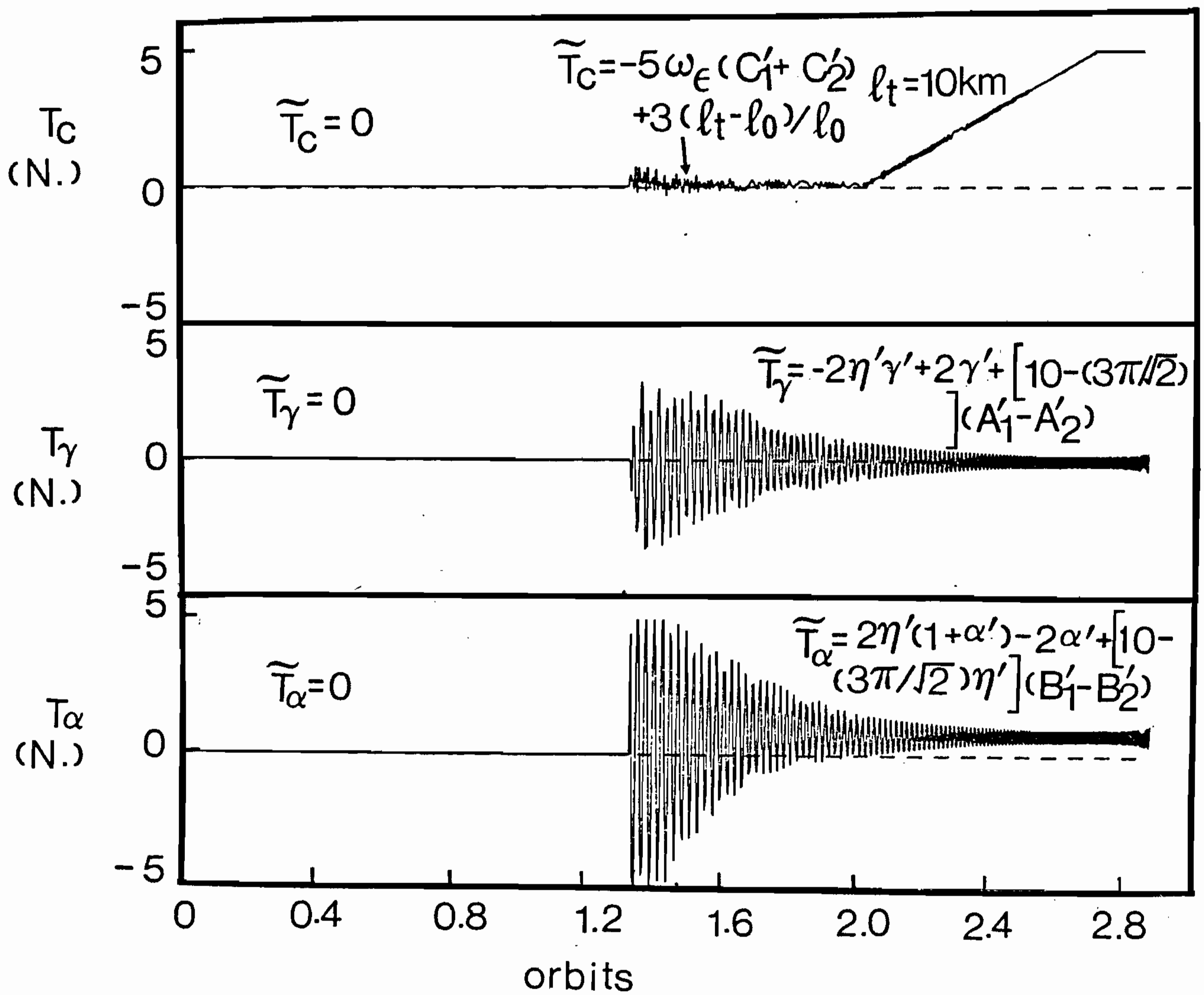

(d) Thruster forces T_α, T_γ and T_c

Fig. 9.5 Dynamical response during retrieval from 100 Km using a length control law at first followed by thruster control with feedback from transverse vibrations

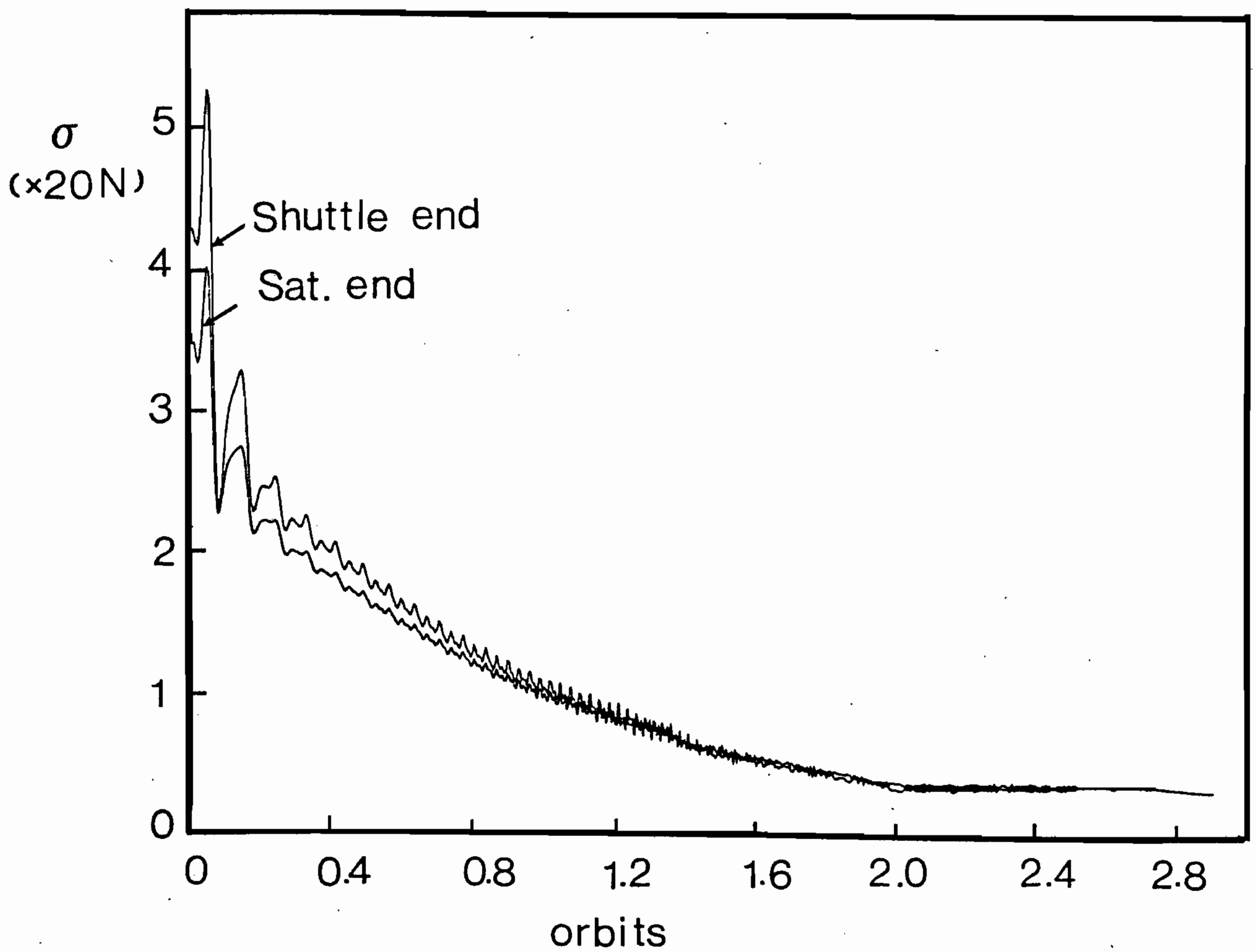

(e) Tension at both ends of the tether

Fig. 9.5 Dynamical response during retrieval from 100 Km using a length control law at first followed by thruster control with feedback from transverse vibrations

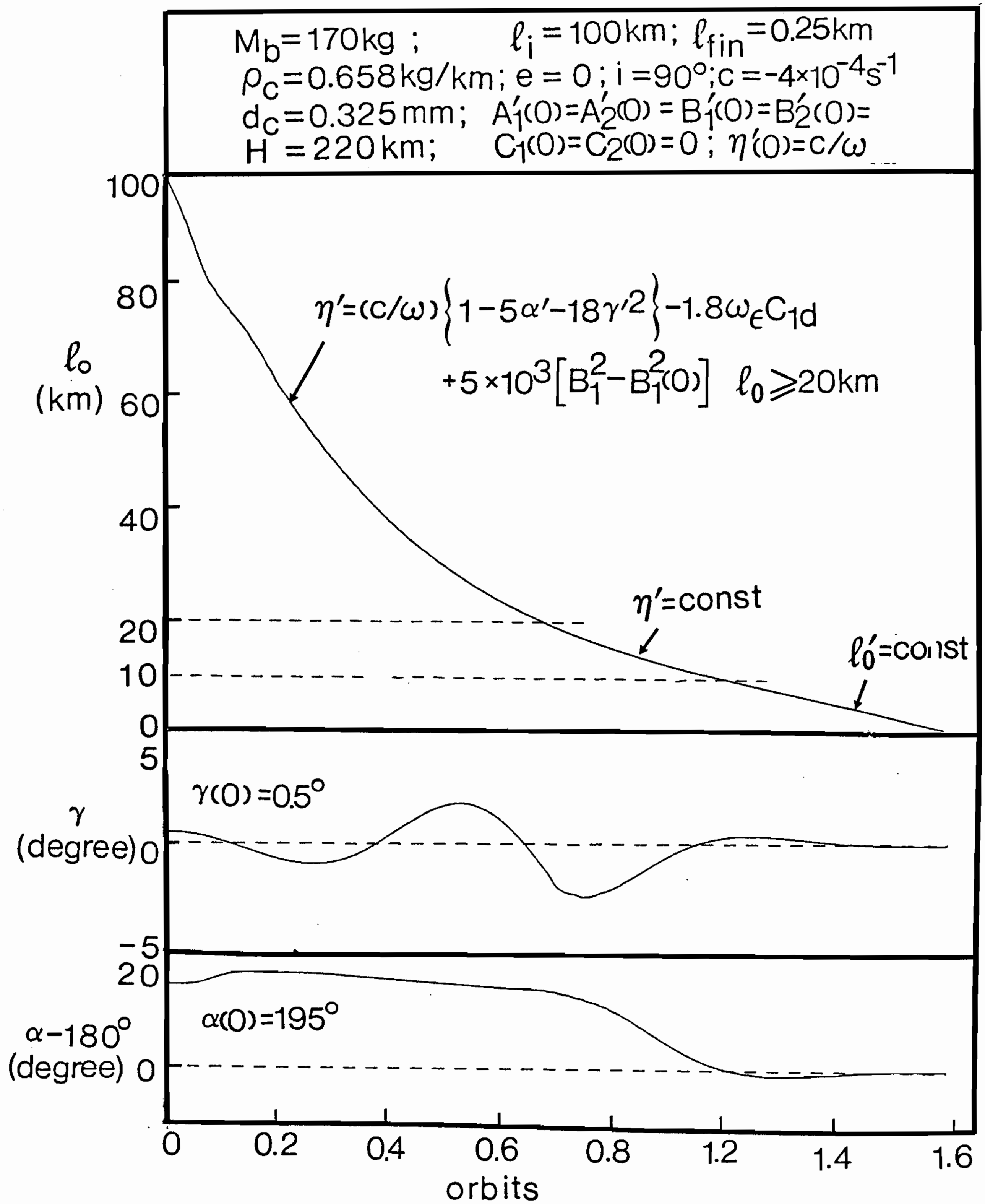

(a) Variation of length ℓ_0 and stable rotations α and γ

Fig. 9.6 Dynamical response during retrieval from 100 Km using a length control law at first followed by thruster control with feedback from transverse vibrations and a fast terminal retrieval scheme

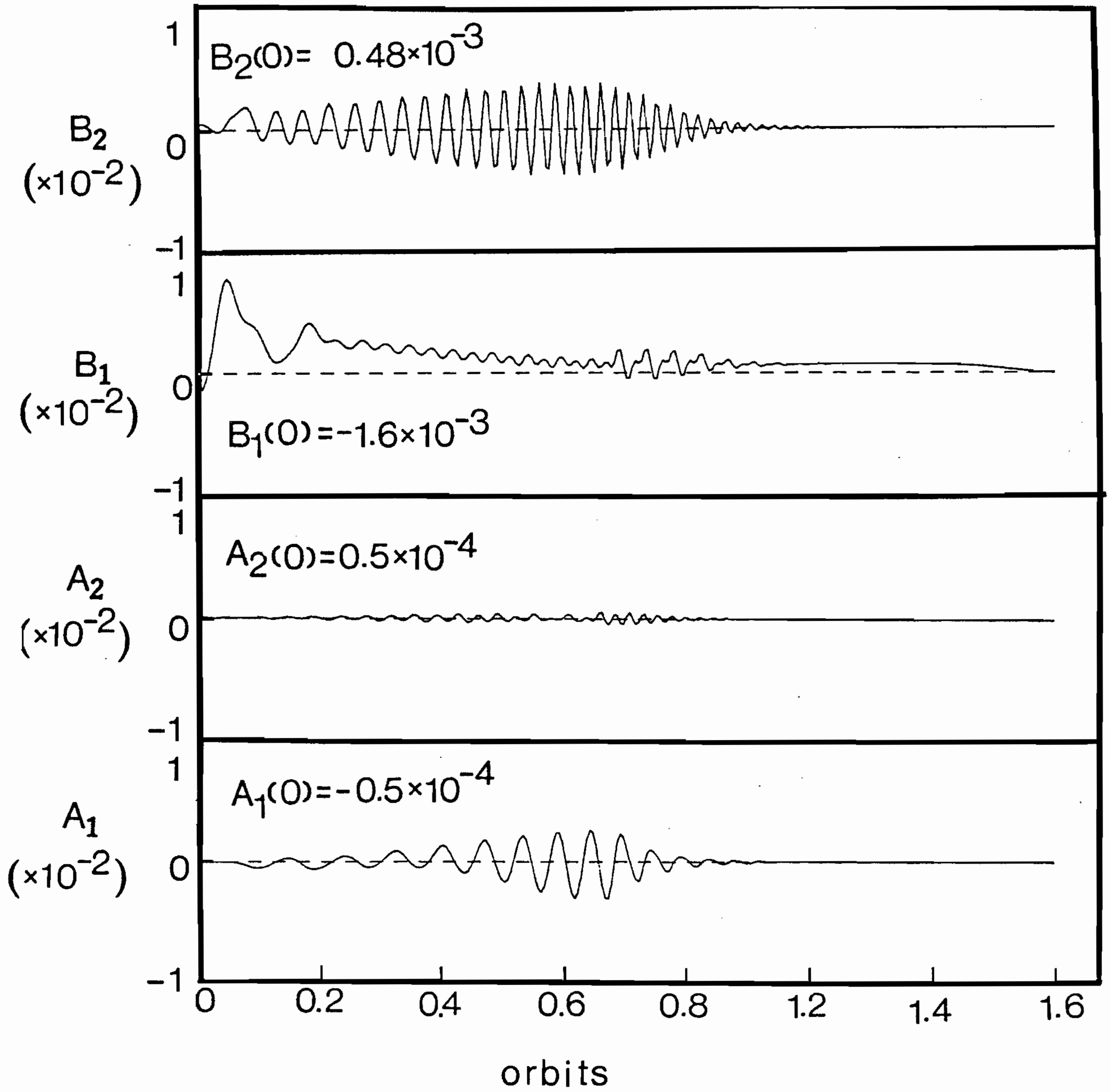

(b) Stable transverse modal coordinates A_1, A_2, B_1 and B_2

Fig. 9.6 Dynamical response during retrieval from 100 Km using a length control law at first followed by thruster control with feedback from transverse vibrations and a fast terminal retrieval scheme

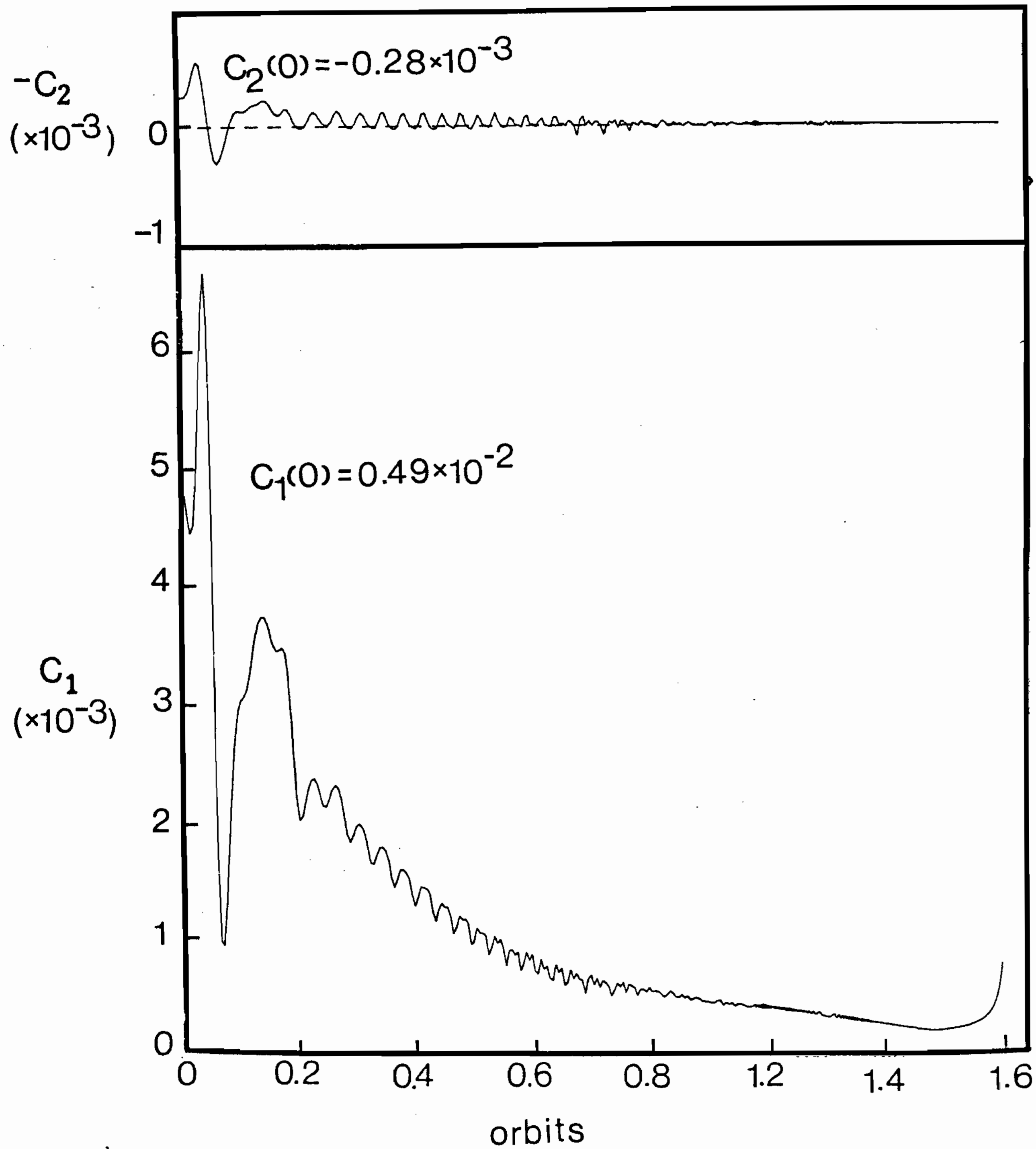

(c) Stable longitudinal vibrations C_1 and C_2

Fig. 9.6 Dynamical response during retrieval from 100 Km using a length control law at first followed by thruster control law at first followed by thruster control with feedback from transverse vibrations and a fast terminal retrieval scheme

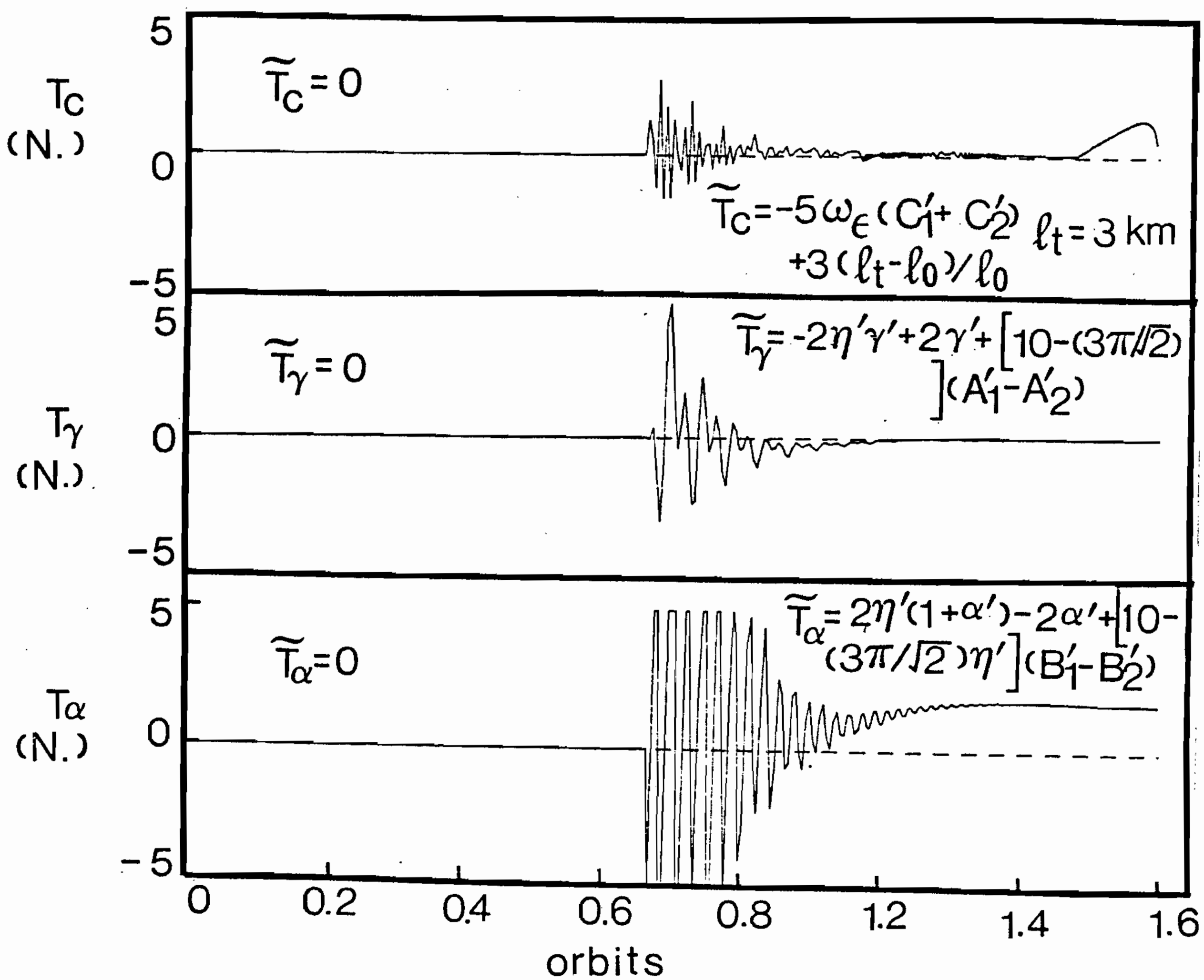

(d) Thruster forces T_α, T_γ and T_c

Fig. 9.6 Dynamical response during retrieval from 100 Km using a length control law at first followed by thruster control with feedback from transverse vibrations and a fast terminal retrieval scheme

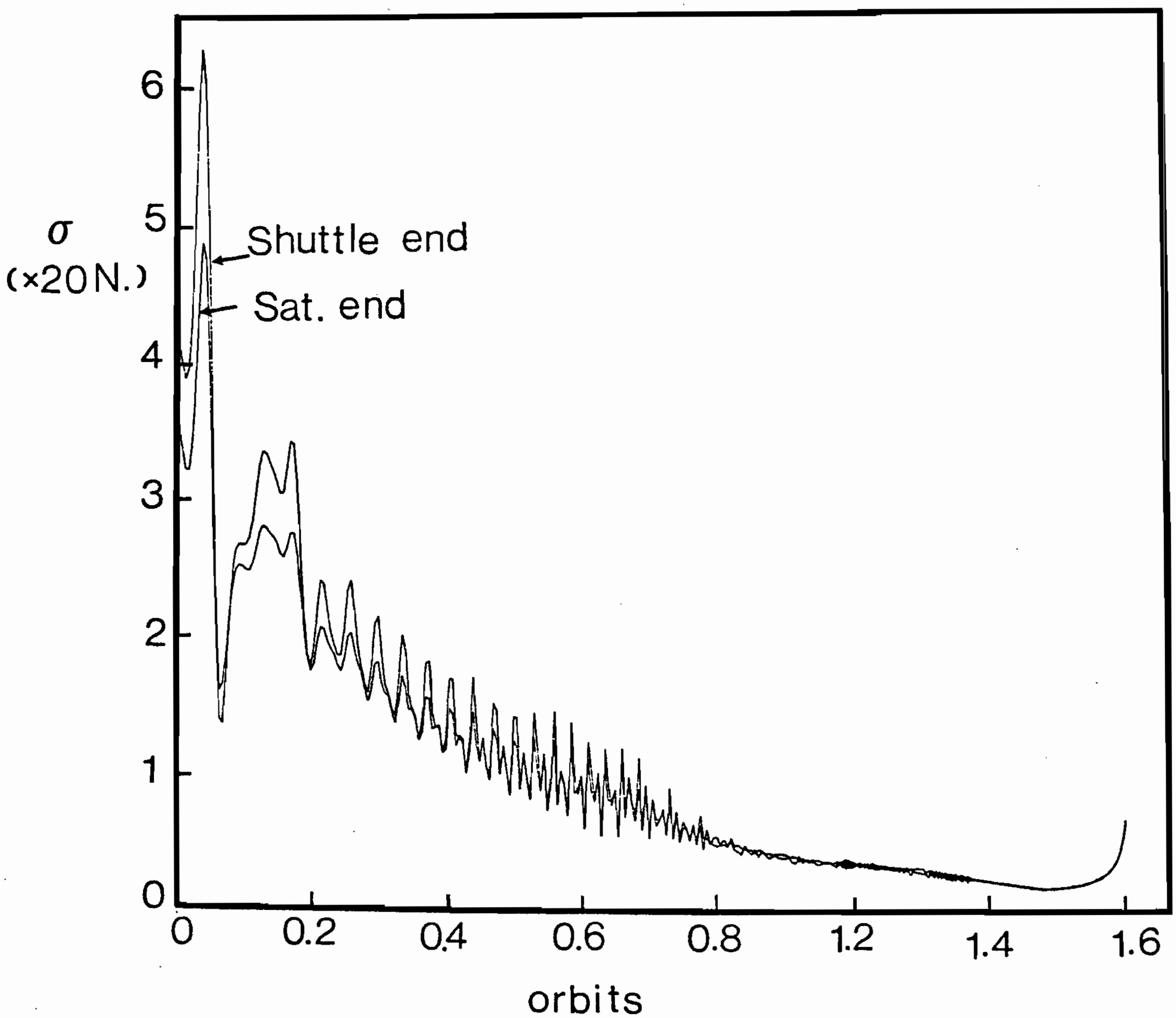

(e) Tension at both ends of the tether

Fig. 9.6 Dynamical response during retrieval from 100 Km using a length control law at first followed by thruster control with feedback from transverse vibrations and a fast terminal retrieval scheme

	Rupp [1975]	Baker et al. [1976]	Kulla [1976]	Buckens [1977]	Kane and Levinson [1977]	Kalaghan et al. [1978]	Modi and Misra [1978]
Three-dimensional motion	No	Yes	No	Yes	Yes	Yes	Yes
Results based on non-linear analysis	No	Yes	Yes	No	No	Yes	No
Tether mass	Yes	Yes	Yes	Yes	No	Yes	Yes
Longitudinal vibration of the tether	Yes	Yes	No	No	No	Masked	Yes
Longitudinal strain variation along the tether	No	No	No	No	No	Masked	No
Transverse vibrations of the tether	Steady state only		Yes	Yes	No	Masked	Yes
Torsional stiffness of the tether	No	No	No	No	No	No	No
Anisotropy of the tether	No	No	No	No	No	No	No
Discretization procedure	...	...	Finite difference	Galerkin	...	Point	Galerkin
Rotational motion of end masses	No	Yes	No	No	No	No	Yes
Offset of the point of attachment at the shuttle	No	No	No	No	No	No	No
Aerodynamic drag	Yes	Yes	Yes	No	No	Yes	No
Rotating atmosphere	No	Yes	No	No	No	Yes	No
Solar radiation	No	No	No	No	No	Yes	No

(Continued to next page)

Table 1. Comparison of Dynamical Models of Shuttle Supported Tethered Subsatellite Systems Used in Various Investigations

	Kohler et al. [1978]	Modi and Misra [1979]	Misra and Modi [1989]	Bainum and Kumar [1980]	Banerjee and Kane [1982]	Glaese and Pastrick [1982]
Three dimensional motion	Yes	Yes	Yes	Yes	Yes	Yes
Results based on non-linear analysis	Yes	No	No	Yes	Yes	*
Tether mass	Yes	Yes	Yes	No	Yes	Yes
Longitudinal vibration of the tether	Yes	Yes	Yes	No	Yes	Yes
Longitudinal strain variation along the tether	Yes	No	Yes	No	Yes	Yes
Transverse vibrations of the tether	Yes	Yes	Yes	No	No	Yes
Torsional stiffness of the tether	Yes	No	No	No	No	No
Anisotropy of the tether	Yes	No	No	No	No	No
Discretization procedure	Finite diff. & fin.elements	Galerkin	Galerkin	...	Galerkin	Galerkin
Rotational motion of end masses	No	Yes	Yes	No	No	Yes
Offset of the point of attachment at the shuttle	No	No	Yes	No	No	No
Aerodynamic drag	Yes	Yes	Yes	Yes	Yes	Yes
Rotating atmosphere	Yes	Yes	Yes	Yes	Yes	Yes
Solar radiation	Yes	No	No	No	No	Yes

* Results are not based on this model

Table 1. Continued

Investigators	Motion Controlled	Type	Control law
Rupp [1975]	2D rotations and stretch	Tension control	$T = K_1 L + C_1 L + K_2 L_c$
Kissel [Baker et al., 1976]	3D rotations and stretch	Tension control	$\frac{T}{m_s + \frac{1}{2} m_t} = (R^2+3)\Omega^2 L + 2\zeta R \Omega \dot{L} - R^2 \Omega^2 L_c$
Kulla [1977]	2D rotations and stretch	Tension control	Kissel law
Kalaghan et al. [1978]	3D rotations and stretch	Tension control	Kissel law
Kohler et al. [1978]	3D rotations and stretch	Tension control	Kissel law
Misra and Modi [1980]	2D rotations, stretch and transverse vibrations	Length rate control	$L' = L_c'[1 + \underset{\sim}{K}_i^T \underset{\sim}{x}_i]$
Bainum and Kumar [1980]	3D rotations and stretch	Optimized tension control	$T - T_0 = K_\ell \ell + K_{\ell'} \ell' + K_\alpha \alpha + K_{\alpha'} \alpha'$
Modi et al. [1981]	3D rotations and stretch	Nonlinear tension control	$T - T_0 = K_\ell \ell + K_{\ell'} \ell' + K_{\gamma'} \gamma'^2$ and several other forms
Bannerjee and Kane [1982]	3D rotations and stretching modes	Thrust augmented torque control	$T_c - T_{co} = K_\alpha \alpha + K_{\alpha'} \alpha' + K_\gamma \gamma + K_{\gamma'} \gamma' + K_\theta \theta + K_{\theta'} \theta'$ $T_c \equiv$ torque Thrusts proportional to α' and γ'

Table 2. Comparison of Control Laws for Shuttle Supported Tethered Subsatellite Systems used by Various Investigators.

TABLE 5.1

Variation of equilibrium state with the tether length;

$e = 0,\ i = 0$

ℓ_0 (Km)	α-180° (degree)	γ (degree)	C_1 (10^{-3})	C_2 (10^{-3})	$\tilde{A}_1$ (m)	$\tilde{A}_2$ (m)	$\tilde{B}_1$ (m)	$\tilde{B}_2$ (m)
10	0	0	0.41	0	0	0	0	0
20	0	0	0.85	-0.01	0	0	0	0
30	0	0	1.30	-0.02	0	0	0	0
40	0	0	1.76	-0.04	0	0	-0.1	0
50	0.01	0	2.24	-0.07	0	0	-0.6	0.2
60	0.05	0	2.73	-0.09	0	0	-2.3	0.7
70	0.19	0	3.24	-0.13	0	0	-9.8	3.1
80	0.76	0	3.77	-0.17	0	0	- 41	14
90	3.01	0	4.31	-0.24	0	0	- 175	55
100	9.96	0	4.85	-0.49	0	0	- 604	178
110	19.67	0	5.38	-0.98	0	0	-1184	320
120	27.61	0	5.88	-1.40	0	0	-1657	418

TABLE 5.2

Variation of quasi-static equilibrium configuration with θ; ℓ_0 = 100 Km;

e = 0.001, i = 0

θ (degree)	α-180° (degree)	γ (degree)	C_1 (10^{-3})	C_2 (10^{-3})	$\tilde{A}_1$ (m)	$\tilde{A}_2$ (m)	$\tilde{B}_1$ (m)	$\tilde{B}_2$ (m)
0	17.3	0	4.830	-0.8206	0	0	-973	273
30	16.3	0	4.836	-0.7709	0	0	-926	262
60	13.6	0	4.851	-0.6401	0	0	-795	230
90	10.0	0	4.852	-0.4856	0	0	-604	179
120	6.8	0	4.854	-0.3737	0	0	-424	127
150	5.0	0	4.854	-0.3222	0	0	-313	94.9
180	4.4	0	4.852	-0.3103	0	0	-278	84.3
210	5.0	0	4.853	-0.3229	0	0	-313	94.9
240	6.8	0	4.854	-0.3741	0	0	-424	127
270	10	0	4.851	-0.4868	0	0	-605	179
300	13.6	0	4.842	-0.6432	0	0	-796	230
330	16.3	0	4.838	-0.7718	0	0	-928	263
360	17.3	0	4.830	-0.8204	0	0	-973	273

TABLE 5.3

Variation of quasi-static equilibrium configuration with θ; ℓ_0 = 100 Km;

e = 0, i = 90°

θ (degree)	α-180° (degree)	γ (degree)	C_1 (10^{-3})	C_2 (10^{-3})	$\tilde{A}_1$ (m)	$\tilde{A}_2$ (m)	$\tilde{B}_1$ (m)	$\tilde{B}_2$ (m)
0	10.9	0.51	4.847	-0.5223	-5.2	8.3	-654	192
30	5.9	0.24	4.864	-0.3472	-2.6	3.9	-370	112
60	13.0	0.03	4.871	-0.2675	0	0	- 83	25
90	5.9	0	5.872	-0.2641	0	0	- 38	11
120	13	0	4.871	-0.2675	0	0	- 83	25
150	5.9	0	4.863	-0.3486	2.6	-3.9	-368	112
180	10.9	0	4.846	-0.5228	5.2	-8.3	-654	192
210	5.9	0	4.864	-0.3471	2.6	-3.9	-369	112
240	13	0	4.872	-0.2673	0	0	- 82	25
270	5.9	0	4.872	-0.2641	0	0	- 38	11
300	13	0.03	4.871	-0.2675	0	0	- 83	25
330	5.9	0.24	4.864	-0.3477	-2.6	3.9	-369	111
360	10.9	0.51	4.846	-0.5228	-5.2	8.3	-654	192

TABLE 5.4

Variation of quasi-static equilibrium configuration with θ; ℓ_0 = 100 Km;

<u>e = 0.001, i = 90°</u>

θ (degree)	α-180° (degree)	γ (degree)	C_1 (10^{-3})	C_2 (10^{-3})	$\tilde{A}_1$ (m)	$\tilde{A}_2$ (m)	$\tilde{B}_1$ (m)	$\tilde{B}_2$ (m)
0	18.2	0.89	4.821	-0.8673	-8.1	13.7	-1016	283
30	11.3	0.46	4.859	-0.5427	-4.7	7.4	- 678	199
60	2.2	0.05	4.883	-0.2703	0	0	- 137	41.9
90	0.6	0	4.872	-0.2638	0	0	-37.6	11.5
120	0.8	0	4.864	-0.2643	0	0	-50.3	15.4
150	2.7	0	4.856	-0.2799	1.2	-1.8	- 168	51.4
180	5.0	0	4.851	-0.3216	2.6	-3.8	- 312	94.6
210	2.6	0	4.856	-0.2801	1.2	-1.8	- 169	51.5
240	0.8	0	4.864	-0.2635	0	0	-50.4	15.4
270	0.6	0	4.872	-0.2641	0	0	-37.6	11.5
300	2.1	0.05	4.879	-0.2751	0	0	- 135	41.2
330	11.3	0.46	4.857	-0.5438	-4.7	7.4	- 679	199
360	18.2	0.89	4.821	-0.8673	-8.1	13.8	-1015	283

APPENDIX A

Differentiating equation (2.3.1) with respect to time, we get,

$$\frac{d}{dt}\left[(M_a + M_c)\vec{R}_a + M_b\,\vec{R}_b + \int_{M_c} \vec{r}_c\,dm\right] = 0 \qquad (A.1)$$

Note that M_a and M_c vary during deployment or retrieval and the limits of integration in the last term are time dependent. However, the sum of M_a and M_c remains constant as the total mass is conserved. Thus,

$$(M_a + M_c)\dot{\vec{R}}_a + M_b\,\dot{\vec{R}}_b + \frac{d}{dt}\int_{M_c} \vec{r}_c\,dm = 0 \qquad (A.2)$$

where

$$\frac{d}{dt}\int_{M_c} \vec{r}_c\,dm = \rho_c \frac{d}{dt}\int_0^{\ell_0(t)} \vec{r}_c(y_c,t)dy_c$$

$$= \rho_c\,\dot{\ell}_0(t)\vec{r}_c(\ell_0,t) + \rho_c\int_0^{\ell_0} \frac{\partial}{\partial t}\vec{r}_c\,dy_c \qquad (A.3)$$

using Leibnitz's rule for differentiation of integrals having variable limits. Now,

$$\int_{M_c} \frac{d}{dt}\vec{r}_c\,dm = \rho_c\int_0^{\ell_0}\left[\left(\frac{\partial}{\partial t} + \dot{\ell}_0\frac{\partial}{\partial y_c}\right)\vec{r}_c\right]dy_c$$

$$= \rho_c\int_0^{\ell_0}\frac{\partial}{\partial t}\vec{r}_c\,dy_c + \rho_c\dot{\ell}_0\left[\vec{r}_c(\ell_0,t)-\vec{r}_c(0,t)\right] \qquad (A.4)$$

Since $\vec{r}_c(0,t)$ is zero in our case, comparing equations (A.3) and (A.4) leads to

$$\frac{d}{dt}\int_{M_c} \vec{r}_c\,dm = \int_{M_c} \frac{d}{dt}\vec{r}_c\,dm \qquad (A.5)$$

APPENDIX B

From (2.7.10),

$$V_{nonorb} = \frac{1}{2} EA \int_0^{\ell_0} \frac{\partial v}{\partial y_c} + \frac{1}{2} [(\frac{\partial u}{\partial y_c})^2 + (\frac{\partial w}{\partial y_c})^2]\}dy_c + \frac{\mu}{2R_0^3} \{M_a[\vec{R}_a \cdot \vec{R}_a$$

$$- 3(\vec{J}_0 \cdot \vec{R}_a)^2] + M_b[\vec{R}_b \cdot \vec{R}_b - 3(\vec{J}_0 \cdot \vec{R}_b)^2] + \rho_c \int_0^{\ell_0} [\vec{R}_c \cdot \vec{R}_c - 3(\vec{J}_0 \cdot \vec{R}_c)^2]dy_c\} \tag{2.3.14}$$

Substituting (2.8.3) - (2.8.5) into (2.3.14),

$$R_a^2 = \vec{R}_a \cdot \vec{R}_a = \frac{1}{M^2} \{M_c^2 \bar{u}^2 + [M_c(\frac{\ell_0}{2} + \bar{v}) + M_b(\ell_0 + v(\ell_0, t))]^2 + M_c^2 \bar{w}^2\} \tag{B.1}$$

$$R_b^2 = \vec{R}_b \cdot \vec{R}_b = \frac{1}{M^2} \{M_c^2 \bar{u}^2 + [M_c(\frac{\ell_0}{2} + \bar{v}) - (M_a + M_c)(\ell_0 + v(\ell_0, t))]^2$$
$$+ M_c^2 w^2\} \tag{B.2}$$

and

$$\int_0^{\ell_0} \vec{R}_c \cdot \vec{R}_c dy_c = \int_0^{\ell_0} \{(u - \frac{M_c}{M} \bar{u})^2 + [y_c + v - \frac{M_c}{M} (\frac{\ell_0}{2} + \bar{v})$$
$$- \frac{M_b}{M} (\ell_0 + v(\ell_0, t))]^2 + (w - \frac{M_c}{M} \bar{w})^2\}dy_c \tag{B.3}$$

Using (2.8.11),

$$\vec{J}_0 = [c\alpha s\gamma,\ c\alpha c\gamma,\ -s\alpha] \begin{Bmatrix} \vec{i}_c \\ \vec{j}_c \\ \vec{k}_c \end{Bmatrix} \tag{B.4}$$

Hence,

$$\vec{J}_0 \cdot \vec{R}_a = -\frac{M_c}{M} [c\alpha s\gamma \bar{u} + c\alpha c\gamma(\frac{1}{2} \ell_0 + \bar{v}) - s\alpha \bar{w}]$$
$$- \frac{M_b}{M} c\alpha s\gamma[\ell_0 + v(\ell_0, t)] \tag{B.5}$$

$$\vec{J}_0\cdot\vec{R}_b = -\frac{M_c}{M}[c\alpha s\gamma\bar{u}+c\alpha c\gamma(\frac{1}{2}\ell_0+\bar{v})-s\alpha\bar{w}]$$

$$+\frac{M_a+M_c}{M}c\alpha s\gamma[\ell_0+v(\ell_0,t)] \quad (B.6)$$

and

$$\vec{J}_0\cdot\vec{R}_c = c\alpha s\gamma(u-\frac{M_c}{M}\bar{u})+c\alpha s\gamma[y_c+v-\frac{M_c}{M}(\frac{\ell_0}{2}+\bar{v})$$

$$-\frac{M_b}{M}(\ell_0+v(\ell_0,t))]-s\alpha(w-\frac{M_c}{M}\bar{w}) \quad (B.7)$$

Putting (B.1) - (B.7) into (2.3.14),

$$V_{nonorb} = \frac{1}{2}EA\int_0^{\ell_0}\{\frac{\partial v}{\partial y_c}+\frac{1}{2}[(\frac{\partial u}{\partial y_c})^2+(\frac{\partial w}{\partial y_c})^2]\}^2 dy_c$$

$$+\frac{1}{2}[V_1+V_2+V_3] \quad (B.8)$$

where

$$V_1 = [\mu/R_0{}^3][M_a\frac{1}{M^2}]\{M_c^2\bar{u}^2+[M_c(\frac{\ell_0}{2}+\bar{v})+M_b(\ell_0+v(\ell_0,t))]^2$$

$$+M_c{}^2\bar{w}^2\}-3M_a\{-\frac{M_c}{M}[c\alpha s\gamma\bar{u}+c\alpha c\gamma(\frac{1}{2}\ell_0+\bar{v})$$

$$-s\alpha\bar{w}]-\frac{M_b}{M}c\alpha c\gamma[\ell_0+v(\ell_0,t)]\}^2 \quad (B.9)$$

$$V_2 = [\mu/R_0{}^3][M_b\frac{1}{M^2}]\{M_c{}^2\bar{u}^2+[M_c(\frac{\ell_0}{2}+\bar{v})-(M_a+M_c)(\ell_0+v(\ell_0,t))]^2$$

$$+M_c{}^2\bar{w}\}-3M_b\{-\frac{M_c}{M}[c\alpha s\gamma\bar{u}+c\alpha s\gamma(\frac{\ell_0}{2}+\bar{v})-s\alpha\bar{w}]$$

$$+\frac{M_a+M_c}{M}c\alpha c\gamma[\ell_0+v(\ell_0,t)]\} \quad (B.10)$$

and

$$V_3 = [\mu/R_a{}^3]M_c \frac{1}{\ell_0} \{\int_0^{\ell_0} \{(u - \frac{M_c}{M}\overline{u})^2 + [y_c + v - \frac{M_c}{M}(\frac{\ell_0}{2} + \overline{v})$$

$$- \frac{M_b}{M}(\ell_0 + v(\ell_0,t))]^2 + (w - \frac{M_c}{M}\overline{w})^2\}$$

$$- 3\int_0^{\ell_0} \{c\alpha s\gamma(u - \frac{M_c}{M}\overline{u}) + c\alpha c\gamma[y_c + v - \frac{M_c}{M}(\frac{\ell_0}{2} + \overline{v})$$

$$- \frac{M_b}{M}(\ell_0 + v(\ell_0,t))] - s\alpha(w - \frac{M_c}{M}\overline{w})\}^2 dy_c \tag{B.11}$$

Due to the basic assumptions made in the Section 2.9, many trivial terms can be neglected. At last the simplified V_{nonorb} will be

$$V_{nonorb} = \frac{EA}{2}\int_0^{\ell_0} \{\frac{\partial v}{\partial y_c} + \frac{1}{2}[(\frac{\partial u}{\partial y_c})^2 + (\frac{\partial w}{\partial y_c})^2]\}^2 dy_c$$

$$+ V_{\alpha\gamma} + V_{uvw} \tag{B.12}$$

where

$$V_{\alpha\gamma} = \frac{1}{2}\omega^2[M_b + \frac{1}{3}M_c](1 - 3c^2\alpha c^2\gamma)\ell_0{}^2 \tag{B.13}$$

and

$$V_{uvw} = \omega^2\{(1 - 3c^2\alpha c^2\gamma)[M_b\,\ell_0\,v(\ell_0,t)$$

$$+ \rho_c\int_0^{\ell_0} y_c\,v\,dy_c] - 3\rho_c\int_0^{\ell_0} c^2\alpha s\gamma c\gamma\,uy_c\,dy_c$$

$$+ 3\rho_c\int_0^{\ell_0} c\gamma c\alpha s\alpha\,wy_c\,dy_c\} \tag{B.14}$$

APPENDIX C

From (2.4.14)

$$T_{nonorb} = \frac{1}{2} M_b \dot{\vec{\ell}}_j \cdot \dot{\vec{\ell}}_j + \frac{1}{2} M_c \frac{1}{\ell_0} \dot{\vec{r}}_c \cdot \dot{\vec{r}}_c \, dy_c \tag{2.4.14}$$

Using (2.9.14) and (2.9.15),

$$\frac{M_b}{2} \dot{\vec{\ell}}_j \cdot \dot{\vec{\ell}}_j = \frac{M_b}{2} \{[(\dot{\alpha}+\dot{\theta})^2 c^2\gamma + \dot{\gamma}^2][\ell_0 + v(\ell_0,t)]^2 + [\dot{\ell}_0(1+\frac{\partial v(\ell_0,t)}{\partial y_c} + \frac{\partial v(\ell_0,t)}{\partial t}]^2\} \tag{C.1}$$

and

$$\frac{1}{2} M_c \frac{1}{\ell_0} \int_0^{\ell_0} \dot{\vec{\gamma}}_c \cdot \dot{\vec{\gamma}}_c \, dy_c = \frac{1}{2} \rho \int_0^{\ell_0} \{[\frac{\partial u}{\partial t} + \dot{\ell}_0 \frac{\partial u}{\partial y_c} - w(\dot{\theta}+\dot{\alpha})s\gamma - (y_c+v)\dot{\gamma}]^2 + [\dot{\ell}_0(1+\frac{\partial v}{\partial y_c}) + \frac{\partial v}{\partial t} + u\dot{\gamma} - (\dot{\theta}+\dot{\alpha})c\gamma w]^2 + [\frac{\partial w}{\partial t} + \dot{\ell}_0 \frac{\partial w}{\partial y_c} + (\dot{\theta}+\dot{\alpha})s\gamma u + (\dot{\theta}+\dot{\alpha})c\gamma(y_c+v)]^2\} dy_c \tag{C.2}$$

Many trivial terms in (C.1) and (C.2) can be neglected if the basic assumption (iv) cited in Section 2 is used, i.e.,

$$u,v,w << \ell_0 \tag{C.3}$$

or

$$\frac{\partial u}{\partial y_c}, \frac{\partial v}{\partial y_c}, \frac{\partial w}{\partial y_c} << 1 \tag{C.4}$$

However, only second order smaller terms are dropped. For example, $v^2(\ell_0,t)$ is dropped compared with ℓ_0^2 in (C.1). Since vibrational displacements y,v,w have high frequencies, its first derivative may not be small and $\dot{\ell}_0$, which represents deployment or retrieval length rate, ranges greatly depending on how fast whether deployment or retrieval is. Hence, it is impossible to tell which one is dominant between $\dot{\ell}_0$ and $\frac{\partial u}{\partial t}$ and so on. Hence, the high order smaller terms are neglected by comparison with the same kind of large term.

Thus, for example, (C.1) equation can be written as

$$\frac{1}{2} M_b \dot{\vec{\ell}}_j \cdot \dot{\vec{\ell}}_j \cong \frac{M_b}{2} \{[(\dot{\alpha}+\dot{\theta})^2 c^2\gamma + \dot{\gamma}^2][\ell_0{}^2 + 2\ell_0 v(\ell_0,t) + v^2(\ell_0,t)] + [\dot{\ell}_0{}^2(1+2\frac{\partial v(\ell_0,t)}{\partial y_c} + (\frac{\partial v(\ell_0,t)}{\partial y_c})^2) + 2\dot{\ell}_0(1 + \frac{\partial v(\ell_0,t)}{\partial y_c})\frac{\partial v(\ell_0,t)}{\partial t} + \frac{\partial v(\ell_0,t)^2}{\partial t}]\} \qquad (C.5)$$

Two second order smaller terms marked ( ) are ignored.

Following the same procedure, many trivial terms in equation (C.2) can be neglected. Rewriting (C.2) as

$$\frac{1}{2} M_c \frac{1}{\ell_0} \int_0^{\ell_0} \dot{\vec{c}} \cdot \dot{\vec{c}}\, dy = \int_0^{\ell_0} (T_1 + T_2 + T_3) dy_c \qquad (C.6)$$

one has

$$T_1 = [\frac{\partial u}{\partial t} + \dot{\ell}_0 \frac{\partial u}{\partial y_c} - w(\dot{\theta}+\dot{\alpha})s\gamma - (y_c+v)\dot{\gamma}]^2 \qquad (C.7)$$

$$T_2 = [\dot{\ell}_0 (1 + \frac{\partial v}{\partial y_c}) + \frac{\partial v}{\partial t} + u\dot{\gamma} - (\dot{\theta}+\dot{\alpha})c\gamma\, w]^2 \qquad (C.8)$$

and

$$T_3 = [\frac{\partial w}{\partial t} + \dot{\ell}_0 \frac{\partial w}{\partial y_c} + (\dot{\theta}+\dot{\alpha})s\gamma u + (\dot{\theta}+\dot{\alpha})c\gamma(y_c+v)]^2 \qquad (C.9)$$

Opening the square term and neglecting the second order smaller terms, T_1 can be written as

$$T_1 = \left(\frac{\partial u}{\partial t}\right)^2 + \dot{\ell}_0^2 \left(\frac{\partial u}{\partial y_c}\right)^2 + (y_c^2+2y_c v)\dot{\gamma}^2 + 2\,\frac{\partial u}{\partial t}\,\dot{\ell}_0\,\frac{\partial u}{\partial y_c}$$

$$- 2\,\frac{\partial u}{\partial t}\,w(\dot{\theta}+\dot{\alpha})s\gamma - 2\,\frac{\partial u}{\partial t}\,(y_c+v)\dot{\gamma} - 2\,\dot{\ell}_0\,\frac{\partial u}{\partial y}\,y_c\,\dot{\gamma}$$

$$+ 2w(\dot{\theta}+\dot{\alpha})s\gamma y_c\,\dot{\gamma} \tag{C.10}$$

$$T_2 = \dot{\ell}_0^2\left(1+2\,\frac{\partial v}{\partial y_c}\right) + \left(\frac{\partial v}{\partial t}\right)^2 + 2\dot{\ell}_0\left(1+\frac{\partial v}{\partial y_c}\right)\frac{\partial v}{\partial t} + 2\left(\dot{\ell}_0+\frac{\partial v}{\partial t}\right)[u\dot{\gamma}$$

$$- (\dot{\theta}+\dot{\alpha})c\gamma w] \tag{C.11}$$

$$T_3 = \left(\frac{\partial w}{\partial t}\right)^2 + \dot{\ell}_0^2\left(\frac{\partial w}{\partial y_c}\right)^2 + (\dot{\theta}+\dot{\alpha})^2 c^2\gamma(y_c^2+2y_c v) + 2\,\frac{\partial w}{\partial t}\,\dot{\ell}_0\,\frac{\partial w}{\partial y_c}$$

$$+ 2\,\frac{\partial w}{\partial t}\,(\dot{\theta}+\dot{\alpha})s\gamma u + 2\,\frac{\partial w}{\partial t}\,(\dot{\theta}+\dot{\alpha})c\gamma(y_c+v) + 2\dot{\ell}_0\,\frac{\partial w}{\partial y_c}$$

$$\cdot\,(\dot{\theta}+\dot{\alpha})c\gamma y_c + 2(\dot{\theta}+\dot{\alpha})^2 s\gamma c\gamma u\, y_c \tag{C.12}$$

Substituting (C.10) - (C.12) into (C.6) and combining, we have

$$\frac{1}{2}\,\rho_c\int_0^{\ell_0}(T_1+T_2+T_3)\,dy_c = \frac{M_c}{2}\,\{\dot{\ell}_0^2 + \frac{1}{3}\,[(\dot{\theta}+\dot{\alpha})^2 c^2\gamma + \dot{\gamma}^2]\ell_0^2\}$$

$$+ \frac{\rho_c}{2}\int_0^{\ell_0}\ \Big[\left(\frac{\partial u}{\partial t}\right)^2 + \left(\frac{\partial v}{\partial t}\right)^2 + \left(\frac{\partial w}{\partial t}\right)^2\Big] + \dot{\ell}_0^2\Big[\left(\frac{\partial u}{\partial y_c}\right)^2 + 2\left(\frac{\partial v}{\partial y_c}\right)^2 + \left(\frac{\partial w}{\partial y_c}\right)^2\Big]$$

$$+ 2\,\dot{\ell}_0\frac{\partial u}{\partial t}\,\frac{\partial u}{\partial y_c} + \frac{\partial v}{\partial t} + \frac{\partial v}{\partial t}\,\frac{\partial v}{\partial y_c} + \frac{\partial w}{\partial t}\,\frac{\partial w}{\partial y_c}] + 2y_c v[(\dot{\theta}+\dot{\alpha})^2 c^2\gamma + \dot{\gamma}^2]$$

$$+ 2(\dot{\theta}+\dot{\alpha})s\gamma\left(u\,\frac{\partial w}{\partial t} - w\,\frac{\partial u}{\partial t}\right) + 2(y_c+v)\Big[(\dot{\theta}+\dot{\alpha})c\gamma\,\frac{\partial w}{\partial t} - \dot{\gamma}\,\frac{\partial u}{\partial t}\Big]$$

$$+ 2\dot{\ell}_0 y_c\Big[(\dot{\theta}+\dot{\alpha})c\gamma\,\frac{\partial w}{\partial y_c} - \dot{\gamma}\frac{\partial u}{\partial y_c}\Big] + 2(\dot{\theta}+\dot{\alpha})s\gamma y_c[\dot{\gamma}w + (\dot{\theta}+\dot{\alpha})c\gamma u]$$

$$+ 2\left(\dot{\ell}_0 + \frac{\partial v}{\partial t}\right)[u\dot{\gamma} - (\dot{\theta}+\dot{\alpha})c\gamma w]\ \}\ dy_c \tag{C.13}$$

Putting (C.5) and (C.13) into (2.4.14) and rearranging it,

$$T_{nonorb} = T_{\alpha\gamma} + T_{uvw} \tag{C.14}$$

where

$$T_{\alpha\gamma} = \frac{1}{2}(M_b + \frac{1}{3}M_c)[(\dot{\alpha}+\dot{\theta})^2c^2\gamma+\dot{\gamma}^2]\ell_0{}^2+ \frac{1}{2}(M_b+M_c)\dot{\ell}_0{}^2 \tag{C.15}$$

$$\begin{aligned}
T_{uvw} = {} & M_b\{[(\dot{\alpha}+\dot{\theta})^2c^2\gamma+\dot{\gamma}^2]v(\ell_0,t)\ell_0+\dot{\ell}_0{}^2\,\frac{\partial v(\ell_0,t)}{\partial y_c} \\
& + \ell_0\,\frac{\partial v(\ell_0,t)}{\partial t}\,(1+\frac{\partial v(\ell_0,t)}{\partial y_c})+(\frac{\partial v(\ell_0,t)}{\partial t})^2\} \\
& + \frac{1}{2}M_c\,\frac{1}{\ell_0}\int_0^{\ell_0}[(\frac{\partial u}{\partial t})^2+(\frac{\partial v}{\partial t})^2+(\frac{\partial w}{\partial t})^2]+\dot{\ell}_0{}^2[(\frac{\partial u}{\partial y_c})^2 \\
& + 2(\frac{\partial v}{\partial y_c})+(\frac{\partial w}{\partial y_c})^2]+2\dot{\ell}_0[\frac{\partial u}{\partial t}\,\frac{\partial u}{\partial y_c} + \frac{\partial v}{\partial t}\,\frac{\partial v}{\partial y_c} + \frac{\partial w}{\partial t}\,\frac{\partial w}{\partial y_c} \\
& - 2(\dot{\theta}+\dot{\alpha})s\gamma(u\,\frac{\partial w}{\partial t} - w\,\frac{\partial u}{\partial t})+2(y_c+v)[(\dot{\theta}+\dot{\alpha})c\gamma\,\frac{\partial w}{\partial t} \\
& - \dot{\gamma}\,\frac{\partial u}{\partial t}]+2(\dot{\theta}+\dot{\alpha})s\gamma y_c[\dot{\gamma}w+(\dot{\theta}+\dot{\alpha})c\gamma u]+2\,\frac{\partial v}{\partial t}\,[u\dot{\gamma} \\
& - (\dot{\theta}+\dot{\alpha})c\gamma w]\}dy_c
\end{aligned} \tag{C.16}$$

APPENDIX D

In this appendix γ, v, w equations are derived.

D.1 DEVELOPMENT OF γ EQUATION

The procedure is similar to the development of α equation. Let us define

$$\delta_\gamma L = L(\alpha,\gamma+s\gamma,u,v,w,\ell_0)-L(\alpha,\gamma,u,v,w,\ell_0) \tag{D.1}$$

Only γ has a generalized virtual displacement.

Using (2.10.3), (2.9.17-19) and (2.9.9-11)

$$\begin{aligned}\delta_\gamma L = \{&-[(1+2\frac{v(\ell_0,t)}{\ell_0})M_b+\frac{1}{3}M_c][(\dot\alpha+\dot\theta)^2 s\gamma c\gamma+\frac{3\dot\theta^2}{1+ec\theta}]\ell_0^2\\
&-3\rho_c\frac{\dot\theta^2}{(1+ec\theta)}c^2\alpha\int_0^{\ell_0} y_c[s(2\gamma)v-c(2\gamma)u-s\gamma tg\alpha w]dy_c\\
&+\rho_c[2\dot\ell_0 s\gamma(\dot\theta+\dot\alpha)\int_0^{\ell_0} w dy_c-2(\dot\theta+\dot\alpha)^2 s\gamma c\gamma\int_0^{\ell_0} y_c v dy_c\\
&+(\dot\theta+\dot\alpha)c\gamma\int_0^{\ell_0}(u\frac{\partial w}{\partial t}-w\frac{\partial u}{\partial t})dy_c-(\dot\theta+\dot\alpha)s\gamma\int_0^{\ell_0}(y_c+v)\frac{\partial w}{\partial t}dy_c\\
&+(\dot\theta+\dot\alpha)c\gamma\dot\gamma\int_0^{\ell_0} y_c w dy_c+(\dot\theta+\dot\alpha)^2 c(2\gamma)\int_0^{\ell_0} y_c u\, dy_c\\
&+(\dot\theta+\dot\alpha)s\gamma\int_0^{\ell_0} w\frac{\partial v}{\partial t}dy_c]\}\delta\gamma+\{[(1+\frac{2v(\ell_0,t)}{\ell_0})M_b+\frac{1}{3}M_c]\dot\gamma\\
&+\rho_c[2\dot\ell_0\int_0^{\ell_0} u\, dy_c+2\dot\gamma\int_0^{\ell_0} y_c v\, dy_c-\int_0^{\ell_0}(y_c+v)\frac{\partial u}{\partial t}dy_c\\
&+(\dot\theta+\dot\alpha)s\gamma\int_0^{\ell_0} y_c w\, dy+\int_0^{\ell_0} u\frac{\partial v}{\partial t}dy_c\}\delta\dot\gamma\end{aligned} \tag{D.2}$$

Integrating $\delta_\gamma L$ with respect to time from t_1 to t_2 and noticing that

$$\delta\gamma(t_1)=\delta\gamma(t_2)\equiv 0 \tag{D.3}$$

$$\delta\dot\gamma=\frac{d}{dt}(\delta\gamma) \tag{D.4}$$

one obtains

$$\int_{t_1}^{t_2} [A_\gamma]\delta\gamma \, dt = \int_{t_1}^{t_2} Q_\gamma \, \delta\gamma \, dt \tag{D.5}$$

where A_γ is defined below and Q_γ is the generalized force corresponding to γ, which is derived in Chapter 3.

Since γ is an independent generalized coordinate, $\delta\gamma$ is arbitrary and the above equation can be satisfied if and only if

$$A_\gamma = Q_\gamma \tag{D.6}$$

This will lead to the γ equation . The final γ equation after ignoring the trivial terms is given by

$$\begin{aligned}
&\ddot{\gamma}\{M_b\ell_0{}^2 + \frac{\rho_c}{3}\ell_0{}^3\} + \dot{\gamma}\{2M_b\ell_0(\dot{\ell}_0 + \frac{\partial v(\ell_0,t)}{\partial t} + \rho_c\ell_0{}^2\dot{\ell}_0\} \\
&+ (\dot{\alpha}+\dot{\theta})^2 s\gamma c\gamma(M_b\ell_0{}^2 + \frac{1}{3}\rho\ell_0{}^3) + \frac{3\dot{\theta}^2}{(1+ec\theta)} c^2\alpha s\gamma c\gamma\ell_0{}^2[M_b \\
&+ \frac{1}{3}\rho_c\ell_0) + \rho_c\,[2\dot{\ell}_0\int_0^{\ell_0} u\,dy_c] + 2\frac{d}{dt}[\dot{\gamma}\int_0^{\ell_0} y_c\, v\, dy_c] \\
&+ (\dot{\theta}+\dot{\alpha})s\gamma\int_0^{\ell_0} y_c\frac{\partial w}{\partial t}dy_c - \frac{d}{dt}\int_0^{\ell_0} y_c\frac{\partial u}{\partial t}dy_c \\
&+ \frac{d}{dt}[(\dot{\theta}+\dot{\alpha})s\gamma\int_0^{\ell_0} y_c\, w\, dy_c\} = Q_\gamma
\end{aligned} \tag{D.7}$$

D.2 DEVELOPMENT OF w EQUATION

Let us define

$$\delta_w L = L(\alpha,\gamma,u,v,w+\delta w,\ell_0) - L(\alpha,\gamma,u,v,w,\ell_0) \tag{D.8}$$

Only w has virtual displacement δw.

Using (2.10.3), (2.9.17-19) and (2.9.9-11),

$$\int_{t_1}^{t_2} \delta_w L dt = \rho_c\{ \int_{t_1}^{t_2}\int_0^{\ell_0} \frac{\partial w}{\partial t}\frac{\partial}{\partial t}\delta w dy_c\, dt + \int_{t_1}^{t_2} \dot{\ell}_0{}^2 \int_0^{\ell_0} \frac{\partial w}{\partial y_c}\frac{\partial}{\partial y_c}\delta w dy_c dt$$

$$+ \int_{t_1}^{t_2} \dot{\ell}_0 \int_0^{\ell_0} (\frac{\partial}{\partial t}\delta w \frac{\partial w}{\partial y_c} + \frac{\partial}{\partial t} w \frac{\partial}{\partial y_c}\delta w) dy_c\, dt$$

$$+ \int_{t_1}^{t_2} (-2)\dot{\ell}_0(\dot{\theta}+\dot{\alpha})c\gamma \int_0^{\ell_0} \delta w dy_c\, dt + \int_{t_1}^{t_2} (\dot{\theta}+\dot{\alpha})s\gamma \int_0^{\ell_0} (u \frac{\partial}{\partial t}\delta w$$

$$- \frac{\partial u}{\partial t}\delta w) dy_c\, dt + \int_{t_1}^{t_2} (\dot{\theta}+\dot{\alpha})c\gamma \int_0^{\ell_0} (y_c+v)\frac{\partial}{\partial t}\delta w\, dy_c\, dt$$

$$+ \int_{t_1}^{t_2} (\dot{\theta}+\dot{\alpha})s\gamma\dot{\gamma} \int_0^{\ell_0} y_c\, \delta w\, dy_c\, dt - \int_{t_1}^{t_2} (\dot{\theta}+\dot{\alpha})c\gamma \int_0^{\ell_0} \frac{\partial v}{\partial t}\delta w\, dy_c\, dt\}$$

$$- EA \int_{t_1}^{t_2}\int_0^{\ell_0} \{\frac{\partial v}{\partial y_c} + \frac{1}{2}[(\frac{\partial u}{\partial y_c}) + (\frac{\partial w}{\partial y_c})^2]\}\frac{\partial w}{\partial y_c}\frac{\partial}{\partial y_c}\delta w\, dy_c\, dt$$

$$- \int_{t_1}^{t_2} \frac{\dot{\theta}^2}{(1+ec\theta)} \int_0^{\ell_0} 3\rho_c c\gamma c\alpha s\alpha \delta w y_c dy_c dt = \int_{t_1}^{t_2} \delta_w W_{np}\, dt$$

$$= - \int_{t_1}^{t_2}\int_0^{\ell_0} Q_w\, dy_c\, dt \qquad (D.9)$$

where Q_w is the generalized force acting on element dy_c of the tether corresponding to w.

Note that

$$\delta w(y_c,t_1) = \delta w(y_c,t_2) \equiv 0 \quad \text{for } y_c \in (0,\ell_0) \qquad (D.10)$$

and the geometric boundary conditions are given by

$$w(0,t) = w(\ell_0,t) = 0 \qquad (D.11)$$

Hence

$$\delta w(0,t) = \delta w(\ell_0,t) = 0 \tag{D.12}$$

Using partial integration law and the above-mentioned conditions (D.10) and (D.12), one obtains

$$\int_{t_1}^{t_2}\int_0^{\ell_0} \{A_w\}\delta w \, dy_c \, dt = \int_{t_1}^{t_2}\int_0^{\ell_0} Q_w \, dy_c \, \delta w \, dt \tag{D.13}$$

Since w is independent, δw is arbitrary. Equation (D.13) can be satisfied if and only if

$$A_w = Q_w \tag{D.14}$$

Finally, one obtains w equation as follows

$$\begin{aligned}
&\frac{D^2}{Dt^2} w+2(\dot{\theta}+\dot{\alpha})[c\gamma(\dot{\ell}_0+ \frac{\partial v}{\partial t})+s\gamma \frac{\partial u}{\partial t}]+ y_c \frac{\partial}{\partial t} [(\dot{\theta}+\dot{\alpha})c\gamma] \\
&\quad - (\dot{\theta}+\dot{\alpha})s\gamma\dot{\gamma}y_c-EA \frac{\partial}{\partial y_c} \{\frac{\partial w}{\partial y_c} [\frac{\partial v}{\partial y_c} + \frac{1}{2}\overline{(\frac{\partial u}{\partial y_c})^2+(\frac{\partial w}{\partial y_c})^2}]\} \\
&\quad + 3 \frac{\dot{\theta}^2}{(1+ec\theta)} s\alpha c\alpha c\gamma y_c = Q_w
\end{aligned} \tag{D.15}$$

where

$$\frac{D[\ ]}{Dt} = (\frac{\partial}{\partial t} + \dot{\ell}_0 \frac{\partial}{\partial y_c})[\ ] \tag{D.16}$$

D.3 DEVELOPMENT OF v EQUATION

Similarly, let us define

$$\delta_v L = L(\alpha,\gamma,u,v+\delta v,w,\ell_0)-L(\alpha,\gamma,u,v,w,\ell_0) \tag{D.17}$$

Using (2.10.3), (2.9.17-19) and (2.9.9-11),

$$\int_{t_1}^{t_2} \delta_v L dt = \int_{t_1}^{t_2} M_b[(\dot{\alpha}+\dot{\theta})^2 c^2\gamma+\dot{\gamma}^2]\ell_0 \delta v(\ell_0,t)dt$$

$$+ \int_{t_1}^{t_2} M_b\dot{\ell}_0{}^2 \frac{\partial\delta v(\ell_0,t)}{\partial y_c} dt + \int_{t_1}^{t_2} M_b\dot{\ell}_0\delta_v[(1 + \frac{\partial v(\ell_0,t)}{\partial y_c})\frac{\partial v(\ell_0,t)}{\partial t}]dt$$

$$+ \int_{t_1}^{t_2} M_b \frac{\partial v(\ell_0,t)}{\partial t} \frac{\partial}{\partial t} \delta v(\ell_0,t)dt+\rho_c\{\int_{t_1}^{t_2}\int_0^{\ell_0} \frac{\partial v}{\partial t}\frac{\partial}{\partial t}\delta v dy_c dt$$

$$+ \int_{t_1}^{t_2} \dot{\ell}_0{}^2 \int_0^{\ell_0} \frac{\partial\delta v}{\partial y_c} dy_c\ dt + \int_{t_1}^{t_2} \dot{\ell}_0 \int_0^{\ell_0} \frac{\partial}{\partial t}\delta v\ dy_c\ dt$$

$$+ \int_{t_1}^{t_2} \dot{\ell}_0 \int_0^{\ell_0} [\frac{\partial v}{\partial y_c}\frac{\partial\delta v}{\partial t} + \frac{\partial v}{\partial t}\ \frac{\partial}{\partial y_c}\delta v]dy_c dt+ \int_{t_1}^{t_2} [(\dot{\theta}+\dot{\alpha})^2c^2\gamma$$

$$+ \dot{\gamma}^2] \int_0^{\ell_0} y_c\delta v dy_c dt+ \int_{t_1}^{t_2} [(\dot{\theta}+\dot{\alpha})c\gamma\frac{\partial w}{\partial t} - \dot{\gamma}\frac{\partial u}{\partial t}] \int_0^{\ell_0} \delta v dy_c dt$$

$$+ \int_{t_1}^{t_2}\int_0^{\ell_0} [u\dot{\gamma}-(\dot{\theta}+\dot{\alpha})c\gamma w] \frac{\partial\delta v}{\partial t} dy_c dt\}-EA \int_{t_1}^{t_2}\int_0^{\ell_0} \{\frac{\partial v}{\partial y_c}$$

$$+ \frac{1}{2} [(\frac{\partial u}{\partial y_c})^2+(\frac{\partial w}{\partial y_c})^2]\} \frac{\partial}{\partial y_c}\delta v dy_c dt- \int_{t_1}^{t_2} \frac{\dot{\theta}^2}{(1+ec\theta)} (1$$

$$- 3c^2\alpha c^2\gamma)M_b\ell_0\delta v(\ell_0,t)dt-\rho_c \int_{t_1}^{t_2} \frac{\dot{\theta}^2}{(1+ec\theta)} (1-3c^2\alpha c^2\gamma)\int_0^{\ell_0} y_c\delta v dy_c dt$$

$$= - \int_{t_1}^{t_2} \delta_v\ w_{np}\ dt \tag{D.18}$$

Note that

$$\delta v(y_c,t_1) = \delta v(y_c,t_2) \equiv 0 \tag{D.19}$$

As for the boundary conditions, we only have one geometric boundary condition at one end of the tether near the shuttle, i.e.,

$$v(0,t) = 0 \tag{D.20}$$

Hence

$$\delta v(0,t) = 0 \tag{D.21}$$

However, at the other end of the tether, a satellite is hung and it can move up and down freely. There is no geometric boundary condition available. Therefore

$$\delta v(\ell_0,t) \neq 0 \tag{D.22}$$

generally.

Using the partial integral law carefully (i.e., remembering that the order of integration with respect to time t and spatial coordinate y_c are not exchangible), one obtains

$$\begin{aligned}&\int_{t_1}^{t_2}\int_0^{\ell_0} \{A_v\}\delta v(y_c,t)dy_c dt + \int_{t_1}^{t_2} \{\overline{A}_v\}\delta v(\ell_0,t)dt \\ &\quad = \int_{t_1}^{t_2}\int_0^{\ell_0} Q_v dy_c dt + \int_{t_1}^{t_2} \overline{Q}_v\, dt\end{aligned} \tag{D.23}$$

where Q_v and $\overline{Q}_v$ are the generalized forces corresponding to $\delta v(y_c,t)$ and $\delta v(\ell_0,t)$ respectively. Since $v(y_c,t)$ and $v(\ell_0,t)$ are independent, $\delta v(y_c,t)$ and $\delta v(\ell_0,t)$ are arbitrary. The above equation can be satisfied if and only if

$$A_v = Q_v \tag{D.24}$$

and

$$\bar{A}_v = \bar{Q}_v \tag{D.25}$$

(D.25) gives a dynamic boundary condition at satellite end of the tether.

Finally, one obtains v equation as well as the dynamic boundary condition at satellite end of the tether as

$$\rho_c \frac{D^2}{Dt^2}[\ell_0+v(y,t)]-\rho_c[(\dot{\alpha}+\dot{\theta})^2c^2\gamma+\dot{\gamma}^2$$
$$+\frac{(3c^2\alpha c^2\gamma-1)\dot{\theta}^2}{(1+ec\theta)}]y_c-2\rho_c\frac{\partial}{\partial t}[(\dot{\theta}+\dot{\alpha})c\gamma w-\dot{\gamma}u]$$
$$-EA\frac{\partial}{\partial y_c}\{\frac{\partial v}{\partial y_c}+\frac{1}{2}[(\frac{\partial u}{\partial y_c})^2+(\frac{\partial w}{\partial y_c})^2]\} = Q_v \tag{D.26}$$

and

$$M_b[(\dot{\alpha}+\dot{\theta})^2c^2\gamma+\dot{\gamma}^2]\ell_0-M_b\frac{D^2}{Dt^2}[\ell_0+v(\ell_0,t)]$$
$$-\frac{\dot{\theta}^2}{(1+ec\theta)}M_b(1-3c^2\alpha c^2\gamma)\ell_0-EA\{\frac{\partial v(\ell_0,t)}{\partial y_c}+\frac{1}{2}[(\frac{\partial u(\ell_0,t)}{\partial y_c})^2$$
$$+(\frac{\partial w(\ell_0,t)}{\partial y_c})^2]\} = -\bar{Q}_v \tag{D.27}$$

It is not difficult to see that equation (D.27) expresses a force equilibrium at the satellite's end of the tether.

APPENDIX E

Let Γ_1 and Γ_2 be the lines of intersection of the orbital plane with the equatorial plane and earth's surface, respectively [See Fig. 3.2(b)]. $_1$ and $_2$ are in the orbital plane. From P, a point on Γ_2, draw a vertical line to the equatorial plane cutting it at H. PH is perpendicular to the equatorial plane. From P also draw a line perpendicular to $_1$, and intersect it at F; plane FPH is exactly perpendiculat to EF. Hence

$$\measuredangle PFH = i$$

now

$$EHsj = PH = FHsi \approx EHs\theta si$$

Hence,

$$sj = si\ s\theta \tag{E.1}$$

Cutting the earth vertically through E.P.H., we get an ellipse representing the shape of the surface. r_{earth} satisfies the equation

$$\frac{(r_{earth}\ cj)^2}{a_0{}^2} + \frac{(r_{earth}\ sj)^2}{b_0{}^2} = 1$$

Thus

$$r_{earth} = a_0 b_0 (b_0{}^2 c^2 j + a_0{}^2 s^2 j)^{-\frac{1}{2}} \tag{E.2}$$

Substituting (E.1) in (E.2),

$$r_{earth} = a_0 b_0 [a_0{}^2 s^2 i s^2 \theta + b_0{}^2 (1 - s^2 i s^2 \theta)]^{-\frac{1}{2}} \tag{E.3}$$

The altitude of any arbitrary point on the tether with the coordinate y_c is easily obtained [see Fig. 3.2(a)] as

$$h = (R_0 - r_{earth} - y_c\ c\alpha\ c\gamma)(\vec{n}\cdot\vec{e}_r) \tag{E.4}$$

where $\vec{n}$ is a unit vector normal to the earth's surface and $\vec{e}_r$ a unit vector along $\vec{R}_0$ direction. Let

$$\vec{n}\cdot\vec{e}_r = \cos\ \xi \tag{E.5}$$

We have

$$tg\ \xi = \frac{1}{r_{earth}}\ \frac{dr_{earth}}{d\theta} \tag{E.6}$$

Thus

$$\vec{n}\cdot\vec{e}_r = \cos\ \xi\ = 1/(1+tg^2\xi)^{\frac{1}{2}} = 1/[1+\frac{1}{r^2_{earth}}\ (\frac{dr_{earth}}{d\theta})^2\ ]^{\frac{1}{2}}$$

while using (E.3),

$$\frac{1}{r_{earth}}\frac{dr_{earth}}{d\theta} = -\ \frac{(a_0{}^2-b_0{}^2)s^2is\theta c\theta}{[(a_0{}^2-b_0{}^2)s^2ic^2\theta+b_0{}^2]} \tag{E.7}$$

Finally, we get

$$h = (R_0 - r_{earth} - y_c\ c\alpha c\gamma)\{1+(a_0{}^2-b_0{}^2)^2s^4is^2\theta c^2\theta$$
$$/[b_0{}^2+(a_0{}^2-b_0{}^2)s^2ic^2\theta]^2\}^{\frac{1}{2}} \tag{E.8}$$

APPENDIX F

α equation

Using the expressions for u, v and w given by (4.1.4), (4.1.5) and (4.1.6) along with (4.1.7) and (4.1.14), one can work out the following integral terms appearing in the α equation (2.11.1):

(i) $$-2\rho_c \frac{d}{dt}\{\dot{\ell}_0 c\gamma \int_0^{\ell_0} y_c \frac{\partial w}{\partial t} dy_c\} =$$

$$-\frac{2\sqrt{2}\nu}{\pi} \sum_{i=1}^{n} \{[1-(-1)^i]/i\}\{(\eta''-F\eta'+3\eta'^2)c\gamma-\eta'\gamma's\gamma]B_i$$

$$+\eta' c\gamma B_i'\}M_b \ell_0^2 \dot{\theta}^2 \qquad \text{(F.1)}$$

(ii) $$\rho_c \frac{d}{dt}\{c\gamma \int_0^{\ell_0} y_c \frac{\partial w}{\partial t} dy_c\}+\rho_c \frac{d}{dt}\{s\gamma\dot{\gamma} \int_0^{\ell_0} y_c\, w\, dy_c\}$$

$$= -\sqrt{2}(-1)^i \nu/i\pi\{c\gamma[B_i''+3(\eta''-F\eta'+3\eta'^2)B_i$$

$$+(6\eta'-F)B_i']+[c\gamma\gamma'^2+s\gamma(\gamma''-F\gamma')B_i\}M_b \ell_0^2 \dot{\theta}^2 \qquad \text{(F.2)}$$

(iii) $$2\rho_c \frac{d}{dt}\{(\dot{\theta}+\dot{\alpha})c^2\gamma \int_0^{\ell_0} y_c\, v\, dy_c\}$$

$$= 2\nu\{[(\alpha''-F-F\alpha')c^2\gamma-2s\gamma c\gamma\gamma'(1+\alpha')+3\eta'(1+\alpha')c^2\gamma]$$

$$\sum_{i=1}^{n} \frac{C_i}{(2i+1)} + (1+\alpha')^2 c^2\gamma \sum_{i=1}^{n} \frac{C_i'}{(2i+1)}\}M_b \ell_0^2 \dot{\theta}^2 \qquad \text{(F.3)}$$

(iv) $$2\rho_c \frac{d}{dt}\{(\dot{\theta}+\dot{\alpha})s\gamma c\gamma \int_0^{\ell_0} y_c\, u\, dy_c\}$$

$$= -(\frac{2\sqrt{2}}{\pi}\nu) \sum_{i=1}^{n} [\frac{(-1)^i}{i}]\{[(\alpha''-F-F\alpha')s\gamma c\gamma+(1+\alpha')c(2\gamma)\gamma'$$

$$+3(1+\alpha')s\gamma c\gamma\eta']A_i+(1+\alpha')s\gamma c\gamma A_i'\}M_b \ell_0^2 \dot{\theta}^2 \qquad \text{(F.4)}$$

where ν and η are defined in the equations (4.2.13) and (4.2.10). Substituting (F.1)-(F.4) into (2.11.1) and divided by $M_b\, \ell_0{}^2\, \dot{\theta}^2$, we will have equation (4.2.12) which is given in the thesis.

<u>A_m equation</u>

Using (2.10.18), equation (4.2.3) becomes

$$\int_0^{\ell_0} \{\frac{D^2}{Dt^2} u - 2(\dot{\ell}_0 + \frac{\partial v}{\partial t})\dot{\gamma} - 2(\dot{\theta}+\dot{\alpha}) s\gamma \frac{\partial w}{\partial t} - [\ddot{\gamma} + (\dot{\theta}+\dot{\alpha})^2 \frac{S(2\gamma)}{2}] y_c$$

$$- \frac{EA}{\rho_c} \frac{\partial}{\partial y_c} [(\frac{\partial u}{\partial y_c})\{\frac{\partial v}{\partial y_c} + \frac{1}{2} [(\frac{\partial u}{\partial y_c}) + (\frac{\partial w}{\partial y_c})^2]\}]$$

$$- \frac{Q_{ua}}{\rho_c}\} \sin \frac{m\pi y_c}{\ell_0} dy_c = 0 \tag{F.5}$$

Since

$$u = \sqrt{2}\, \tilde{A}_n \sin \frac{n\pi y_c}{\ell_0} \tag{F.6}$$

$$w = \sqrt{2}\, \tilde{B}_n \sin \frac{n\pi y_c}{\ell_0} \qquad n = 1,2...N \tag{F.7}$$

$$v = \tilde{C}_1 y_c + \tilde{C}_i\, y_c{}^3 \tag{F.8}$$

where $\tilde{A}_n$, $\tilde{B}_n$ are dimensional quantities,

$$\tilde{A}_n = A_n\, \ell_0 \tag{F.9}$$

$$\tilde{B}_n = B_n\, \ell_0 \tag{F.10}$$

and summation convention is assumed for simplicity, i.e., summation is carried out with respect to a dummy index n. With the above, we have

$$\frac{\partial u}{\partial y_c} = \sqrt{2}\ (\frac{n\pi}{\ell_0})\tilde{A}_n \cos\frac{n\pi y_c}{\ell_0} \tag{F.11}$$

$$\frac{\partial w}{\partial y_c} = \sqrt{2}\ (\frac{n\pi}{\ell_0})\tilde{B}_n \cos\frac{n\pi y_c}{\ell_0} \tag{F.12}$$

$$\frac{\partial u}{\partial t} = \sqrt{2}\ \dot{\tilde{A}}_n \sin\frac{n\pi y_c}{\ell_0} - \sqrt{2}\ \tilde{A}_n(\frac{\dot{\ell}_0}{\ell_0})(\frac{n\pi y_c}{\ell_0}) \cos\frac{n\pi y_c}{\ell_0} \tag{F.13}$$

$$\frac{\partial w}{\partial t} = \sqrt{2}\ \dot{\tilde{B}}_n \sin\frac{n\pi y_c}{\ell_0} - \sqrt{2}\ \tilde{B}_n(\frac{\dot{\ell}_0}{\ell_0})(\frac{n\pi y_c}{\ell_0}) \cos\frac{n\pi y_c}{\ell_0} \tag{F.14}$$

$$\begin{aligned}\frac{\partial^2 u}{\partial t^2} = {} & \sqrt{2}\ \ddot{\tilde{A}}_n \sin\frac{n\pi y_c}{\ell_0} - 2\sqrt{2}\ \dot{\tilde{A}}_n(\frac{\dot{\ell}_0}{\ell_0})(\frac{n\pi y_c}{\ell_0}) \cos\frac{n\pi y_c}{\ell_0} \\ & - \sqrt{2}\ \tilde{A}_n(\frac{n\pi y_c}{\ell_0})[\frac{\ddot{\ell}_0}{\ell_0} - 2(\frac{\dot{\ell}_0}{\ell_0})^2]\cos\frac{n\pi y_c}{\ell_0} \\ & - \sqrt{2}\ \tilde{A}_n(\frac{n\pi y_c}{\ell_0})^2(\frac{\dot{\ell}_0}{\ell_0})^2 \sin\frac{n\pi y_c}{\ell_0}\end{aligned} \tag{F.15}$$

$$\begin{aligned}\frac{\partial^2 w}{\partial t^2} = {} & \sqrt{2}\ \ddot{\tilde{B}}_n \sin\frac{n\pi y_c}{\ell_0} - 2\sqrt{2}\ \dot{\tilde{B}}_n(\frac{\dot{\ell}_0}{\ell_0})(\frac{n\pi y_c}{\ell_0})\cos\frac{n\pi y_c}{\ell_0} \\ & - \sqrt{2}\ \tilde{B}_n(\frac{n\pi y_c}{\ell_0})[\frac{\ddot{\ell}_0}{\ell_0} - 2(\frac{\dot{\ell}_0}{\ell_0})^2]\cos\frac{n\pi y_c}{\ell_0} \\ & - \sqrt{2}\ \tilde{B}_n(\frac{n\pi y_c}{\ell_0})^2(\frac{\dot{\ell}_0}{\ell_0})^2 \sin\frac{n\pi y_c}{\ell_0}\end{aligned} \tag{F.16}$$

$$\frac{\partial^2 u}{\partial y \partial t} = \sqrt{2}\ \{\dot{\tilde{A}}_n\left(\frac{n\pi}{\ell_0}\right)\cos\frac{n\pi y_c}{\ell_0} + \tilde{A}_n\left[-\frac{n\pi}{\ell_0}\left(\frac{\dot{\ell}_0}{\ell_0}\right)\cos\frac{n\pi y_c}{\ell_0}\right.$$

$$\left. + \left(\frac{n\pi}{\ell_0}\right)^2\left(\frac{\dot{\ell}_0}{\ell_0}\right) y_c \sin\frac{n\pi y_c}{\ell_0}\right]\} \tag{F.17}$$

$$\frac{\partial^2 w}{\partial y \partial t} = \sqrt{2}\ \{\dot{\tilde{B}}_n\left(\frac{n\pi}{\ell_0}\right)\cos\frac{n\pi y_c}{\ell_0} + \tilde{B}_n\left[-\frac{n\pi}{\ell_0}\left(\frac{\dot{\ell}_0}{\ell_0}\right)\cos\frac{n\pi y_c}{\ell_0}\right.$$

$$\left. + \left(\frac{n\pi}{\ell_0}\right)^2\left(\frac{\dot{\ell}_0}{\ell_0}\right) y_c \sin\frac{n\pi y_c}{\ell_0}\right]\} \tag{F.18}$$

where $n = 1,2\ldots N$, and

$$\frac{\partial v}{\partial y_c} = \tilde{C}_1 + 3\ \tilde{C}_2\ y_c{}^2 \tag{F.19}$$

$$\frac{\partial v}{\partial t} = \dot{\tilde{C}}_1\ y_c + \dot{\tilde{C}}_2\ y_c{}^3 \tag{F.20}$$

With above, the integral in equation (F.5) can be carried out term by term without difficulty although the algebra is tedious. Since

$$\frac{D}{Dt}(\ ) = \left(\frac{\partial}{\partial t} + \dot{\ell}_0\frac{\partial}{\partial y_c}\right)(\quad) \tag{F.21}$$

$$\frac{D^2}{Dt^2}(\ ) = \left(\frac{\partial}{\partial t} + \dot{\ell}_0\frac{\partial}{\partial y_c}\right)\left(\frac{\partial}{\partial t} + \dot{\ell}_0\frac{\partial}{\partial y_c}\right)(\quad)$$

$$= \frac{\partial^2}{\partial t^2} + 2\dot{\ell}_0\frac{\partial^2}{\partial t \partial y_c} + \ddot{\ell}_0\frac{\partial}{\partial y_c} + \dot{\ell}_0{}^2\frac{\partial^2}{\partial y_c{}^2} \tag{F.22}$$

The first term in the equation (F.5) can be integrated now using (F.22). We have,

(i) $$\int_0^{\ell_0} \frac{\partial^2 u}{\partial t^2} \sqrt{2} \sin \frac{m\pi y_c}{\ell_0} dy_c = \ell_0 \{\ddot{\tilde{A}}_m - 4\dot{\tilde{A}}_n (\frac{\dot{\ell}_0}{\ell_0})(C_{mn}$$

$$- 2\tilde{A}_n [\frac{\ddot{\ell}_0}{\ell_0} - 2(\frac{\dot{\ell}_0}{\ell_0})^2] C_{mn} - 2\tilde{A}_n (\frac{\dot{\ell}_0}{\ell_0})^2 D_{mn}\} \tag{F.23}$$

where

$$C_{mn} = \begin{cases} -\frac{m}{4} & , \quad n = m \\ -\frac{mn}{(m^2-n^2)} (-1)^{m+n}, & n \neq m \end{cases} \tag{F.24}$$

and

$$D_{mn} = \begin{cases} (\frac{\pi^2}{6} m^2 - \frac{1}{4}) & , \quad n = m \\ \frac{4mn^2}{(m^2-n^2)^2} (-1)^{m+n}, & n \neq m \end{cases} \tag{F.25}$$

(ii) $$\int_0^{\ell_0} \ell_0^2 \frac{\partial^2 u}{\partial y_c^2} \sqrt{2} \sin \frac{m\pi y}{\ell_0} dy_c = -\dot{\ell}_0^2 (\frac{m\pi}{\ell_0})^2 \tilde{A}_m \ell_0 \tag{F.26}$$

(iii) $$\int_0^{\ell_0} \ddot{\ell}_0 \frac{\partial u}{\partial y_c} \sqrt{2} \sin \frac{m\pi y_c}{\ell_0} dy_c = \ddot{\ell}_0 \tilde{A}_n E_{mn} \tag{F.27}$$

where

$$E_{mn} = \begin{cases} 0 & , \quad m + n = \text{even} \\ \frac{4mn}{m^2-n^2} & , \quad m + n = \text{Odd} \end{cases} \tag{F.28}$$

(iv) $$\int_0^{\ell_0} 2\dot{\ell}_0 \frac{\partial^2 u}{\partial y_c \partial t} \sqrt{2} \sin \frac{m\pi y_c}{\ell_0} dy_c = 2\dot{\ell}_0[\dot{\tilde{A}}_n - (\frac{\dot{\ell}_0}{\ell_0})\tilde{A}_n]E_{mn}$$

$$+4\dot{\ell}_0{}^2/\ell_0 \tilde{A}_n F_{mn} \quad \text{(F.29)}$$

where

$$F_{mn} = \begin{cases} 0 & , \quad m + n = \text{even} \quad n \neq m \\ \frac{m^2\pi^2}{4} & , \quad n = m \\ \frac{-4mn^3}{(m^2-n^2)^2} & , \quad m + n = \text{odd} \end{cases} \quad \text{(F.30)}$$

The other integrals are:

(v) $$\int_0^{\ell_0} - 2\dot{\ell}_0 \dot{\gamma} \sqrt{2} \sin \frac{m\pi y_c}{\ell_0} dy_c = 2\sqrt{2} \dot{\ell}_0 \dot{\gamma}/m\pi[(-1)^m-1]\ell_0 \quad \text{(F.31)}$$

(vi) $$\int_0^{\ell_0} -y_c\ddot{\gamma}\sqrt{2} \sin \frac{m\pi y_c}{\ell_0} dy_c = \sqrt{2} \ddot{\gamma} \ell_0{}^2(-1)^m/m\pi \quad \text{(F.32)}$$

(vii) $$\int_0^{\ell_0} - y_c(\dot{\alpha}+\dot{\theta})^2 s\gamma c\gamma\sqrt{2} \sin \frac{m\pi y_c}{\ell_0} dy_c$$

$$= \sqrt{2}(\dot{\alpha}+\dot{\theta})^2 s\gamma c\gamma \ell_0{}^2(-1)^m/m\pi \quad \text{(F.33)}$$

(viii) $$\int_0^{\ell_0} - 2 \frac{\partial v}{\partial t} \dot{\gamma} \sqrt{2} \sin \frac{m\pi y_c}{\ell_0} dy_c$$

$$= -2\sqrt{2} \dot{\gamma}\{\dot{\tilde{C}}_1 \dot{\ell}_0{}^2(-1)^{m+1}/m\pi+\dot{\tilde{C}}_2 \ell_0{}^4[\frac{(-1)^{m+1}}{m\pi}$$

$$+ \frac{6(-1)^m}{m^3} \frac{1}{\pi^3}]\} \quad \text{(F.34)}$$

$$\text{(ix)} \quad \int_0^{\ell_0} -3\,\frac{\dot{\theta}^2}{(1+ec\theta)}\,c^2\alpha s\gamma c\gamma y_c\sqrt{2}\,\sin\frac{m\pi y_c}{\ell_0}\,dy_c$$

$$= -3\sqrt{2}\,\dot{\theta}^2/(1+ec\theta)c^2\alpha s\gamma c\gamma\,\ell_0{}^2(-1)^{m+1}/(m\pi) \tag{F.35}$$

$$\text{(x)} \quad \int_0^{\ell_0} -\frac{EA}{\rho_c}\frac{\partial}{\partial y_c}\{\frac{\partial u}{\partial y_c}\{\frac{\partial v}{\partial y_c}+\frac{1}{2}[(\frac{\partial u}{\partial y_c})^2+(\frac{\partial w}{\partial y_c})^2]\}\}\sqrt{2}\,\sin\frac{m\pi y_c}{\ell_0}\,dy_c$$

This integral is rather complex. Integrating by parts, it turns out to be

$$= \sqrt{2}\,\frac{EA}{\rho_c}\frac{m\pi}{\ell_0}[\int_0^{\ell_0}\frac{\partial u}{\partial y_c}\frac{\partial v}{\partial y_c}\cos\frac{m\pi y_c}{\ell_0}\,dy_c$$

$$+\frac{1}{2}\int_0^{\ell_0}\frac{\partial u}{\partial y_c}[(\frac{\partial u}{\partial y_c})^2+(\frac{\partial w}{\partial y_c})^2]\cos\frac{m\pi y_c}{\ell_0}\,dy_c]$$

$$= \sqrt{2}\,\frac{EA}{\rho_c}\,m\pi\,[I_1+I_2] \tag{F.36}$$

$$I_1 = \frac{1}{\ell_0}\int_0^{\ell_0}\frac{\partial u}{\partial y_c}\frac{\partial v}{\partial y_c}\cos\frac{m\pi y_c}{\ell_0}\,dy_c$$

$$= \frac{1}{\ell_0}\int_0^{\ell_0}[\tilde{C}_1+3\tilde{C}_2\,y_c{}^2]\sqrt{2}\tilde{A}_n\frac{n\pi}{\ell_0}\cos\frac{n\pi y_c}{\ell_0}\cos\frac{m\pi y_c}{\ell_0}\,dy_c$$

$$= \sqrt{2}\,\tilde{A}_n(n\pi)/\ell_0\{\tilde{C}_1\int_0^{\ell_0}\cos\frac{n\pi y_c}{\ell_0}\cos\frac{m\pi y_c}{\ell_0}\,dy_c$$

$$+\,3\tilde{C}_2\int_0^{\ell_0}y_c{}^2\cos\frac{n\pi y_c}{\ell_0}\cos\frac{m\pi y_c}{\ell_0}\,dy_c\}$$

$$= \frac{\sqrt{2}m\pi}{2\ell_0}\tilde{A}_m\,\tilde{C}_1+3\sqrt{2}\,\tilde{C}_2(\tilde{A}_n/\ell_0)G_{mn}\,(n\pi) \tag{F.37}$$

where

$$G_{mn} = \begin{cases} \left(\frac{\pi^2}{6} m^2 + \frac{1}{4}\right) \frac{\ell_0^{\,3}}{m^2\pi^2} & , \quad n = m \\ \frac{2\ell_0^{\,3}}{(m^2-n^2)^2} (-1)^{m+n} \frac{(m^2+n^2)}{\pi^2} & , \quad n \neq m \end{cases} \tag{F.38}$$

$$I_2 = \frac{1}{2\ell_0} \int_0^{\ell_0} \frac{\partial u}{\partial y_c} \left[\left(\frac{\partial u}{\partial y_c}\right)^2 + \left(\frac{\partial w}{\partial y_c}\right)^2\right] \cos \frac{m\pi y_c}{\ell_0} \, dy_c$$

$$= \frac{1}{2\ell_0} \int_0^{\ell_0} \sqrt{2}\, \tilde{A}_n \frac{n\pi}{\ell_0} \cos \frac{n\pi y_c}{\ell_0} \left[2\, \tilde{A}_s \frac{s\pi}{\ell_0} \cos \frac{s\pi y_c}{\ell_0} \tilde{A}_k \frac{k\pi}{\ell_0} \cos \frac{k\pi y_c}{\ell_0}\right.$$

$$\left. + 2\tilde{B}_s \frac{s\pi}{\ell_0} \cos \frac{s\pi y_c}{\ell_0} \tilde{B}_k \frac{k\pi}{\ell_0} \cos \frac{k\pi y_c}{\ell_0}\right] \cos \frac{m\pi y}{\ell_0} \, dy_c$$

$$= \sqrt{2}\, \tilde{A}_n \left(\frac{n\pi}{\ell_0^{\,2}}\right)\left(\frac{s\pi}{\ell_0}\right)\left(\frac{k\pi}{\ell_0}\right)(\tilde{A}_s \tilde{A}_k + \tilde{B}_s \tilde{B}_k) \int_0^{\ell_0} \cos \frac{n\pi y_c}{\ell_0} \cos \frac{s\pi y_c}{\ell_0}$$

$$\cos \frac{k\pi y_c}{\ell_0} \cos \frac{m\pi y_c}{\ell_0} \, dy_c$$

where n, s, k are dummy indices. Let $\xi = \frac{\pi y_c}{\ell_0}$,

$$\int_0^{\ell_0} \cos \frac{n\pi y_c}{\ell_0} \cos \frac{s\pi y_c}{\ell_0} \cos \frac{k\pi y_c}{\ell_0} \cos \frac{m\pi y_c}{\ell_0} \, dy_c$$

$$= \frac{\ell_0}{\pi} \int_0^{\pi} \cos n\xi \cos s\xi \cos k\xi \cos m\xi \, d\xi$$

$$= \begin{cases} 0 & \pm m \pm n \pm s \pm k \neq 0 \\ \frac{\ell_0}{16} , & \pm m \pm n \pm s \pm k = 0 \end{cases} \tag{F.39}$$

Hence

$$I_2 = (\frac{\sqrt{2}}{16})(1/\ell_0{}^3)\pi^3 \sum_{\pm m\pm n\pm s\pm k=0} nsk\ \tilde{A}_n(\tilde{A}_s\ \tilde{A}_k + \tilde{B}_s\ \tilde{B}_k) \qquad (F.40)$$

$$(xi)\ \int_0^{\ell_0} \frac{1}{\rho_c} Q_{ua} \sin\frac{m\pi y_c}{\ell_0} dy_c = P_{AM}\ \ell_0{}^2\ \dot{\theta}^2 \qquad (F.41)$$

P_{AM} is given in (4.2.37).

Substituting the integrals from (i) to (xi) into the equation (F.5), one obtains the $\tilde{A}_m$ equation as

$$\ell_0\{\ddot{\tilde{A}}_m - 4\dot{\tilde{A}}_n(\frac{\dot{\ell}_0}{\ell_0})C_{mn} - 2\tilde{A}_n[(\frac{\ddot{\ell}_0}{\ell_0}) - 2(\frac{\dot{\ell}_0}{\ell_0})^2]C_{mn} - 2\tilde{A}_n(\frac{\dot{\ell}_0}{\ell_0})^2 D_{mn}\}$$

$$- \dot{\ell}_0{}^2(\frac{m\pi}{\ell_0})^2\tilde{A}_m\ell_0 + \ddot{\ell}_0\tilde{A}_n E_{mn} + 2\dot{\ell}_0[\dot{\tilde{A}}_n - \tilde{A}_n(\frac{\dot{\ell}_0}{\ell_0})]E_{mn}$$

$$+ 4\dot{\ell}_0{}^2/\ell_0\tilde{A}_n F_{mn} + 2\sqrt{2}\dot{\ell}_0\dot{\gamma}/m\pi[(-1)^m - 1]\ell_0 + \sqrt{2}\ddot{\gamma}\ell_0{}^2(-1)^m/(m\pi)$$

$$+ \sqrt{2}(\dot{\alpha}+\dot{\theta})^2 s\gamma c\gamma\ell_0{}^2(-1)^m/(m\pi) - 2\sqrt{2}\dot{\gamma}\{\dot{\tilde{C}}_1\ell_0{}^2(-1)^{m+1}/(m\pi)$$

$$+ \dot{\tilde{C}}_2\ell_0{}^4[(-1)^{m+1}/(m\pi) + 6(-1)^m/(m^3\pi^3)]\} + (EA\pi^2/\rho_c\ell_0)m\{m\tilde{A}_m\tilde{C}_1$$

$$+ 6\tilde{C}_2\tilde{A}_n nG_{mn} + \frac{1}{8}(\pi/\ell_0)^2 \sum_{\pm m\pm n\pm s\pm k=0} nsk(\tilde{A}_s\ \tilde{A}_k + \tilde{B}_s\tilde{B}_k)\tilde{A}_n\}$$

$$- 2(\dot{\alpha}+\dot{\theta})s\gamma\ell_0\dot{\tilde{B}}_m - 4(\dot{\alpha}+\dot{\theta})s\gamma(\frac{\dot{\ell}_0}{\ell_0})\tilde{B}_n\ell_0 C_{mn}$$

$$- [(\ddot{\alpha}+\ddot{\theta})s\gamma + \dot{\gamma}c\gamma(\dot{\alpha}+\dot{\theta})]\ell_0\tilde{B}_m = P_{AM}\ \ell_0{}^2\dot{\theta}^2 \qquad (F.42)$$

Using nondimensionalized quantities A_i, B_i, C_1, C_2, η which are defined earlier and changing independent variable t to θ, equation (F.42) can be nondimensionalized. For $i = 1, 2$, $m = 1$ gives A_1 equation while $m = 2$ yields A_2 equation, which are given in (4.2.16) and (4.2.19), respectively.

It might be noted that B_m equations are quite similar to A_m equations. C_1 and C_2 equations involve even more algebra. However, the procedure is the same. These procedures are omitted here for brevity.

APPENDIX G

The first row of the matrix [A] is determined by the length change feedback control law. Assume that the length change law has the form as

$$\eta' = C[1-K_\alpha \alpha'-K_\gamma \gamma'^2] \qquad (F.1)$$

where C is retrieval constant and K_α, K_γ are the gains. K_α, K_γ are positive while C is negative. Differentiating η' with respect to θ, we get

$$\eta'' + K_\alpha C\alpha''+2K_\gamma c\gamma'\gamma'' = 0 \qquad (F.2)$$

The first row of the matrix [A] is determined. Using equation (4.3.5), one can write that,

$$[A_{11}]_{3\times 3} = \begin{bmatrix} 1 & cK_\alpha & 2cK_\gamma \gamma' \\ -\frac{4\sqrt{2}}{\pi}\nu c\gamma B_1 + \frac{3\sqrt{2}\nu}{2\pi}(2B_1-B_2)\,, & (1+\frac{1}{3}\nu)c^2\gamma+2\nu c^2\gamma(\frac{1}{3}C_1+\frac{1}{5}C_2) + \frac{\sqrt{2}}{\pi}\nu s\gamma c\gamma(2A_1-A_2)\,, & \frac{\sqrt{2}\nu}{2\pi} s\gamma(2B_1-B_2) \\ \frac{4\sqrt{2}}{\pi}\nu A_1 - \frac{3\sqrt{2}\nu}{2\pi}(2A_1-A_2)\,, & \frac{\sqrt{2}\nu}{2\pi}s\gamma(2B_1-B_2)\,, & (1+\frac{1}{3}\nu)+2\nu(\frac{1}{3}C_1+\frac{1}{5}C_2) \end{bmatrix}$$

(F.3)

$$\{A\}_{3\times 6} = \begin{Bmatrix} 0 & 0 & 0 & 0 & 0 & 0 \\ 0 & 0 & 0 & 0 & \frac{\sqrt{2}\nu c\gamma}{\pi} & -\frac{\sqrt{2}\nu c\gamma}{2\pi} \\ 0 & 0 & -\frac{\sqrt{2}\nu}{\pi} & \frac{\sqrt{2}\nu}{2\pi} & 0 & 0 \end{Bmatrix}$$

$$\{A_{21}\}_{6\times 3} = \begin{Bmatrix} \begin{array}{l}\{\frac{2}{35}(1+\frac{1}{2}\nu+C_1+C_2) \\ -\frac{1}{2}(1+\frac{1}{5}\nu)\}/\Delta\end{array} & \begin{array}{l}\{(\frac{-2\sqrt{2}}{35}/\pi)\nu c\gamma(2B_1-B_2) \\ +(1+\frac{1}{5}\nu)(12\sqrt{2}/\pi^3) \\ \cdot(B_1-\frac{1}{8}B_2)\}/\Delta\end{array} & \begin{array}{l}\{(\frac{2\sqrt{2}}{35}/\pi)\nu(2A_1-A_2) \\ -(1+\frac{1}{5}\nu)(12\sqrt{2}/\pi^3) \\ \cdot(A_1-\frac{1}{8}A_2)\}/\Delta\end{array} \\ \begin{array}{l}\{-\frac{2}{15}(1+\frac{1}{2}\nu+C_1+C_2) \\ +\frac{1}{2}(1+\frac{1}{3}\nu)\}/\Delta\end{array} & \begin{array}{l}\{\frac{2}{15}(\sqrt{2}/\pi)\nu c\gamma(2B_1-B_2) \\ -(1+\frac{1}{3}\nu)(12\sqrt{2}/\pi^3) \\ \cdot(B_1-\frac{1}{8}B_2)\}/\Delta\end{array} & \begin{array}{l}\{\frac{-2\sqrt{2}}{15}/\pi(2A_1-A_2) \\ +(1+\frac{1}{3}\nu)(12\sqrt{2}/\pi^3) \\ (A_1-\frac{1}{8}A_2)\}/\Delta\end{array} \\ \frac{3}{2}A_1 - \frac{4}{3}A_2 & -s\gamma\, B_1 & -\frac{\sqrt{2}}{\pi} \\ \frac{4}{3}A_1 + \frac{3}{2}A_2 & -s\gamma\, B_2 & \frac{\sqrt{2}}{2\pi} \\ \frac{3}{2}B_1 - \frac{4}{3}B_2 & s\gamma A_1 + \frac{\sqrt{2}}{\pi}c\gamma & 0 \\ \frac{4}{3}B_1 + \frac{3}{2}B_2 & s\gamma A_2 - \frac{\sqrt{2}}{2\pi}c\gamma & 0 \end{Bmatrix} \tag{F.6}$$

where

$$\Delta = [(1 + \frac{1}{3}\nu)\frac{2}{35} - \frac{2}{15}(1 + \frac{1}{5}\nu)] \tag{F.6}$$

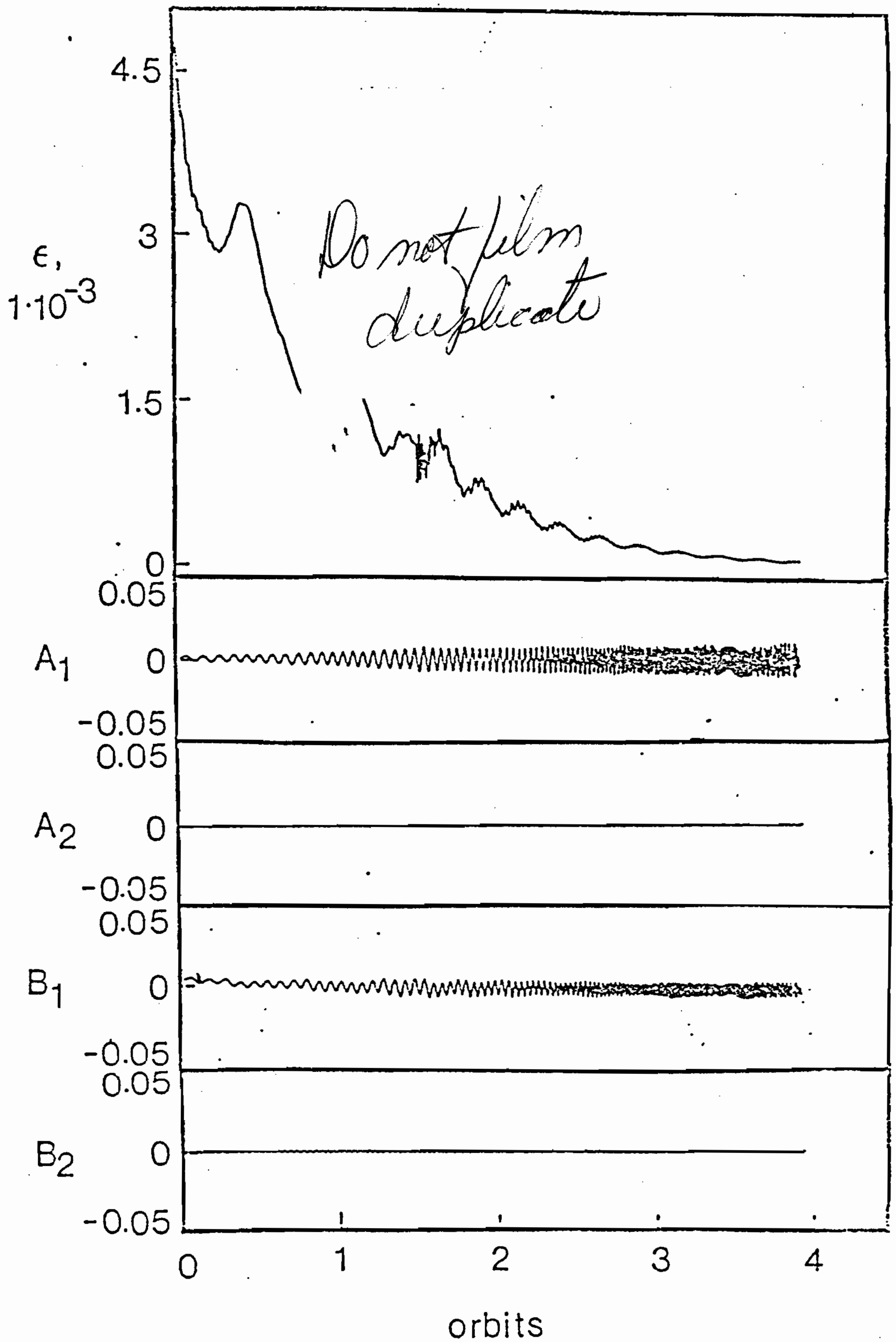

(b) Longitudinal strain and transverse modal coordinates A_1, A_2, B_1 and B_2

Fig. 8.10 Dynamical response (both rotations and vibrations) during retrieval from 100 Km with the linear strain model and using length rate law (8.5.3)